Polymer Brushes via Surface-Initiated Controlled Radical Polymerization: Synthesis, Characterization, Properties, and Applications

Raphaël Barbey, Laurent Lavanant, Dusko Paripovic, Nicolas Schüwer, Caroline Sugnaux, Stefano Tugulu, and Harm-Anton Klok*

École Polytechnique Fédérale de Lausanne (EPFL), Institut des Matériaux, Laboratoire des Polymères, Bâtiment MXD, Station 12, CH-1015 Lausanne, Switzerland

Received February 5, 2009

Contents

1. Introduction

Polymer brushes are ultrathin polymer coatings consisting of polymer chains that are tethered with one chain end to an interface, which generally is a solid substrate. At high grafting densities, i.e. when the distance between neighboring

* To whom correspondence should be addressed. E-mail: harm-anton.klok@epfl.ch. Fax: +41 21 693 5650. Telephone: +41 21 693 4866.

10.1021/cr900045a CCC: $71.50 © 2009 American Chemical Society
Published on Web 10/21/2009

Raphaël Barbey was born in Saint-Imier (Bern, Switzerland) in 1980. He received his M.Sc. degree in chemical and biochemical engineering from the École Polytechnique Fédérale de Lausanne (EPFL, Switzerland) in 2004. After a one year academic internship working on the development of reaction calorimetry applied to polymerization reactions in supercritical fluids, he joined the group of Prof. H.-A. Klok. He is currently pursuing his doctoral studies in the field of polymer brushes and their use for biomedical and bioanalytical applications.

Laurent Lavanant was born in 1979 in Rennes (France) and graduated from the École Nationale Supérieure de Chimie de Paris (France) and the University Pierre et Marie Curie (Paris, France) with a master in chemical engineering and molecular chemistry, respectively. He received his Ph.D. degree in 2005 from the University of Rennes (France) after working with Jean-François Carpentier. After postdoctoral research with H.-A. Klok from 2005 to 2007, he is now a research scientist at Sensile Medical AG (Hägendorf, Switzerland) and works on the development of medical devices.

grafting points is small, steric repulsion leads to chain stretching and a brush-type conformation of the surface-tethered chains. At lower grafting densities, surface-tethered polymer chains can adopt various other conformations, which are referred to as mushroom or pancake.[1–4]

Polymer brushes can be prepared following two main strategies: (i) the *grafting to* and (ii) the *grafting from* strategies.[3] The *grafting to* strategy involves the attachment of prefabricated polymers via either physisorption[5–12] (Figure 1A) or covalent bond formation (chemisorption) (Figure 1B).[13–20] Although experimentally very straightforward, the *grafting to* strategy suffers from several limitations, which make it difficult to produce thick and very dense polymer brushes. Steric repulsions between polymer chains hamper the formation of dense polymer brushes.[21,22] Furthermore, with increasing polymer molecular weight, the reaction between the polymer end-group and the complementary group on the substrate surface becomes less efficient.

Dusko Paripovic was born in 1981 and studied at the Faculty of Technology and Metallurgy in Belgrade (Serbia) to obtain his degree in organic chemical technology and polymer engineering. He completed his diploma thesis in the group of Prof. Morbidelli at ETH Zürich in 2006. Currently he works with Prof. H.-A. Klok at EPF Lausanne pursuing his Ph.D. on the topic of biofunctionalized polymer brushes.

Nicolas Schüwer was born in Besançon (France) in 1984. He obtained his bachelor degree in chemistry from the University of Franche-Comté (France) and his master degree in physical chemistry from Åbo Akademi (Turku, Finland). He is currently working as a Ph.D. student with Prof. H.-A. Klok at the École Polytechnique Fédérale de Lausanne (Switzerland).

Caroline Sugnaux was born in Morges (Vaud, Switzerland) in 1984. After accomplishing her master thesis in the group of Prof. S. Mecking (Konstanz, Germany), she obtained her master degree in molecular and biological chemistry in 2008 from the École Polytechnique Fédérale de Lausanne (EPFL, Switzerland). She is currently carrying out a Ph.D. thesis under the supervision of Prof. H.-A. Klok.

In the *grafting from* approach (Figure 1C), the polymerization is directly initiated from initiator-functionalized surfaces.[3,22–25] Controlled/"living" polymerization techniques[26,27] are particularly attractive for the preparation of polymer brushes

Stefano Tugulu was born in Ahlen (Germany) in 1974. He received his diploma degree in chemistry from the University of Bielefeld (Germany) in 2001. In 2007 he obtained his Ph.D. working with Prof. H.-A. Klok on functional polymer brushes prepared via surface-initiated controlled radical polymerizations at the Max Planck Institute for Polymer Research (Mainz, Germany) and at the École Polytechnique Fédérale de Lausanne (Switzerland). He is currently working as a R&D project manager in the field of medical device technology at Thommen Medical (Waldenburg, Switzerland).

Harm-Anton Klok was born in 1971 and studied chemical technology at the University of Twente (Enschede, The Netherlands) from 1989 to 1993. He received his Ph.D. in 1997 from the University of Ulm (Germany) after working with M. Möller. After postdoctoral research with D. N. Reinhoudt (University of Twente) and S. I. Stupp (University of Illinois at Urbana−Champaign), he joined the Max Planck Institute for Polymer Research (Mainz, Germany) in early 1999 as a project leader in the group of K. Müllen. In November 2002, he was appointed to the faculty of the École Polytechnique Fédérale de Lausanne (EPFL, Switzerland).

following the *grafting from* strategy, as they allow accurate control over brush thickness, composition, and architecture.[28–31] Examples include anionic polymerization,[32–34] cationic polymerization,[34–37] ring-opening polymerization,[38–46] and ring-opening metathesis polymerization.[47–51] Conventional free radical polymerization has also found widespread use for the synthesis of polymer brushes.[22,52–64] Most of the polymer brushes produced by the *grafting from* approach, however, are prepared using surface-initiated controlled radical polymerization techniques.

This article concentrates exclusively on polymer brushes prepared via surface-initiated controlled radical polymerization and is an attempt to summarize the state-of-the-art in this field. The following sections will successively discuss the synthesis of polymer brushes via surface-initiated controlled radical polymerization, the characterization of these surface-tethered polymers, as well as their properties and applications.

2. Synthesis

2.1. Polymerization Strategies

Among the different controlled/"living" polymerization techniques, radical-based strategies are most frequently used. Compared to other controlled/"living" polymerization methods, radical-based polymerization reactions have several advantages, notably in terms of compatibility with both aqueous and organic media as well as a high tolerance toward a wide range of functional groups. In the following sections, the four major surface-initiated controlled radical polymerization (SI-CRP) techniques will be discussed in detail. Table 1 provides an overview of the different polymer brushes that have been prepared using SI-CRP. The brushes in Table 1 are classified according to the nature of the polymer backbone. For each polymer, Table 1 indicates both the CRP techniques that have been used and the different brush architectures that have been produced.

2.1.1. Surface-Initiated Atom Transfer Radical Polymerization (SI-ATRP)

Among the different controlled radical polymerization techniques that are available, atom transfer radical polymerization (ATRP) has been most extensively used to produce polymer brushes. Compared to other controlled radical polymerization techniques, ATRP is chemically extremely versatile and robust. ATRP was first reported in 1995[65–67] and has been extensively reviewed.[68–72] ATRP relies on the reversible redox activation of a dormant alkyl halide-terminated polymer chain end by a halogen transfer to a transition metal complex. The formal homolytic cleavage of the carbon−halogen bond, which results from this process, generates a free and active carbon-centered radical species at the polymer chain end. This activation step is based on a single electron transfer from the transition metal complex to the halogen atom, which leads to the oxidation of the transition metal complex. Then, in a fast, reversible reaction, the oxidized form of the catalyst reconverts the propagating radical chain end to the corresponding halogen-capped dormant species. Many parameters, such as ligand to transition metal ratio, Cu^{II} to Cu^{I} ratio, type of ligand, counterion, solvent, or initiator, influence the performance of (SI)-ATRP and thus offer the possibility to fine-tune the reaction.[73–81]

SI-ATRP was first reported in 1997 by Huang and Wirth, who successfully grafted poly(acrylamide) (PAM) brushes from benzylchloride-derivatized silica particles.[82] Shortly thereafter, Ejaz et al. described the preparation of poly(methyl methacrylate) (PMMA) brushes that were grown from 2-(4-chlorosulfonylphenyl)ethyl silane self-assembled monolayers (SAMs) obtained using the Langmuir−Blodgett technique.[83] These authors found that addition of free, sacrificial initiator (*p*-toluenesulfonyl chloride) was necessary to achieve a controlled polymerization. In the absence of sacrificial initiator, the initiator concentration and, related to this, the concentration of the deactivating Cu^{II} species was too low to allow a controlled polymerization. Instead of adding a sacrificial initiator, another strategy to overcome the insufficient deactivator concentration that results from surface-confined ATRP is to add the deactivating Cu^{II} species directly to the polymerization solution. This was successfully demonstrated by Matyjaszewski et al. for the synthesis of

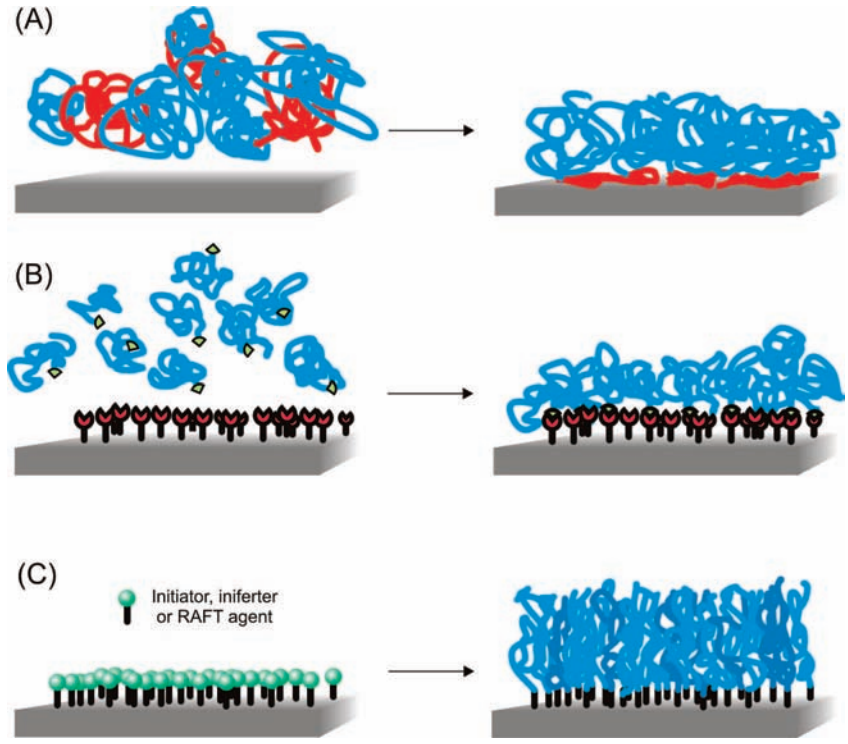

Figure 1. Synthetic strategies for the preparation of polymer brushes: (A) physisorption of diblock copolymers via preferential adsorption of the red blocks to the surface (*grafting to* approach); (B) chemisorption via reaction of appropriately end-functionalized polymers with complementary functional groups at the substrate surface (*grafting to* approach); (C) polymer brushes grown via surface-initiated polymerization techniques (*grafting from* approach).

polystyrene (PS) brushes from bromoisobutyrate-functionalized silicon wafers.[84]

A significant increase in the rate of SI-ATRP was observed for polymerizations carried out in polar and, in particular, aqueous media.[75,78,85,86] Jones et al. synthesized 50-nm-thick PMMA brushes in a controlled fashion within 4 h of polymerization time using a $Cu^{I}Br$/2,2′-bipyridine (bpy) catalyst system in a water/methanol mixture as solvent.[87] A purely aqueous-based system was used by Huang et al. for the preparation of 700-nm-thick poly(2-hydroxyethyl methacrylate) (PHEMA) brushes via "water-accelerated" SI-ATRP using a mixed halide $Cu^{I}Cl/Cu^{II}Br_2$/bpy catalyst system (Scheme 1).[88] As described by Matyjaszewski et al., the use of such mixed halide systems represents, because of the higher free energy of dissociation of the C−Cl bond compared to the C−Br bond, a valuable tool to shift the equilibrium between dormant and propagating radical species on the side of dormant species, which leads to an increase over the control of the polymerization.[89]

In SI-ATRP, chain growth starts from an ATRP initiator that is immobilized on a substrate. The same transition metal complexes that mediate SI-ATRP, however, can also be used to grow polymer brushes in a controlled fashion from surfaces modified with a conventional radical initiator. This process is referred to as surface-initiated reverse ATRP (SI-RATRP). SI-RATRP has been successfully used by Sedjo et al. to prepare PS and PS-*b*-PMMA brushes from a conventional radical azo-functionalized silica substrate using $Cu^{II}Br_2$/bpy complex as deactivating agent.[90] Later, Wang et al. described the synthesis of PMMA brushes from peroxide-derivatized substrates in the presence of $Cu^{II}Cl_2$/bpy complex.[91,92]

The (possible) presence of residual amounts of the metal catalyst in polymers prepared via (SI)-ATRP often raises concerns, in particular with the use of these materials in (bio)medical applications. Matyjaszewski and co-workers have developed an ATRP variant that allows to overcome these concerns and which makes it possible to reduce the concentration of the copper catalyst to a few ppm and increases the tolerance toward oxygen or other radical traps in the polymerization system. This ATRP variant is referred to as activators (re)generated by electron transfer ATRP or A(R)GET ATRP.[93–97] A(R)GET ATRP involves the use of reducing agents, such as ascorbic acid, Sn^{II} 2-ethylhexanoate, or Cu^{0}, to continuously restore Cu^{I} from Cu^{II} and has also been successfully applied to surface-initiated polymerization.[98–104]

Summarizing, SI-ATRP has been proven to be an excellent technique to prepare polymer brushes. ATRP is chemically versatile, compatible with a large assortment of monomers and functional groups, and tolerates a relatively high degree of impurities. In particular, ATRP is relatively insensitive toward small residual traces of oxygen, which are readily removed by oxidation of the ATRP catalyst. The fact that most of the standard ATRP catalyst systems, as well as surface immobilizable initiators, are commercially available in ready-to-use quality or can be synthesized relatively easily also makes ATRP an attractive technique from an experimental point of view. SI-ATRP, however, also has limitations. In particular, the controlled polymerization of monomers that can complex or react with the metal catalyst, such as pyridine-containing or acidic monomers, can be challenging. For pyridinic monomers, this problem can be partially overcome by using highly coordinative tri- or tetradentate ligands to form the catalytic transition metal complex.[105,106]

The preparation of acidic polymer brushes has been accomplished via ATRP of the corresponding sodium salts.[107–113] An interesting exception has been reported in a recent publication by Jain et al., who reported the first example of successful direct SI-ATRP of a protonated acidic monomer, 2-(methacryloyloxy)ethyl succinate (MES).[113] Another limitation of (SI)-ATRP is related to the transition metal catalyst, which can be difficult to remove. Residual traces of

Table 1. Overview of Polymer Brushes Prepared via Surface-Initiated Controlled Radical Polymerization

Polymer	Chemical structure	Surface-initiated polymerization technique[a]			
		ATRP	RAFT	NMP	PIMP
METHACRYLATES (Neutral)					
PAHMA poly(6-azidohexyl methacrylate)	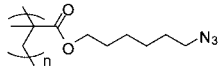		H[626] B[626]		
PBIEMA poly(2-(2-bromoisobutyryloxy)ethyl methacrylate)	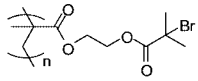	H[221] R[221,246] (hyperbranched)			
PBMA poly(*n*-butyl methacrylate)	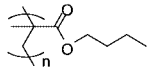	H[286,287,339,434,442,736-739] B[286,287,736] R[272]			B[215]
PBzMA poly(benzyl methacrylate)	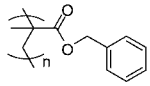	H[226,589] B[487,672] R[226,487]			
PCDMA poly(cadmium dimethacrylate)	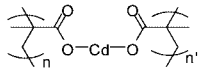	H[379,740] B[635,740] R[635]			
PDDMA poly(dodecyl methacrylate)	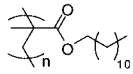	H[395]		H[408]	
PDEAEMA poly(2-(diethylamino)ethyl methacrylate)	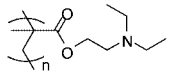	H[109,343,693,741]			
PDHPMA poly(2,3-dihydroxypropyl methacrylate)	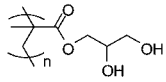	H[342,343,448,465,742] R[619,719]			
PDMAEMA poly(2-(dimethylamino)ethyl methacrylate)	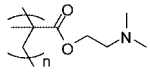	H[88,109,287,288,290,299,338,342,349,360,361,378,387,388,397,416,421,426,427,439,482,494,518,522,529,532,533,555,563,581,594,608,609,661,692,695,728,729,742-750] B[88,218,219,286,287,338,360,361,388,397,439,482,494,495,507,608,736,744,750,751] R[272,427,609,642,750]	H[480,481] B[120,122,143,481,752]		H[208] R[222]
PDPAEMA poly(2-(diisopropylamino)ethyl methacrylate)	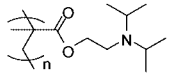	H[343]			
PEEMA poly(1-ethoxyethyl methacrylate)	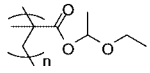	H[753,754]			
PEGDMA poly(ethylene glycol dimethacrylate)	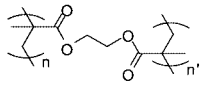	H[253,255,755] R[226,231,364]	R[131,756]		R[228,229]
PEMA poly(ethyl methacrylate)	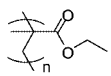	H[101]			H[208]
PEMOMA poly(3-ethyl-3-(methacryloyloxy)-methyloxetane)	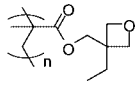	H[264] B[264]			
PFMMA poly(ferrocenylmethyl methacrylate)	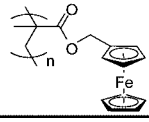	H[664]			

Table 1. Continued

Polymer	Chemical structure	Surface-initiated polymerization technique[a]			
		ATRP	RAFT	NMP	PIMP
PGAMA poly(2-gluconamidoethyl methacrylate)	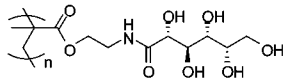	H[342,757]			
PGMA poly(glycidyl methacrylate)	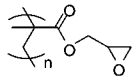	H[87,225,250,257-260,295,339,355,356,474,475,510,579,618,621-623,719,758-761] B[257,338,482,621,672,758,762] R[225,619,620,719]	H[125,252,763] B[125,763]		B[631]
PHDFDMA poly(heptadecafluorodecyl methacrylate)	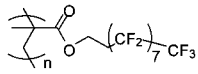	H[764]			
PHEMA poly(2-hydroxyethyl methacrylate)	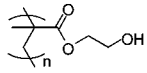	H[87,88,105,192,243,251,254,255,278,284,285,288,289,291,300,303,309,328,342-344,358,361,365-367,378,387,397,416,419,482,503,508,516,522,564,579-581,597-600,602,603,605,726,759,765-774] ARGET[104] B[87,88,111,217-219,284,288,289,328,354,361,472,486,508,516,562,744,750,761,769] R[271,750]	H[121,140,143,353] B[143]	B[354] R[156,169]	H[199,208,256,525]
PHosMA poly(hostasol-derivatized methacrylate)	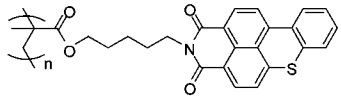	R[770]			
PHPMA poly(2-hydroxypropyl methacrylate)	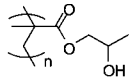	H[343]			
PiBMA poly(isobutyl methacrylate)	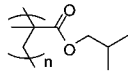	H[461,462]			
PiBoMA poly(isobornyl methacrylate)	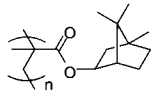	H[416]			
PLAMA poly(2-lactobionamidoethyl methacrylate)	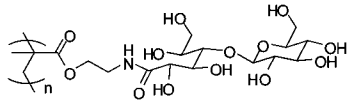	H[775]			
PLDMA poly(lead dimethacrylate)	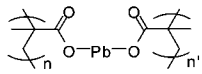	H[776]			
PMAA poly(methacrylic acid) *(sodium salt form, cf **PMAA(Na)**)*					H[200,202,208,213,214,281,584,681] B[200,681] R[228,229]
PMAd poly(5'-methacryloyladenosine)	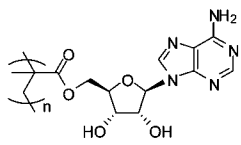	H[777] R[777]			
PMAIG poly(3-O-methacryloyl-1,2:5,6-di-O-isopropylidene-D-glucofuranose)	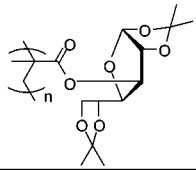	H[246,624,778] R[246]			

Table 1. Continued

Polymer	Chemical structure	Surface-initiated polymerization technique[a]			
		ATRP	RAFT	NMP	PIMP
PMDPAB poly(4-(10-methacryloydecyloxy)-4'-pentylazobenzene)	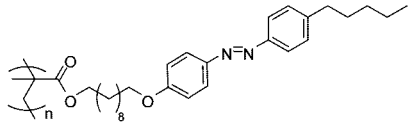	H[779,780]			
PMEMA poly(2-methoxyethyl methacrylate)	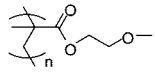	H[308,309,781] B[781]			
PMES poly(2-(methacryloyloxy)ethyl succinate)	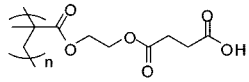	H[113]			
PMMA poly(methyl methacrylate)		H[74,83,87,101,105,156,192,218,219,221,235-240,249,282,288,295,303,309,310,326,338,345,346,360,372,376,384,386,391,392,395,397,398,406,411,412,416,417,428-431,435-437,444,451,453,458,464-466,467,482,484,487,489,493,498,505,507,511,515,519,545,570,579-581, 587,591,596,638,666,734,740,744,746,755,758,761,762,765,770,782-796 Reverse[91,92,401,519,550,551] B[87,110,217-219,248,262,264,284,288,289,327,338,360,369,396,397,444,482,487,505,507,562,635,669,672,740,744,758,761,784,785,797-800 Reverse[90,401] R[221,225,231,271,444,487,635,655,770,797,801,802]	H[117,120,122,123,128,135,139,143,144,146,340,404,413] B[117,120,122,139,143,144,626] R[756]	B[156,169] R[156,169,432]	H[207,209,211,280,407,803,804] B[201,207,211,407]
PMUr poly(5'-methacryloyluridine)	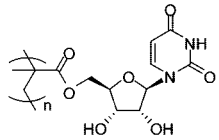	H[777] R[777]			
PNHSMA poly(*N*-hydroxysuccinimide methacrylate)	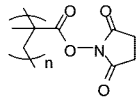	H[381,382]			
PNMEMA poly(2-(*N*-morpholino)ethyl methacrylate)	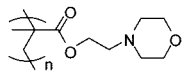	H[342,759,805]			
PNVOCMA poly(4,5-dimethoxy-2-nitrobenzyl methacrylate)	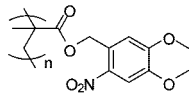	H[806]			
PODMA poly(octadecyl methacrylate)	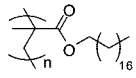	H[395]			
POMA poly(octyl methacrylate)	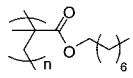				H[210] B[210]
PPEGDMA poly(poly(ethylene glycol) dimethacrylate)	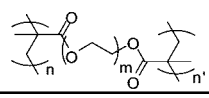	H[254]			H[256] R[230]

Table 1. Continued

Polymer	Chemical structure	Surface-initiated polymerization technique[a]			
		ATRP	RAFT	NMP	PIMP
PPEGMA$_m$ poly(poly(ethylene glycol) methacrylate)	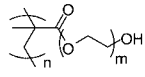	H[101,234,251,254,298,307,351,352,359,360,369,377,388,389,470,486,495,508,517,600-602,604,632,746,760,764,807] B[234,351,369,388,486,495,508,562,760,808] R[234,307,552]	H[125] B[125]		H[202,509] R[230]
PPEGMEMA$_m$ poly(poly(ethylene glycol) methyl ether methacrylate)	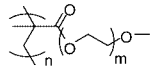	H[103,252,292,294,307,308,385,393,494,497,507,531,542,543,552,556,567,575,590,593,628,629,659,687,689,702,711,725,731,759,768,771,805,809-811] Reverse[550] ARGET[101,103,658] B[494,507,543,669] R[233,307,422,427,552]	H[120,812] B[120]		H[210,256] B[210]
PPeMMA poly(3-perylenylmethyl methacrylate)	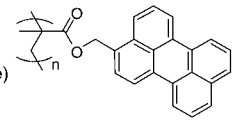	R[655]			
PPOSSMA poly(heptaisobutyl POSS™-derivatived propyl methacrylate)	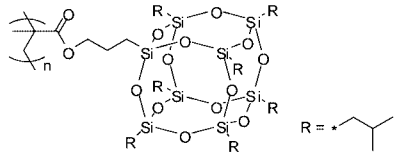	H[813]			
PSMA poly((2,2-dimethyl-1,3-dioxolan-4-yl)methyl methacrylate)	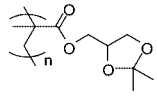	H[166,625]			
PSP poly(spirobenzopyran-functionalized methacrylate)	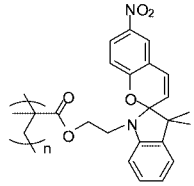	B[797] R[797,801,802,814]			
Pt*B*AEMA poly(2-(*tert*-butylamino)ethyl methacrylate)	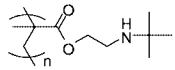	H[233] R[233]			
Pt*B*MA poly(*tert*-butyl methacrylate)	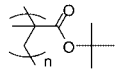	H[416,435,461,608,609,815] B[608] R[609]		H[544]	
PTFEMA poly(trifluoroethyl methacrylate)	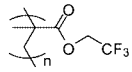	H[397,516,746,799] B[397,516,543,760,799]			
PTMSMA poly(trimethylsilyl methacrylate)	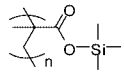	H[378]			
PTMSPMA poly(3-(trimethoxysilyl)propyl methacrylate)	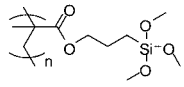	H[350,527]			
PZMA 2-(perfluoroalkyl)ethyl methacrylate)	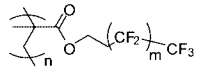	H[521]			
METHACRYLATES (Charged)					
PBIMHFP poly(2-(1-butylimidazolium-3-yl) ethyl methacrylate hexafluorophosphate)	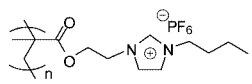	H[816]			

Table 1. Continued

Polymer	Chemical structure	Surface-initiated polymerization technique[a]			
		ATRP	RAFT	NMP	PIMP
PCBMA poly(carboxybetaine methacrylate)	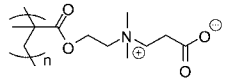	H[612,617,702,817]			
PEMEICl poly(1-ethyl 3-(2-methacryloyloxy ethyl) imidazolium chloride)	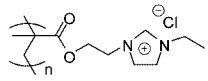	H[662,818]			
PMAA(Na) poly(sodium methacrylate)	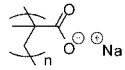	H[111,112,555,576,614,819] B[110,111]			H[199,202]
PMEP poly(2-methacryloyloxyethyl phosphate)	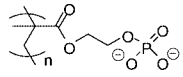	H[555,562,569,651,820,821] B[562]			
PMETAC poly((2-(methacryloyloxy)ethyl)-trimethylammonium chloride)	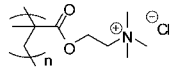	H[81,110,296,342,502,536,553,557-559,644,646,649,652,663,697,698,821,822] B[110] R[712]			
PMPC poly(2-(methacryloyloxy)ethyl phosphorylcholine)	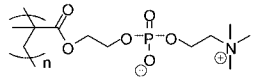	H[301,342,577,621,709,711,735,742,751,815,823,824] B[621,751] R[620]			
PSBMA poly(sulfobetaine methacrylate)	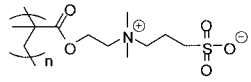	H[339,633,701,702,731,817,825-828]	H[119] B[119]		
PSEMA poly(2-sulfatoethyl methacrylate)	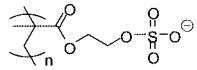	H[805,820]			
PSPMA(K) poly(potassium 3-sulfopropyl methacrylate)	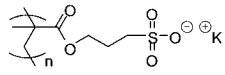	H[504,521,660,730,742,829,830] R[712]			H[199]
ACRYLATES (Neutral)					
PAA poly(acrylic acid) *(sodium salt form, cf **PAA(Na)**)*		R[233,690]	H[133] B[668] R[134]	H[647,831] B[647]	H[523] B[215] R[490,523]
PAAb poly(acrylated antibody)	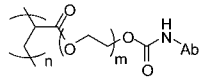				R[718]
PBA poly(*n*-butyl acrylate)	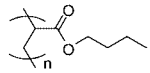	H[87,99,371,395,411,420,436,462,463,485,498,785,832-834] ARGET[99,100,102] B[410,785,833] ARGET[102] R[223]	H[124,127,134,144,146,413] B[127,134,144]	H[163,178-181,185,187-189,341] B[181,185,341] R[191]	H[491]
PBAEA poly(2-(bromoacetyloxy)ethyl acrylate)	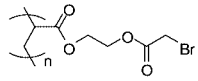	H[223] R[223] (hyperbranched)			
PBPEA poly(2-(2-bromopropionyloxy)ethyl acrylate)	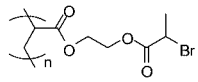	H[220,221] R[220,221] (hyperbranched)			
PBzA poly(benzyl acrylate)	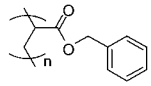	B[835]			
PCPPUA poly(11-(4'-cyanophenyl-4"-phenoxy)undecyl acrylate)	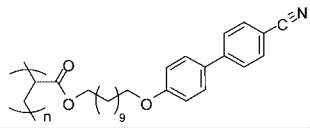	H[473] B[473]			

Table 1. Continued

Polymer	Chemical structure	Surface-initiated polymerization technique[a]			
		ATRP	RAFT	NMP	PIMP
PDMAEA poly(2-(dimethylamino)ethyl acrylate)	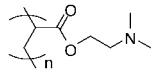		B[668]	H[185] B[185] R[191]	
PEA poly(ethyl acrylate)	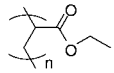	H[405,476,498,511] B[476]		H[179,180]	H[208]
PEGDA poly(ethylene glycol diacrylate)	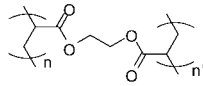	R[224]			
PFA poly(fluorescein acrylate)	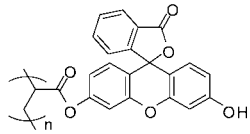				H[525]
PHDDA poly(1,6-hexanediol diacrylate)	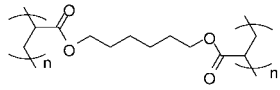				H[526]
PHDFDA poly(heptadecafluorodecyl acrylate)	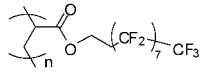	H[84,836] B[667]			
PHEA poly(2-hydroxyethyl acrylate)	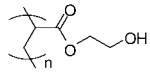	H[394,536]			
PLCA poly(mesogen-functionalized acrylate)	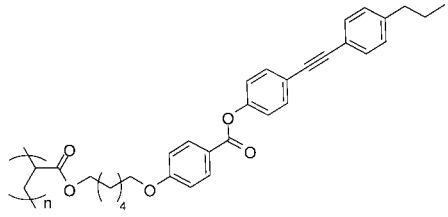	H[837]			
PMA poly(methyl acrylate)		H[74,84,216,217,339, 468,471-473,515,608, 667,668,744,770,838-840] B[84,216-218,471-473, 608,667,668,744,769, 770,838-840]	H[134,135,144,146,148, 149] B[122,134,144] R[134]	B[195]	
POA poly(octyl acrylate)	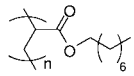				H[525]
PODA poly(octadecyl acrylate)	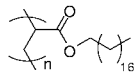	H[721,722]			
PPEGA poly(poly(ethylene glycol) acrylate)	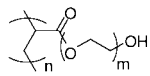				H[525,526] R[524,718]
PPEGASF poly(poly(ethylene glycol) acrylate succinyl fluorescein)	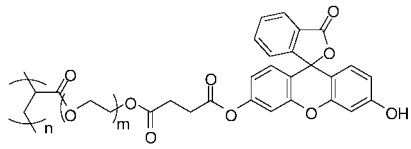				R[524]
PPEGMEA poly(poly(ethylene glycol) methyl ether acrylate)	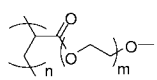	H[483]			
PPFPA poly(pentafluoropropyl acrylate)	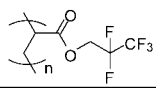	B[667,839]			

Table 1. Continued

Polymer	Chemical structure	Surface-initiated polymerization technique[a]			
		ATRP	RAFT	NMP	PIMP
P*t*BA poly(*tert*-butyl acrylate)	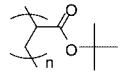	H[105,106,220,221,241,242,276,330,403,449,453,462,463,608,610,611,613,615,719,770,841,842] B[84,106,608,634,719,727,770,833,838] R[220,221]	H[549] B[549]	H[190,195] B[195]	H[407,525]
PTFEA poly(trifluoroethyl acrylate)	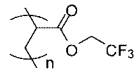	B[667]			H[525,526]
PTMSA poly(trimethylsilyl acrylate)	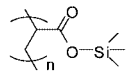	H[378]			
PTPAA poly(triphenylamine acrylate)	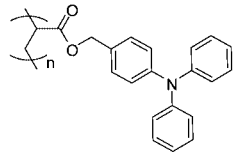	H[843,844]			
ACRYLATES (Charged)					
PAA(Na) poly(sodium acrylate)	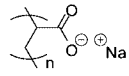	H[469,582,694] R[654]			H[203]
METHACRYLAMIDES					
PHPMAM poly(*N*-(2-hydroxypropyl) methacrylamide)	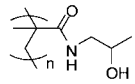		H[142]	H[647] B[647]	
PMAM poly(methacrylamide)					H[208]
PMPDSAH poly((3-methacryloylamino)propyl)-dimethyl-(3-sulfopropyl)ammonium hydroxide)	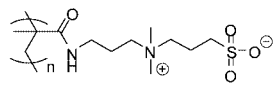	H[845]			
ACRYLAMIDES					
PAGA poly(*N*-acryloyl glucosamine)	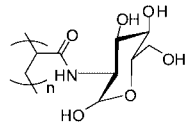		H[147] B[147]		
PAM poly(acrylamide)		H[82,232,265,274,275,283,290,309,313,400,478,492,500,501,505,512,732,733,739,784,846-850] B[399,505,784] R[232,578]	H[145]		H[208,523,851] R[523]
PAMPS(K) poly(potassium 2-acrylamido-2-methylpropane sulfonate)	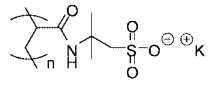	H[852]			
PCBAM poly(carboxybetaine derivatized acrylamide)	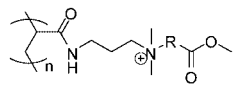 R=CH_2, $(CH_2)_3$, $(CH_2)_5$	H[616,617]			
PCyPAM poly(*N*-cyclopropyl acrylamide)	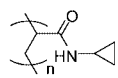	H[431]			
PDMAM poly(*N*,*N*-dimethylacrylamide)		H[311,312,486,538-541,639,724] B[486,537,538]	H[117,146,763] B[117,763]	H[630]	H[199,200,202,203,205,206,208,509] B[215] R[202,222]

Table 1. Continued

Polymer	Chemical structure	Surface-initiated polymerization technique[a]			
		ATRP	RAFT	NMP	PIMP
PDMAPAM poly(*N*-(3-(dimethylamino)propyl) acrylamide)	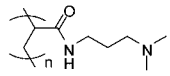				H[200] B[200,215]
PDMAPAMMI poly(*N*-(3-(dimethylamino)propyl) acrylamide methiodide)	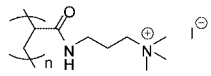				H[199,200] B[200]
PHMAM poly(*N*-hydroxymethyl acrylamide)	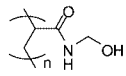	H[849]			
PMBAM poly(*N,N'*-methylenebisacrylamide)	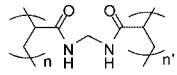	R[227,232,363,424]			
PMEAM poly(methoxyethylacrylamide)	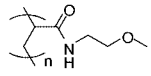	H[538,540] B[538,540]			
PN-BocAHAM poly(*N*-(6-(*N*-*tert*-butoxy-carbonylaminooxy)hexyl)acrylamide)	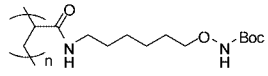	R[578]			
PNIPAM poly(*N*-isopropyl acrylamide)	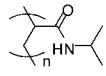	H[224,234,243,250,279,290,297,302,328,345,368,375,378,414,418,431,447,455,459,475,477,486,488,499,506,513,520,534,537,538,540,555,561,565,566,568,571-574,585,586,590,639,645,650,653,657,674-677,680,682,683,685,708,762,781,853-858] B[234,328,475,486,537,538,540,562,781] Reverse[401] R[224,227,234,363,422,424,642,650,654,690]	H[136,138,146,147,859] B[141,147,668]	H[647]	H[204,206,212,490,631,681] B[631,681] R[490]
PPEGMEAM$_m$ poly(poly(ethylene glycol) methyl ether acrylamide)	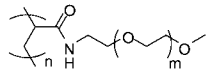	H[860]			
STYRENIC (Neutral)					
PAS poly(acetoxystyrene)	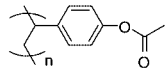			H[169] B[169]	
PCMS poly(4-chloromethylstyrene)	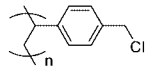	H[247,249] R[248] (hyperbranched)	H[118] B[118]	H[544]	H[202] R[202,222]
PDVB poly(divinylbenzene)	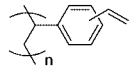	B[263]			
PFMS poly(4-(perfluoroalkyl)-oxymethylstyrene)	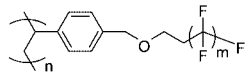			H[161] B[161]	
PGL poly(*tert*-butoxy-vinylbenzyl-polyglycidol)	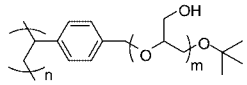	R[467]			
PMS poly(4-methylstyrene)	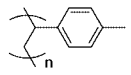	B[514]			
PODVBPheA poly(*N'*-octadecyl-*N*$^{\alpha}$-(4-vinyl)-benzoyl-L-phenylalanineamide)	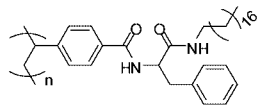	H[723,861]			
PPFS poly(2,3,4,5,6-pentafluorostyrene)	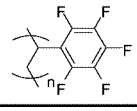	H[248,263,388,439,516,770] B[248,257,263,439,516,667] R[248]	B[118]		

Table 1. Continued

Polymer	Chemical structure	Surface-initiated polymerization technique[a]			
		ATRP	RAFT	NMP	PIMP
PSd8 poly(deuterated styrene)	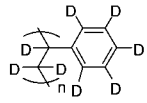	H[840] B[840]		H[193]	
PS polystyrene	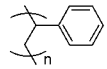	H[84,105,126,192,216,262,277,309,326,327,331,339,354,370,373,374,380,396,399,402,411,433,435,436,443,444,451,455,458,465-467,471,479,498,514,595,608,635,643,667,668,719,727,737,762,770,785,786,793,795,800,835,838,862-870] Reverse[90] B[84,216,262,327,354,396,399,410,444,471,476,494,514,608,635,667,668,672,719,727,762,770,785,797,800,835,838] Reverse[90] ARGET[102] R[233,443,444,467,627,871]	H[117,122,124,127-130,132,134,135,137,141,144,146,148,413,530,546,548] B[117,122,126,127,134,139,141,144,481,549,668] R[134,450,547]	H[156,158-169,171,177,182-186,192,194,235-242,341,409,432,441,456,457,592,630,647,872-874] B[156,161,162,169,171,181,184,185,341,647,874] R[156,169,191,194,432]	H[200,201,207,208,407,875] B[200,201,207,211,215,407]
PSLS poly(salen ligand-derivatized styrene)	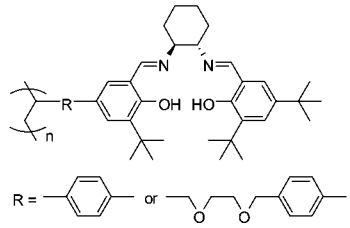	R[627]			
PSPEG poly(4-(poly(ethylene glycol) methyl ether)styrene)	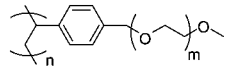			H[162] B[162]	
PVA poly(4-vinylaniline)	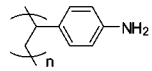	H[876]			
PVBCB poly(4-vinylbenzocyclobutene)	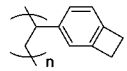			R[194]	
PVQ poly(vinylquinoline derivative)	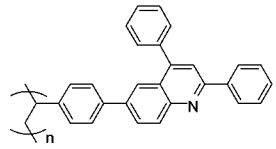	H[454]			
STYRENIC (Charged)					
PSS(Na) poly(sodium 4-styrenesulfonate)	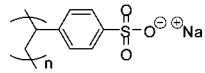	H[109,112,252,351,353,378,449,460,496,742,807,808,877-879] B[351,808]	B[119]	H[170,354] B[354]	
PVB(Na) poly(sodium 4-vinylbenzoate)	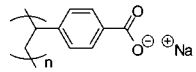	H[109]			
PVBIHFP poly(1-(4-vinylbenzyl)-3-butyl-imidazolium hexafluorophosphate)	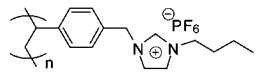	H[880]			
PYRIDINIC					
P2VP poly(2-vinylpyridine)	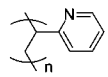	H[106,634,881,882] B[106,634,882]			
P3VP poly(3-vinylpyridine)	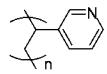			H[165,166]	

Table 1. Continued

Polymer	Chemical structure	Surface-initiated polymerization technique[a]			
		ATRP	RAFT	NMP	PIMP
P4VP poly(4-vinylpyridine)	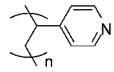	H[105,106,261,423,475,528,637] B[106,475,798] R[364]	R[131]	H[170,544,874] B[171,874]	
Others					
PAN poly(acrylonitrile)		H[347,443] R[443,871]			
PIA poly(itaconic acid)	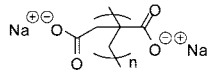	H[112,819]			
PMAn poly(maleic anhydride)			R[450]	R[194]	
PNVI poly(*N*-vinylimidazole)	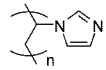	R[650]			
PNVP poly(*N*-vinyl-2-pyrrolidone)	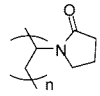	H[883,884]	H[752] B[752]		H[208]
PTMI poly(*m*-isopropenyl-α,α'-dimethyl-benzyl isocyanate)	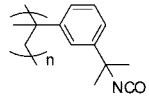		R[547]		
PVDMA poly(2-vinyl-4,4-dimethyl azlactone)	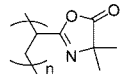	H[885]			

[a] H, B, and R refer to homopolymer, block copolymer, and random copolymer brushes. The superscripts are references to the relevant publications.

Scheme 1. Preparation of PHEMA-*b*-PDMAEMA Diblock Copolymer Brushes via SI-ATRP from 2-Bromoisobutyrate-Functional Thiol SAMs on Gold Surfaces[88]

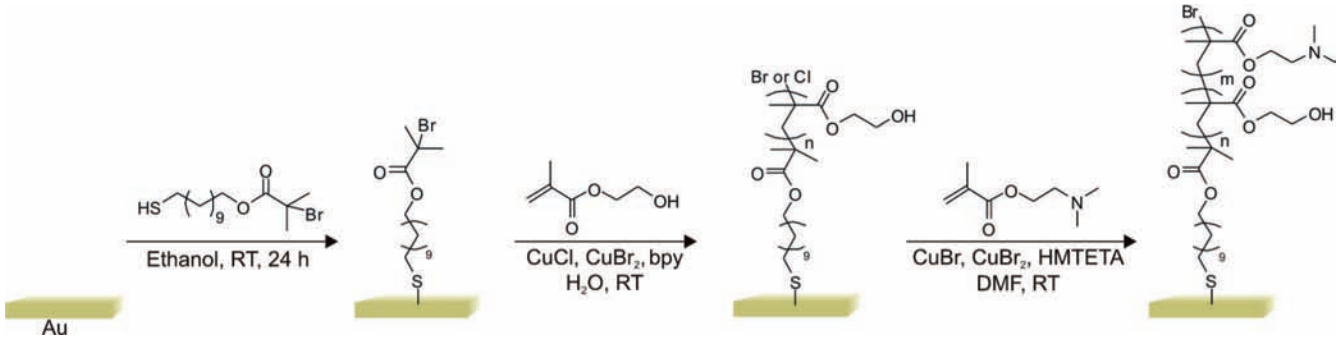

catalysts in the final polymer brushes might have undesirable consequences for applications, such as in the biomedical or electronic industry. However, some methods, in particular A(R)GET ATRP, have been developed that allow to reduce the amount of copper to the level of a few ppm.[72]

2.1.2. Surface-Initiated Reversible-Addition Fragmentation Chain Transfer (SI-RAFT) Polymerization

In contrast to ATRP, where the equilibrium between the dormant and active, propagating chains is based on reversible termination, reversible-addition fragmentation chain transfer (RAFT) polymerization is based on reversible chain transfer.[114–116] A distinct advantage of RAFT polymerization is its relative simplicity and versatility, since conventional free radical polymerizations can be readily converted into a RAFT process by adding an appropriate RAFT agent, such as a dithioester, dithiocarbamate, or trithiocarbonate compound, while other reaction parameters, such as monomer, initiator, solvent, and temperature, can be kept constant. RAFT polymerization has also been successfully used to prepare polymer brushes via surface-initiated polymerization. SI-RAFT can be performed using two different strategies, which use either surface-immobilized conventional free radical initiators or surface-immobilized RAFT agents (Scheme 2). These two different strategies will be discussed in more detail in the following paragraphs.

Scheme 2. SI-RAFT Polymerization: (A) Bimolecular Process as Reported by Baum and Brittain[117] for the Preparation of PMMA Brushes from Azo-Functionalized Silicon Wafers; (B) R-Group Approach To Grow PBA Brushes from Dithiobenzoate Modified Silica Nanoparticles as Described by Li and Benicewicz;[127] (C) Z-Group Approach for the Grafting of PMA Brushes from Silica Particles Supported Trithiocarbonate Derivative[146]

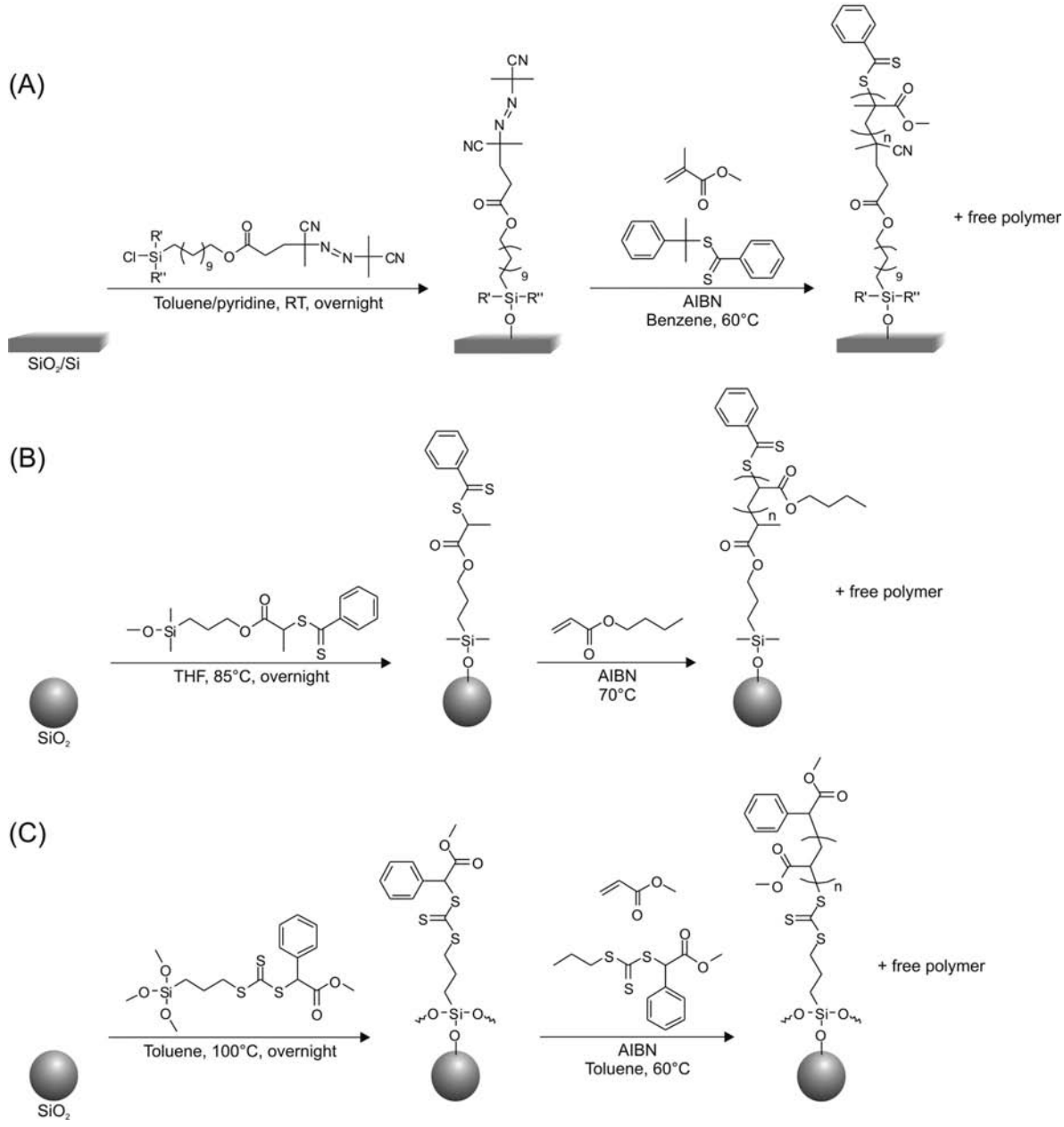

An early example of SI-RAFT polymerization was reported by Baum and Brittain, who prepared 30-nm-thick PMMA brushes as well as 11-nm-thick PS and poly(*N*,*N*-dimethylacrylamide) (PDMAM) brushes from azo-functionalized silicon wafers in the presence of the chain transfer agent (CTA) 2-phenylprop-2-yl dithiobenzoate and free initiator (2,2′-azoisobutyronitrile (AIBN)) (Scheme 2A).[117] Addition of free initiator (e.g., AIBN) was shown to facilitate polymer brush growth not only because it acts as a scavenger for possible trace amounts of impurities in the polymerization mixture but also since it increases the amount of radicals in the system, which are necessary to avoid early termination by CTA capping, as the concentration of the surface initiators is particularly low. Several other groups used the same strategy to grow poly(chloromethylstyrene) (PCMS),[118] poly(pentafluorostyrene) (PPFS),[118] poly(sulfobetaine methacrylate) (PSBMA),[119] poly(sodium 4-styrenesulfonate) (PSS(Na)),[119] PMMA,[120] poly(poly(ethylene glycol) methyl ether methacrylate) (PPEGMEMA),[120] and poly(2-(dimethylamino)ethyl methacrylate) (PDMAEMA)[120] brushes from azo-functionalized substrates or to graft PHEMA brushes from surfaces bearing peroxide groups.[121]

In addition to the use of free radical initiator-modified substrates, as was described in the previous paragraph, SI-RAFT can also be carried out using surface-immobilized RAFT agents. The RAFT agent can be immobilized in two different ways, which are referred to as the R-group and Z-group approaches (parts B and C, respectively, of Scheme 2). In the R-group approach, the RAFT agent is attached to the surface via the leaving and reinitiating R group. This strategy has been used to prepare a wide variety of polymer brushes from dithiobenzoate- or trithiocarbonate-derivatized silicon wafers,[122–125] silica (nano)particles,[126–132] titania[133] or CdSe[134] nanoparticles, cotton,[135] gold nanoparticles,[136] cellulose,[137] or multiwalled

Scheme 3. SI-NMP of Styrene from a TEMPO-Functionalized Silicon Wafer, as Reported by Husseman et al[156]

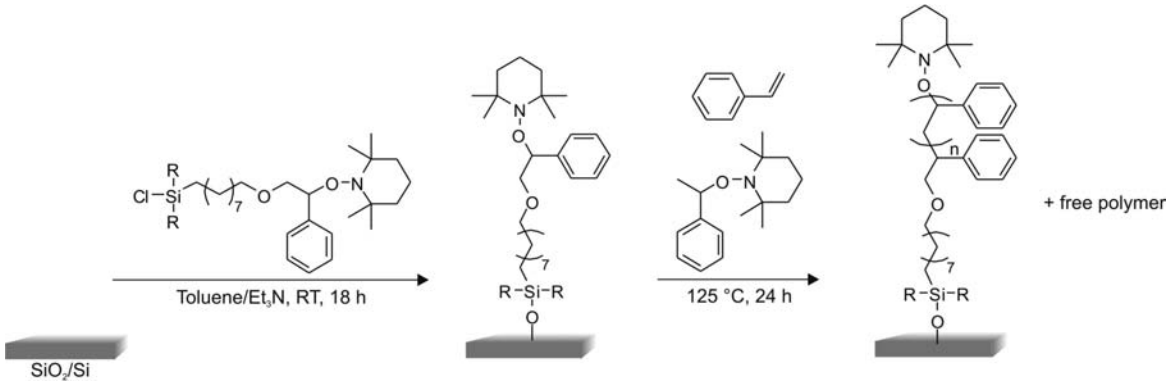

carbon nanotubes (carbon MWNTs).[138–142] The Z-group approach is based on the immobilization of the RAFT agent via the stabilizing Z group and has been successfully used to prepare a variety of methacrylic, acrylic, styrenic, and acrylamide-based brushes.[143–149]

Compared to other CRP techniques, RAFT polymerization is extremely versatile and tolerates a wide range of (sensitive) functional groups. A drawback of RAFT polymerization is that it involves the use of chain transfer agents that are usually not commercially available and which need to be prepared via multistep synthesis. SI-RAFT polymerization methods that involve the use of surface-immobilized CTAs have specific limitations. The R-group approach, comparable to a *grafting from* process, always involves the surface detachment of the RAFT agent during the polymerization, which might broaden the molecular weight distribution via bimolecular termination at an unusually high rate, whereas the Z-group approach, which can be compared with a *grafting to* approach, might suffer from a decrease of brush grafting densities with increasing brush length, since the RAFT agent anchored to the surface will be less and less accessible.[126,144,146]

2.1.3. Surface-Initated Nitroxide-Mediated Polymerization (SI-NMP)

Nitroxide-mediated polymerization is based upon reversible activation/deactivation of growing polymer chains by a nitroxide radical.[150–155] Husseman et al. reported the first example of surface-initiated nitroxide-mediated polymerization (SI-NMP) and successfully produced up to 120-nm-thick PS brushes from 2,2,6,6-tetramethylpiperidinyloxy (TEMPO) functionalized chlorosilane SAMs supported on silicon substrates (Scheme 3).[156] In SI-NMP the maximum number of persistent radicals[157] is limited by the total number of initiator moieties on the substrate surface, which is, especially for planar substrates with low specific surface areas, relatively low. Consequently, the reversible capping becomes ineffective due to the quasi infinite dilution of persistent radicals in the reaction medium. In their contribution, Husseman et al. managed to overcome this issue by adding a predetermined amount of "free" alkoxyamine to the reaction mixture. The addition of free (sacrificial) initiator, however, leads to the formation of free, non-surface-attached polymer and requires an additional, final washing step to remove physisorbed polymer from the resulting polymer brushes. Husseman et al. also found that the number average molecular weight (M_n) and the polydispersity index (M_w/M_n) of the grafted PS are almost equal to the values of free polymer in solution. Nitroxide-mediated polymerization was also used by several other groups for the formation of PS brushes from TEMPO-functionalized silicon wafers or glass slides,[158–163] magnetite[164–166] or titanium[166,167] nanoparticles, steel,[168] Merrifield resins,[169] carbon,[168] and carbon MWNTs.[170,171] In addition, several other polymer brushes, such as poly(3-vinylpyridine) (P3VP),[165,166] poly(4-vinylpyridine) (P4VP),[170,171] PSS(Na),[170] and poly(4-(poly(ethylene glycol) methyl ether)styrene) (PSPEG) brushes,[162] have been successfully prepared via SI-NMP from TEMPO-modified substrates.

A drawback of TEMPO-mediated polymerization is that its utility is essentially limited to styrenic monomers. NMP has been found to yield acrylic polymers with low M_n and relatively high polydispersities compared to those of polymers prepared from styrenic monomers.[153,172] Especially with acrylic and methacrylic monomers, chain growth and reversible deactivation compete with β-H elimination of the growing polymer chain.[173] Studies were conducted in order to find a more universal alkoxyamine initiator as an alternative to TEMPO-based systems.[174,175] First, an acyclic β-phosphonylated nitroxide, *N-tert*-butyl-*N*-[1-diethylphosphono-(2,2-dimethylpropyl)] nitroxide (DEPN), was identified as a good candidate for NMP of acrylic and styrenic monomers. However, a slightly higher percentage of termination reactions was observed for DEPN-mediated polymerizations of styrenic monomers compared to TEMPO-mediated polymerizations.[176,177] Parvole et al. developed a strategy to grow poly(*n*-butyl acrylate) (PBA) and poly(ethyl acrylate) (PEA) brushes from azo-grafted surfaces by adding DEPN, which acts as a chain growth moderator (so-called bimolecular polymerization system).[178–180] Instead of using a conventional free radical initiator-modified substrate, DEPN-mediated polymerizations can also be carried out using surface-immobilized DEPN. This strategy has been used for the preparation of PS,[177,181–186] PBA,[181,185,187–189] and poly(2-(dimethylamino)ethyl acrylate) (PDMAEA) brushes.[185] Another alternative to prepare styrenic, acrylic, or acrylamide- or acrylonitrile-based polymer brushes involves the use of α-hydrido nitroxide, which was identified to yield well controlled bulk polymerizations.[175] These α-hydrido nitroxide compounds were successfully used as a free initiator to moderate the SI-NMP from TEMPO-functionalized surfaces[190,191] or from α-hydrido nitroxide-functionalized surfaces.[192–195]

In conclusion, SI-NMP represents a valuable method for the controlled fabrication of polymer brushes. An advantage of SI-NMP is that no further catalysts are required. This obviates the need for additional purification steps and reduces the chance to introduce impurities, which is advantageous, especially for sensitive applications, e.g. in the electronic and biomedical sector. The relatively high polymerization

Scheme 4. Preparation of PS-*b*-PMMA Brushes by SI-PIMP from a Benzyl-*N*,*N*-diethyldithiocarbamate-Derivatized Silicon Substrate[207]

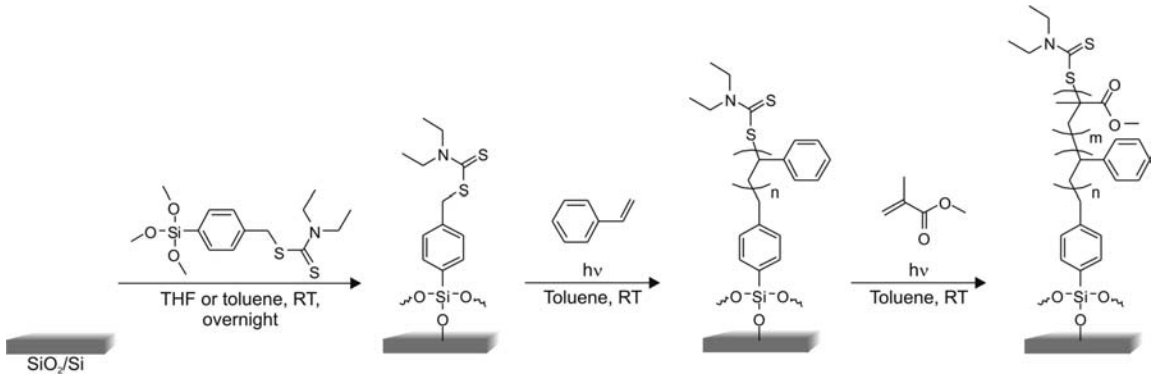

temperatures, however, may cause problems when thermally sensible monomers are used. Another drawback of NMP is that controlled polymerization requires judicious choice of the mediating nitroxide for a particular monomer. This is further hampered by the fact that many mediating radicals are not commercially available and need to be prepared, which requires an additional synthetic effort.

2.1.4. Surface-Initiated Photoiniferter-Mediated Polymerization (SI-PIMP)

The concept of iniferter-mediated polymerization, which is based on the use of a special class of nonconventional initiators (named iniferters), was proposed by Otsu et al. in 1982.[196,197] Iniferters are molecules that can simultaneously act as *ini*tiators, trans*fer* agents, and *ter*minators. The controlled nature of the polymerization relies on the photolytic dissociation of the photoiniferter molecule into a reactive carbon-centered radical and a relatively stable dithiocarbamyl radical. While the carbon-centered radical readily undergoes addition of monomer units to *ini*tiate chain propagation, the persistent dithiocarbamyl radical does not participate in initiation but acts as a trans*fer* agent and induces reversible *ter*mination of the growing polymer chain (*iniferter*).[198] In the absence of termination or transfer reactions, the polymerization proceeds only during irradiation of light and via a predominantly controlled radical polymerization mechanism, which is based on reversible termination. Since the concentration of radicals, and therefore the rate of polymerization, is directly related to the intensity of irradiating light, surface-initiated photoiniferter-mediated polymerization (SI-PIMP) is spatially and temporally coupled to the location, intensity, and duration of UV irradiation.[199,200]

Otsu et al. reported the first example of SI-PIMP, which involved the use of a photoiniferter (dithiocarbamate derivative)-functionalized PS gel for the preparation of various surface-attached di- and triblock copolymers.[201] Matsuda and co-workers extensively used SI-PIMP to prepare a wide variety of polymer brushes from benzyl-*N*,*N*-diethyldithiocarbamate-functionalized substrates. Among others, PDMAM, poly(acrylic acid) (PAA), poly(*N*-isopropyl acrylamide) (PNIPAM), PCMS, poly(poly(ethylene glycol) methacrylate) (PPEGMA), poly(sodium methacrylate) (PMAA-(Na)), and poly(methacrylic acid) (PMAA) brushes were prepared via this strategy.[202–206] De Boer et al. used a trimethoxysilane-modified benzyl-*N*,*N*-diethyldithiocarbamate derivative to modify the surface of silicon substrates and grow PS brushes (Scheme 4). These authors reported the successful preparation of up to 100-nm-thick PS brushes within 15 h of irradiation with 365 nm UV light.[207]

The fact that SI-PIMP is usually carried out without additional "free" deactivating species has led to a controversial discussion about the controlled nature of this technique, since the concentration of the deactivating dithiocarbamyl radicals is considered not to be sufficient to effectively convert propagating polymer chains to the corresponding dormant species. To study the living nature of this polymerization technique, several groups have performed kinetic studies.[200,207–209] Studies of the SI-PIMP of methyl methacrylate performed by Rahane et al. indicated a pseudoliving behavior due to irreversible termination reactions, leading to the loss of surface free radicals, with increasing exposure time. The nonlinear growth of the PMMA brushes as a function of irradiation time was mainly attributed to bimolecular termination reactions, rather than chain transfer to monomer.[209] To circumvent irreversible termination reactions, Luo et al. as well as Rahane et al. reported a strategy to increase the amount of deactivating species, which are mandatory to provide a controlled radical polymerization behavior, by adding tetraethylthiuram disulfide to the polymerization mixture as a source of deactivating dithiocarbamyl radicals.[210,211]

The limitations of SI-PIMP are related to the fact that only photostabile surfaces and monomers can be used. Gold is a very challenging substrate, since exposure to UV light leads to the deterioration of the initiator (here the iniferter) SAMs.[207] However, recently, Vancso and co-workers successfully prepared PNIPAM[212] and PMAA[213,214] brushes from benzyl-*N*,*N*-diethyldithiocarbamate-modified gold substrates by means of a UV lamp emitting at 300 nm coupled with a 280 nm cutoff filter. Furthermore, SI-PIMP requires surfaces that are readily accessible for UV exposure. For instance, microchannels, tubes, or small cavities are difficult to modify, since these substrates are difficult to irradiate and an inhomogeneous distribution of light intensity might cause inhomogeneous brush growth. On the other hand, SI-PIMP provides a versatile route to 2D- and 3D-microstructured polymer brushes without being particularly limited to special types of monomers. Furthermore, SI-PIMP does not require the removal of polymerization catalyst and is therefore especially suitable for the preparation of material surfaces for biomedical or electronic applications.

2.2. Control of Architecture

In addition to allowing relatively accurate control over brush thickness, the use of surface-initiated controlled radical polymerization (SI-CRP) also enables control and variation of the architecture of polymer brushes. SI-CRP has been

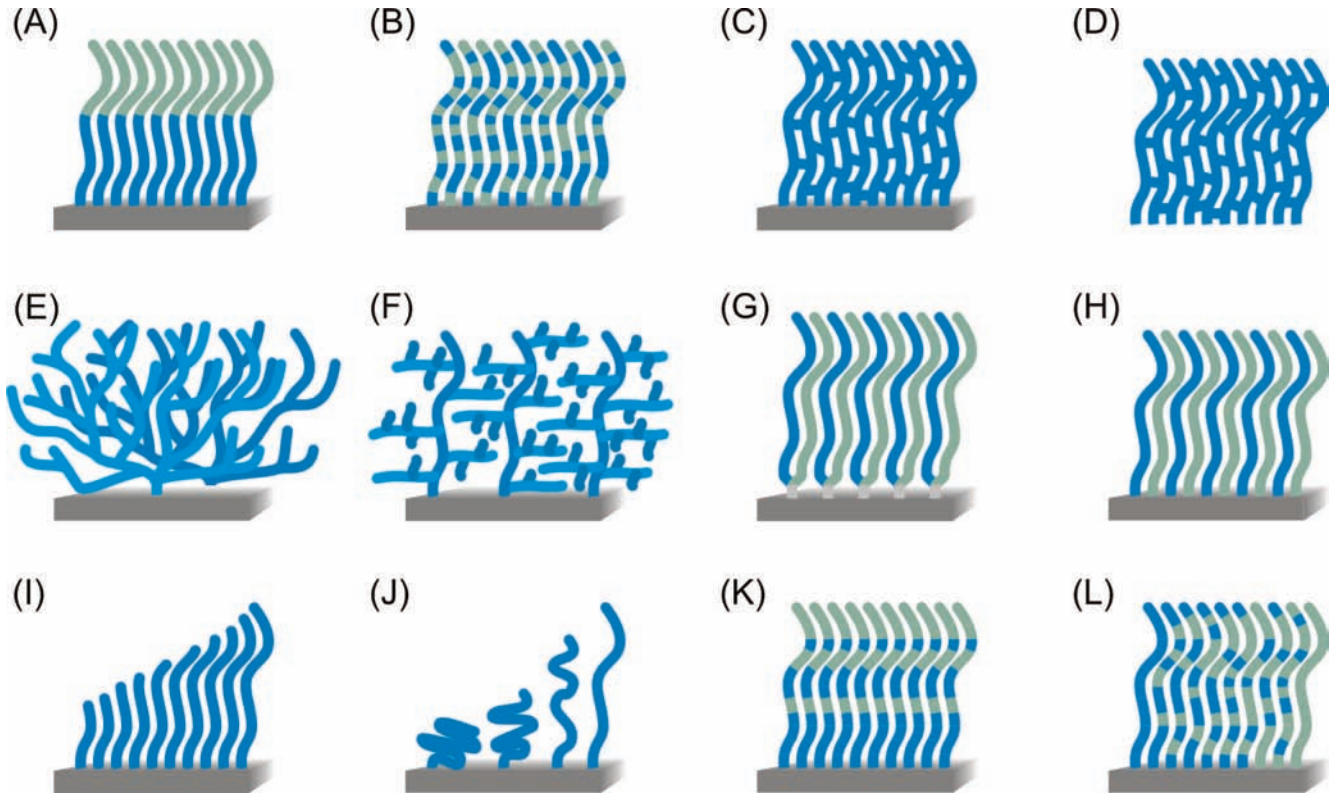

Figure 2. Overview of different polymer brush architectures that can be prepared via surface-initiated controlled radical polymerization. (A) block copolymer brushes (section 2.2.1); (B) random copolymer brushes (section 2.2.2); (C) cross-linked polymer brushes (section 2.2.5); (D) free-standing polymer brushes (section 2.2.6); (E) hyperbranched polymer brushes (section 2.2.4); (F) highly branched polymer brushes (section 2.2.4); (G) Y-shaped binary mixed polymer brushes (section 2.2.3); (H) standard binary mixed brushes (section 2.2.3); (I) molecular weight gradient polymer brushes (section 2.2.7); (J) grafting density gradient polymer brushes (section 2.2.7); (K, L) chemical composition gradient polymer brushes (section 2.2.7).

successfully used to prepare block and random copolymer brushes as well as gradient brushes. Furthermore, binary brushes, various branched polymer brush architectures, as well as cross-linked and free-standing brushes have also been produced using SI-CRP. All of these different architectures will be discussed in this section. Finally, this section will also discuss the different strategies that have been developed to vary and control the initiator surface concentration and consequently the grafting density of the tethered polymer chains.

2.2.1. Block Copolymer Brushes

After homopolymer brushes, SI-CRP techniques have been mostly used to prepare block copolymer brushes (Figure 2A). These are usually synthesized either to confirm the livingness of the SI-CRP or to prepare nanostructured phase-separated thin films (see section 4.1). Table 2 gives an overview of the different types of diblock copolymer brushes that have been prepared so far. In addition to the nature of the first, surface-tethered, and second blocks, Table 2 also indicates for each diblock copolymer brush the SI-CRP technique(s) that have been used.

The first diblock copolymer brush synthesized via SI-CRP was reported by Otsu et al. in 1986.[201] In their work, the authors used a cleavable photoiniferter immobilized on a PS gel to prepare surface-attached PS-*b*-PMMA diblock copolymers. Nakayama and Matsuda later reported the successful formation of PDMAM-*b*-PS, PDMAM-*b*-PAA, PDMAPAM-*b*-PDMAM, and PDMAM-*b*-PBMA diblock copolymer brushes from dithiocarbamated PS films via sequential SI-PIMP of the corresponding monomers.[215] In 1999, Husseman et al. and Matyjaszewski et al. prepared block copolymer brushes using other SI-CRP strategies.[84,156] Husseman et al. reported a PS-*b*-(PS-*co*-PMMA) block copolymer brush grown from TEMPO-functionalized silicon substrates via nitroxide-mediated polymerization,[156] whereas Matyjaszewski et al. reported the successful synthesis of PS-*b*-poly(methyl acrylate) and PS-*b*-P*t*BA diblock copolymer brushes from 2-bromoisobutyrate-derivatized silicon wafers via SI-ATRP.[84] Later, Baum and Brittain used SI-RAFT to prepare PS-*b*-PDMAM and PDMAM-*b*-PMMA diblock copolymer brushes from azo-functionalized silicon wafers in the presence of 2-phenylprop-2-yl dithiobenzoate as chain transfer agent.[117]

In addition to diblock copolymer brushes, SI-CRP has also been used to prepare triblock copolymer brushes. In their seminal paper, Otsu et al. already reported the synthesis of surface-attached PS-*b*-PMMA-*b*-PS, PS-*b*-poly(*p*-chlorostyrene)-*b*-PMMA, and PS-*b*-PMMA-*b*-PMA triblock copolymers via SI-PIMP.[201] Nakayama et al. used SI-PIMP to produce PDMAPAM-*b*-PS-*b*-PDMAPAM triblock copolymer brushes.[200] SI-ATRP has been used to grow PS-*b*-PMA-*b*-PS,[216] PMA-*b*-PS-*b*-PMA,[216] PMA-*b*-PMMA-*b*-PHEMA,[217,218] or PMMA-*b*-PDMAEMA-*b*-PMMA brushes.[218] Triblock copolymer brushes comprising two oppositely charged polyelectrolyte blocks, PMETAC-*b*-PMMA-*b*-PMAA(Na), were successfully prepared via SI-ATRP by Osborne et al.[110] Genzer and co-workers critically investigated the feasibility of SI-ATRP to produce multiblock copolymer brushes and reported the successful preparation of multiblock copolymer brushes composed of up to three (PMMA-*b*-PHEMA) or (PMMA-*b*-PDMAEMA) se-

Table 2. Overview of Diblock Copolymer Brushes Prepared by Surface-Initiated Controlled Radical Polymerization(s)

	Second block									
First block	Poly(methacrylate)		Poly(acrylate)		Poly(acrylamide)		Poly(styrene)		Poly(vinylpyridine)	
Poly(methacrylate)										
PAHMA	PMMA	ATRP[626]								
PBMA	PDMAEMA	ATRP[286,287,736]								
PBzMA							PS	ATRP[672]		
PCDMA	PMMA	ATRP[740]								
PDMAEMA	PGMA	ATRP[338]					PPFS	ATRP[439]		
	PHEMA	ATRP[361,750]					PS	ATRP[494]		
	PMMA	ATRP[360]						RAFT[481]		
	PPEGMA	ATRP[388]								
	P*t*BMA	ATRP[608]								
PEMOMA	PMMA	ATRP[264]								
PGMA	PPEGMA	RAFT[125]					PPFS	ATRP[257]		
PHEMA	PDMAEMA	ATRP[88,361] RAFT[143]	PMA	ATRP[769]	PNIPAM	ATRP[328]				
	PMMA	ATRP[284,288,289]								
	PPEGMA	ATRP[508]								
	PTFEMA	ATRP[516]								
PMAA					PNIPAM	PIMP[681]				
PMAA(Na)	PHEMA	ATRP[111]								
PMMA	PBzMA-*co*-PMMA	ATRP[487]	PBA	ATRP[785]	PAM	ATRP[505,784]	PS	RAFT[122,139,144]	P4VP	ATRP[798]
	PCDMA	ATRP[740]	PMA	RAFT[144]	PNIPAM	RATRP[401]		PIMP[211,407]		
	PDMAEMA	RAFT[120,122,143] ATRP[218,360,397,482,507,744]						ATRP[444]		
	PGMA	ATRP[338,482,672,758]								
	PHEMA	ATRP[87,744,761]								
	PMMA	ATRP[758]								
	PTFEMA	ATRP[397]								
PMPC	PDMAEMA	ATRP[751]								
	PGMA	ATRP[621]								
	PMPC	ATRP[751]								
PPEGMA	PDMAEMA	ATRP[388,495]			PNIPAM	ATRP[234]	PSS(Na)	ATRP[351]		
	PGMA	RAFT[125]								
	PHEMA	ATRP[486,508]								
	PMMA	ATRP[369]								
	PTFEMA	ATRP[760]								
PPEGMEMA	PDMAEMA	ATRP[507] RAFT[120]					PS	ATRP[494]		
	POMA	PIMP[210]								
	PTFEMA	ATRP[543]								
PSBMA							PSS(Na)	RAFT[119]		
PTFEMA	PHEMA	ATRP[516]								
	PMMA	ATRP[397,799]								
Poly(acrylate)										
PAA							PS	NMP[647]		
PBA	PDMAEMA	NMP[185]	PMA	RAFT[144]			PS	RAFT[127]		
	PMMA	ATRP[785]	P*t*BA	ATRP[833]				ARGET[102] NMP[181,341]		
PEA							PS	ATRP[476]		

Table 2. Continued

First block	Second block: Poly(methacrylate)		Poly(acrylate)		Poly(acrylamide)		Poly(styrene)		Poly(vinylpyridine)	
PMA	PDMAEMA	ATRP/RAFT[668]	PBA	RAFT[144]			PPFS	ATRP[667]		
	PHEMA	ATRP[472]	PCPPUA	ATRP[473]			PS	ATRP[216,471]		
			PHDFDA	ATRP[667]						
			PPFPA	ATRP[667,839]						
			P*t*BA	ATRP[608,838]						
			PTFEA	ATRP[667]						
P*t*BA			PMA	NMP[195]			PS	RAFT[549]	P2VP	ATRP[106,882]
									P4VP	ATRP[106]
Poly(acrylamide)										
PAM	PHEMA	ATRP[781]								
	PMMA	ATRP[784]								
PDMAM	PBMA	PIMP[215]	PAA	PIMP[215]	PMEAM	ATRP[538]				
	PGMA	RAFT[763]			PNIPAM	ATRP[538]				
	PHEMA	ATRP[486]								
	PMMA	RAFT[117]								
PDMAPAM	PMAA	PIMP[200]			PDMAM	PIMP[215]	PS	PIMP[200]		
PMEAM					PDMAM	ATRP[538]				
					PNIPAM	ATRP[538,540]				
PNIPAM	PGMA	PIMP[631]			PAGA	RAFT[147]			P4VP	ATRP[475]
	PHEMA	ATRP[486]			PDMAM	ATRP[537,538]				
	PPEGMA	ATRP[234]								
Poly(styrene)										
PAS							PS	NMP[169]		
PCMS							PPFS	RAFT[118]		
PFMS							PS	NMP[161]		
PPFS	PDMAEMA	ATRP[439]					PDVB	ATRP[263]		
	PHEMA	ATRP[516]								
	PMMA	ATRP[248]								
PS	PDMAEMA	NMP[185]	PAA	NMP[647]	PAM	ATRP[399]	PFMS	NMP[161]	P4VP	NMP[171]
	PGMA	ATRP[762]		ATRP/RAFT[668]	PDMAM	RAFT[117]	PMS	ATRP[514]		
	PHEMA	NMP[354]	PBA	ATRP[134,410,785]	PNIPAM	ATRP/RAFT[668]	PPFS	ATRP[667]		
	PMMA	PIMP[207]	PBzA	ATRP[835]		RAFT[141]	PS	ATRP/RAFT[668]		
		RATRP/ATRP[90]	PHDFDA	ATRP[667]				NMP[184]		
		ATRP[262,327,396,444,800]	PMA	ATRP[84,216,770]			PSPEG	NMP[162]		
	PMMA-*co*-PCDMA	ATRP[635]		RAFT[122,134,144]			PS-*co*-PMMA	NMP[156,169]		
	PMMA-*co*-PS	NMP[156,169]	PPFPA	ATRP[667]						
			P*t*BA	ATRP[84,608,719,727,770,838]						
			PTFEA	ATRP[667]						
PSd8			PMA	ATRP[840]						
PSP-*co*-PMMA							PS	ATRP[797]		
PSS(Na)	PHEMA	ATRP[354]								
	PPEGMA	ATRP[351,808]								
Others										
P2VP			P*t*BA	ATRP[634,882]						
P4VP					PNIPAM	ATRP[475]	PS	NMP[874]		
PNVP	PDMAEMA	RAFT[752]								

quences.[219] The authors found that the nature of the surface-attached macroinitiator and the nature of the monomer used for the subsequent block are important parameters that influence the success of the surface-initiated block copolymerization process. While multiblock copolymer brushes composed of PMMA and PHEMA were readily prepared, the synthesis of PMMA-*b*-PDMAEMA brushes proved to be much more difficult. The authors discovered that while chains terminated with PDMAEMA did not reinitiate appreciably to MMA, the chain ends remained intact and would allow further polymerization of DMAEMA.

The importance of the efficiency of the reinitiation step for the synthesis of well-defined (multi)block copolymer brushes was also underlined by Kim et al., who investigated the preparation of surface-tethered triblock copolymers composed of PMA, PMMA, and PHEMA.[217] These authors found that quenching the polymerization after the synthesis of each block with a large excess of $Cu^{II}Br_2$ preserved >95% of the active chain ends. In contrast, when just a simple solvent rinsing step was applied between the synthesis of the different blocks, only 85−90% of the active chains were able to reinitiate polymerization.

2.2.2. Random Copolymer Brushes

Random copolymer brushes (Figure 2B) can be prepared by SI-CRP of a mixture of two or more monomers. Random copolymer brushes have been mainly prepared to tune the properties such as hydrophilicity as well as stimuli-responsiveness (see section 4.1). Table 3 gives an overview of the different binary copolymer brushes that have been produced using SI-CRP. While most random copolymer brushes are composed of linear polymer chains, SI-CRP has also been used to produce branched[202,220–223] and cross-linked[131,194,224–232] polymer brushes.

Due to differences in monomer reactivity, the composition of a copolymer brush is not necessarily identical to the monomer feed. Ignatova et al. have prepared various copolymer brushes either via SI-NMP from TEMPO-functionalized stainless steel substrates or via SI-ATRP from chloropropionated surfaces and used the composition of the free copolymer that is formed in solution as a measure for the composition of copolymer brushes.[191,233] Copolymerization of an equimolar mixture of 2-(dimethylamino)ethyl acrylate (DMAEA) with styrene (S) or butyl acrylate (BA) as comonomers resulted in copolymers with molar compositions of 40:60 and 45:55, respectively, whereas copolymerization of equimolar amounts of 2-(*tert*-butylamino)ethyl methacrylate (*t*BAEMA) and acrylic acid (AA) or styrene (S) afforded copolymers with compositions of 47:53 (*t*BAEMA:AA) and 40:60 (*t*BAEMA:S). Neoh and coworkers used XPS analysis to compare the monomer feed composition to the final surface composition.[234] In their study, the authors showed that a PNIPAM-*co*-PPEGMA copolymer brush containing 1.8 mol % PEGMA was formed from a polymerization solution composed of 1 mol % PEGMA.

2.2.3. Binary Brushes

Binary mixed brushes (Figure 2G and H) are composed of two distinct polymer chains immobilized on a solid substrate with high grafting density.[3] Depending on the specific arrangement of the polymer chains, random, alternating, and gradient binary brushes can be distinguished. Zhao was the first to grow binary mixed brushes via SI-CRP and prepared PMMA/PS binary brushes from mixed self-assembled monolayers (SAMs) of ATRP and NMP initiators.[235] In addition to mixed SAMs, vapor deposition of an ATRP initiator followed by backfilling with an NMP initiator has also been used to form gradient binary mixed PMMA/PS brushes.[236] One possible complication in the synthesis of binary mixed brushes from a surface modified with a mixture of orthogonal initiators is phase separation of the initiators, which can prevent the formation of a truly mixed binary polymer brush. To overcome this problem, Zhao and He synthesized a difunctional ATRP/NMP initiator-functionalized silane (Y-silane), which was subsequently used to prepare mixed binary PMMA/PS brushes.[237] Using this difunctional initiator, the effects of molecular weight on the solvent-induced self-assembly[238] and the changes in surface morphology[239,240] of mixed PMMA/PS brushes were studied. The difunctional Y-silane initiator was also used to graft well-defined P*t*BA/PS mixed brushes from silica nanoparticles.[241,242] Wang and Bohn reported the preparation of gradient mixed PNIPAM/PHEMA brushes.[243] These brushes were prepared via SI-ATRP from SAMs on gold. In a first step, a PNIPAM brush was grown from a spatially uniform initiator SAM. Using electrochemical etching, the PNIPAM brushes were partially removed, following by backfilling with the ATRP initiator and surface-initiated polymerization of PHEMA.

2.2.4. Hyperbranched, Comb-Shaped, and Highly Branched Brushes

In addition to linear brushes, SI-CRP techniques have also been used to prepare architecturally more complex brushes including hyperbranched, comb-shaped, and highly branched polymer brushes.

Hyperbranched polymer brushes (Figure 2E) can be prepared in a one step reaction by self-condensing vinyl polymerization (SCVP)[244] of AB* inimers (*ini*tiator−mono*mer*) from appropriately initiator-modified substrates.[245] Inimers contain both a polymerizable double bond (A) and a group capable of initiating the polymerization of vinyl groups (B*). Mori et al. described the preparation of hyperbranched polymer brushes via atom transfer radical (co)polymerization of the AB* inimers, 2-(2-bromopropionyloxy)ethyl acrylate and 2-(2-bromoisobutyryloxy)ethyl methacrylate, respectively.[220,221,245,246] Other groups have modified halloysite nanotubes via self-condensing atom transfer radical (co)polymerization of 2-(bromoacetyloxy)-ethyl acrylate (BAEA)[223] or chloromethylstyrene (CMS).[247] Xu et al. have prepared hyperbranched PPFS/silicon hybrids by copolymerization of CMS and pentafluorostyrene from ATRP initiator-functionalized silicon substrates.[248] Mu et al. have used a hyperbranched PCMS brush grafted from silica nanoparticles to initiate the subsequent polymerization of MMA.[249]

Comb-shaped polymer brushes can be prepared by first growing a homopolymer brush that contains functional groups in the side chains, followed by modification of the side chains with ATRP initiator groups or photoiniferter moieties and a second polymerization step to graft the arms.[202,222,250–252] For example, ATRP initiating groups were attached to PGMA brushes by reaction of the epoxide moieties with halogenated propionic acid derivatives. These ATRP initiator-modified PGMA brushes were subsequently used to prepare PGMA-*cb*-PNIPAM,[250] PGMA-*cb*-PPEGMEMA,[252] and PGMA-*cb*-PSS(Na) brushes.[252] Along the

Table 3. Overview of Random Copolymer Brushes Prepared by Surface-Initiated Controlled Radical Polymerization

	Monomer 2									
Monomer 1	Methacrylate		Acrylate		Acrylamide		Styrenic		Others	
Methacrylate										
BIEMA	MMA	ATRP[221]								
BMA	DMAEMA	ATRP[272]								
BzMA	EGDMA	ATRP[226]								
	MMA	ATRP[487]								
CDMA	MMA	ATRP[635]								
DHPMA	GMA	ATRP[619,719]								
DMAEMA	BMA	ATRP[272]			NIPAM	ATRP[642]	CMS	PIMP[222]		
	HEMA	ATRP[750]								
	*t*BMA	ATRP[609]								
EGDMA	BzMA	ATRP[226]							4VP	ATRP[364]
	MAA	PIMP[228,229]								RAFT[131]
	MMA	ATRP[231]								
GMA	DHPMA	ATRP[619,719]								
	MMA	ATRP[225]								
	MPC	ATRP[620]								
HEMA	DMAEMA	ATRP[750]					S	NMP[169]		
	MMA	ATRP[271]								
HosMA	MMA	ATRP[770]								
MAA	EGDMA	PIMP[228,229]								
METAC	SPMA(K)	ATRP[712]								
MMA	BIEMA	ATRP[221]					S	ATRP[444]		
	BzMA	ATRP[487]						NMP[156,169,432]		
	CDMA	ATRP[635]					SP	ATRP[797,801,802,814]		
	EGDMA	ATRP[231]								
	GMA	ATRP[225]								
	HEMA	ATRP[271]								
	HosMA	ATRP[770]								
	PeMMA	ATRP[655]								
MPC	GMA	ATRP[620]								
PEGDMA	PEGMA	PIMP[230]								
PEGMA	PEGDMA	PIMP[230]			NIPAM	ATRP[234]				
	PEGMEMA	ATRP[307,552]								
PEGMEMA	PEGMA	ATRP[307,552]			NIPAM	ATRP[422]				
	*t*BAEMA	ATRP[233]								
PeMMA	MMA	ATRP[655]								
SPMA(K)	METAC	ATRP[712]								
*t*BAEMA	PEGMEMA	ATRP[233]	AA	ATRP[233]			S	ATRP[233]		
*t*BMA	DMAEMA	ATRP[609]								
Acrylate										
AA					AM	PIMP[523]	S	RAFT[134]		
					NIPAM	ATRP[690]				
						PIMP[490]				
AAb			PEGA	PIMP[718]						
AA(Na)					NIPAM	ATRP[654]				
BA			BAEA	ATRP[223]						
			DMAEA	NMP[191]						
BAEA			BA	ATRP[223]						
BPEA			*t*BA	ATRP[220,221]						
DMAEA			BA	NMP[191]			S	NMP[191]		
EGDA					NIPAM	ATRP[224]				
MA							S	RAFT[134]		
PEGA			AAb	PIMP[718]						
			PEGASF	PIMP[524]						
PEGASF			PEGA	PIMP[524]						
*t*BA			BPEA	ATRP[220,221]						
Acrylamide										
AM			AA	PIMP[523]	MBAM	ATRP[232]				
					N-BocAHAM	ATRP[578]				
DMAM							CMS	PIMP[202,222]		
MBAM					AM	ATRP[232]				
					NIPAM	ATRP[227,363,424]				
N-BocAHAM					AM	ATRP[578]				
NIPAM	DMAEMA	ATRP[642]	AA	ATRP[690]	MBAM	ATRP[227,363,424]			NVI	ATRP[650]
	PEGMA	ATRP[234]		PIMP[490]						
	PEGMEMA	ATRP[422]	AA(Na)	ATRP[654]						
			EGDA	ATRP[224]						
Styrenic										
CMS	DMAEMA	PIMP[222]			DMAM	PIMP[202,222]				
GL							S	ATRP[467]		
S	HEMA	NMP[169]	AA	RAFT[134]			SLS	ATRP[627]	AN	ATRP[443,871]
	MMA	ATRP[444]	DMAEA	NMP[191]			GL	ATRP[467]	MAn	RAFT[450]
		NMP[156,169,432]	MA	RAFT[134]						NMP[194]
									TMI	RAFT[547]
									VBCB	NMP[194]
SLS							S	ATRP[627]		
SP	MMA	ATRP[797,801,802,814]								
Others										
4VP	EGDMA	ATRP[364]								
		RAFT[131]								
AN							S	ATRP[443,871]		
MAn							S	RAFT[450]		
								NMP[194]		
NVI					NIPAM	ATRP[650]				
TMI							S	RAFT[547]		
VBCB							S	NMP[194]		

same lines, the hydroxyl groups of PHEMA and PPEGMA brushes have been used to introduce ATRP initiating 2-bromoisobutyrate moieties,[251] and PCMS brushes have been modified with dithiocarbamate derivatives to allow SI-PIMP.[202,222]

The synthetic strategies developed for the preparation of comb-shaped brushes can be readily extended to highly branched or arborescent brushes (Figure 2F) by repetition of the (co)polymerization/postmodification sequence using appropriate functional monomers to act as grafting points. Matsuda and co-workers, for example, prepared highly branched polymer brushes via successive photopolymerization of a CMS-containing monomer(s) mixture, followed by dithiocarbamylation.[202,222] Xu et al. reported the formation of highly branched PPFS brushes via surface-initiated atom transfer radical copolymerization of CMS and pentafluorostyrene from a surface-immobilized difunctional ATRP initiator.[248]

2.2.5. Cross-linked Brushes

Cross-linked polymer brushes (Figure 2C) can be prepared via two main pathways, namely the surface-initiated homo- or copolymerization of bifunctional monomers and the postmodification of polymer brushes with appropriate cross-linking agents. The homopolymerization of ethylene glycol dimethacrylate derivatives via either SI-ATRP[253–255] or SI-PIMP[256] is probably the easiest way to prepare cross-linked polymer brushes. The addition of a cross-linkable comonomer to the polymerization mixture is also widely used for the preparation of cross-linked brushes. Already in 1998, Wirth and co-workers successfully prepared cross-linked polyacrylamide (PAM) brushes on the interior surface of silica capillaries by adding 2% of *N*,*N*′-methylenebisacrylamide (MBAM) to the ATRP polymerization solution.[232] The use of ethylene glycol di(meth)acrylates as comonomers for the preparation of cross-linked brushes has been extensively reported for SI-ATRP,[224,231] SI-RAFT,[131] or SI-PIMP.[228–230]

In addition to the homo- or copolymerization of bifunctional monomers, cross-linked brushes can also be obtained by postmodification of appropriately functional polymer brushes. A widely used strategy is based on the postmodification of linear PGMA brushes with (di)amines such as ethylenediamine,[257] 1,4-phenylenediamine,[258] or octylamine.[225] Edmondson et al. reported the use of methanolic NaOH to induce internal cross-linking via the pendent epoxide groups along the side chain of linear PGMA brushes.[259,260] Loveless et al. showed that P4VP brushes can be reversibly cross-linked by the addition of a bis(Pd^{II}-pincer) compound, which noncovalently coordinates to the vinylpyridine units of the polymer brush.[261]

The preceding paragraphs have outlined two strategies that can be used to deliberately prepare cross-linked polymer brushes. Cross-linking, however, can also occur in a less controlled manner as a result of side reactions during SI-CRP. Huang et al., for example, found that detachment of PHEMA brushes from gold substrates afforded insoluble polymer films.[88] The insolubility of the grafted PHEMA was attributed to intermolecular cross-linking via transesterification. In another report, it was observed that PPEGMA brushes detach in the form of continuous films from silicon substrates upon exposure to cell culture medium, which also suggests that these brushes cross-link during surface-initiated polymerization.[254]

2.2.6. Free-Standing Brushes

In the previous section, various approaches were discussed that can be used to prepare cross-linked polymer brushes. If these cross-linked brushes are prepared on substrates that can be dissolved or sacrificed, then this provides opportunities to produce free-standing 2D polymer films (Figure 2D) as well as polymer hollow spheres or tubes. This section will give an overview of different free-standing brushes, either in the form of 2D films or hollow spheres or tubes, that have been prepared following this rationale.

Huck and co-workers described the preparation of quasi-2D polymer films by delaminating cross-linked PGMA brushes grown from ATRP initiator-functionalized gold substrates upon electrolysis.[259] The same group studied the buckling process in these patterned quasi-2D films by locally applying a short electrolysis pulse to cleave the gold−sulfur bond, which tethers the film to the gold substrate.[260]

Hollow polymeric nanospheres have been prepared by HF etching of silica nanoparticles coated with a cross-linked polymer shell. Mandal et al. grafted PBzMA-*co*-PEGDMA brushes via SI-ATRP from SiO_2 particles to obtain hollow polymer particles after HF etching of the sacrificial silica cores.[226] Other methods to create such architectures are based on postmodification of linear polymer brushes to produce cross-linked shells, either via internal ring-opening reaction of moieties along the polymer brush, addition of a cross-linker, or UV irradiation. Hawker and co-workers, for example, prepared random PS-*co*-PVBCB and PS-*co*-PMAn copolymer brushes via NMP from silica nanoparticles. In their study, they used the cyclobutene groups of PVBCB chains as thermal cross-linking agent or a diamine cross-linker to react with PMAn groups.[194] Fu et al. prepared cross-linked hollow nanospheres via SI-ATRP.[262,263] PS-*b*-PMMA coated silica nanoparticles were irradiated with UV to induce decomposition of the PMMA outer shell and cross-linking of the PS shell. After HF treatment of the core, well-defined hollow nanospheres were obtained.[262] A related strategy was used by the same authors to prepare thin films of agglomerated and cross-linked hollow polymer nanospheres.[263] To this end, PPFS-*b*-PDVB block copolymer brushes were grown from silica nanoparticles using SI-ATRP. UV irradiation of the block copolymer-modified nanoparticles leads to inter- and intramolecular cross-linking of the residual double bonds in the PDVB layer, which simultaneously covalently stabilizes the PDVB shell of the particles and connects the individual particles to form a continuous film. Removal of the silica core with HF afforded a porous fluoropolymer film. Recently, Morinaga reported another strategy to prepare hollow nanospheres. The PEMO layer of PEMO-*b*-PMMA grafted silica particles was internally cross-linked by cationic ring-opening reaction of the oxetane groups catalyzed with boron trifluoride diethyl etherate, followed by HF etching to remove the silica core.[264]

The strategies discussed above can be easily extended to the preparation of polymeric nanotubes when porous membranes or nanowires instead of nano- or microparticles are used as sacrificial substrates. Cui et al. reported the formation of PNIPAM-*co*-PMBAM copolymer nanotubes by growing the corresponding polymer brushes within a anodic aluminum oxide (AAO) membrane by SI-ATRP followed by the dissolution of the AAO membrane in 1 M NaOH solution.[227]

2.2.7. Gradient Brushes

Gradient brushes are brushes wherein one or more physicochemical properties vary continuously along the substrate.[265–270] Gradient brushes prepared via SI-CRP can be subdivided into four groups; chemical composition gradient brushes (Figure 2K and L), grafting density gradient brushes (Figure 2J), molecular weight gradient brushes (Figure 2I), or brushes prepared by a combination of several gradient architectures.[266]

Xu et al. prepared PMMA/PHEMA gradient copolymer brushes via SI-ATRP by gradually adding an ATRP solution of HEMA to the MMA polymerization mixture.[271] Instead of creating chemical composition gradients parallel to the substrate, polymer brushes can also be prepared that have a composition gradient perpendicular to the substrate. Such composition gradient brushes have been reported by Beers and co-workers, who prepared PBMA/PDMAEMA composition gradient brushes via SI-ATRP from silicon substrates by using a microchannel filled with a solution gradient of both monomers.[272]

Grafting density gradient polymer brushes can be obtained by SI-CRP from substrates covered with a surface concentration gradient of polymerization initiators, iniferters, or chain transfer agents, which can be prepared using various strategies. Wu et al. prepared gradient initiating layers by means of the methodology developed by Chaudhury and Whitesides.[273] Briefly, an initiator concentration gradient along the substrate was generated by vapor diffusion of a 1-trichlorosilyl-2-(*m*/*p*-chloromethylphenyl)ethane/paraffin oil mixture followed by backfilling with *n*-octyl trichlorosilane (OTS).[274,275] This initiator gradient layer was subsequently used to graft PAM brushes via SI-ATRP following the conditions reported by Huang and Wirth.[82] Instead of first generating an initiating gradient layer followed by backfilling with an ATRP inactive silane, grafting density gradient brushes can also be prepared by first forming a gradient of inactive silane followed by backfilling with an ATRP initiator. This strategy has been used to produce density gradient P*t*BA brushes.[276] Based on the strategy of Wu et al., Zhao developed a method to prepare grafting density gradients of two chemically different polymer brushes propagating in opposite directions by vapor deposition of an ATRP initiator onto the substrate and then backfilling with a NMP initiator. The resulting gradient mixed initiator SAM was subsequently used for the preparation of density gradient binary mixed PMMA/PS brushes.[236] In addition to vapor deposition, there are various other strategies to generate substrates covered with an initiator density gradient layer. Liu et al. used a linear temperature gradient stage to generate a gradual variation in the thickness of a dip-coated PGMA layer, which was then proportionally derivatized with 2-bromo-2-methylpropionic acid followed by the ATRP of styrene.[277] Washburn and co-workers produced initiator gradient films by means of gradual addition of ATRP initiator to a test tube containing an OTS-modified silicon wafer and then grew PHEMA brushes.[278] Wang et al. used an electrochemical gradient to selectively desorb hexadecanethiol from a gold substrate followed by backfilling of the free areas with an ATRP initiator from which PNIPAM brushes were successively grown.[279] Wang and Bohn further described the preparation of density gradient binary mixed PNIPAM/PHEMA brushes where the grafting density of each polymer varies in opposite directions along the substrate.[243] Their strategy involved a gradual chemical etching of PNIPAM brushes grown from uniform ATRP initiator SAM on gold followed by backfilling of the etched surface sites with fresh ATRP initiator for the subsequent surface-initiated polymerization of HEMA.

Molecular weight (i.e., thickness) gradient brushes have been prepared using both SI-PIMP and SI-ATRP. Harris et al. described the synthesis of PMMA[280] and PMAA[281] thickness gradient brushes from photoiniferter-modified silicon substrates using a movable photomask, which permits creation of a UV exposure time gradient along the substrate. A similar strategy was followed by Matsuda and co-workers, who used a movable sample stage instead of moving the photomask.[199] The same group also reported on the use of a gradient neutral-density filter to introduce a continuous and unidirectional change of the irradiation intensity during the photopolymerization for the preparation of molecular weight gradient films.[200] PMMA,[282] PAM,[265,283] and PHEMA-*b*-PMMA[284] thickness gradient brushes were successfully prepared via SI-ATRP by continuously and gradually removing the polymerization solution from the chamber containing the ATRP initiator-functionalized substrate ("draining" method) with a μ-pump. Tomlinson et al. used a dipping sample holder that allowed control of the longitudinal position of the ATRP initiator-functionalized substrates in a discrete or semicontinuous manner to prepare "step height", respectively, molecular weight gradient polymer brushes.[219] Beers and co-workers generated PHEMA molecular weight gradient brushes using microchannel-confined SI-ATRP, which allowed them to control the lateral composition of the polymerization mixture.[285] The same group also prepared PDMAEMA-*b*-PBMA block copolymer brush gradients consisting of a uniform PBMA bottom block and a molecular weight gradient PDMAEMA top block by gradually filling the chamber containing the living PBMA brushes coated substrate with the second ATRP solution.[286,287]

By combining some of the methods described above, Genzer and co-workers have prepared orthogonal gradient polymer brushes where physicochemical properties, such as molecular weight and density of a given polymer or molecular weights of two polymers, vary independently in orthogonal directions.[288–291] Such orthogonal gradient brushes are ideal candidates for high-throughput structure−property investigations.

2.2.8. Variation of Brush Density

In the previous section, various strategies have been presented that can be used to cover substrates with a polymer brush density gradient. The control and variation of brush density will be discussed in more detail in this section. In contrast to the previous section, which concentrated on density gradients, the focus here will be on techniques that can be used to homogeneously cover surfaces with a polymer brush coating of controlled density.

The most commonly used method to vary brush density is based on the modification of the substrate from which the brush is grown with a mixture of an initiator-functionalized compound and a "dummy" compound that is not able to initiate the polymerization reaction. This approach has been used for the preparation of PPEGMEMA,[292–294] PMMA,[295] PMETAC,[296] and PGMA[295] brushes from mixed thiol self-assembled monolayers on gold substrates, to grow PNIPAM,[297] PPEGMA,[298] and PDMAEMA[299] brushes from mixed disulfide monolayers on gold, to generate PPEGMA,[254] PMAA(Na),[111] and PHEMA[300] brushes from mixed trimethoxysilane monolayers on silicon wafers, as well as

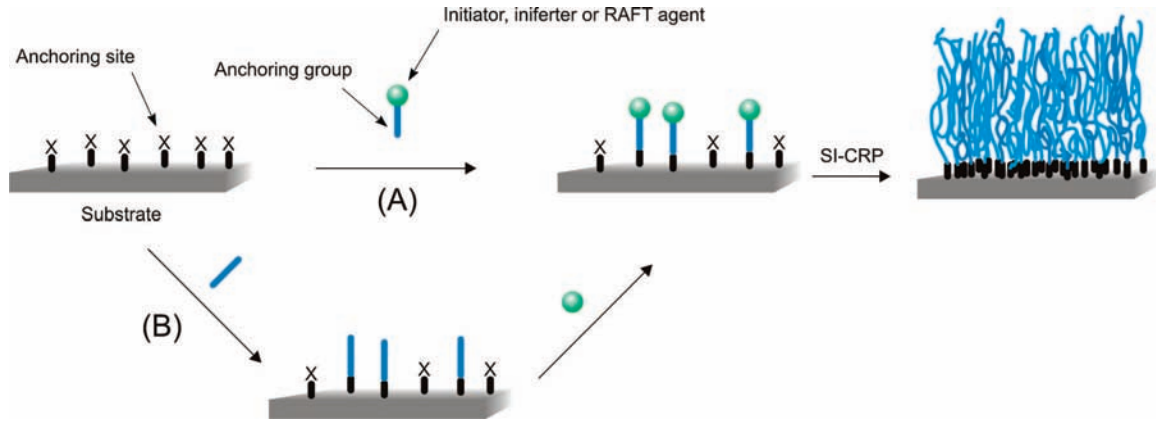

Figure 3. Substrate surface modification with initiator, iniferter, or RAFT agent: (A) one step strategy; (B) multistep strategy.

for the synthesis of PMPC,[301] PNIPAM,[302] PHEMA,[303] and PMMA[303] brushes from mixed trichloro- or monochlorosilane-functionalized silicon substrates. Usually, the initiator functionalized and "dummy" molecules have similar chemical structures and are assumed to have good affinity to the substrate such that the relative amount of both compounds in solution is equal to that on the surface.[304–306] However, XPS studies on mixed trimethoxysilane[111] as well as mixed thiol[294] SAMs have revealed a nonideal behavior when comparing surface and solution compositions.

A second strategy to vary the initiator surface concentration and brush density involves postmodification of a precursor amino-, hydroxyl-, or allyl-terminated SAM with a compound that is able to initiate ATRP. Brown et al., for example, modified substrates with different surface concentrations of ATRP initiating groups by postmodifying the amine groups of a 3-(aminopropyl)trimethoxysilane (APTS) layer with different molar ratios of 2-bromoisobutyryl bromide and propionyl bromide. These mixed-initiator layer-modified substrates were subsequently used to prepare PPEGMA brushes.[307] Bao et al. used mixtures of 2-bromopropionyl bromide and 2-methylpropionyl bromide to derivatize hydroxyl-terminated monolayers on gold, which were then used to grow PMMA and PHEMA brushes.[303] Along the same lines, hydroboration of mixed octadecyltrichlorosilane/15-hexadecenyltrichlorosilane layers has been used to introduce hydroxyl groups that were selectively reacted with 2-bromoisobutyryl bromide and subsequently used for the preparation of PMEMA, PPEGMEMA, PHEMA, PAM, PMMA, and PS brushes with variable grafting densities.[308,309] Statistical UV photodecomposition of the surface-fixed 2-(4-chlorosulfonylphenyl)ethyl trichlorosilane ATRP initiator was used by Yamamoto et al. to control the density of PMMA brushes.[310]

The Langmuir−Blodgett technique provides another tool to modify substrates with a controlled surface concentration of initiator and generate polymer brushes with controlled densities. This method was successfully used to transfer defined monolayers of 2-(4-chlorosulfonylphenyl)ethyl-[83] or nitroxide-functionalized[158,159] alkoxysilanes onto silicon wafers, which were subsequently used to graft PMMA and, respectively, PS brushes.

Kizhakkedathu et al. grafted PDMAM brushes from ATRP initiator-functionalized PS latex particles, which were synthesized with different initiator concentrations by changing the feed ratio of styrene to initiator (2-(methyl-2′-chloropropionato)ethyl acrylate) during the particle preparation.[311] Instead of varying the mole fraction of initiator-modified monomer during particle synthesis, the same group demonstrated that the brush density can also be controlled by careful basic hydrolysis of grafted polymer chains from the latex particles.[312]

Finally, Wu et al. reported an interesting strategy to prepare highly dense PAM brushes on PDMS substrates. Mechanical stretching of the PDMS substrate during both the initiator functionalization step and the following SI-ATRP resulted in a highly dense PAM brush upon relief of the strain.[313]

2.3. Variation of Substrate

SI-CRP techniques have been used to grow polymer brushes from a wide variety of different substrates. In order to graft polymer brushes, the substrate surface needs to be modified with an appropriate initiator, iniferter, or RAFT agent, which can be introduced either in a single step or via a multistep protocol (Figure 3). The one step protocols require the use of molecules that contain the appropriate initiator, iniferter, or RAFT agent as well as functional groups that can react with complementary functional groups on the substrate surface. Alternatively, the substrate surface can be modified with molecules that introduce certain functional groups, which can then be modified with the desired initiator, iniferter, or RAFT agent in a subsequent (series of) reaction(s). The focus of this section will be on the modification of the substrate surface with the initiator, iniferter, or RAFT agent needed for the SI-CRP process. This section consists of eight parts, which will successively discuss the preparation of polymer brushes via SI-CRP from silicon oxide, silicon, metal oxide, clay mineral, gold, metal and semiconductor, carbon, and polymer surfaces. For each of these classes of substrates, the discussion will concentrate on the surface chemistry that is available to introduce functional groups that allow SI-CRP.

2.3.1. Polymer Brushes Grafted from Silicon Oxide

Among the different substrates that have been used to produce polymer brushes via SI-CRP, silicon oxide has been most extensively used. Table 4 provides an overview of the different initiators, iniferters, and RAFT agents that have been used to graft polymer brushes from silicon oxide surfaces. For each example, Table 4 specifies the nature of the anchoring group, the chemical structure of the initiator, iniferter, or RAFT agent, the polymerization technique, as well as the nature and geometry of the substrate surface. Since the focus of this section is on the surface chemistries

Table 4. Overview of Initiators, Iniferters, and RAFT Agents That Have Been Used To Grow Polymer Brushes from Silicon Oxide Surfaces

Anchoring group	Initiator/iniferter/RAFT agent	Immobilization protocol: Single step	Immobilization protocol: Multi step	SI-CRP technique	Substrate and substrate geometry	Ref
	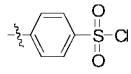	×		ATRP	Oxidized silicon wafer (planar)	310,570
		×		ATRP	SiO_2 layer deposited onto Au (planar)	310
		×		ATRP	SiO_2 layer deposited onto Al (planar)	796
		×		ATRP	Quartz (planar)	655
		×		ATRP	Glass filter (porous; pore diameter: 5 μm)	792
	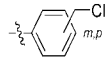	×		ATRP	Oxidized silicon wafer (planar)	232,267,274,552,847,848
		×		ATRP	Glass slide (planar)	674
		×		ATRP	Fused silica capillary (inner diameter: 50 μm)	232,674
		×		ATRP	Silica nanoparticle	850,857
		×		ATRP	Porous silica microparticle	82,302,642,676,848,855
		×		ATRP	Opal film (porous; pore diameter: 16 nm)	850
			×	ATRP	Oxidized silicon wafer (planar)	309,781
		×		ATRP	Oxidized silicon wafer (planar)	84,106,156,216,219,221,225,235,236,271,276,278,282-291,301,307,567,594,603,604,608,615,634,635,644,654,667669,684,686,689,693,709,741,743,751,769,784,797,799,801,809,813,837, 838,840
		×		ATRP	Glass slide (planar)	290,567,594,743,837
		×		ATRP	Silicon ATR crystal (planar)	216,667,838,839
		×		ATRP	Quartz (planar)	802
		×		ATRP	Fused silica capillary (inner diam.: 100 μm)	726
		×		ATRP	Fused silica capillary (inner diam.: 75 μm)	770
		×		ATRP	Glass filter (porous; pore diameter: 2-20 μm)	839
		×		ATRP	Silica nanoparticle	220,801,802,811
		×		ATRP	Silica microparticle	797
		×		ATRP	Silica microparticle (nanoporous)	721-723
		×		ATRP	Etched silicon wafer (pore diameter: 50 nm)	346
		×		ATRP	Oxidized silicon AFM tip (complex geometry)	666
		×		ATRP	Silica nanoparticle	886
	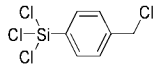	×		ATRP	Silica nanoparticle	262,263,876
		×		ATRP	Au/SiO_2 Core/shell spherical colloids	887
	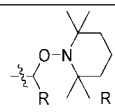 R = Me or Ph	×		NMP	Oxidized silicon wafer (planar)	156,161,162,190,236
	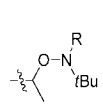 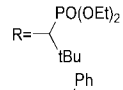	×		NMP	Silica nanoparticle	181,188,886
	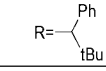	×		NMP	Silica nanoparticle	194
	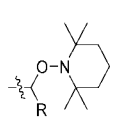 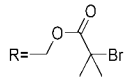	×		NMP/ATRP (bifunctional)	Oxidized silicon wafer (planar)	237,238,240
	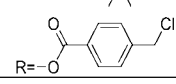	×		NMP/ROP (bifunctional)	Oxidized silicon wafer (planar)	329
	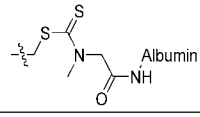		×	PIMP	Glass slide (planar)	206
	 R=−Me		×	RAFT	Oxidized silicon wafer (planar)	122
	R=−H		×	RAFT	Silica nanoparticle	131
	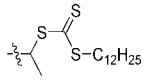		×	RAFT	Silica nanoparticle	888

Table 4. Continued

Anchoring group	Initiator/iniferter/RAFT agent	Immobilization protocol: Single step	Immobilization protocol: Multi step	SI-CRP technique	Substrate and substrate geometry	Ref
	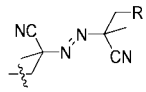 R=−H	×		Reverse ATRP	Oxidized silicon wafer (planar)	90
		×		Bimolecular RAFT	Oxidized silicon wafer (planar)	117
		×		Bimolecular RAFT	Silicon ATR crystal (planar)	117
		×		Bimolecular NMP	Oxidized silicon wafer (planar)	178
	R=-~-	×		Bimolecular NMP	Silica nanoparticle	179,886
	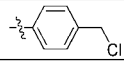		×	ATRP	Oxidized silicon wafer (planar)	732
		×		ATRP	Porous silica microparticle	226
		×		ATRP	Oxidized silicon wafer (planar)	625,734,735,779
		×		ATRP	Quartz (planar)	779
		×		ATRP	Silica nanoparticle	264,788,789,795,800
		×		ATRP	Si/SiO_2 core/shell nanowire	755
		×		ATRP	Porous silica monoliths (pore diameter: 50 and 80 nm)	767
			×	ATRP	Oxidized silicon wafer (planar)	566,628,776
			×	ATRP	Silica nanoparticle	98,683,740,853,869
			×	ATRP	Quartz (planar)	623
			×	ATRP	Fe_3O_4/SiO_2 core/shell nanoparticle	877
			×	ATRP	Silica nanoparticle	765,841,879
			×	ATRP	Oxidized silicon wafer (planar)	739
			×	ATRP	Silica nanoparticle	249
			×	ATRP	Silica nanoparticle	737,738,864,866
	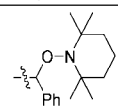		×	NMP	Mesoporous silica nanoparticle (size: 600nm; pore diameter 2.6 nm)	872
		×		NMP	Oxidized silicon wafer (planar)	158,873
		×		NMP	Oxidized Si_3N_4 AFM tip	159
	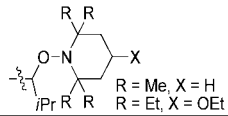 R = Me, X = H R = Et, X = OEt	×		NMP	Oxidized silicon wafer (planar)	163
	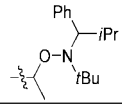	×		NMP	Oxidized silicon wafer (planar)	873
	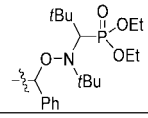	×		NMP	Oxidized silicon wafer (planar)	873
		×		NMP	Silica nanoparticle	177,182,184
	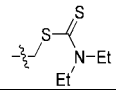		×	PIMP	Silica nanoparticle	803,875
	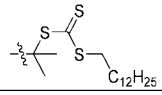		×	RAFT	Mesoporous silica nanoparticle (size: 100 nm; pore diameter: 2 nm)	129
			×	RAFT	Oxidized silicon wafer (planar)	123
	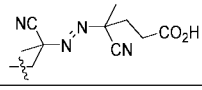		×	Bimolecular RAFT	Porous silica microparticle	756
	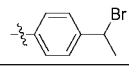		×	ATRP	Oxidized silicon wafer (planar)	326,327
	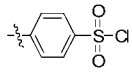	×		ATRP	Oxidized silicon wafer (planar)	83,591,624
		×		ATRP	Glass membrane (pore diameter: 500 nm)	622
		×		ATRP	Oxidized silicon wafer (planar)	632
		×		ATRP	Glass slide (planar)	632
		×		ATRP	Silica nanoparticle	627,777
			×	ATRP	Oxidized silicon wafer (nanostructured)	587

Table 4. Continued

Anchoring group	Initiator/iniferter/RAFT agent	Immobilization protocol: Single step	Immobilization protocol: Multi step	SI-CRP technique	Substrate and substrate geometry	Ref
MeO MeO–Si– MeO (continued)		×		ATRP	Oxidized silicon wafer (planar)	111,254,576,600,729
		×		ATRP	Glass slide (planar)	111,254,576,600, 602,729,817
		×		ATRP	Si/SiO_2 core/shell nanowire	755
			×	ATRP	Oxidized silicon wafer (planar)	307,578,680,690,774,852
			×	ATRP	Glass slide (planar)	578,728
			×	ATRP	Silica nanoparticle	745
	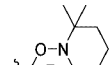 R_1=–H R_2=–Ph	×		NMP	Oxidized silicon wafer (planar)	235,647
	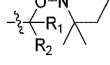 R_1=–Me R_2= 	×		NMP	Oxidized silicon wafer (planar)	354
	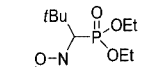 R_1=–H R_2= 		×	NMP	Silica nanoparticle	184
	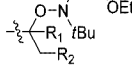 R_1=–Me R_2= 		×	NMP	Silica nanoparticle	187
	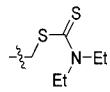	×		PIMP	Oxidized silicon wafer (planar)	207,209,211,280, 281,631,681
			×	PIMP	Porous silica microparticle	229
	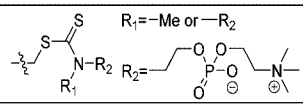 R_1=–Me or –R_2		×	PIMP	Glass slide (planar)	205
		×		RAFT	Oxidized silicon wafer (planar)	125
	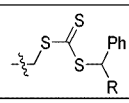 R=–H		×	RAFT	Silica nanoparticle	859
	R=–H and R=–CO_2Me	×		RAFT	Silica nanoparticle	146
	R=–CO_2Me		×	RAFT	Silica nanoparticle	144
	–SH	×		Bimolecular RAFT	Glass slide (planar)	763
MeO Me–Si– MeO			×	ATRP	Oxidized silicon wafer (planar)	328
Me MeO–Si– Me		×		RAFT	Silica nanoparticle	127
Me EtO–Si– Me		×		ATRP	Oxidized silicon wafer (planar)	815
		×		ATRP	Silica nanoparticle	109,759,786,794,805
		×		ATRP	Silsesquioxane microgel nanoparticle	870
		×		ATRP	CdS/SiO_2 core/shell nanoparticle (size: 53 nm)	787
	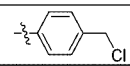	×		ATRP	Silica nanoparticle	863
			×	RAFT	Silica nanoparticle	128,626
Me Si Me			×	ATRP	Oxidized silicon wafer (planar)	331
			×	ATRP	Silicon ATR crystals (planar)	331
Et H–Si– Et		×		ATRP	Oxidized silicon wafer (planar)	330
Me Cl–Si– Me		×		ATRP	Oxidized silicon wafer (planar)	102,303,330,570,575, 577,582,609,611,621, 692,733,758,783
		×		ATRP	Silica nanoparticles	99,687,785,791, 834,835,865,871
		×		ATRP	Silsesquioxane microgel nanoparticle	870
		×		ATRP	Oxidized poly(methylsiloxane) nanofilament	620
		×		ATRP	Porous silica microparticle	793
		×		ATRP	Silica nanoparticle	126
		×		ATRP	Porous silica microparticle	793

Table 4. Continued

Anchoring group	Initiator/iniferter/RAFT agent	Immobilization protocol: Single step	Immobilization protocol: Multi step	SI-CRP technique	Substrate and substrate geometry	Ref
Me Cl—Si— Me (continued)		×		ATRP	Silica nanoparticle	862
		×		ATRP	Oxidized silicon wafer (planar)	867
	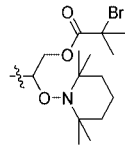	×		ATRP/NMP	Silica nanoparticle	241,242
	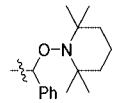	×		NMP	Oxidized silicon wafer (planar)	156,190
	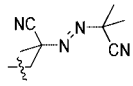	×		Bimolecular NMP	Oxidized silicon wafer (planar)	178
		×		Bimolecular RAFT	Oxidized silicon wafer (planar)	117
		×		Bimolecular RAFT	Silicon ATR crystals (planar)	117
	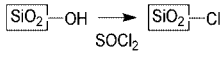	×		ATRP	Porous silica microparticle	339
					Glass slide and oxidized silicon wafer (planar)	338
	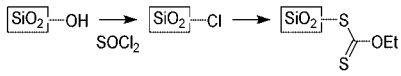		×	RAFT	Oxidized silicon wafer (planar)	340
	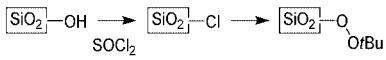		×	Reverse ATRP	Oxidized silicon wafer (planar)	91
			×	Bimolecular NMP	Silica nanoparticle	341
	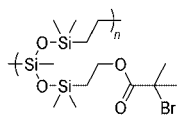			ATRP	Porous silica microparticle	675
	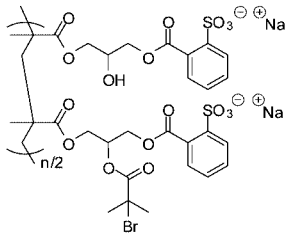	x		ATRP	Oxidized silicon wafer (planar)	343
	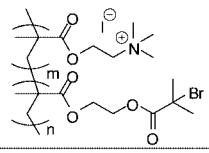	x		ATRP	Silica nanoparticle	342
	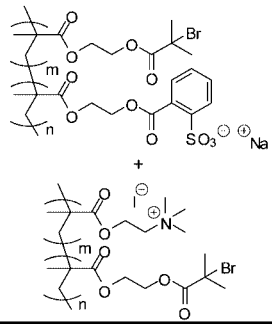		x (LbL[a])	ATRP	Oxidized silicon wafer and glass slide (planar)	345

Table 4. Continued

Anchoring group	Initiator/iniferter/RAFT agent	Immobilization protocol: Single step	Immobilization protocol: Multi step	SI-CRP technique	Substrate and substrate geometry	Ref
	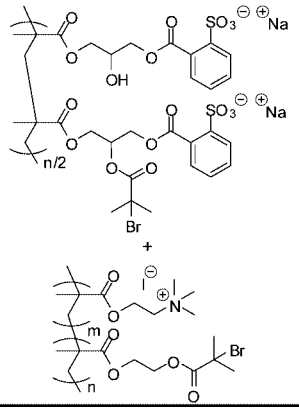		x (LbL[a])	ATRP	Oxidized silicon wafer (planar)	344

[a] LbL: layer-by-layer deposition.

that are available to introduce polymerization active groups and to avoid unnecessary lengthening of the table, the nature of the linker that connects the anchoring group and the initiator, iniferter, or RAFT agent is not specified.

Polymer brushes have been grafted from a wide range of silicon oxide substrates including wafers, glass or quartz slides, porous and nonporous particles, as well as capillaries and membranes. Polymer brushes are also frequently produced from thin silicon oxide layers that have been deposited onto metallic substrates. For the modification of silicon oxide surfaces with initiators, iniferters, or RAFT agents, two general strategies are available, which will be discussed in the following paragraphs. The first strategy, which is most frequently used, is based on the chemisorption (covalent attachment) of organosilane molecules. A second possibility to modify silicon oxide surfaces with functional groups that can initiate SI-CRP is based on the physisorption of polyelectrolyte macroinitiators.

The use of organosilane reagents to introduce functional groups that can initiate or mediate SI-CRP is a direct extension of the concept of organosilane self-assembled monolayers (SAMs), which have been extensively investigated since the 1980s.[314] Commonly, SiO_2 surfaces are activated prior to the grafting step to clean the surface and maximize the number of silanol groups. Usually, H_2SO_4/H_2O_2 mixtures (piranha) or oxygen plasma are employed. These procedures render the surface hydrophilic and promote the formation of a thin layer of water onto the SiO_2 surface. There is a general consensus that trace amounts of water are essential for the formation of a well-packed monolayer of organosilane molecules.[315] The formation of organosilane SAMs on silicon oxide surfaces is believed to proceed via a sequence of surface adsorption, hydration, and silanization steps. In this process, silanol groups (Si−OH) on the SiO_2 surface react with organosilane molecules such as $R-SiR'_xCl_{3-x}$ or $R-SiR'_x(O(CH_2)_nCH_3)_{3-x}$ through a condensation reaction to form Si−O−Si chemical bonds.[316,317] This process is not necessarily limited to the surface and, under certain conditions, the organosilane SAM may develop in three dimensions because the dehydration may happen between organosilane monomers and SAM instead of between organosilane monomers and surface functional groups.[317] The chemisorption of organosilane molecules to silicon oxide substrates is a reaction that is very sensitive to many experimental parameters, such as reaction time, temperature, or water content.[318–324] In addition to the reaction conditions, also the structure of the organosilane reagent and, specifically, the number of hydrolyzable groups influence the quality of the resulting organosilane layer. The chemisorption of both mono- (R_3SiX), di- (R_2SiX_2), and tri- ($RSiX_3$) functional organosilanes, where X is a hydrolyzable group (usually X = Cl, OR, NMe_2), has been investigated extensively.[325] Monofunctional organosilane molecules (R_3SiX) are attractive in terms of the reproducibility of the organosilane layer because only one type of grafting is possible. Trifunctional organosilane molecules ($RSiX_3$) are more reactive compared to their monofunctional analogues but are capable of polymerizing in the presence of water. In addition to covalent attachment, 2D horizontal polymerization and 3D surface-induced polycondensation are possible.[325] Difunctional organosilane molecules (R_2SiX_2) are the least frequently used silanes to modify silicon oxide substrates. In addition to covalent attachment, chemisorption of difunctional organosilanes on silicon oxide can also lead to vertical polymerization and the formation of a thicker (i.e., nonmonolayer) organosilane film.[325]

For the modification of silicon oxide surfaces with functional groups that can initiate or mediate SI-CRP, many organosilane reagents that contain one polymerization active group and one (−$SiMe_2Cl$, −$SiMe_2OEt$) or three hydrolyzable groups (−$Si(OMe)_3$, −$Si(OEt)_3$, −$SiCl_3$) have been used. In addition, several examples of organosilane molecules functionalized with one polymerization active group and two hydrolyzable groups such as −$SiMe(OEt)_2$[326,327] or −$SiMe(OMe)_2$[328] have been reported. Finally, a few examples of organosilane molecules functionalized with two orthogonal polymerization active groups and one or three hydrolyzable groups have been described.[237,238,240–242,329] The use of these asymmetric difunctional initiator-terminated SAMs, which have been referred to as Y-SAMs, was presented in section 2.2.3.

As discussed above, the chemisorption of organosilane reagents on silicon oxide can be a very delicate process, which, among others, is sensitive to moisture. To overcome the problem of moisture sensitivity, Rühe and co-workers developed an ATRP initiator functionalized with hydridosilane groups (−$Si(Et)_2H$) to modify SiO_2 surfaces.[330] In this

case, a covalent bond is formed between the silicon atom of the hydridosilane and the oxygen atom of a hydroxyl group on the surface, presumably upon the elimination of hydrogen. The distinct advantage of hydridosilanes is that they are stable even in moist environments. A different approach to overcome the moisture sensitivity of initiators or iniferters functionalized with organosilane moieties has been developed by Brittain and co-workers.[331] These authors reported a multistep process that starts with the grafting of an allyldimethylsilane derivative onto the SiO_2 surface, followed by postfunctionalization of the organosilane layer with an ATRP initiator. This strategy is based on earlier work by Shimada and co-workers, who reported the modification of silica gel using allylorganosilanes.[332] In refluxing toluene, deallylation of allylsilanes takes place under the formation of an Si−O−Si bond with the silicon oxide substrate. This method of surface functionalization has the merit that allylsilanes are stable toward hydrolysis and can be purified by silica gel chromatography.[332]

Although organosilane reagents have been very extensively used to modify silicon oxide substrates with functional groups that can initiate or mediate SI-CRP, the resulting polymer brushes are tethered via Si−O−Si bonds, which are thermally labile and susceptible to hydrolytic cleavage.[333,334] Recently, it was shown that poly(poly(ethylene glycol) methacrylate) (PPEGMA) brushes, prepared by SI-ATRP from glass or silicon oxide substrates modified with a trimethoxysilane-based ATRP initiator, detach rapidly from the substrate when high density brushes were incubated in cell culture medium.[254] The reason for the detachment is still controversial, but it was proposed that detachment of the brushes involves cleavage of Si−O bonds that are located at the interface between the brush and the substrate.[315,335] Possible explanations for the detachment of the PPEGMA brushes may be osmotic stresses that act on the brushes in the cell culture medium as well as steric crowding. Both of these factors could induce additional tension along the already stretched polymer brush backbones, which could promote hydrolysis of the Si−O bonds and detachment of the brush. In two recent reports, it has been demonstrated that polymer/surface interactions can generate tensions along polymer backbones that are sufficient to mechanically break covalent bonds.[336,337] One possibility to overcome this problem could be to graft polymer brushes via more robust Si−C bonds instead of Si−O bonds. It has been shown, for example, that chlorinated SiO_2 surfaces (SiO_2−Cl) are effective initiators for surface-initiated ATRP from oxidized silicon wafers,[338] glass slides,[338] or porous silica microparticles.[339] In these cases, the resulting polymer brushes are covalently attached to the SiO_2 surfaces via stable Si−C bonds. Alternatively, SiO_2−Cl surfaces can be postmodified to initiate RAFT,[340] reverse ATRP,[91] or bimolecular NMP[341] SI-CRP reactions.

In addition to the use of low molecular weight organosilane molecules, a second approach to modify silicon oxide substrates with ATRP initiators is based on the physisorption of ATRP initiator-modified polyelectrolytes. Armes and co-workers have designed a cationic trimethylammonium-based ATRP macroinitiator and an anionic sulfate-based ATRP macroinitiator, which were electrostatically adsorbed onto ultrafine anionic sols[342] and aminated (cationic) planar oxidized silicon wafers, respectively.[343] Recently, the layer-by-layer (LbL) deposition of the two oppositely charged polyelectrolyte macroinitiators discussed above, or analogues, has been used to functionalize planar silicon oxide substrates.[344,345]

As indicated in Table 4, SI-CRP has been used to graft polymer brushes from silicon oxide surfaces of various geometries. This section concludes with a few remarks on the effects of the substrate geometry on the SI-CRP process. Recently, Genzer, Gorman, and co-workers have investigated the effect of confinement on the molecular weight and polydispersity of polymer brushes prepared by SI-ATRP.[346] To this end, porous silicon oxide (etched silicon wafer) and porous anodic aluminum oxide (AAO) membranes with a nominal pore size of ∼50 and ∼200 nm were used as templates for the *grafting from* polymerization of methyl methacrylate (MMA). It was found that, under identical polymerization conditions, PMMA grown from porous substrates had a much lower molecular weight and a broader molecular weight distribution compared to PMMA prepared via solution ATRP. These differences were attributed to confinement effects, which were related to reduced growth rates and more polydisperse chains. Kruk, Matyjaszewski, and co-workers, shortly thereafter, reported an improved SI-ATRP protocol that allows grafting of polymer brushes from the surfaces of cylindrical and spherical mesopores with improved control over film thickness and with polydispersities comparable to those obtained in well-controlled solution polymerization.[347] This improved control was achieved by the addition of appropriate amounts of deactivating Cu^{II} species in the polymerization reaction.

2.3.2. Polymer Brushes Grafted from Silicon

In contrast to silicon oxide, only a relatively small number of reports has been published that describe the preparation of polymer brushes from silicon surfaces. Table 5 presents an overview of the different ATRP initiators and RAFT agents that have been used to allow SI-CRP from silicon surfaces.

The grafting of polymer brushes from silicon surfaces is attractive, since the polymer chains are tethered via robust Si−C bonds. This process starts with the preparation of a hydrogen-terminated silicon surface (Si−H), which can be obtained by treating a pristine silicon oxide substrate with dilute hydrofluoric acid to remove the native oxide layer.[348] After that, functional groups that are able to initiate or mediate SI-CRP can be immobilized in either a one step process or a multistep process.

Most frequently, the initiators or RAFT agents are immobilized on silicon substrates via UV-induced coupling of *p*- or *o*-chloromethylstyrene to provide a stable initiator monolayer attached via robust Si−C bonds.[248] The Si−H group on the silicon surface can be homolytically dissociated by UV irradiation to form a radical site, which reacts readily with an alkene to give rise to a surface-tethered alkyl radical on the β-carbon. The radical subsequently abstracts an H atom from the adjacent Si−H bond. The abstraction creates a new reactive silicon radical to allow the above reaction to propagate as a chain reaction on the Si−H surface.[348] The resulting chloromethylbenzene-functionalized surfaces either can be used to directly initiate SI-ATRP[250,251,349–358] or can be postmodified with a RAFT agent.[143] Along the same lines, ω-unsaturated alkyl ester[118,119,257,359,360] and 4-vinylaniline[234] have also been photoimmobilized on silicon and subsequently postmodified with ATRP initiating groups[234,257,359,360] or RAFT agents[118,119] to allow SI-CRP. Kang and co-workers have demonstrated that halogenated silicon surfaces (Si−X; X = Cl, Br), obtained via chlorination or bromination of

Table 5. Overview of Initiators and RAFT Agents That Have Been Used To Grow Polymer Brushes from Planar Silicon Substrates

Anchoring group	Initiator/RAFT agent	Immobilization protocol: Single step	Immobilization protocol: Multi step	SI-CRP technique	Polymer	Ref
Direct halogenation: PCl_5: Si-Cl; NBS: Si-Br		×		ATRP	PHEMA, PDMAEMA	361
UV-induced coupling:	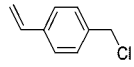	×		ATRP	P4VP	890
		×		ATRP	PDMAEMA	349
		×		ATRP	PHEMA, PPEGMA, PHEMA-*cb*-PHEMA, PPEGMA-*cb*-PPEGMA	251
		×		ATRP	PGMA, PGMA-*cb*-PNIPAM	250
		×		ATRP	PTMSPMA	350
		×		ATRP	PPEGMA	351,352
		×		ATRP	PSS(Na)	351,353,354
		×		ATRP	PGMA	355,356
		×		ATRP	PHEMA-*cb*-(PS-*b*-PPEGMA)	357
		×		ATRP	PHEMA	358
		×		ATRP	PPFS	248
UV-induced coupling followed by chlorosulfonation:	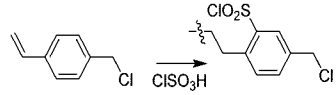		×	ATRP	PPFS	248
UV-induced coupling and postmodification:	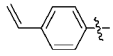 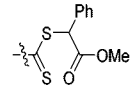		×	RAFT	PMMA, PHEMA, PDMAEMA-*b*-PMMA, PDMAEMA-*b*-PHEMA	143
			×	ATRP	PPEGMA, PNIPAM	234
UV-induced coupling and postmodification:	 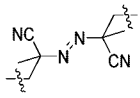		×	Bimolecular RAFT	PSBMA, PSBMA-*b*-PSS	119
			×		PSBMA, PSBMA-*b*-PSS	119
			×		PCMS	118
	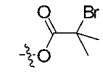		×	ATRP	PGMA	257
			×	ATRP	PPEGMA	359
			×	ATRP	PDMAEMA, PPEGMA, PMMA	360

the hydrogen-terminated silicon surfaces, are themselves effective initiators for SI-ATRP.[361]

2.3.3. Polymer Brushes Grafted from Metal Oxide Surfaces

An increasing number of publications describes the grafting of polymer brushes from metal oxide surfaces via SI-CRP. Table 6 presents an overview of the different initiators and RAFT agents that have been used to grow brushes from metal oxide surfaces. The different substrates are listed alphabetically in this table. To date, most examples of CRP initiated from metal oxide surfaces have employed aluminum, titanium, or iron oxide substrates. Only very few examples of polymer brushes grafted from other metal oxide surfaces such as indium tin oxide, copper oxide, nickel oxide, zinc oxide, and magnesium oxide have been reported.

Porous alumina membranes have been modified with polymer brushes via SI-ATRP. Both one step and two step protocols have been used to graft ATRP initiator-functionalized organosilanes. The Al−O−Si bond formed upon reaction of the organosilane moieties with the surface hydroxyl groups of the substrate is the strongest and hydrolytically most stable in the metal−O−Si series, although its strength is inferior to that of the Si−O−Si bond.[362] The two step approach for the modification of alumina substrates with ATRP initiators starts with the immobilization of 3-aminopropyltrimethoxysilane followed by postmodification with 2-bromo-2-methylpropionyl bromide.[227,363,364] Alternatively, trichlorosilane-functionalized ATRP initiators such as [(11-(2-bromo-2-methyl)propionyloxy)undecyl]-trichlorosilane[346,365–367] and 1-(trichlorosilyl)-2-[*m*/*p*-(chloromethyl)phenyl]ethane[368] can be grafted in a one step reaction to the alumina substrate.

Similar to alumina substrates, ATRP initiators functionalized with triethoxy- or trichlorosilane moieties have been used to modify the surface of Fe_3O_4 nanoparticles.[369–377] In these cases, the polymer brushes are believed to be tethered through a Fe−O−Si bond. Alternatively, ligand-exchange reactions can be used to graft ATRP initiators onto surfactant-coated Fe_3O_4 nanoparticles. Hatton and co-workers prepared oleic acid-coated magnetic nanoparticles and replaced the surfactant with ricinoleic acid, which was further functionalized with an ATRP initiator.[378] Similarly, oleic acid stabilized Fe_3O_4 or Fe_2O_3 nanoparticles were ligand-exchanged with 3-chloropropionic acid[379,380] or 2-bromoisobutyric acid[381,382] to allow SI-ATRP. It has been suggested that binding of these organic acids to the iron oxide surface involves the interaction of the carboxylic groups of these molecules with a trivalent iron atom located on the substrate surface.[378] While the interaction between carboxylic acids and Fe_3O_4 is relatively weak and reversible, phosphonic acids/phosphonates form stronger bonds.[383] Various NMP and ATRP initiator-functionalized phosphonates have been prepared and grafted onto Fe_3O_4 particles.[164–166,384] Another strategy to allow SI-CRP from iron oxide surfaces is based on the catecholic amino acid L-3,4-dihydroxyphenylalanine (L-DOPA), which is found in the adhesive proteins secreted by mussels and believed to play a critical role in their adhesion to a wide variety of substrates.[385] Inspired by these observations, Messersmith and co-workers prepared catechol-

Table 6. Overview of Initiators and RAFT Agents That Have Been Used To Grow Polymer Brushes from Metal Oxide Surfaces

Substrate	Substrate geometry	Anchoring group	Initiator/ RAFT agent	Immobilization protocol: Single step	Immobilization protocol: Multi step	SI-CRP technique	Polymer	Ref
Al_2O_3	Porous (pore size: 200 nm)			×		ATRP	PHEMA	365-367
							PMMA	346
	Porous (pore size: 20, 100, 200 nm)		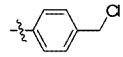	×		ATRP	PNIPAM	368
	Porous (pore size: 200 nm)				×	ATRP	PNIPAM-*co*-PMBAM	227,363
	Porous (pore size: 100 nm)				×	ATRP	PEGDMA	364
CuO_x and NiO_x (native oxide onto Cu and Ni respectively)	Planar			×		ATRP	PMMA, PTFEMA, PDMAEMA, PHEMA, PMMA-*b*-PTFEMA, PTFEMA-*b*-PMMA, PMMA-*b*-PDMAEMA	397
Fe_3O_4	Nanoparticle (diameter: 22 nm)		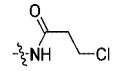		×	ATRP	PPEGMA	369
							PMMA	
	Nanoparticle (diameter: 9 nm)			×		ATRP	PS	370
							PBA	371
	Nanoparticle (diameter: 9 nm)		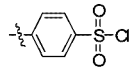	×		ATRP	PMMA	372
							PS	373,374
							PNIPAM	375
	Nanoparticle (diameter: 60 nm)		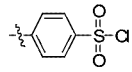	×		ATRP	PMMA	376
	Nanoparticle (diameter: 6 nm)	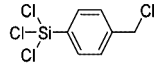		×		ATRP	PPEGMA	377
	Nanoparticle (diameter: 13 nm)	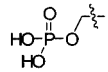		×		ATRP	PMMA	384
	Nanoparticle (diameter: 10 nm)	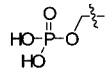	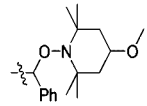	×		NMP	P3VP, PS	164-166
	Nanoparticle (diameter: 11 nm)				×	ATRP	PHEMA, PNIPAM, PSS(Na)	378
	Nanoparticle (diameter: 10 nm)	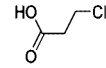		×		ATRP	PCDMA	379
	Nanoparticle (diameter: 5 nm)	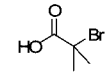		×		ATRP	PNHSMA	381,382
Fe_xO_y (native oxide onto 316L stainless steel)	Planar	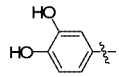		×		ATRP	PPEGMA	385
γ-Fe_2O_3	Nanoparticle (diameter: 4–10 nm)	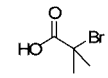		×		ATRP	PDMAEMA	426
							PS	868
$MnFe_2O_4$	Nanoparticle (diameter: 9 nm)	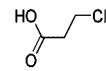		×		ATRP	PS	380
ITO (Indium Tin Oxide)	Planar			×		ATRP	PTPAA	843,844
	Planar		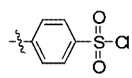	×		ATRP	PFMMA	664

Table 6. Continued

Substrate	Substrate geometry	Anchoring group	Initiator/ RAFT agent	Immobilization protocol: Single step	Immobilization protocol: Multi step	SI-CRP technique	Polymer	Ref
$Mg(OH)_2$	Nanoparticle		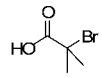	×		ATRP	PS	869
	Nanoparticle (diameter: 70 nm)			×		ATRP	PS-*b*-PMMA	396
	Nanoparticle (diameter: 50–100 nm)		 R = H and Me	×		ATRP	PBA, PMMA, PODMA, PDDMA	395
TiO_2	Nanoparticle (diameter: 25–70 nm)		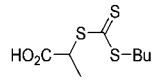	×		RAFT	PAA	133
	Nanoparticle (diameter: 15 nm)	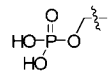	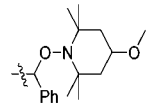	×		NMP	P3VP, PS	166,167
	Nanoparticle (diameter: 15 nm)				×	ATRP	PMMA	386
TiO_2	Nanoparticle (diameter: 34 nm)							391
TiO_2 (native TiO_2 onto NiTi and Ti-6Al-4V alloys)	Planar	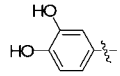		×		ATRP	PMMA	392
TiO_2 (native TiO_2 onto Ti)	Planar						PPEGMEMA	385,393
TiO_2 (native TiO_2 onto Ti)	Planar	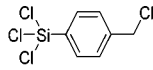		×		ATRP	PHEMA	387
							PPEGMA-*b*-PDMAEMA, PPFS	388
				×		ATRP	PGAMA	757
							PPEGMA	389
ZnO	Nanoparticle (diameter: 25 nm)			×		ATRP	PHEA	394
							PCMS	247

modified ATRP initiators, which were successfully immobilized onto the native iron oxide layer of 316L stainless steel via adsorption from aqueous solution.[385]

In addition to alumina and iron oxide surfaces, organosilane-based reagents have also been used to allow SI-ATRP from TiO_2 substrates.[386–389] In this case, the polymer brushes produced are believed to be tethered via Ti−O−Si bonds. Fadeev and co-workers have shown that monolayers of nonfunctionalized organosilane molecules, such as $C_{18}H_{37}Si(CH_3)_2Cl$, grafted on TiO_2 substrates showed poor hydrolytic stability compared to the corresponding $C_{18}H_{37}P(O)(OH)_2$ monolayer. This difference in stability was attributed to the low stability of the Ti−O−Si bond and the strong interactions between the phosphonic acid groups and the TiO_2 surface, respectively.[390] Phosphonic acid-functionalized NMP initiators have been used to allow SI-NMP from the surface of TiO_2 nanoparticles.[166,167] Another molecule that has been used to allow SI-CRP from planar and spherical TiO_2 surfaces is the catechol-functionalized ATRP initiator developed by the group of Messermith.[385,391–393] Finally, Charpentier and co-workers have prepared the RAFT agent 2-(((butylsulfanyl)carbonothioyl)sulfanyl)propanoic acid, which can be attached via the free carboxylic acid group to the surface of TiO_2 nanoparticles.[133]

In addition to alumina, iron oxide, and titanium dioxide, also several other metal oxide substrates have been used to grow polymer brushes via SI-CRP. ATRP initiators functionalized with organosilane moieties such as $-SiCl_3$ and $-SiOEt_3$ have been used to functionalize planar indium tin oxide and zinc oxide nanoparticles, respectively.[247,394] SI-ATRP from magnesium dihydroxide ($Mg(OH)_2$) nanoparticles has been achieved via the direct attachment of ATRP initiators such as 2-bromopropionyl bromide, 2-chloropropionyl chloride, or 2-bromoisobutyryl bromide.[395,396] Polymer brushes have also been grafted from flat nickel and copper surfaces via SI-ATRP.[397] Attempts to modify the surface of these metals with chlorosilane reagents failed and resulted in extensive corrosion. Instead, a triethoxysilane-functionalized ATRP initiator was used. The triethoxysilane derivative was first hydrolyzed to the corresponding silanol ($-Si(OH)_3$) and then reacted with hydroxyl groups on the metal surface.

2.3.4. Polymer Brushes Grafted from Clay Mineral Surfaces

SI-CRP techniques have also been used to prepare clay mineral polymer nanocomposites. Table 7 provides a summary of different initiators, iniferters, and RAFT agents that have been used to graft polymer brushes from clay mineral surfaces using SI-CRP.

Organosilane-modified ATRP initiators have been used to allow SI-CRP from various clay minerals, including

Table 7. Overview of Initiators, Iniferters, and RAFT Agents That Have Been Used To Grow Polymer Brushes from Clay Mineral Surfaces

Substrate	Substrate geometry	Anchoring group	Initiator/iniferter/ RAFT agent	Immobilization protocol: Single step	Immobilization protocol: Multi step	SI-CRP technique	Polymer	Ref
Attapulgite	Nanofibrillar silicate		Hyperbranched macroinitiator 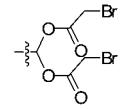		×	ATRP	PMMA	398
			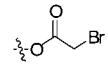		×	ATRP	PS, PS-*b*-PAM	399
							PAM	400
Halloysite	Layered silicate		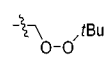		×	Reverse ATRP	PMMA-*b*-PNIPAM	401
			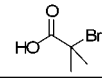	×		ATRP	PBAEA, PBAEA-*co*-PBA	223
Magadiite	Layered silicate		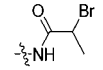		×	ATRP	PS	402
Mica	Layered silicate		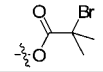	×		ATRP	P*t*BA	403,891
Montmorillonite	Layered silicate		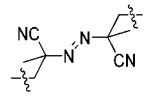	×		Bimolecular NMP	PDDMA	408
			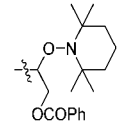	×		NMP	PS	409
			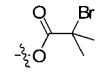	×		ATRP	PS-*b*-PBA	410
							PS, PBA, PMMA	411
							PMMA	412
							PS	892
			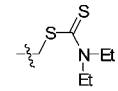	×		PIMP	PS, PMMA, P*t*BA, PMMA-*b*-PS	407
		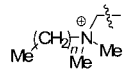	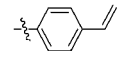	×		Bimolecular RAFT	PS, PBA, PMMA	413
Laponite (Montmorillonite)	Layered silicate		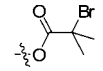	×		ATRP	PNIPAM	414
Cloisite 30B (organically modified Montmorillonite)	Layered silicate		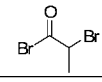	×		ATRP	PEA	405
Palygorskite	Layered silicate		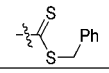		×	RAFT	PMMA	404
Zirconium phosphonate: 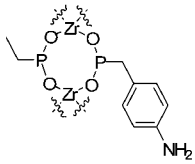	Lamellar structure		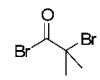	×		ATRP	PMMA	406

attapulgite,[398–400] halloysite,[401] magadiite,[402] mica,[403] and palygorskite.[404] Cloisite 30B, a bis-2-hydroxyethyl-modified montmorillonite, and an amine-functionalized zirconium phosphate clay have been functionalized with ATRP initiating groups by reaction of the hydroxyl and amine groups with 2-bromopropionyl bromide[405] and 2-bromo-2-methylpropionyl bromide,[406] respectively. In addition to covalent immobilization, also noncovalent electrostatic interactions have been used to modify clay mineral surfaces with functional groups that can initiate or mediate SI-CRP. This approach has been used for example to modify the surface of halloysite with 2-bromoisobutyric acid.[223] Noncovalent interactions have also been used to modify montmorillonite. Sodium montmorillonite has ion-exchange capacities due to the presence of sodium ions in the interlayer spacing, which can be replaced by ionic species. Ion-exchange reactions have been used to intercalate initiators, iniferters, or RAFT agents functionalized with ionic anchoring groups such as trim-

Table 8. Overview of Initiators, Iniferters, and RAFT Agents That Have Been Used To Grow Polymer Brushes from Gold Surfaces

Anchoring group	Initiator/iniferter/ RAFT agent	Immobilization protocol: Single step	Immobilization protocol: Multi step	SI-CRP technique	Substrate and substrate geometry	Ref
		×		ATRP	Thin layer onto Si_3N_4 (nanostructured)	586,650,651
		×		ATRP	Thin layer onto quartz (planar)	101,296,659,697
		×		ATRP	Thin layer onto silicon chip (planar)	292
		×		ATRP	Thin layer onto glass slide or silicon wafer (planar)	105,110,243,258-260,294,295,307, 553,555,559,561,562,565,572,574, 579,581,585,586,610,612,644,649,660-662,697,698,701,712,730,825,842,856
	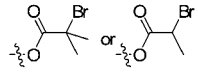	×		ATRP	-	261,564,580
		×		ATRP	Nanoparticle (diameter: 1–50 nm)	420,429,430,568
			×	ATRP	Thin layer onto glass slide or silicon wafer (planar)	74,217,303,417,605,610,682,685
			×	ATRP	Nanoparticle (diameter: 1–50 nm)	428,684
	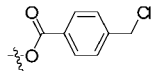		×	ATRP	Thin layer onto glass slide (planar)	881
	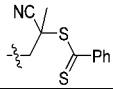		×	RAFT	Nanoparticle (diameter: 3.2 nm)	136
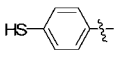	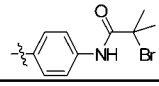		×	ATRP	Thin layer onto silicon wafer (planar)	418
		×		ATRP	Thin layer onto glass slide or silicon wafer (planar)	87,88,112,231,253,297-299,416,596-599,604,736,748,772,819,845
	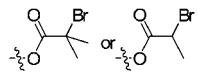	×		ATRP	Gold surface (planar)	563
		×		ATRP	-	708
		×		ATRP	Nanoparticle (diameter: 3–20 nm)	224,421-424,426,427,431,775
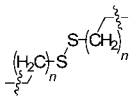		×		ATRP	Thin layer onto polycarbonate track-etched membrane	677
		×		ATRP	Nanorod (size: 40 × ~10 nm)	657
	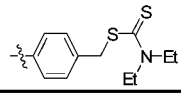	×		PIMP	Nanoline onto silicon wafer (size: 250 nm)	212,584
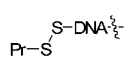	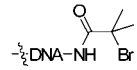	×	×	ATRP	Thin layer onto glass (planar)	419

ethylammonium, in the individual layers of sodium montmorillonite.[407–413] Ion-exchange reactions have also been applied to intercalate an ATRP initiator in laponite,[414] a synthetic hectorite, which is chemically quite similar to montmorillonite.[415]

2.3.5. Polymer Brushes Grafted from Gold Surfaces

Gold has been very extensively used as a substrate to graft polymer brushes via SI-CRP. Most of the examples that have been reported use SI-ATRP, and only a few reports describe the modification of gold surfaces with SI-PIMP or SI-RAFT. The gold substrates that have been used can be classified into two groups: (i) gold films deposited by metal vapor deposition onto flat substrates such as silicon wafers, glass, and quartz slides as well as substrates with more complex geometries such as AFM tips and (ii) gold nanoparticles. Table 8 gives a summary of the initiators, iniferters, and RAFT agents that have been used to produce polymer brushes via SI-CRP. The remainder of this section will successively discuss the modification of planar gold substrates and gold nanoparticles.

Both one step and two step protocols have been used to attach ATRP initiators onto planar gold substrates. In the first case, ATRP initiator-functionalized disulfides or thiols are directly grafted onto gold surfaces. The most popular ATRP initiator-functionalized disulfide and thiol are $(BrC(CH_3)_2COO(CH_2)_{11}S)_2$[416] and $BrC(CH_3)_2COO(CH_2)_{11}SH$,[295] respectively. Two step protocols for the modification of gold substrates start with the formation of a hydroxyl-functionalized disulfide or thiol SAM, which is subsequently esterified to introduce the ATRP initiator.[417] In most instances, the ATRP initiating group and the thiol or disulfide group are separated by a long alkyl spacer. Other spacers have also been used, however. He et al. converted a SAM of 4′-nitro-1,1′-biphenyl-4-thiol adsorbed onto a gold-coated silicon wafer into a cross-linked 4′-amino-1,1′-biphenyl-4-thiol monolayer by electron beam irradiation. Then, the ATRP initiator, bromoisobutyryl bromide, was added and attached through the formation of an amide bond,

Table 9. Overview of Initiators and RAFT Agents That Have Been Used To Grow Polymer Brushes from Metal and Semiconductor Surfaces

Substrate	Substrate geometry	Anchoring group	Initiator/ RAFT agent	Immobilization protocol: Single step	Immobilization protocol: Multi step	SI-CRP technique	Polymer	Ref
CdSe	Nanoparticle (size: 525 nm)	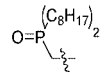	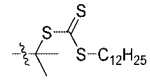	×		RAFT	PS, PMA, PBA, PS-*co*-PAA, PS-*co*-PMA, PS-*b*-PMA, PS-*b*-PBA	134
CdSe	Nanoparticle (size: 3–4 nm)	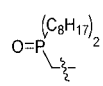	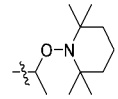	×		NMP	PS, PS-*co*-PMMA	432
CdS	Nanoparticle (size: 4.5 nm)			×		ATRP	PBA	100
Fe (plate)	Planar	Electrograting: 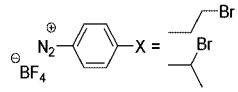		×		ATRP	PBMA	434
							PS, PMMA	435
							PS, PMMA, PBA	436
Fe (Stainless steel)	Planar	Electrograting: 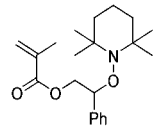		×		NMP	PS-*co*-PDMAEA, PBA-*co*-PDMAEA	191
Fe (Stainless Steel)	Planar	Electrograting: 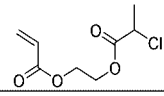		×		ATRP	PS	433
							P*t*BAEMA, P*t*BAEMA-*co*-PAA, P*t*BAEMA-*co*-PS, P*t*BAEMA-*co*-PPEGMA	233
GaAs (single crystal wafer)	Planar				×	ATRP	PMMA	437
Ge-F (Ge treated by HF)	Planar	UV-induced coupling: 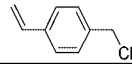		×		ATRP	PPFS, PDMAEMA, PDMAEMA-*b*-PPFS	439

to create a surface bound initiator monolayer.[418] He and co-workers have used DNA hybridization to prepare surface tethered double helical structures that can be used to initiate SI-ATRP.[419]

A variety of strategies is available to modify the surface of gold nanoparticles with functional groups that enable SI-CRP. Ligand-exchange reactions between stabilizing ligands and ligands functionalized with initiators, iniferters, or RAFT agents are a convenient way to modify the surface of gold nanoparticles with functional groups that can initiate or mediate SI-CRP. Hallensleben and co-workers, for example, have used dodecanethiol-stabilized gold nanoparticles and replaced this alkanethiol by the ATRP initiator-functionalized thiol $BrC(CH_3)_2COO(CH_2)_{11}SH$.[420] Ligand-exchange reactions have also been used to modify citrate-stabilized gold nanoparticles. Since the bond strength between Au and S is stronger than that between Au and citrate, citrates can be exchanged with disulfide-functionalized ATRP initiators such as $(BrC(CH_3)_2COO(CH_2)_{x=2-11}S)_2$.[224,421–427]

In addition to the direct ligand-exchange strategy discussed above, gold nanoparticles can also be functionalized with ATRP initiating or RAFT groups following two step post-modification strategies. As an example, gold nanoparticles have been prepared in the presence of 11-mercapto-1-undecanol and were subsequently esterified with 2-bromoisobutyryl bromide as initiator for ATRP[428] or 4-cyanopentanoic acid dithiobenzoate as RAFT agent.[136]

A third strategy for the preparation of gold nanoparticles modified with functional groups that enable SI-CRP involves the use of the appropriate ATRP initiator functionalized with thiols or disulfides as ligands for the nanoparticles synthesis. This strategy, however, requires mild reductive conditions to avoid cleavage of ester bonds. Fukuda and co-workers have developed a protocol to coat gold nanoparticles with an ATRP initiator group by the simple one-pot reduction of $HAuCl_4 \cdot 4H_2O$ with slow addition of sodium borohydrate in the presence of an ATRP initiator-functionalized disulfide $(BrC(CH_3)_2COO(CH_2)_{11}S)_2$.[429,430] An alternative approach involves the rapid addition of sodium borohydride to an ethyl acetate solution of $HAuCl_4 \cdot 4H_2O$ and the ATRP initiator-functionalized disulfide $(BrC(CH_3)_2COO(CH_2)_6S)_2$.[431]

2.3.6. Polymer Brushes Grafted from Metal and Semiconductor Surfaces

Section 2.3.3 has discussed strategies to graft polymer brushes via SI-CRP from metal oxide surfaces. Table 9, in contrast, presents an overview of different initiators and RAFT agents that have been used to graft polymer brushes from nonoxide metallic and semiconductor substrates.

Similar to gold nanoparticles, ligand-exchange reactions have also been used to functionalize CdSe nanoparticles and CdS quantum dots with initiators and RAFT agents. These

nanoparticles are typically stabilized by tri-*n*-octylphosphine oxide ligands. NMP[432] and ATRP[100] initiator-functionalized as well as RAFT agent[134]-containing phosphines have been attached to CdSe and CdS via ligand-exchange chemistry. This is accomplished by first replacing the tri-*n*-octylphosphine oxide ligands by pyridine, followed by exchange with appropriate functionalized ligands.

Various electrochemical approaches have been used to modify stainless steel and iron substrates with functional groups that can initiate or mediate SI-CRP. Jérôme and co-workers have electrografted the inimer 2-chloropropionate ethyl acrylate to steel surfaces to form a dense layer of ATRP macroinitiators. This work also showed that copper catalysts, the usual first choice for ATRP reactions, reacted electrochemically to corrode the steel surface, necessitating the use of Grubbs type and nickel complex catalysts.[233,433] A similar strategy was also used to coat steel surfaces with an NMP initiator.[191] An alternative approach to modify iron surfaces is based on the electrochemical reduction of ATRP initiator-functionalized aryl diazonium salts.[434–436]

ATRP initiator-functionalized thiols have been used to allow SI-ATRP from GaAs surfaces. The first step in this process is treatment of the substrate with concentrated HCl to remove the native oxide layer. After that, the GaAs substrate was functionalized with 6-mercapto-1-hexanol to form a hydroxy-terminated GaAs, which was subsequently postfunctionalized with 2-bromoisobutyryl bromide.[437] Similar to the case of silicon surfaces, exposure of pristine germanium chips to aqueous HF produces a uniform hydrogen-terminated surface (Ge−H). ATRP initiators have been immobilized via UV-induced coupling (i.e., hydrogermylation)[438] of vinylbenzyl chloride on the Ge−H surface. In this case, the ATRP initiator is linked to the surface via a Ge−C bond.[439]

2.3.7. Polymer Brushes Grafted from Carbon Surfaces

SI-CRP has been used to modify a broad range of carbon-based materials, including carbon nanotubes, carbon black particles, diamond, and graphite. Table 10 presents a summary of initiators, iniferters, and RAFT agents that have been used to allow SI-CRP from carbon substrates.

Since carbon nanotubes (and carbon in general) do not possess any functional groups that facilitate chemical modifications, these substrates first need to be activated to introduce appropriate chemical handles. Carboxylic acid-functionalized single (SWNTs) and multiwalled carbon nanotubes (MWNTs), for example, can be obtained by oxidation of the pristine nanotubes with HNO_3 or H_2SO_4/HNO_3 and subsequently converted into the corresponding acid chloride via reaction with thionyl chloride.[440] Acid chloride-functionalized carbon nanotubes have been modified in a single step by esterification of appropriate hydroxyl-functionalized NMP[170,441] or ATRP[442–444] initiators. Alternatively, acid chloride-functionalized nanotubes can be reacted with ethanolamine or ethyleneglycol, generating hydroxyl-substituted nanotubes, which can be further modified with the ATRP initiator 2-bromo-2-methylpropionyl[246,440,445–449] or a carboxylic acid RAFT agent.[140] RAFT agents have been introduced by reacting acid chloride-functionalized nanotubes with 2-hydroxyethyl-2′-bromoisobutyrate, which have been subsequently converted into a RAFT agent.[138,139,141,450]

In addition to the modification of oxidized carbon nanotubes, several other strategies have been reported that allow the introduction of functional groups that can initiate or mediate SI-CRP. Chehimi and co-workers have reported the electrochemical reduction of brominated aryl diazonium salts to introduce initiators for ATRP onto the surface of MWNT.[451] SWNTs have been modified via a multistep protocol starting with the grafting of phenyl diazonium compounds, which were then further modified with a RAFT agent[145] or ATRP initiator.[452] The 1,3-dipolar cycloaddition reaction between SWNT and octanal and 4-hydroxyphenyl glycine has been used to produce phenol-functionalized nanotubes which were further derivatized with 2-bromoisobutyryl bromide.[453] Following a similar approach, 2-chloropropionyl chloride was attached to amino-functionalized nanotubes.[454] Radical addition reactions have also been used to modify carbon nanotubes. Atom transfer radical addition[455] and free radical functionalization[456,457] reactions have been used to modify carbon nanotubes with ATRP initiators and, respectively, NMP initiators.

The strategies discussed above for the functionalization of carbon nanotubes have also been used to modify a variety of other carbon substrates. The oxidation of carbon surfaces followed by the immobilization of ATRP initiators via one step or multistep protocols has been used to modify the surface of carbon nanoparticles,[458–460] ultradispersed diamond particles,[461] Herringbone graphite nanofibers,[462,463] carbon fibers,[464] and pure carbon spheres.[465] The electrochemical reduction of brominated aryl diazonium salts has been used to introduce ATRP initiators onto diamond films[466] and planar glassy carbon substrates.[435,467]

2.3.8. Polymer Brushes Grafted from Polymer Surfaces

An increasing number of publications describes the grafting of polymer brushes from polymer substrates using SI-CRP techniques. Figure 4 shows the four principal strategies that are used to modify polymer substrates with initiators, iniferters, or RAFT agents that allow SI-CRP. Polymer surfaces bearing suitable functional groups allow the direct attachment of initiators, iniferters, or RAFT agents (Figure 4A). In contrast, many inert polymers require an appropriate pretreatment or activation to introduce functional groups, onto which initiators, iniferters, or RAFT agents can then be attached (Figure 4B). A third approach to grow polymer brushes from polymer substrates involves the use of polymeric initiators or RAFT agents (Figure 4C). The fourth approach uses irradiation or plasma treatment to directly grow brushes from inert polymer substrates under CRP conditions (Figure 4D). Each of these four strategies will be discussed in more detail in the following sections.

2.3.8.1. Polymer Brushes Grafted from Functional Polymer Surfaces. A straightforward strategy to allow SI-CRP from polymer substrates is to graft initiators, iniferters, or RAFT agents onto prefabricated polymer substrates which contain nucleophilic or electrophilic groups (Figure 4A). Table 11 gives an overview of various functional polymers that have been used as substrates to attach initiators, iniferters, and RAFT agents to allow SI-CRP.

Cellulose has been extensively used as a substrate to graft polymer brushes via SI-CRP. Carlmark and Malmström have reported a single step protocol to convert the pendant hydroxyl groups present on the cellulose surface into ATRP initiators. The cellulose hydroxyl groups were esterified with 2-bromoisobutyryl bromide in the presence of triethylamine.[468] This protocol, and similar strategies using 2-bromoisobutyryl bromide analogues, has been used to modify

Table 10. Overview of Initiators and RAFT Agents That Have Been Used To Grow Polymer Brushes from Carbon Surfaces

Substrate	Activation procedure	Anchoring group	Initiator/RAFT agent	Immobilization protocol: Single step	Immobilization protocol: Multi step	SI-CRP technique	Polymer	Ref
Singlewalled carbon nanotube (SWNT)		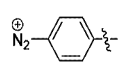			×	RAFT	PAM	145
		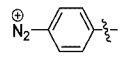			×	ATRP	PBA	452
		1-3 dipolar cycloaddition: 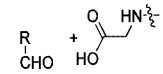			×	ATRP	PMMA, P*t*BA	453
		1-3 dipolar cycloaddition: 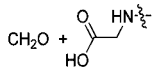			×	ATRP	PVQ	454
								
	$SOCl_2$				×	ATRP	PMPC, PLAMA	445
		Electrografting: 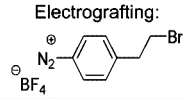		×		ATRP	PS, PMMA	451
	1. HNO_3 2. $SOCl_2$			×		ATRP	PBMA	442
Multiwalled carbon nanotube (MWNT)	1. $K_2Cr_2O_7/H_2SO_4$ 2. $SOCl_2$			×		ATRP	PS, PAN, PS-*co*-PAN	443
	$SOCl_2$			×		ATRP	PMMA, PS, PS-*b*-PMMA, PMMA-*b*-PS	444
							PBIMHFP	816
							PS, PS-*b*-P*t*BA	446
	1. HNO_3 2. $SOCl_2$				×	ATRP	PMMA, PMMA-*b*-PHEMA	440
							PNIPAM	447
							PDHPMA	448
							P*t*BA, PSS(Na)	449
							PMAIG	246
							PNIPAM	138
	1. HNO_3 2. $SOCl_2$		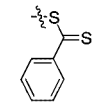		×	RAFT	PMMA, PMMA-*b*-PS	139
							PHEMA	140
							PS, PS-*b*-PNIPAM	141
							PS-*co*-PMAn	450
	1. H_2SO_4/HNO_3 2. $SOCl_2$		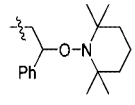		×	NMP	PSS(Na), P4VP	170
							PS	441
		Coupling by atom transfer radical addition: 			×	ATRP	PS, PNIPAM	455
Nitrogen-doped MWNT	Benzoyl peroxide	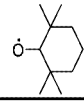			×	NMP	PS	456,457
Carbon black (nanoparticles; diameter: 30 nm)	1. HNO_3 2. $SOCl_2$				×	ATRP	PS, PMMA	458
							PNIPAM	459
							PSS(Na)	460
Carbon black (carboxylate-stabilized nanoparticles; diameter 120–500 nm)					×	ATRP	PDMAEMA, PDMAEMA-*co*-PHEMA, PDMAEMA-*b*-PHEMA	750
							PBA, P*t*BA	832,833

Table 10. Continued

Substrate	Activation procedure	Anchoring group	Initiator/RAFT agent	Immobilization protocol: Single step	Immobilization protocol: Multi step	SI-CRP technique	Polymer	Ref
Diamond (ultrananocrystalline thin film deposited onto silicon wafer)		Electrografting: 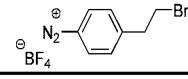		×		ATRP	PS, PMMA	466
Ultradispersed diamond (4–6 nm diamond nanocrystals coated by a fullerene-like carbon matrix aggregated into particles 20–50 nm in diameter)	1. HNO_3 2. $SOCl_2$		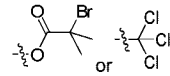	×		ATRP	PiBMA, P*t*BMA	461
Glassy carbon (planar)		Electrografting: 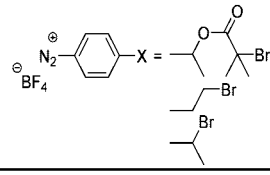		×		ATRP	PS, PMMA, PGL PS, PMMA, P*t*BMA	467 435
Herringbone graphitic carbon nanofiber (cross section: 150 nm)	1. HNO_3 2. $SOCl_2$			×		ATRP	PBA, PiBMA, P*t*BA	462,463
Carbon fiber (cross section: 6 μm)	HNO_3			×		ATRP	PMMA	464
Pure carbon sphere (diameter: 400-900 nm)	1. HNO_3/H_2SO_4 2. $SOCl_2$				×	ATRP	PS, PMMA, PDHPMA	465
Aligned carbon nanotube	HNO_3				×	ATRP	PNIPAM	858

cellulose substrates such as regenerated cellulose membranes,[469–471] paper filters,[468,471–475] or cotton fibers.[476] Related approaches have also been used to modify other polysaccharides such as dextran,[477] chitosan particles,[478,479] and chitosan films.[471] To enhance the accessibility of the hydroxyl groups and to facilitate higher degrees of substitution, Perrier and co-workers pretreated cellulose fibers with aqueous NaOH. After extensive washing with first ethanol and then tetrahydrofuran (THF), these substrates were reacted with 2-chloro-2-phenylacetyl chloride and subsequently treated with phenyl magnesium chloride in the presence of carbon disulfide to generate a cellulose-bound RAFT agent.[137,480,481] In addition to cellulose and dextran, the direct esterification with 2-bromoisobutyryl bromide or analogues has also been used to modify a variety of other hydroxyl functional polymers with ATRP initiating groups. Examples include microspheres made of a copolymer of divinylbenzene and 2-hydroxyethyl methacrylate (PDVB-*co*-PHEMA),[482] films made of a copolymer of 2-hydroxyethyl methacrylate and methyl methacrylate (PHEMA-*co*-PMMA),[483] ramie fibers,[484] starch granules,[485] hydroxylated and PEG-functionalized polystyrene beads,[486] Wang resin,[487] and hydroxyl-functionalized poly(ethyleneterephthalate) (PET) track-etched membranes.[488] In analogous fashion, also amino-functionalized polyaniline substrates were modified with the ATRP initiator bromoacetylbromide.[489]

In addition to hydroxyl-functionalized polymer substrates, halogenated and epoxide-functionalized polymer substrates are also conveniently modified with initiators or chain transfer agents that allow SI-CRP. Allyl and benzyl chloride groups can be reacted with sodium *N*,*N*-diethyldithiocarbamate to introduce iniferter groups for SI-PIMP. This protocol has been used to functionalize nanoparticles made of a copolymer of styrene and 4-chloromethylstyrene (PS-*co*-PCMS)[490] as well as cross-linked PVC beads[491] and Merrifield resins.[229] In a similar fashion, initiators for NMP can be introduced onto the surface of Merrifield resin by reaction of the sodium salt of 2,2,6,6-tetramethylpiperidinyloxy (TEMPO).[169] *N*-*tert*-Butyl-*N*-[1-diethylphosphono-(2,2-dimethylpropyl)] nitroxide (DEPN), a stable radical used for NMP, was attached to latex particles made of PS-*co*-PCMS via atom transfer radical addition (ATRA).[185] Finally, ATRP initiators were grafted onto the surface of poly(glycidyl methacrylate) (PGMA) via the reaction between the epoxy groups of PGMA and the carboxylic acid group of 2-bromo-2-methylpropionic acid.[277]

In one example, solid phase peptide synthesis was used to prepare peptide chains, which were bound to a Wang resin. The N-terminus of these peptide sequences was subsequently converted into a carboxylic acid group by coupling of glutaric anhydride. Further functionalization by reaction with the benzylic amine of a fluorine-labeled alkoxyamine yielded a NMP initiator tethered to the N-terminus of the peptide.[195] A multistep protocol has also been used to graft ATRP initiators onto a poly(ethylene-*co*-acrylic acid) substrate. For initiator immobilization, the carboxylic acid groups on the film were converted to acid chloride groups and subsequently reacted with (di)ethanolamine to provide hydroxyl groups onto which 2-bromoisobutyryl bromide initiator was attached.[492] The surface modification of cross-linked poly(dicyclopentadiene) films with ATRP initiators has also been achieved using a two step protocol. In this case, double bonds present at the surface of the polymer were reacted with mercaptoethanol to generate hydroxyl groups, which were subsequently reacted with 2-bromoisobutyryl bromide.[493]

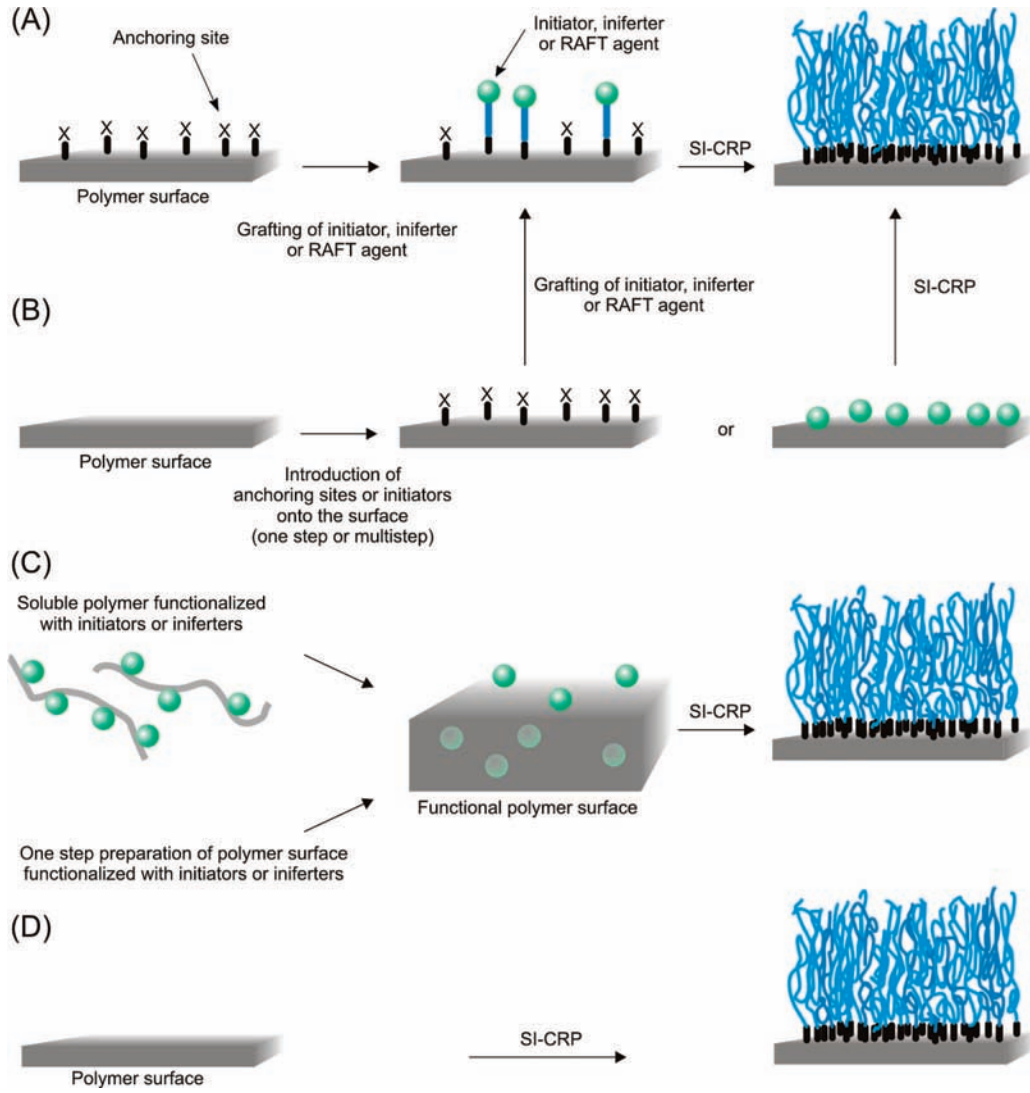

Figure 4. Strategies to graft polymer brushes from polymer surfaces: (A) polymer brushes grafted from functional polymer surfaces; (B) polymer brushes grafted from inert polymer surfaces; (C) direct SI-CRP from initiator-, iniferter-, or RAFT agent-functionalized polymer surfaces; (D) radiation/plasma-mediated SI-CRP.

Poly(vinylidene fluoride) (PVDF) films represent a very interesting substrate to grow polymer brushes, as they allow direct ATRP using the secondary fluorinated sites for initiation.[494]

2.3.8.2. Polymer Brushes Grafted from Inert Polymer Surfaces. Polymer substrates that lack functional groups that can act as handles to introduce moieties to initiate or mediate SI-CRP require a pretreatment or activation step (Figure 4B). Table 12 gives an overview of different inert polymer substrates, which have been modified with initiators, iniferters, or RAFT agents. For each of the substrates, Table 12 also indicates the activation protocol that has been used.

A variety of plasma and oxidative surface treatments is available to modify inert polymer substrates with hydroxyl or carboxylic acid groups, which can be further modified with 2-bromoisobutyryl bromide or analogues to allow SI-ATRP. In this way, ATRP initiating groups have been introduced onto the surface of polypropylene hollow fiber membranes using ozone pretreatment,[495] onto poly(tetrafluoroethylene) (PTFE) substrates using hydrogen plasma and ozone pretreatment,[496] within PMMA microcapillaries using oxygen plasma pretreatment,[497] and onto ground tire rubber particles using oxidative hydrolysis pretreatment NaOH/$KMnO_4$.[498] Alternatively, the surface hydroxyl groups may be modified with trichlorosilane derivatives. This strategy has been used to modify oxygen plasma-treated poly(ethylene terephthalate) (PET) and poly(ethylene naphthalate) (PEN) substrates with functional groups that can act as initiators for ATRP.[499] Chlorosilane-based ATRP initiators have also been employed to modify various silanol-activated PDMS substrates, which can be obtained via exposure to UV ozone,[313,500,501] oxygen plasma,[502] or treatment with HCl.[503] Unsal et al. converted the surface epoxide groups of porous poly(glycidyl methacrylate-*co*-ethylene dimethacrylate) (PGMA-*co*-PEDMA) particles into hydroxyl groups, which were subsequently modified with the ATRP initiator containing alkoxysilane 3-(2-bromoisobutyramido)propyl(triethoxy)-silane.[504] In the case of PET, alkaline hydrolysis generates both hydroxyl and carboxyl groups, which can subsequently be converted into acid chloride moieties via further oxidation and PCl_5 treatment. After that, ATRP initiators can be grafted using a two step protocol, which starts with an amidation reaction using diethanolamine followed by esterification of the hydroxyl groups with bromopropionyl bromide.[505] Ulbricht and co-workers have used $KMnO_4/H_2SO_4$ to introduce carboxylic acid groups onto the surface of PET, followed by amidation with ethanolamine and esterification of the resulting hydroxyl groups with bromopropionyl bromide to

Table 11. Overview of Functional Polymer Substrates That Have Been Modified with Initiators, Iniferters, and RAFT Agents To Generate Polymer Brushes via SI-CRP

Substrate and substrate geometry	Anchoring site	Anchoring group	Initiator/iniferter /RAFT agent	Immobilization protocol: Single step	Immobilization protocol: Multi step	SI-CRP technique	Polymer brush	Ref
Cellulose (porous membrane, regenerated)	–OH			×		ATRP	PAA	469
				×		ATRP	PPEGMA	470
Cellulose (porous membrane, regenerated)	–OH	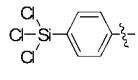	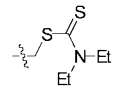		×	PIMP	PEGDMA-*co*-PMAA	228
Cellulose (fiber, filter paper)	–OH			×		ATRP	PMA, PMA-*b*-PHEMA	468,472
							PCPPUA	473
							PGMA	474
Cellulose (fiber, filter paper)	–OH		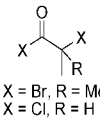 X = Br, R = Me X = Cl, R = H	×		ATRP	PNIPAM, P4VP, PNIPAM-*b*-P4VP, P4VP-*b*-PNIPAM, PGMA	475
Cellulose (fiber, filter paper)	–OH				×	RAFT	PS	137
							PDMAEMA	480,481
							PDMAEMA-*b*-PS	481
Cellulose (filter paper, microcrystalline cellulose, dialysis membrane, lyocell fiber)	–OH			×		ATRP	PMA	471
Cellulose (Cotton fiber)	–OH		 R = Ph, SMe		×	RAFT	PS, PMMA, PMA	135
Cellulose (Cotton fiber)	–OH			×		ATRP	PEA, PEA-*b*-PS	476
Chitosan (film)	–OH			×		ATRP	PMMA	471
Chitosan (bead)	–OH			×		ATRP	PAM	478
Chitosan (particle)	–OH			×		ATRP	PS	479
Dextran (cross-linked microsphere, Sephadex G50)	–OH			×		ATRP	PNIPAM	477
Merrifield resin (particle, 100–400 mesh)	–Cl		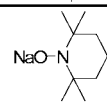	×		NMP	PAS, PS, PAS-*b*-PS, PS-*b*-(PMMA-*co*-PS), PS-*co*-PHEMA	169
Merrifield resin (particle)	–Cl		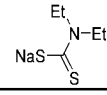	×		PIMP	PAA-*co*-PEGDMA	229
PDVB-*co*-PHEMA (microsphere)	–OH			×		ATRP	PMMA, PMMA-*b*-PDMAEMA, PMMA-*b*-PMETAC, PMMA-*b*-PGMA	482
PE-*co*-PAA (film)	–COCl	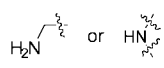			×	ATRP	PAM	492
PET (film)	$-CO_2-$				×	ATRP	PS	893
PET (track-etched membrane, pore diameter: 80 and 330 nm)	–OH			×		ATRP	PNIPAM	488
PGMA (film deposited onto silicon wafer)			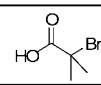	×		ATRP	PS	277
PHEMA-*co*-PMMA (film)	C–OH					ATRP	PPEGMEA	483

Table 11. Continued

Substrate and substrate geometry	Anchoring site	Anchoring group	Initiator/iniferter /RAFT agent	Immobilization protocol: Single step	Immobilization protocol: Multi step	SI-CRP technique	Polymer	Ref
Poly(aniline) (powder)	C–NH_2		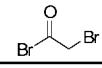	×		ATRP	PMMA	489
Poly(dicyclopentadiene) (film)					×	ATRP	PMMA	493
PS-*co*-PCMS (nanoparticle, diameter: 400 nm)	C–Cl		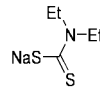	×		PIMP	PNIPAM	490
PS-*co*-PCMS (latex particle, diameter 60 nm)	C–Cl		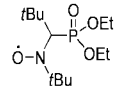	×		NMP	PBA, PS, PDMAEA, PS-*b*-PDMAEA, PBA-*b*-PDMAEA	185
PS hydroxylated (cross-linked bead, diameter: 100 μm, commercially available)	C–OH		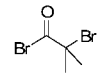	×		ATRP	PPEGMA, PPEGMA-*b*-PHEMA	486
PS functionalized with PEG (cross-linked bead, diameter: 10-200 μm, commercially available)	C–OH			×		ATRP	PNIPAM, PDMAM, PPEGMA, PNIPAM-*b*-PHEMA, PDMAM-*b*-PHEMA, PPEGMA-*b*-PHEMA	486
PVC (film)	C–Cl	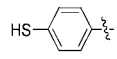			×	ATRP	PDMA, PDMA-co-PNIPAM	894
PVC (cross-linked bead, diameter: 1mm)	C–Cl		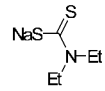	×		PIMP	PBA	491
PVDF (film)	C–F	- (direct ATRP)				ATRP	PPEGMEMA, PDMAEMA, PPEGMEMA-*b*-PS, PDMAEMA-*b*-PS	494
Ramie (fiber)	C–OH		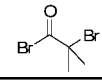	×		ATRP	PMMA	464
Starch (granule)	C–OH		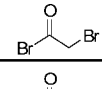	×		ATRP	PBA	465
Wang resin (diameter: 150–300 μm)	C–OH		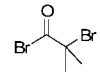	×		ATRP	PMMA, PMMA-*b*-(PBzMA-*co*-PMMA)	467
Wang resin (peptide-modified)	C–NH_2	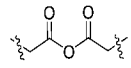	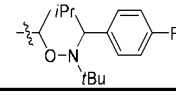		×	NMP	P*t*BA-*b*-PMA	195

produce a PET substrate functionalized with ATRP initiators.[506] PVDF films can be hydroxylated by exposing the pristine substrate to aqueous LiOH followed by successive reductions with $NaBH_4$ and diisobutylaluminium hydride (DIBAL-H). The resulting hydroxylated surfaces have been modified with 2-bromoisobutyryl bromide[507] and 4,4-azobis(4-cyanopentanoic acid)[120] to allow SI-ATRP and, respectively, surface-initiated bimolecular RAFT polymerization. Nylon can be hydroxylated by reacting the amide bonds with formaldehyde to give the corresponding *N*-methylol derivative. This strategy has been used by Kang and co-workers to modify nylon membranes with ATRP initiating groups by esterification with 2-bromoisobutyryl bromide.[508] PDVB microspheres have been functionalized with ATRP initiating groups via hydroboration/oxidation of the pendant vinyl groups, followed by esterification with bromopropionyl bromide.[482]

In addition to the hydroxyl and carboxylic acid groups that have been discussed so far, several other functional groups can also be used to activate "inert" polymer substrates and allow the attachment of initiators or iniferters for SI-CRP. Segmented polyurethane (PU) films, for example, were treated with chloromethyl methyl ether to introduce $-CH_2Cl$ groups, which were subsequently modified with sodium *N*,*N*-diethyldithiocarbamate trihydrate to provide a diethyldithiocarbamate-functionalized substrate.[509] These modified PU substrates allowed the growth of polymer brushes via SI-PIMP. Cross-linked poly(styrene-*co*-divinylbenzene) (PS-*co*-PDVB) beads were chlorosulfonated using chlorosulfonic acid and modified with 2-chloroethyl amine to produce 2-chloroethyl sulfonamide ATRP initiator groups.[510] Alternatively, the chlorosulfonated polymer beads can be modified in a multistep process with *N*-chlorosulfonamide groups, which can be used to initiate SI-ATRP.[511,512]

All of the strategies discussed so far to functionalize "inert" polymer substrates with ATRP or NMP initiators or RAFT agents are based on multistep synthetic protocols. There are, however, several alternative protocols that allow modification of "inert" polymer substrates with SI-CRP active functional groups in a single step. Polypropylene, for example, can be

Table 12. Overview of Inert Polymer Substrates That Have Been Modified with Initiators, Iniferters, and RAFT Agents To Allow SI-CRP

Substrate and substrate geometry	Activation protocol	Anchoring site or initiator	Anchoring group	Initiator/iniferter /RAFT agent	Immobilization protocol: Single step	Immobilization protocol: Multi step	SI-CRP technique	Polymer brush	Ref
Ground tire rubber (particle)	$NaOH / KMnO_4$	C–OH			×		ATRP	PS, PMMA, PEA, PBA	498
HDPE	Maleic anhydride	$–CO_2H$		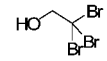	×		ATRP	PMMA	519
HDPE	No activation	C–H, C–C		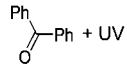	×		Reverse ATRP	PMMA	519
Nylon (membrane pore size: 1.2 μm)	Formaldehyde	C–OH			×		ATRP	PHEMA, PPEGMA, PHEMA-*b*-PPEGMA	508
PDMS (planar)	HCl	–OH			×		ATRP	PHEMA	503
PDMS (stamp)	O_2 plasma	–OH			×		ATRP	PMETAC	502
PDMS (microfluidic chips)	UV / ozone	–OH		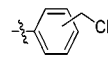	×		ATRP	PAM	500
PDMS (planar)					×		ATRP	PAM	501
					×		ATRP	PAM	313
PDMS (planar)	No activation			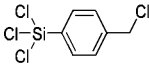	×		ATRP	PPEGMA	517
PTFE (film)	H_2 plasma / O_3 treatment	C–OH			×		ATRP	PSS(Na)	496
PDVB (bead, diameter 3 μm)	Halogenated with HCl			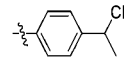			ATRP	PS, PS-*b*-PMS	514
PDVB (microsphere)	Hydroboration	C–OH			×		ATRP	PHEMA, PDMAEMA	482
PDVB (bead, diameter 2.36 μm)	Halogenated with HBr			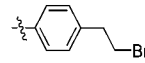			ATRP	PGMA	895
PET and PEN (film)	O_2 plasma	C–OH			×		ATRP	PNIPAM	499
PET (film)	$NaOH/CH_3COOH$ further oxidation	–COCl				×	ATRP	PMMA, PAM, PMMA-*b*-PAM	505
PET (track-etched membranes, pore diameter: 400 nm)	$KMnO_4 / H_2SO_4$	$–CO_2H$				×	ATRP	PNIPAM	506, 896
PGMA-*co*-PEDMA (porous particles: diameter 5.8 μm, pore size 40 nm)	Acidic hydrolysis	C–OH			×		ATRP	PSPMA(K)	504
PGMA-*co*-PMMA (film)	Air plasma	C–OH			×		ATRP	PEGMEMA	725
PMMA (capillary)	O_2 plasma	C–OH			×		ATRP	PPEGMEMA	497
Polyurethane (film)	Chloromethylation	C–Cl		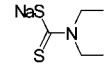	×		PIMP	PPEGMA, PDMAM	509
Polyimide (film)	Chloromethylation			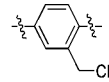			ATRP	PPFS, PTFEMA, PHEMA, PPFS-*b*-PHEMA, PTFEMA-*b*-PHEMA	516
Polyimide (film, Kapton®)	Chloromethylation			C–Cl			ATRP	P4VP	897

Table 12. Continued

Substrate and substrate geometry	Activation protocol	Anchoring site or initiator	Anchoring group	Initiator/iniferter /RAFT agent	Immobilization protocol: Single step	Immobilization protocol: Multi step	SI-CRP technique	Polymer	Ref
PP (planar)	Halogenation with Br_2			C–Br			ATRP	PNIPAM	513
PP (planar)	No activation	C–H, C–C	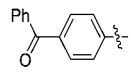		×		ATRP	PDMAEMA	518
PP (hollow fiber membrane, pore diameter: 40–200 nm)	O_3 / O_2	C–OH			×		ATRP	PEGMEMA, PDMAEMA	495
PS-*co*-PDVB (particle, diameter: 353 nm)	Chloromethylation			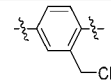			ATRP	PMMA, PMA	515
PS-*co*-PDVB (bead, 420–590 μm)	Cholorosulfonation	$-SO_2Cl$		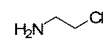	×		ATRP	PGMA	510
PS-*co*-PDVB (bead, 420–590 μm)	Cholorosulfonation	$-SO_2Cl$				×	ATRP	PMMA, PEA	511
PS-*co*-PDVB (bead, 210–420 μm)								PAM	512
PS-*co*-PDVB (bead)	Chloromethylation	C–Cl		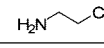	×		ATRP	PNVP	883
PVDF (film)	LiOH/$NaBH_4$/DIBAL-H	C–OH			×		ATRP	PMMA, PPEGMEMA, PPEGMEMA-*b*-PDMAEMA	507
PVDF (film)	LiOH/$NaBH_4$/DIBAL-H	C–OH	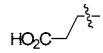	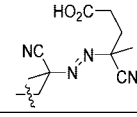		×	Bimolecular RAFT	PMMA, PPEGMEMA	120

photobrominated to generate alkyl bromide groups that can be used directly to initiate SI-ATRP.[513] Similarly, the surface vinyl groups of PDVB microspheres can be hydrochlorinated using HCl to generate chloroethylbenzene moieties that can initiate ATRP.[514] Cross-linked PS latex particles[515] and Kapton,[516] an aromatic polyimine, have been modified with benzylchloride groups capable of initiating ATRP via chloromethylation using trioxane/chlorotrimethylsilane/$SnCl_4$ and, respectively, paraformaldehyde/chlorotrimethylsilane/$SnCl_4$. Polydimethylsiloxane (PDMS) substrates can be modified with benzylchloride moieties by vapor deposition of 4-(chloromethyl)phenyl trichlorosilane followed by a hydrolysis step. This generates a surface-confined benzylchloride-functionalized semi-interpenetrating network that can be used to initiate ATRP.[517] In contrast to all other techniques that are available to modify PDMS substrates with functional groups that can initiate or mediate SI-CRP, this strategy obviates the need for UV/ozone pretreatment. Another very interesting approach that allows the one step modification of "inert" polymer substrates is based on benzophenone photochemistry. Under UV radiation, benzophenone can abstract a hydrogen atom from neighboring aliphatic C−H groups to form a C−C bond. The benzophenone group in benzophenonyl 2-bromoisobutyrate has been used as an anchor to promote the immobilization of ATRP initiator on PP.[518] Alternatively, benzophenone was grafted onto high-density polyethylene (HDPE) and used as an initiator for reverse ATRP.[519]

2.3.8.3. Direct Polymerization from Initiator-, Iniferter-, or RAFT Agent-Modified Polymer Surfaces. The previous two sections have discussed a variety of possibilities to postmodify prefabricated polymer substrates with functional groups that can initiate or mediate SI-CRP. An alternative approach to prepare polymer brushes involves the synthesis of polymers that contain those functional group and which can be processed to form surfaces from which SI-CRP can be initiated. Table 13 provides an overview of different initiator-, iniferter-, and RAFT agent-modified polymers and polymer particles which have been used as substrates for SI-CRP.

A variety of initiator or iniferter-functionalized polymers has been prepared and used to graft polymer brushes via SI-CRP. PCMS prepared via free radical polymerization was spin coated onto PS substrates and used to initiate ATRP.[520] Mecerreyes and co-workers synthesized a copolymer composed of 2-(2-bromoisobutyryloxy)ethyl methacrylate and methyl methacrylate (PBIEMA-*co*-PMMA) which was used to allow SI-ATRP from patterned silicon surfaces.[521] A structurally related copolymer of 2-(bromoisobutyryloxy)-ethyl acrylate and 2-(trimethylammonium iodide)ethyl methacrylate (PBIEA-*co*-PTMAEMA) was developed by Baker, Bruening, and co-workers and used to coat polyethersulfone membranes via layer-by-layer self-assembly with macroinitiators for SI-ATRP.[522] Photoiniferter-based macroinitiators have been prepared by free radical copolymerization of (methacryloylethylene dioxycarbonyl)benzyl *N*,*N*-diethyldithiocarbamate (MEDCBDC)[210,256] or vinylbenzyl *N*,*N*-diethyldithiocarbamate (VBDC).[200,222] Alternatively, photoiniferter-functionalized polymers can be prepared, for example, via postmodification of PCMS with sodium diethyldithiocarbamate.[523] Polymer films able to initiate PIMP have also been fabricated via photopolymerization of a mixture of acrylates, methacylates, or styrene in the presence of iniferters.[230,524–526] In this case, polymer chains capped with iniferters are present on the surface of the resulting polymers and were reactivated to initiate PIMP.

In addition to soluble polymers, also a range of polymer micro- and nanoparticles functionalized with initiators, iniferters, and RAFT agents has been prepared and used as substrates to graft polymer brushes via SI-CRP. Emulsion

Table 13. Overview of Initiator-, Iniferter-, or RAFT Agent-Functionalized Polymers That Have Been Used as Substrates To Prepare Polymer Brushes via SI-CRP

Substrate and substrate geometry	Substrate preparation	Initiator/iniferter /RAFT agent	SI-CRP technique	Polymer	Ref
PBIEA-*co*-PTMAEMA (adsorbed onto porous and planar poly(ether sulfon membrane)	Free radical polymerization		ATRP	PHEMA, PDMAEMA	522
P*t*BA-*co*-PEGDA/PBIEA core/shell particle (diameter: 140 nm)	Seed emulsion polymerization		ATRP	PPEGMEMA	531
PBIEMA-*co*-PMMA (film)	Free radical polymerization		ATRP	PSPMA(K), PZMA	521
PS-*co*-PDVB/PBIEMA-*co*-PDVB core/shell particle (diameter: 50 nm)	Seed emulsion polymerization		ATRP	PDMAEMA	532,533
PS/PBPEA and PS/PBPEA-*co*-PS-*co*-PDVB core/shell particles (diameter: 920 nm)	Seed emulsion polymerization		ATRP	PNIPAM	534,535
PBPEA-*co*-PS-*co*-PDVB particle (diameter: 100 nm)	Emulsion polymerization		ATRP	PHEA, PMETAC	536
PS/PCPEA core/shell particle (diameter: 587 nm)	Shell-growth emulsion polymerization		ATRP	PNIPAM	537
PS/PCPEA-*co*-PS or PBPEA-*co*-PS core/shell particle (diameter: 509–551 nm)	Shell-growth emulsion polymerization	 X = Br, Cl	ATRP	PNIPAM, PDMAM, PMEAM, PNIPAM-*b*-PDMAM, PDMAM-*b*-PMEAM, PDMAM-*b*-PNIPAM, PMEAM-*b*-PNIPAM	538
PS/PCPEA-*co*-PS core/shell particle (diameter: 551 nm)	Shell-growth emulsion polymerization		ATRP	PDMAM	539
PS/PCIEA core/shell particle (diameter: 509–580 nm)	Shell-growth emulsion polymerization		ATRP	PDMAM, PMEAM, PNIPAM, PMEAM-*b*-PNIPAM	540
			ATRP	PDMAM	311,541
PCMS particle (diameter: 100 nm)	Emulsion polymerization		ATRP	PTMSPMA	527
PCMS (film spin coated onto PS)	Free radical polymerization	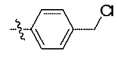	ATRP	PNIPAM	520
PCMS derivatized (film spin coated onto QCM crystal)	Post-functionalization		PIMP	PAM, PAA, PAM-*co*-PAA	523
PCMS-*co*-PDVB particle (diameter: 160nm)	Emulsion polymerization	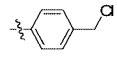	ATRP	P4VP	528
PCMS-*co*-PEGDMA particle (diameter: 500–600 μm)	Emulsion polymerization	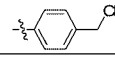	ATRP	PDMAEMA	529
PDVB particle (diameter: 2 μm)	Precipitation polymerization	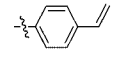	Bimolecular RAFT	PS	530
PDVB-*co*-PS en capped with initiator for NMP (porous membrane, pore size: 50–1000 nm)	NMP	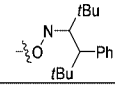	NMP	PCMS, P4VP, P*t*BMA	544
Poly(phthalazinone ether sulfone ketone), (nanoporous membrane, pore size: 10 nm; chloromethylated)	Chloromethylation	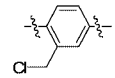	ATRP	PPEGMEMA	542
Poly(acrylates) (complexe composition, Iniferter-functionalized)	Photopolymerization in the presence of iniferter (polymer chains end-capped with iniferter)		PIMP	PPEGA-*co*-PPEGASF	524
				PPEGMA, PHEMA, PTFEA, POA, P*t*BA	525
Poly((meth)acrylates), Poly(thiol ene) (film, complexe composition; iniferter-functionalized)				PTFEA, PPEGA	526
PPEGDMA (film, iniferter-functionalized)				PPEGDMA-*co*-PEGMA, PPEGDMA, PMAA	230
PS (film, cross-linked; iniferter-functionalized)				PPEGDMA-*co*-PEGMA	230
Poly(methacrylates) (complex composition, iniferter-functionalized)	Photopolymerization in the presence of MEDCBDC	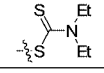	PIMP	PPEGMEMA	210,256
Poly(ether imide) (microporous membrane, chloromethylated)	Membrane obtained by the by the phase inversion technique	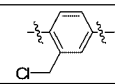	ATRP	PPEGMEMA, PPEGMEMA-*b*-PTFEA	543
PVBDC-*co*-PS (film)	Free radical polymerization	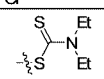	PIMP	PCMS-*co*-PDMAM, PCMS-*co*-PDMAEMA	222
				PDMAM, PDMAPAM, PMAA, PS, PDMAPAMMI, PDMAPAMMI-*b*-PMAA	200
PVPBMP-*co*-PDVB (microcellular monolith surface)	Free radical polymerization		ATRP	PMMA	545

Table 14. Overview of Polymer Substrates That Have Been Used To Graft Polymer Brushes via Direct Radiation/Plasma-Mediated SI-CRP

Substrate and substrate geometry	Radiation/plasma activation	SI-CRP technique	Polymer	Ref
Cellulose (fibers)	γ-radiation	Bimolecular RAFT	PS	548
PP (planar)	γ-radiation	Bimolecular RAFT	PS	546
PP (planar)	γ-radiation	Bimolecular RAFT	PS-*co*-PTMI	547
PE-*co*-PP (planar)	γ-radiation	Bimolecular RAFT	P*t*BA, P*t*BA-*b*-PS	549
PE (planar)	γ-radiation in air	Reverse ATRP	PMMA	551
PVDF (microfiltration membrane, pore size 450 nm)	UV/air	Reverse ATRP	PMMA, PPEGMEMA	550
PTFE (film)	Ar plasma/air	Bimolecular RAFT	PGMA	252
PTFE-*co*-PHFE (film)	O_2 plasma	Bimolecular RAFT	PHEMA	121

(co)polymerization of chloromethylstyrene has been used in several cases to prepare chloromethyl-functionalized polymer particles that can be used to initiate SI-ATRP.[527–529]

The residual double bonds on the surface of cross-linked PDVB microspheres have been used to graft brushes by bimolecular RAFT.[530] Heterophase polymerization techniques have also been employed to prepare core/shell particles composed of an inert core and an outer shell containing functional groups that are able to initiate ATRP. Seed emulsion polymerization, for example, has been used to synthesize P*t*BA/poly(2-(2-bromoisobutyryloxy)ethyl acrylate) (PBIEA),[531] PS/poly(2-(2-bromoisobutyryloxy)ethyl methacrylate) (PBIEMA),[532,533] PS/poly(2-(2-bromopropionyloxy)ethyl methacrylate) (PBPEA), and PS/PBPEA-*co*-PS-*co*-PDVB[534–536] core/shell particles. Similarly, shell-growth emulsion polymerization has been used to prepare ATRP initiator-functionalized PS/poly(2-(2-chloropropionyloxy)ethyl acrylate) (PCPEA),[537] PS/PCPEA-*co*-PS,[538,539] PS/PBPEA-*co*-PS[538] and PS/poly(2-(2-chloroisobutyryloxy)ethyl acrylate) (PCIEA)[311,540,541] core/shell particles.

Polymers functionalized with groups that can initiate ATRP or NMP have also been used to grow brushes from porous polymer substrates. Phase inversion has been used to prepare ATRP initiator-functionalized porous polymer membranes based on chloromethylated poly(phthalazinone ether sulfone ketone)[542] and poly(ether imide).[543] Porous polymer monoliths have been prepared by copolymerization of styrene and divinylbenzene (PS-*co*-PDVB) initiated by alkoxyamine initiator. After preparation of the polymer, the capped radicals located at the surface of the pores of the monolith were used to initiate NMP.[544] ATRP initiator-functionalized polymer monoliths have been prepared by emulsion copolymerization of divinylbenzene and ATRP initiator-functionalized 4-hydroxystyrene derivatives, which were subsequently used for the SI-ATRP of MMA.[545]

2.3.8.4. Direct Radiation/Plasma-Mediated Polymerization. The previous three sections have presented a broad range of strategies that can be used to prepare polymer substrates with functional groups that can initiate or mediate SI-CRP. Even in the absence of such functional groups, however, brushes can be grown from polymer substrates when they are exposed to UV or γ-irradiation or upon plasma treatment. Table 14 provides a summary of different polymer substrates that have been used to graft brushes via direct radiation or plasma-mediated SI-CRP.

Using γ-irradiation to initiate polymerization and cumyl phenyldithioacetate as a RAFT agent, Barner et al. grafted polymer brushes from polypropylene lanterns[546,547] and cellulose filters.[548] Similarly, Hill and co-workers have modified the surface of polyethylene-*co*-polypropylene (PE-*co*-PP) sheets using 1-phenylethyl phenyldithioacetate as RAFT agent.[549] In these examples, γ-radiation was used to generate radicals both on the polymer surface and in the monomer solution. Monomer radicals and radicals formed on the surface generate propagating chains, which subsequently add to the dithiocarbamyl group of the RAFT agent. In the course of the reactions, both grafted polymer (on the surface) and free, nongrafted polymer (in the solution) are generated. UV and γ-radiation have been used to activate PVDF[550] and PE[551] substrates and allow surface-initiated reverse ATRP. Peroxide initiators have been generated directly on PTFE surfaces via radiofrequency argon plasma pretreatment, followed by air exposure[252] or on PTFE-*co*-poly(hexafluoropropylene) (PHFP) film via oxygen plasma treatment[121] and were used as initiating site for bimolecular RAFT.

2.4. Patterning Strategies

Patterned polymer brushes are not only of interest for many applications, ranging from microelectronics to biomaterials,[552] but are also useful tools to study fundamental questions of surface-tethered polymer films, such as swelling behavior.[553] Patterned polymer brushes can be prepared via SI-CRP following either "bottom-up" or "top-down" strategies. While the former are based on the decoration of the substrate surface with a pattern of initiator or iniferter molecules, the latter strategies involve the selective removal of surface-attached polymer chains. A wide variety of technologies is available for the preparation of patterned polymer brushes via SI-CRP using both "bottom-up" and "top-down" approaches. These techniques are summarized in Table 15 and will be discussed in the subsequent sections.

2.4.1. Microcontact Printing

Microcontact printing (μCP) is one of the most extensively used techniques to create patterned polymer brushes. In μCP, an elastomeric PDMS stamp is used to print a pattern of molecules onto the surface of a substrate.[554] μCP was first applied to the preparation of patterned SAMs of alkanethiols on gold. After the first printing step, the nonprinted areas can be backfilled with another thiol molecule that contains a different functional group, which leads to a chemically patterned surface.

To obtain patterned polymer brushes, μCP can be used either to directly print a "polymerization-active" ink or to print a passive pattern, which is then backfilled in a second step with a molecule containing a polymerization initiator or iniferter. The second strategy is illustrated in Figure 5. As "polymerization-active" inks, both low molecular weight[260,292,297,343,499,553,555–559] and polymeric initiator/iniferter-functionalized molecules have been used.[343] Also for the second approach, both low molecular weight initiator/iniferter molecules[87,110,259,416,560–566] and polymers have been used to pattern the substrate surface with a passive layer.[567,568] μCP

Table 15. Overview of Different Techniques That Have Been Used To Prepare Patterned Polymer Brushes via SI-CRP

Technique	Substrate	Polymerizations technique	Details	Ref
Microcontact printing (μCP)	Au	ATRP	μCP of "inert molecule" followed by backfilling with the ATRP initiator.	87,110,416, 561-563,565
	SiO_2	ATRP	μCP of "inert" molecule followed by backfilling with APTS,[a] which was then reacted with BMPA[b] in order to give a patterned ATRP initiator surface.	566
	Au	ATRP	μCP of a thiol initiator; using this technique single patterned brushes[259,260,292,297,553,557-559,564,569] or multicomponent brushes[555] can be obtained.	258-260,292, 297,553,555, 557-559,564, 569
	SiO_2, Polymer (PET,[d] PEN[e])	ATRP	μCP of a silane initiator (polymer surfaces need to be activated by plasma oxidation).	499
	SiO_2	ATRP	μCP of a polyelectrolyte macroinitiator (electrostatic adsorption).	343
	Glass	ATRP	μCP of a polymer on the glass substrate. The "free" surface was reacted with a silane initiator by vapor deposition.	567
	Polymer	ATRP	μCP of a polymer on the substrate. The "free" surface was covered with gold colloids. Subsequently a thiol initiator was attached onto the gold surface.	568
	Au	PIMP	Formation of a mixed SAM[f] by μCP.	212
Electron beam-assisted methods	SiO_2	ATRP	The electron beam was used to selectively destroy the initiator.	326,327,570
	Au	ATRP	The electron beam was used to selectively "activate" an amino hydrochloride SAM,[f] which was then reacted with BiBB[c] to give a patterned initiator surface.	573
	Au	ATRP	The electron beam was used to create a mixed SAM[f] by irradiation-promoted exchange reaction of the aliphatic SAM[f] by aminothiol. The amino end-groups were then reacted with BiBB[c] to give a patterned initiator surface.	572
	Au	ATRP	The electron beam was used to reduce selectively the terminal nitro groups into amino groups, which were subsequently reacted with BiBB.[c]	418,571
	SiO_2	ATRP	The electron beam was used to create holes in a PMMA spin coated film. Subsequently the resulting "free" SiO_2 surface was cleaned with oxygen plasma and reacted with a monochlorosilane initiator (gas phase silanation).	575
	SiO_2	ATRP	The electron beam was used to pattern a spin coated film on a silicon wafer. A gold layer was then deposited and the resist was lifted off leading to a patterned gold/SiO_2 surface. A thiol ATRP initiator was then deposited on the gold part.	574,856
UV-assisted methods	Polymer	PIMP	Selective polymerization using a light sensitive initiator ("photoiniferter"). The substrate contains a photoiniferter and a UV "inert" copolymer.	199,200,230, 256,526
	Au	ATRP	Selective destruction of the polymer brush; from the UV-etched area a new brush can be grown.	579-581
	SiO_2	ATRP	Selective destruction of the initiator by UV exposure through a photomask.	576,577
	SiO_2	ATRP	Selective destruction of the APTS[a] monolayer. The remaining amino groups were reacted with BiBB[c] to create a patterned initiator surface.	578
	Si	ATRP	Selective grafting of the ATRP initiator; VBC[g] was reacted with pure Si surface upon UV irradiation.	353,354
	Glass	PIMP	Photopolymerization from a substrate patterned with chromium, the initiator only attaches to the glass, which leads to a patterned polymer/chromium surface.	207
	SiO_2	ATRP	Selective immobilization of the initiator on a SiO_2 surface patterned with resist.	552
	Ti, Stainless steel	ATRP	A spin coated film on a metal surface was patterned by UV exposure through a photomask. ATRP initiator was grafted on the "free" metal surface generated by the UV etching.	385
	SiO_2	ATRP	A solution of polystyrene containing a photoacid generator was spin coated onto the top of a poly(*tert*-butyl acrylate) brush; exposure to UV light through a mask resulted in the photogeneration of acid in specific areas of the overlayer, which locally hydrolyzed the poly(*tert*-butyl acrylate) brush.	190
	SiO_2	ATRP	A SAM[f] of poly(ethylene glycol) on a silicon surface was exposed to oxygen plasma through a patterned photoresist (patterned using UV exposure). The etched regions were then backfilled with an initiator for ATRP.	582
SPM-assisted methods	Au	ATRP	An AFM tip was employed as a "nanotool" to selectively remove the "inert" thiol SAM[f] (nanoshaving). Subsequently, the freshly exposed gold surfaces were backfilled with the thiol ATRP initiator. A similar process was applied to selectively remove an area of a polymer brush.[586]	585
	SiO_2	ATRP	A conductive AFM tip was used to locally oxidize an ODTS[h] SAM.[f] The oxidized area was subsequently covered with a hydroxyl-terminated silane, which was further reacted with BiBB.[c]	587
	Au	ATRP	An AFM tip was used as a "pen" to imprint thiol initiator on a surface ("dip pen" lithography[588]).	292
	Si	PIMP	"Dip-pen" lithography[588] was used to deposit gold nanowires on a silicon substrate. A disulfide iniferter was then selectively attached on those gold wires.	584
Nanoimprint and contact lithography	SiO_2	ATRP	A copolymer containing ATRP initiating groups was spin coated and the resulting film patterned using nanoimprint lithography.	521
	SiO_2	ATRP	Nanoimprint lithography was used to fabricate holes in a spin coated PMMA film, which was subsequently backfilled with an ATRP initiator-containing silane.	575
	SiO_2/Glass	ATRP/NMP	A patterned polymeric mold was used to template a second liquid photopolymer resin layer, which included ATRP or NMP initiator and was subsequently UV polymerized to allow pattern transfer.	192,589,630

[a] APTS: 3-(aminopropyl)tri(m)ethoxysilane. [b] BMPA: 2-bromo-2-methylpropionic acid. [c] BiBB: bromoisobutyryl bromide. [d] PET: poly(ethylene terephthalate). [e] PEN: poly(ethylene naphthalate). [f] SAM: self-assembled monolayer. [g] VBC: 4-vinylbenzyl chloride. [h] ODTS: octadecyl trichlorosilane.

has been mostly carried out using thiol-based inks on gold substrates,[87,110,258–260,292,297,416,553,555,557–559,561–565,569] but it has also been successfully applied to silicon wafers[343,499,560,566] as well as to polymer substrates such as poly(ethylene

terephthalate) or poly(ethylene naphthalate).[499] While μCP has been mostly used to prepare topographically patterned brushes such as illustrated in Figure 5, Zhou et al. developed a general μCP-based route that allows access to laterally patterned multicomponent brushes.[555] The approach developed by these authors involved μCP of an ATRP initiator-functionalized thiol, followed by SI-CRP and deactivation of "living" chain ends. By repeating this sequence of steps three times, it was possible to generate a PMAA/PMEP/PNIPAM/PDMAEMA quaternary brush.[555]

In all the examples discussed above, μCP was used to pattern the substrate surface from which the polymer brushes were grown. In an alternative approach, van Poll et al. have shown that a hydrophilic/hydrophobic patterned thiol SAM on gold prepared by μCP can be used as a master to generate chemically patterned PDMS substrates from which PPEGMA brushes could be grown using SI-ATRP.[556]

2.4.2. Electron Beam-Assisted Methods

Electron beam irradiation has been explored in different ways as a tool to produce patterned polymer brushes. Using a focused electron beam or an appropriate mask, electron beam irradiation can be used to selectively decompose surface-attached polymerization initiators or the living ends of surface-tethered polymer chains. This strategy was used by Maeng et al. to generate patterned PMMA and PS brushes by irradiating an ATRP initiator layer through a TEM grid as a mask.[326] In a subsequent report, by taking advantage of the living character of ATRP and by repeating the irradiation step, these authors went one step further and used this strategy to prepare a rectangular PMMA micropattern onto a polystyrene brush.[327] Tsujii et al. studied the influence of the electron beam dose on the patterning process. In their study, these authors found that doses larger than 2000 $\mu C/cm^2$ were sufficient to decompose a monolayer of the ATRP initiator 2-(4-chlorosulfonylphenyl)ethyl trichlorosilane.[570]

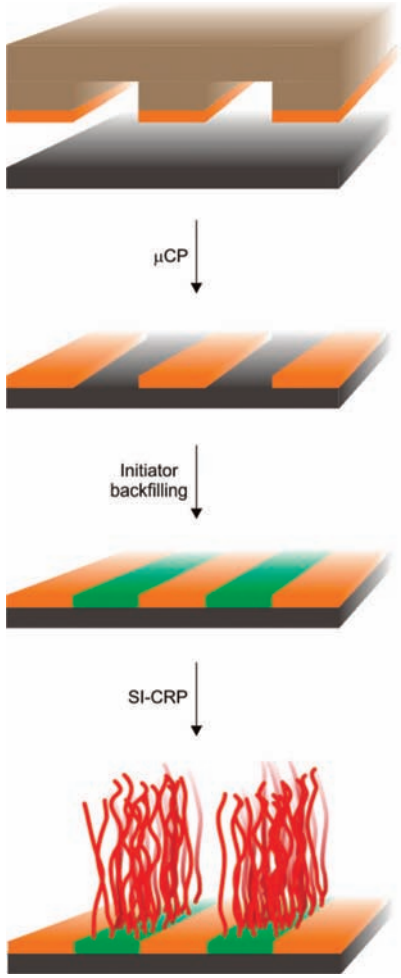

Figure 5. Preparation of a patterned polymer brush via microcontact printing (μCP) of a passivating pattern, followed by backfilling with an initiator- or iniferter-modified molecule and subsequent SI-CRP.

In addition to selectively decomposing surface-immobilized initiators or active polymer chain ends, electron beam irradiation can also be used in a bottom-up fashion to produce patterned, initiator-modified substrates. Using electron beam irradiation, He et al. generated cross-linked 4′-amino-1,1′-biphenyl-4-thiol patterns into a 4′-nitro-1,1′-biphenyl-4-thiol SAM.[418,571] In a subsequent step, the amino groups were reacted with 2-bromoisobutyryl bromide to give a patterned ATRP initiator surface. Similar to Tsujii et al.,[570] He at al. also observed that the surface concentration of amino groups was dependent on the electron beam dose.[571] By monitoring the obtained brush thickness as a function of the electron dose, a threshold value of about 40 $\mu C/cm^2$ at which all nitro groups were converted was found.

Zharnikov and co-workers have reported two other interesting electron beam-assisted approaches for the preparation of patterned polymer brushes. The first approach is referred to as the irradiation-promoted exchange reaction and is based on the generation of chemical and structural defects in an inert alkanethiol SAM, which promotes exchange reactions with functional thiols that can be further derivatized with, for example, ATRP initiating groups.[572] The second strategy was based on the observation that 11-amino-undecanethiol SAMs that were exposed to electron irradiation prior to attachment of the ATRP initiator (bromoisobutyryl bromide) afforded thicker PNIPAM brushes as compared to pristine SAMs that were modified with the same initiator. The authors speculated that the repressed reactivity of the pristine SAM was due to binding of an oxygen-containing quencher moiety.[573]

Electron beam irradiation can also be used to generate patterned substrates that allow selective attachment of initiator molecules. Zauscher and co-workers have created gold squares in the size range of 100 nm to 4 μm on silicon wafers by lift-off electron beam lithography. To this end, a PMMA film was spin coated on a silicon wafer and subsequently patterned by selective exposure to the electron beam. After evaporation of a layer of chromium and a layer of gold, the developed resist was lifted off, leaving behind the desired gold patterned silicon wafer. Onto these gold patterns, a thiol initiator can be attached selectively to allow the growth of a polymer brush.[574]

Jonas et al. used electron beam irradiation to create circular holes with diameters from 35 nm to several micrometers in a spin coated PMMA film onto a SiO_2 surface. Subsequently, a silane initiator was attached on the "free" SiO_2 surface. After that, the remaining polymer mask was removed, the unmodified surface backfilled with an inert silane, and the polymer brush grown using SI-CRP.[575]

2.4.3. UV Irradiation-Assisted Methods

Similar to electron beam irradiation, UV irradiation can be used in several ways to produce patterned polymer brushes. Among the different possible techniques, surface-

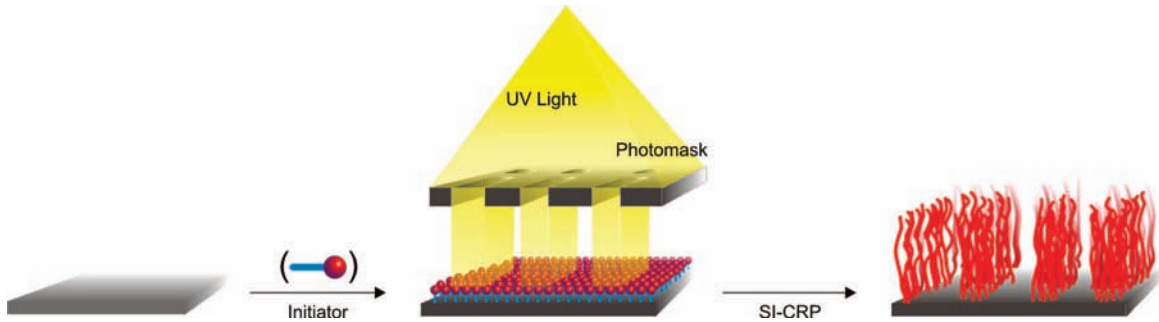

Figure 6. UV irradiation-assisted preparation of patterned polymer brushes. In this example, UV irradiation is used to selectively decompose initiator molecules in areas that are not covered by the photomask. Subsequent SI-CRP only generates polymer brushes in areas that were not exposed to UV irradiation.[576,577] Reproduced with permission from ref 576. Copyright 2006 Wiley-VCH Verlag GmbH & Co. KGaA.

initiated photoiniferter-mediated polymerization (SI-PIMP) is particularly convenient, since the polymerization requires photolytic dissociation of a photoiniferter molecule. Already in 1996, Nakayama and Matsuda demonstrated that patterned homopolymer and block copolymer brushes based on *N*,*N*-dimethylacrylamide, *N*-(3-(dimethylamino)propylacrylamide), methacrylic acid, or styrene can be grown from photoiniferter-modified polymer films.[200] Several other examples have been reported since then, either using photoiniferter-modified polymer films as the substrate[199,215,222,230,256,524,526] or by grafting photoiniferter-modified silanes onto glass surfaces.[202,205] Higashi et al. demonstrated the possibility of creating multicomponent polymer brushes using SI-PIMP by irradiating sequentially a selective area of a polymer containing a photoiniferter in the presence of a certain monomer.[199] This strategy allowed successive growth of up to five different brushes on five different regions of the same substrate. De Boer et al. prepared patterned PMMA, PS, and PS-*b*-PMMA brushes on glass substrates using SI-PIMP.[207] These brushes were grafted from chromium patterned glass substrates using a trimethoxysilane-modified photoiniferter that only binds to the glass substrate.

UV irradiation has also been used to photodecompose surface-bound ATRP initiators.[576,577] By using a photomask, ATRP initiator patterned substrates can be prepared, and during the subsequent polymerization step, brushes will only grow in areas that were not exposed to UV irradiation (Figure 6). Kamitani et al. have used UV irradiation to (partially) decompose a 3-(aminopropyl)trimethoxysilane (APTS) SAM.[578] The remaining intact amino groups could be further modified to generate ATRP initiating sites for SI-CRP. Yamamoto et al. used grazing-angle reflection−absorption infrared spectroscopy to monitor the photodecomposition of 2-(4-cholorosulfonylphenyl)ethyl trichlorosilane on a silicon wafer.[310] In their experiments, the authors found that a 20 min irradiation time was sufficient to photodecompose 90% of the initiator layer. In general, however, results from photodecomposition experiments are difficult to compare, since different studies use different UV light sources and variable light source−substrate distances, among others.

Kang, Neoh, and co-workers have used the UV-induced hydrosilylation to produce micropatterned monolayers of 4-vinylbenzyl chloride (VBC) on hydrogen-terminated silicon substrates.[353,354] The VBC moieties could be used to initiate SI-ATRP, while the unmodified areas of the substrate could be further modified to allow SI-RAFT or SI-NMP to produce micropatterned binary brushes.

In addition to deactivating surface-immobilized initiators, or functional groups that can be used to introduce polymerization-active groups, UV irradiation can also be used to selectively degrade (etch) polymer brushes. Zhou et al. have used this strategy to prepare patterned polymer brushes by exposing a polymer brush-covered substrate to UV irradiation through a photomask.[579–581] An etching rate of ~10 nm/h was observed for poly(methacrylate) brushes. The authors further demonstrated that it is possible to selectively and completely remove the polymer brush layer, modify the etched substrate with a polymerization initiator, and generate a patterned binary PHEMA/PMMA brush by SI-ATRP of a second monomer.[581] Husemann et al. prepared patterned binary PAA/P*t*BA brushes via selective, UV-mediated deprotection of the *tert*-butyl ester groups.[190] This was accomplished by spin coating a solution of polystyrene containing a photoacid generator onto a P*t*BA brush, followed by exposure to 248 nm irradiation through a mask.

In addition to the examples discussed above, UV irradiation has also been used in a more conventional fashion to prepare thin, patterned photoresist layers.[385,582,583] The uncovered substrate can then be modified with a polymerization initiator and used to grow a polymer brush after lift-off of the photoresist material.

2.4.4. SPM-Assisted Methods

Although they are relatively slow and not very amenable to mass production, scanning probe microscopy (SPM)-based patterning techniques offer a high spatial resolution (down to 20 nm).[584] Zauscher and co-workers have used the nanoshaving technique to graft patterned PNIPAM brushes from gold substrates.[585,586] This method uses an AFM tip as a nanomechanical tool to selectively produce a pattern in an alkanethiol resist. The freshly exposed gold surface in the trenches can be backfilled with a thiol-modified initiator and used to start SI-CRP. Another strategy to generate patterned ATRP initiator substrates is based on the use of an AFM tip to locally oxidize regions in a *n*-octadecyl trichlorosilane SAM.[587] The oxidized areas could be further functionalized with a polymerization initiator and were used to grow PMMA brushes. AFM tips can also be used to directly "write" molecules on a substrate surface; this technique is referred to as "dip-pen" nanolithography.[588] Ma et al. used this method to produce spots and lines of a thiol-functionalized ATRP initiator on gold.[292] Zapotoczny et al. used dip-pen nanolithography to deposit gold nanowires on silicon substrates.[584] In a second step, thiol-functionalized iniferters could be selectively immobilized on the gold nanostructures and were subsequently used to grow polymer brushes.

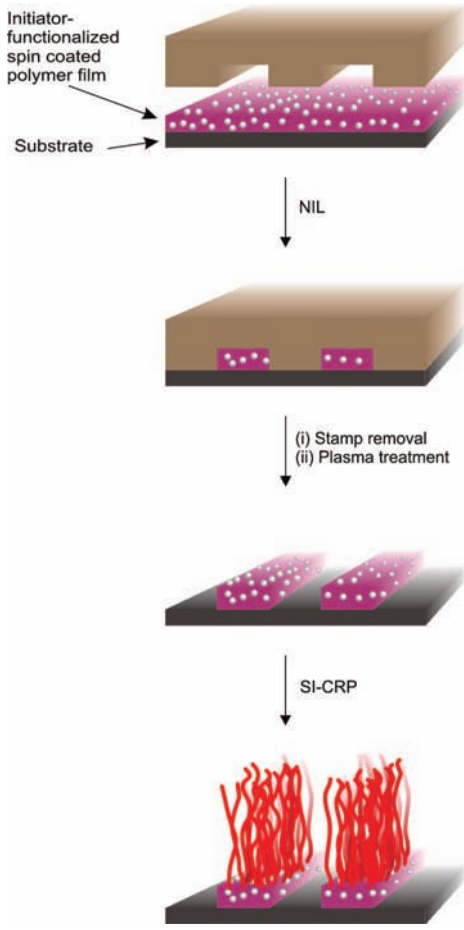

Figure 7. Preparation of patterned polymer brushes via nanoimprint lithography (NIL) of a thin polymerization initiator-functionalized polymer film.

2.4.5. Nanoimprint and Contact Lithography

Genua et al. have used nanoimprint lithography (NIL) to generate a patterned thin film of an ATRP initiator-functionalized copolymer (Figure 7).[521] After removal of the residual polymer in the trenches by an oxygen plasma treatment, these imprinted surfaces were used to grow poly(3-sulfopropyl methacrylate) and fluorinated poly(methacrylate) brushes via SI-ATRP. NIL was used by Jonas et al. to prepare a patterned PMMA substrate where the trenches, after an oxygen plasma treatment, could be backfilled with a polymerization initiator.[575]

Another imprint method that has found use to prepare patterned polymer brushes is "nanocontact molding". In this technique, a patterned polymeric mold is used to template a second liquid photopolymer resin, which can include ATRP or NMP initiator molecules and which is subsequently UV-polymerized to allow pattern transfer.[192,589]

Liu et al. used a method referred to as "capillary force lithography" to create binary patterned brushes.[590] This process started with spin coating a thin polystyrene layer onto an ATRP initiator-functionalized substrate. Then, a PDMS mold was placed over the spin coated film and the system was annealed in an oven. After this heat treatment, the mold was removed, leaving a polystyrene pattern on an ATRP initiator-functionalized substrate. A first surface-initiated polymerization was performed from the uncovered ATRP initiating sites, which was followed by removal of the residual polystyrene and a second SI-ATRP step.

2.4.6. Other Patterning Techniques

In addition to the techniques discussed in the previous sections, a number of other tools has also been used to prepare patterned polymer brushes. Several of these techniques will be highlighted below.

Ejaz et al. prepared mixed monolayers of 2-(4-chlorosulfonylphenyl)ethyl trimethoxysilane and *n*-octadecyl trimethoxysilane on a silicon wafer.[591] Due to the immiscibility of the two silanes, a phase-separated monolayer was formed, which was used to prepare random patterned brushes. Using Langmuir−Blodgett lithography, Brinks et al. managed to produce regularly structured patterns of an NMP initiator-modified silane, which was subsequently used to generate striped polymer brush patterns.[163]

Andruzzi et al. used reactive ion etching to prepare structured oligo(ethylene glycol)-modified polystyrene brushes.[162] To this end, parylene was vapor deposited on a polymer brush-covered substrate. Standard photolithographic patterning, followed by reactive ion etching and peeling off the parylene layer, affords the structured polymer brush.

Plasma techniques have also been used to produce patterned polymer brushes. Teare et al. prepared patterned maleic anhydride modified poly(tetrafluoroethylene) substrates using pulsed plasma deposition through a copper grid.[592] The deposited maleic anhydride groups could be postmodified to introduce polymerization initiators. Lego et al. demonstrated that plasma activation can be used to prepare hydroxyl-functionalized mica substrates, which can be used to attach ATRP initiators.[403]

Lahann and co-workers have used chemical vapor deposition of [2.2]paracyclophane-4-methyl-2-bromoisobutyrate to coat a broad variety of substrates with ATRP initiator groups.[593] In combination with a microstencil, this technique could be used to prepare patterned polymer brushes.

Electrochemistry can also be used to generate patterned brushes, as demonstrated by Slim et al.[594] Their strategy used a scanning electrochemical microscope to selectively destroy a bromoisobutyrate alkyl silane SAM on glass or silicon substrates via a spatially controlled electrochemical dehalogenation reaction. Schubert and co-workers used another approach, which was based on the selective conversion of an alkyl SAM.[595] In this example, a conductive mask was placed on an alkyl SAM-coated substrate. After that, a voltage was applied to the mask for a short time period, which converted the alkyl end-groups of the SAM into carboxylic acid moieties to which an ATRP initiator can be attached.

Sankhe et al. modified a classical office inkjet printer and developed an automated patterning method based on inkjet printing.[596] They used this method to directly print gradients or patterns of thiol-functionalized ATRP initiator onto gold substrates, which were subsequently amplified by surface-initiated polymerization of methyl methacrylate.

2.5. Postmodification of Polymer Brushes

Although radical-based chain polymerizations are characterized by a relatively high functional group tolerance, there are still various functional groups that cannot be introduced into polymer brushes via direct surface-initiated polymerization of the corresponding monomer. This can be due to reaction of these functional groups with the propagating radical chain ends or due to interaction of the functional groups with the polymerization catalyst,

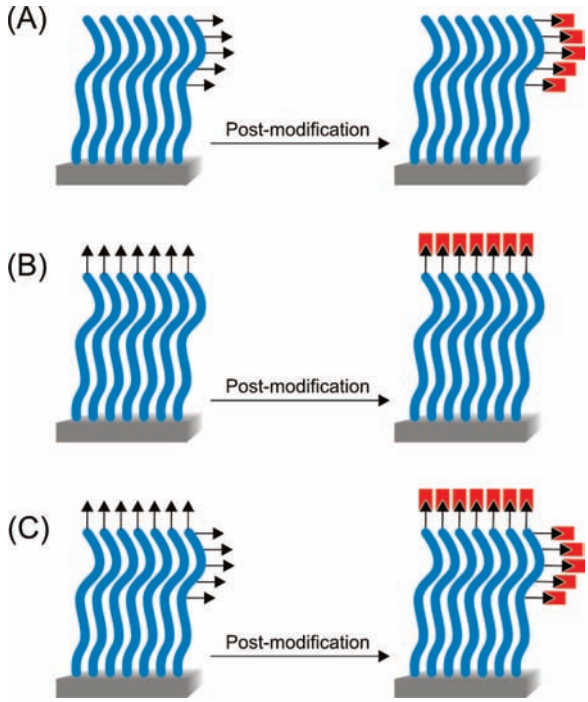

Figure 8. Postmodification of polymer brushes: (A) side chain modification; (B) chain end modification; (C) side chain and chain end modification.

among others. Such sensitive functional groups, however, may be introduced by postmodification of precursor polymer brushes, which contain appropriate reactive groups that are compatible with surface-initiated controlled radical polymerization. As schematically illustrated in Figure 8, postmodification of polymer brushes can involve modification of side-chain functional groups (Figure 8A), modification of the polymer chain end (Figure 8B), as well as a combination of both of them (Figure 8C). In the following six sections, the postmodification of hydroxyl groups, carboxylic acid groups, carboxylic ester groups, epoxide groups, and other side-chain functional groups as well as chain end modification of polymer brushes prepared via surface-initiated controlled radical polymerization will be discussed. Postmodification is usually carried out to adjust the surface properties of polymer brushes or to introduce functional groups that can act as an anchor for further modification. While the major focus of the following sections is on postmodification chemistry, Tables 16−21, which give an overview of the different reactions that can be used to modify side chains and terminal functional groups, also briefly highlight the applications of the modified brushes. Properties and applications of polymer brushes prepared via SI-CRP will be discussed more in detail in section 4.

2.5.1. Postmodification of Hydroxyl-Functionalized Polymer Brushes

Hydroxyl-functionalized polymer brushes have been extensively used as substrates for postmodification reactions. Table 16 gives an overview of several reactions that have been used to modify hydroxyl-side chain functionalized polymer brushes. From the top to the bottom, Table 16 shows approaches that have been used to modify hydroxyl-side chain functionalized brushes with hydrophobic groups, carboxylic acid moieties, and halogen functionalities as well as various strategies to prepare biofunctional polymer brushes and several other options for postmodification. In the remainder of this section, one or several examples of reactions from these different groups will be discussed in more detail.

The modification of hydroxyl-containing polymer brushes with hydrophobic (e.g., fluorinated) groups has been used to tailor the barrier properties, wettability, and etch resistance of polymer brushes, among others. In most cases, these functional groups were introduced via reaction with the corresponding acid chlorides. Bantz et al. studied the kinetics of the acylation of PHEMA with $C_7H_{15}COCl$ and demonstrated that 0−80% of the hydroxyl groups could be modified by controlling the reaction time.[597] In a subsequent report, these authors investigated the acylation of PHEMA with a homologous series of hydrocarbon acid chlorides ($C_nH_{2n+1}COCl$; n = 1, 7, 11, 13, 15, and 17) and observed a decrease in hydroxyl group conversion with increasing hydrocarbon chain length.[598] The same group also reported an interesting strategy for the preparation of fluorocarbon/hydrocarbon block copolymer brushes.[599] These block-type polymer brushes were obtained by acylation of a PHEMA brush with C_6F_5COCl, followed by a controlled alkaline hydrolysis step, which regenerates PHEMA in the top layer, followed by reacylation with hydro- or fluorocarbon acid chlorides.

Hydroxyl-containing polymer brushes have been modified with carboxylic acid groups to produce double responsive brushes, to generate templates for the synthesis of polymer/metal hybrids or to introduce handles for further chemical modification. Carboxylic acid-modified polymer brushes are usually obtained by reacting the precursor hydroxyl-functionalized brushes with an excess of succinic anhydride in the presence of a base, such as pyridine.[328,342,359,448]

The modification of hydroxyl-functional polymer brushes with halogen moieties is of interest, as it can open the way to comb-shaped polymer brushes and also allow further derivatization reactions. Hydroxyl side-chain functional groups can be esterified with 2-bromoisobutryl bromide to introduce ATRP initiating side-chain functional groups.[251] Chlorination of hydroxyl-containing polymer brushes with $SOCl_2$ is a convenient way to introduce chloroalkyl functional groups that can be further modified using nucleophilic substitution reactions.[352,358,359]

Hydroxyl-containing polymer brushes such as PHEMA and PPEGMA have been extensively used as platforms to immobilize peptides, proteins, or other biologically active functional groups. PHEMA and PPEGMA are attractive substrates to fabricate biofunctional or bioactive surface coatings, since they combine nonbiofouling properties with a high density of hydroxyl groups that are available for postmodification. Several strategies have been developed to activate the hydroxyl groups of polymer brushes and allow the immobilization of bioactive molecules. A very popular approach involves the activation of the hydroxyl groups with *p*-nitrophenyl chloroformate (NPC), which generates a carbonate intermediate that can be reacted with the N-terminal amine group of short peptides[389,600,601] or other amine-functionalized moieties.[602] Examples of other alternative reagents that have been used to prepare protein-functionalized polymer brushes include 1,1′-carbonyldiimidazole (CDI)[552] and *N*,*N*′-disuccinimidyl carbonate (DSC).[603,604] Alternatively, PHEMA brushes have been reacted with succinic anhydride to generate carboxylic acid groups, which can then be further modified with amine-function-

Table 16. Overview of Reactions That Have Been Used To Postmodify Hydroxyl Side Chain-Functionalized Polymer Brushes

Polymer brush substrate	Modified polymer brush	Reaction conditions	Conversion	Application	Ref
PHEMA	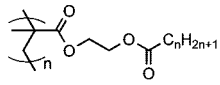	Acylation with acetyl chloride	-	-	88
			93%	-	772
		Acylation with octanoyl chloride	-	Stationary phase for capillary electrochromatography	726
			82%	-	772
			90%	Pervaporation membranes	365
		Acylation with cinnamoyl chloride	-	-	88
		Acylation with lauroyl chloride	77%	-	772
		Acylation with myristoyl chloride	68%	-	772
		Acylation with palmitoyl chloride	64%	-	772
			90%	Pervaporation membranes	365
		Acylation with stearoyl chloride	37%	-	772
PHEMA	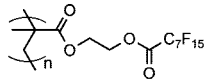	Acylation with pentadecafluorooctanoyl chloride	90%	Pervaporation membranes	365
			-	Increase CO_2 permeability of composite membrane	255
PHEMA	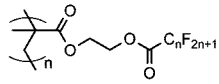	Acylation with perfluoroalkyl and perfluoroaryl acid chlorides	70–85%	-	598
			0–80%	-	597
			-	-	769
PHEMA	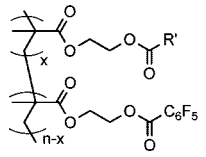	1. Acylation with perfluorobenzoyl chloride 2. Surface hydrolysis with KOH to recover hydroxyl group 3. Acylation with R'OCl	~80%	Barrier coatings	599
PHEMA	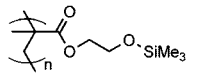	Reaction with trimethylchlorosilane to form the corresponding silyl ethers	-	Hydrophobic surface increasing etch resistance	579, 580
PHEMA	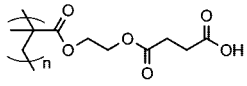	Esterification with succinic anhydride, pyridine	-	Double-responsive copolymer brushes	328
PPEGMA	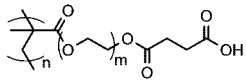	Esterification with succinic anhydride, pyridine	65%	-	359
PDHPMA	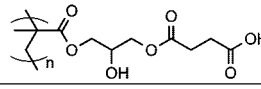	Esterification with succinic anhydride, triethylamine, pyridine	-	-	342
			-	Template for the synthesis of polymer-metal hybrids	448
PHEMA	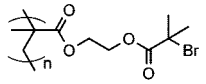	Esterification with 2-bromoisobutyryl bromide	-	-	579
			~100%	Macroinitiator for the preparation of comb-shaped polymer brushes	251
PPEGMA	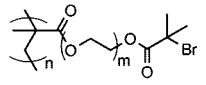	Esterification with 2-bromoisobutyryl bromide	~100%	Macroinitiator for the preparation of comb-shaped polymer brushes	251
PHEMA	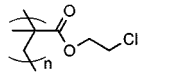	$SOCl_2$, pyridine	~20%	Reactive group for further modification	358
PPEGMA	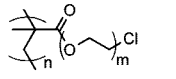	$SOCl_2$, pyridine	70%	-	359
			~32%	Insertion of reactive group for further modification	352
PHEMA	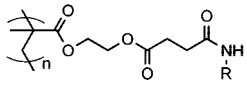	1. Succinic anhydride/DMAP 2. NHS/EDC activation 3. Coupling of gentamicin or collagen (R).	-	Antibacterial (gentamicin) and cell adhesive (collagen) surfaces	387
PHEMA	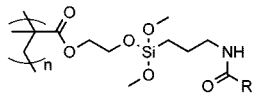	1. Reaction with (3-aminopropyl) trimethoxysilane) 2. Coupling of activated penicillin. R = penicillin.	-	Antibacterial surfaces	387
PHEMA	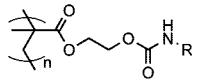	1. NPC activation 2. Coupling with peptide/DMAP. R = peptide containing RGD sequence	-	Specific cell adhesion on a non-biofouling substrate	600
PPEGMA	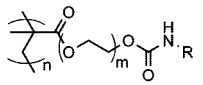	1. NPC activation 2. Coupling with peptide. R = peptide containing RGD sequence	-	Specific cell adhesion on a non-biofouling substrate	600,601

Table 16. Continued

Polymer brush substrate	Modified polymer brush	Reaction conditions	Conversion	Application	Ref
PPEGMA	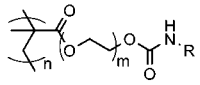	1. NPC activation 2. Coupling with peptide. R = peptide containing GFOGER sequence	-	Specific cell adhesion on a non-biofouling substrate	389
PPEGMA	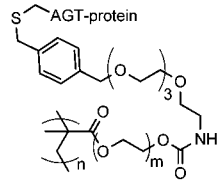	1. NPC activation 2. Benzylguanine derivative/DMAP 3. AGT-mediated protein immobilization	-	Protein microarrays	602
PPEGMA	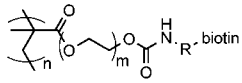	1. DSC/DMAP activation 2. Coupling with biotin or poly(L-lysine) derivatives	-	Non-biofouling polymer films, protein and cell micropatterns	604
PPEGMA	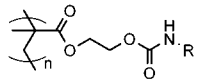	1. CDI activation 2. Coupling of protein. R = human immunoglobulin.	-	Micropatterning of proteins	552
PHEMA	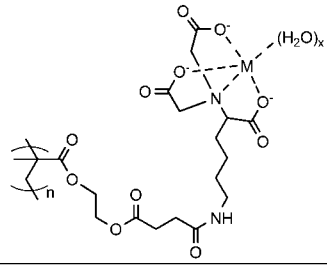	1. Succinic anhydride/DMAP 2. EDC/NHS activation 3. Aminobutyl-NTA 4. Coordination of M: Cu^{II}, Ni^{II}, Fe^{III}	- -	Purification of His-tagged proteins MALDI sample plates	366,367 605,606
PHEMA	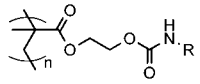	1. DSC/DMAP activation 2. Coupling with RNH_2. R = C_{16} (1); PEG_{20} (2); PEG_{50} (3); C_8F_{15} (4) and others.	90% (1) 87±11% (2) 79±5% (3) 43±6% (4)	Reactive microcontact printing, reactive microcapillary patterning	603
PHEMA	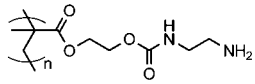	1. CDI activation 2. Ethylendiamine	-	Capillary electrochromatography	726
PPEGMA	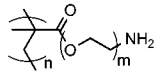	1. $SOCl_2$ 2. Ethylenediamine	43%	-	359
PPEGMA	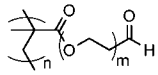	Oxidation with a mixture of acetic anhydride and dimethyl sulfoxide	63%	-	359

alized (bio)molecules using standard peptide coupling conditions.[366,367,387,605,606]

A final postmodification reaction that is worth mentioning is the conversion of hydroxyl side-chains into aldehyde groups. This has been accomplished with a conversion of 63% by exposing PPEGMA brushes to a mixture of acetic anhydride and DMSO at room temperature for 8 h.[359] The resulting aldehyde-functionalized brushes are interesting substrates to allow immobilization of peptides and proteins via reductive alkylation.[607]

2.5.2. Postmodification of Carboxylic Acid-Functionalized Polymer Brushes

Side chain carboxylic acid-functionalized polymer brushes can be prepared via direct polymerization of monomers such as, for example, methacrylic acid[213,281] or acrylic acid.[133,523] Although SI-PIMP of these monomers works well, direct SI-ATRP of (meth)acrylic acid has been reported to be challenging.[70] Poly(methacrylic acid) and poly(acrylic acid) brushes, however, can be prepared via direct ATRP of sodium methacrylate[110] and sodium acrylate, respectively.[582] Baker and Bruening recently proposed the direct SI-ATRP of 2-(methacryloyloxy)ethyl succinate (MES), which was the first example of direct ATRP of a protonated acidic monomer.[113] Most frequently, however, carboxylic acid-functionalized polymer brushes are obtained via deprotection of an appropriate side chain-protected precursor, such as, for instance, poly(*tert*-butyl methacrylate) (section 2.5.3).[461,608,609] Alternatively, carboxylic acid-functionalized polymer brushes can be prepared via postmodification of other side-chain functional brushes, as was discussed in the previous section.

Polymer brushes with carboxylic acid side-chain functionalities have been frequently used as platforms for postmodification reactions. Table 17 provides an overview of different reactions that have been used to postmodify carboxylic acid-functional polymer brushes. Table 17 only includes examples of polymer brushes that are obtained via direct SI-CRP of the corresponding (protected) carboxylic acid functional monomer and does not include carboxylic acid-functionalized polymer brushes that are the products of other postmodification reactions.

Postmodification of carboxylic acid side chain-functionalized polymer brushes generally aims at the im-

Table 17. Overview of Reactions That Have Been Used To Postmodify Carboxylic Acid Side-Chain Functional Polymer Brushes

Polymer brush substrate	SI-CRP technique	Modified polymer brush	Reaction conditions	Application	Ref
PAA	SI-ATRP	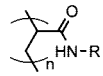	1. EDC/NHS 2. Protein coupling R = anti-CRP;[613] avidin;[582] BSA-FITC;[582] BSA-biotin;[582] BSA;[610] RNase A.[611]	Immunosensor, Protein binding, Protein immobilization	582,610, 611,613
PAA	SI-ATRP	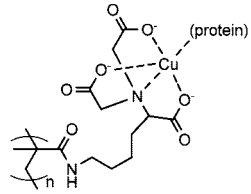	1. EDC/NHS 2. aminobutyl-NTA 3. Copper complexation 4. Protein binding Protein = BSA;[610] anti-IgG;[610] myoglobin;[610] RNase A.[611]	Protein binding, Protein immobilization	610,611
PMAA	SI-ATRP	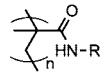	1. NHS/EDC 2. Protein coupling R = silk sericin	Inhibition of bacterial adhesion, promotion of osteoblast function	614
PMAA	SI-PIMP	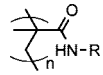	1. NHS/DCC[281] or EDC[213] 2. Peptide coupling R = RGD peptide	Cell adhesion	213,281
PCBMA	SI-ATRP	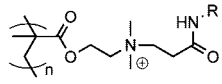	1. EDC/NHS 2. Protein coupling R = anti-hCG	Protein immobilization	612
PMES	SI-ATRP	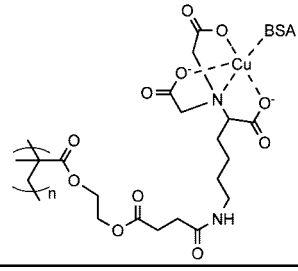	1. EDC/NHS 2. aminobutyl-NTA 3. Copper complexation 4. BSA binding	Protein binding	113

mobilization of biomolecules (peptides[213,281] or proteins)[582,610–614] or binding motifs (e.g., N^{α},N^{α}-bis(carboxymethyl)-L-lysine (aminobutyl-NTA)) that can allow biomolecule immobilization.[113,610,611] The resulting peptide- or protein-modified polymer brushes have attracted interest for applications such as biosensing as well as promoting cell adhesion and reducing bacterial adhesion. Postmodification of poly(carboxylic acid) brushes starts with activation of the carboxylic acid side-chain functional groups, followed by reaction with a nucleophilic group (usually an amine) of the peptide/protein or binding ligand (aminobutyl-NTA) of interest. The first step is usually carried out using 1-ethyl-3-(3-dimethylaminopropyl)carbodiimide hydrochloride (EDC) and *N*-hydroxysuccinimide (NHS) as activating agents.

2.5.3. Postmodification of Carboxylic Ester-Functionalized Polymer Brushes

The majority of postmodification reactions that have been reported with carboxylic ester side-chain functionalized polymer brushes are deprotection reactions that serve to generate the corresponding carboxylic acid-functionalized brushes. The rationale behind the use of these ester-protected brushes (generally *tert*-butyl ester) is to avoid possible complications that can occur using the direct polymerization of the corresponding monomers, especially in the case of SI-ATRP. Table 18 provides an overview of different reactions that have been used to postmodify carboxylic ester-functionalized polymer brushes. Most of the reported examples involve the use of poly(*tert*-butyl (meth)acrylate), but several other carboxylic ester-functionalized brushes have been used as well.

Poly(*tert*-butyl (meth)acrylate) brushes are useful precursors for the preparation of poly((meth)acrylic acid) brushes. Two different strategies are available for the deprotection of poly(*tert*-butyl (meth)acrylate) brushes: (i) acidic hydrolysis and (ii) pyrolysis. Acidic hydrolysis is widely exploited, and a variety of conditions can be used. In the case of polymer brushes that are tethered to the substrate via an ester linkage, however, the deprotection reaction may be accompanied by brush cleavage. Sanjuan and Tran compared the acidolysis of poly(*tert*-butyl methacrylate) brushes using a strong acid (hydrochloric acid, HCl) with that mediated by a weaker acid (trifluoroacetic acid, TFA).[609] Deprotection with TFA was found to proceed at a much slower rate but also resulted in significantly less brush cleavage. Pyrolysis represents an attractive alternative protocol to deprotect poly(*tert*-butyl (meth)acrylate) brushes.[608,615] Heating these brushes to 190−200 °C for ∼30 min removes essentially quantitatively the protecting groups. In contrast to the acid-mediated deprotection, pyrolysis reduces the risk of brush cleavage of ester-linked polymer brushes.

In addition to poly(*tert*-butyl (meth)acrylate), various other carboxylic ester side-chain functional polymer brushes have been prepared, which have been subjected to postmodification reactions. Pei et al., for example, used 5 M HCl to partially hydrolyze the side chains of PHEMA-grafted carbon nanotubes and generate metal chelating carboxylic acid groups.[140] Jiang and co-workers have used polycarboxybetaine ester brushes as precursors to produce

Table 18. Overview of Reactions That Have Been Used for the Postmodification of Carboxylic Ester Side-Chain Functional Polymer Brushes

Polymer brush substrate	SI-CRP technique	Modified polymer brush	Reaction conditions	Application	Ref
P*t*BA	SI-ATRP		Hydrolysis with 10% HCl	-	84,608,838
			Hydrolysis with CF_3COOH	-	220,462,613,719
			Hydrolyis with methanesulfonic acid	-	105,610,842
			Hydrolysis with 37% HCl, dioxane	-	276,634
			Hydrolysis by iodotrimethylsilane	-	241
			Pyrolysis: 190–200 °C	-	106,608,611,615,770
	SI-NMP		Deposition of PS solution containing the photo acid generator bis(tert-butylphenyl)iodonium triflate on P*t*BA brushes, following by exposure to 248 nm UV light	Patterning	190
P*t*BMA	SI-ATRP		Hydrolysis with 10% HCl	-	609
			Pyrolysis: 200 °C	-	608
			Hydrolysis with CF_3COOH	-	461,609
PHEMA	SI-RAFT		Hydrolysis with HCl 5M	-	140
PCBAM	SI-ATRP	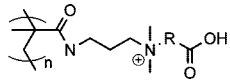	Hydrolysis of methyl ester or ethyl ester with NaOH R = CH_2; $(CH_2)_3$; $(CH_2)_5$	-	616,617
PNHSMA	SI-ATRP	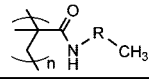	Substitution with primary amines R = $(CH_2)_7$; $(CH_2)_{11}$; $(CH_2)_{13}$; $(CH_2)_{15}$	-	381,382

nontoxic and nonfouling zwitterionic brushes.[616,617] Compared to the free acids, the use of carboxybetaine ester monomers resulted in an increased surface coverage and also obviated problems due to autopolymerization of the unprotected monomers. Finally, Parvin et al. have grafted poly(*N*-hydroxysuccinimide methacrylate) (PNHSMA) brushes via SI-ATRP from iron oxide nanoparticles.[381,382] These active ester brushes were subsequently converted with seven primary amines containing 7, 11, 13, or 15 methylene units to generate a library of poly(methacrylamide)-modified iron oxide particles.[382] The authors' rationale for choosing the active ester monomer rather than opting for direct SI-ATRP of the corresponding alkyl methacrylamides was to avoid complications due to, for example, catalyst complexation or other side reactions during the polymerization.

2.5.4. Postmodification of Epoxide-Functionalized Polymer Brushes

Poly(glycidyl methacrylate) (PGMA) is a versatile platform for postmodification reactions. Table 19 gives an overview of the different postmodification reactions that have been used to derivatize PGMA. Most of the examples in Table 19 are based on polymer brushes that were prepared using SI-ATRP.[225,250,257–260,355,356,618–623] In one example, the postmodification of PGMA brushes prepared by SI-RAFT was reported.[252] Roughly, postmodification reactions that have been used to derivatize PGMA can be subdivided into four groups: (i) the preparation of cross-linked brushes, (ii) the preparation of macroinitiators, (iii) biomolecule immobilization, as well as (iv) several other postmodification reactions. Each of these different groups will be briefly discussed below.

Huck and co-workers have explored the cross-linking of PGMA brushes as a way to generate quasi-2D polymer nanoobjects.[225,258–260] These authors used both amines as well as methanolic NaOH to induce cross-linking. Both monofunctional and bifunctional amines have been used to cross-link PGMA brushes. Cross-linking reactions with primary amines are possible, since the secondary amine group that is formed after the first ring-opening step can open a second epoxide ring.[225] For the 1,4-phenylene diamine-induced cross-linking, two reaction pathways have been proposed: (i) the diamine links two epoxide groups or (ii) the alkoxide ion generated by the first epoxide ring-opening acts as a nucleophile to start a ring-opening chain reaction.[258] Cross-linking of PGMA brushes via ring-opening chain reaction can also be achieved by exposing the polymer layers to 2 M methanolic NaOH for 25 min at 60 °C.[259,260]

Kang, Neoh, and co-workers have used PGMA brushes as platforms to synthesize macroinitiators for the preparation of comb-shaped polymer brushes.[250,252] To this end, ATRP initiating groups were introduced by exposing the polymer brushes to a solution containing 2-chloropropionic acid or 2-bromo-2-methylpropionic acid at elevated temperature (60−70 °C) for up to 24 h.

The epoxide pendant groups of PGMA also provide opportunities for biomolecule immobilization. Two different approaches have been reported to immobilize proteins on PGMA brushes. The first approach involves the direct immobilization of the protein of interest via a nucleophilic ring-opening reaction of one of its amine groups with the epoxide groups in the brush.[355,619] Since most proteins contain multiple amine groups, this strategy, however, does not allow much control over the orientation of the immobilized protein.

Table 19. Overview of Postmodification Reactions That Have Been Used To Derivatize PGMA Brushes

	Modified polymer brush	Reaction conditions	Application	Ref
Crosslinking	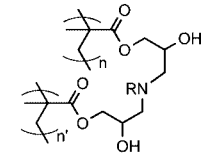	Octylamine, ethanol, 60 °C, 4 h	-	225
	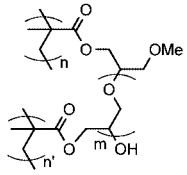	2M methanolic NaOH, 60 °C, 25 min	Preparation of quasi-2D polymer objects	259,260
	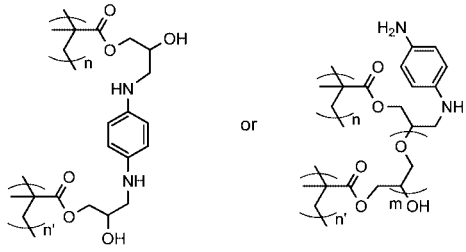	Ethanolic solution of 1,4-phenylenediamine, 60 °C, 30 min	Preparation of quasi-2D polymer objects	258
Macroinitiator	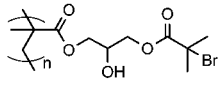	2-bromo-2-methylpropionic acid, THF, 70 °C, overnight	Comb brush synthesis	252
	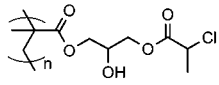	2-chloropropionic acid, DMF, 60 °C, 24 h	Comb brush synthesis	250
Biomolecule immobilization	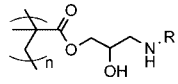	Ring-opening of epoxide with amine groups of the protein. R = Glucose oxidase	Development of glucose biosensor	355
	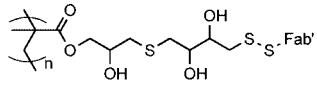	1. Dithiothreitol, RT, 15 h 2. 2,2-dithiodipyridine and 2-thiopyridone (2TP), RT, 1.5 h 3. Selective reaction with cystein residue of Fab' fragment. Fab' = antibody fragment	Site-directed antibody immobilization	620,621
	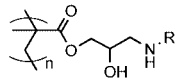	Ring-opening of epoxide with nucleophile group of the protein. R = Penicillin G acylase	-	619
Other	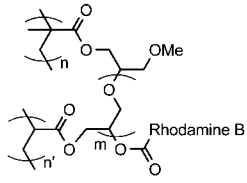	1. Crosslinking; methanolic NaOH 2. Rhodamine B/EDC coupling with residual hydroxyl group	-	259
	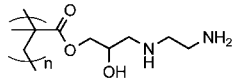	Excess ethylenediamine, RT, 10 h	-	257
	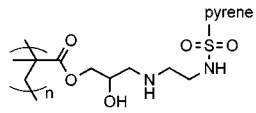	Ring-opening of epoxide with *N*-(1-pyrenylsulfonyl) ethylenediamine	Nitrite-selective fluorescent sensor	356
	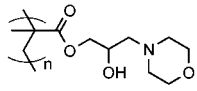	Ring-opening of epoxide with morpholine	-	618
	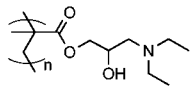	Ring-opening of epoxide with diethylamine	-	622
	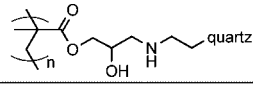	Ring-opening with a surface functionalized with primary amine groups	Quartz wafer bonding	623

Cysteine, which is an amino acid with lower natural abundance than the amino group-bearing lysine, offers better opportunities for the site-directed protein immobilization. Protein immobilization via cysteine residues can be accomplished via thiol−disulfide interchange reactions. To this end, Iwasaki and co-workers have prepared disulfide-containing copolymer brushes of 2-methacryloyloxyethyl phosphorylcholine and glycidyl methacrylate.[620,621] The glycidyl methacrylate moieties were first reacted with dithiothreitol and subsequently with 2,2-dithiodipyridine to introduce disulfide functional groups that were used to immobilize antibody fragments.

Two final examples that are worth mentioning are the postmodification of PGMA brushes with fluorophores to fabricate ion sensors[356] and the use of PGMA brushes as a reactive layer to facilitate substrate wafer bonding.[623] In the first example, approximately 25% of the epoxide groups in PGMA was modified with *N*-(1-pyrenylsulfonyl)ethylenediamine to generate a nitrite-selective fluorescent sensor. In the later example, a PGMA brush grafted from a quartz wafer using SI-ATRP was used as a reactive platform to allow covalent binding of a second aminopropyl-modified wafer.

2.5.5. Postmodification of Other Side-Chain Functional Polymer Brushes

In addition to the hydroxyl-, carboxylic acid-, carboxylic ester-, and epoxide-functionalized brushes discussed in the previous sections, also several other side chain-functionalized polymer brushes have been used as templates for postmodification reactions. Table 20 gives an overview of these polymer brushes, summarizes the reactions that have been used for their postmodification, and lists applications of the modified brushes. The postmodification reactions shown in Table 20 can be divided into three groups: (i) quaternization, (ii) deprotection, and (iii) several other postmodification reactions, each of which will be shortly elaborated upon below.

Tertiary amine- or pyridine-containing brushes such as PDMAEMA, PDMAEA, and poly(4-vinylpyridine) (P4VP) are often quaternized to generate antibacterial surfaces or polymer brushes with pH-dependent surface properties. A wide variety of alkylhalide reagents have been used for the quaternization. The nature of the alkylhalide reagent determines both the degree of modification and the properties of the resulting polymer brush. For the modification of PDMAEMA with 1-bromooctane, 1-bromodecane, and benzylbromide, Ignatova et al. reported quaternization yields between 60 and 75%, depending on the quaternization agent used.[191] Cheng et al. found that the antibacterial properties of quaternized PDMAEMA brushes also depend on the nature of the alkylhalide reagent.[529]

A second class of postmodification reactions includes deprotection reactions to deblock protected sugar-modified polymer brushes,[246,624] to generate aminooxy groups that can be glycosylated,[578] or to prepare poly(2,3-dihydroxypropyl methacrylate) brushes.[166,625]

In addition to the quaternization and deprotection reactions discussed above, several other interesting postmodification reactions have been reported. Loveless et al. reported the reversible cross-linking of P4VP brushes using bis(Pd^{II}-pincer) complexes.[261] The cross-linking of these brushes could be reversed by the addition of DMAP, which competes with P4VP for binding to the pincer ligand. Li and Benicewicz have employed the copper catalyzed dipolar cycloaddition reaction ("click chemistry") to modify azide-functionalized poly(methacrylate) brushes with various acetylene reagents.[626] Jones and co-workers have prepared catalytically active, polymer brush supported salen-Co^{III} complexes by metalation of the corresponding salen-modified brushes (PSLS).[627] These catalytically active brushes were investigated for the hydrolytic kinetic resolution of racemic epoxides.

2.5.6. (Selective) Chain End Postmodification

The previous sections have discussed various approaches to modify functional groups present in the side chains of polymer brushes prepared via SI-CRP. Among others, one attractive feature of SI-CRP is that the polymer chains contain reactive end-groups, which can not only be used to reinitiate polymerization but may also be explored for postmodification. If the reactivity of the polymer chain end is orthogonal to that of the side-chain functional groups, then selective end-modification becomes possible. Alternatively, chain end modification may compete with side chain modification (or vice versa), resulting in polymer brushes that are modified both at the side chains as well as at the chain end. Table 21 provides an overview of reactions that have been used to (selectively) modify the chain end of polymer brushes prepared via SI-CRP. Table 21 is subdivided into two parts. The upper part shows examples where postmodification of the polymer chain end occurs concurrently with side chain modification. The lower part of Table 21 lists examples of selective chain end postmodification.

Simultaneous chain end and side chain modification occurs when polymer brushes prepared via SI-ATRP are halogenated or modified with side chain carboxylic acid groups and subsequently reacted with a protein.[352,358,387] Simultaneous chain end and side chain modification also takes place when PDMAEMA brushes, which have been generated via SI-ATRP, are treated with 4,4′-bipyridine and 1,6-dibromohexane to introduce viologen moieties.[349]

In contrast to the examples discussed above, the defined end-groups of polymer chains grafted by SI-CRP techniques also provide possibilities for selective chain end modification. The halogen end-group of polymer brushes prepared via SI-ATRP either can be used to directly introduce the functional group of interest or can be further modified with reactive groups that allow subsequent derivatization. The first strategy has been used to immobilize collagen and heparin at the chain end of PHEMA and,[358,387] respectively, PNIPAM brushes.[375] Yao et al. have modified the chain end of PPEGMEMA brushes prepared via SI-ATRP with tris-(2-aminoethyl)amine, which was further derivatized with disuccinimidyl octanedioate to allow immobilization of different proteins.[628] Lee et al. converted the terminal bromide functional group of PPEGMEMA brushes prepared via SI-ATRP into an azide group, which generates a versatile platform for further modification using click chemistry.[629] Selective chain end functionalization is also possible with polymer brushes prepared via SI-PIMP or SI-NMP. The *N*,*N*-diethyldithiocarbamyl end-groups of a PNIPAM brush prepared by SI-PIMP, for example, can be exchanged for an amino-functionalized TEMPO radical under irradiation.[212] Selective end-functionalization of brushes grown via SI-NMP is possible by adding an alkoxyamine derivative with the desired functionality during brush growth.[630]

Table 20. Overview of Reactions That Have Been Used To Postmodify Various Side Chain-Functionalized Polymer Brushes

	Polymer brush substrate	SI-CRP technique	Reactive group	Modified polymer brush	Reaction conditions	Application	Ref
Quaternization	PDMAEMA	SI-ATRP		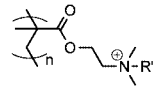	Quaternization with bromoethane, bromohexane and bromododecane (R': C_2H_5, C_6H_{13}, $C_{12}H_{25}$)	Antibacterial surface	349,387,495, 518,529,728, 729,749
	PDMAEMA	SI-RAFT		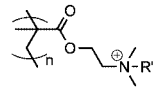	Quaternization with bromoethane, bromohexane, bromooctane and bromododecane (R': C_2H_5, C_6H_{13}, C_8H_{17}, $C_{12}H_{25}$)	Antibacterial surface	480,752
	PDMAEMA	SI-ATRP		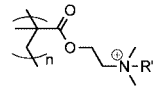	Quaternization with methyl iodide	-	482,609,661,692
	PDMAEMA	SI-ATRP		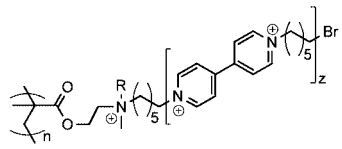	Incorporation of viologen moieties via reaction with a stoichiometric mixture of 1,6-dibromohexane and 4,4'-dipyridine.	Antibacterial surface	349
	PDMAEA	SI-NMP		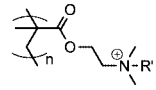	Quaternization with bromooctane, bromododecane and benzyl bromide (R': C_8H_{17}, $C_{13}H_{25}$, C_7H_7)	Antibacterial surface	191
	P4VP	SI-ATRP		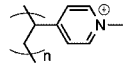	Quaternization of amine with methyl iodide	pH responsive surface	106
Deprotection	PMAIG	SI-ATRP	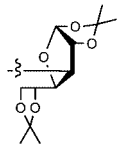	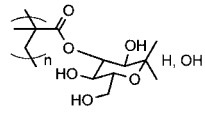	Deprotection of the isopropylidenyl groups with formic acid	Synthesis of glucopolymer brushes	624
	PSMA	SI-ATRP SI-NMP		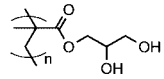	Hydrolysis of the acetal with MeOH/HCl	-	166,625
	PN-BocAHAM	SI-ATRP	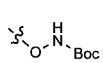	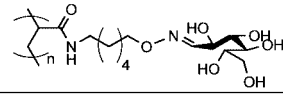	1. Boc-deprotection: HCl 2. Glycosylation: lactose/ glucose, $Na[B(CN)H_3]$	Carbohydrate arrays	578
Others	P4VP	SI-ATRP		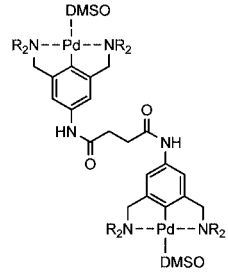	Addition of a DMSO solution containing either crosslinker bis(Pd^{II}-pincer), or crosslinker/DMAP. The surface was allowed to equilibrate for several hours (Only structure of the crosslinker is presented)	Reversible cross-linked polymer brushes	261
	PS	SI-NMP		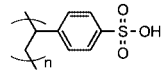	Sulfonation: fuming H_2SO_4/SO_3	-	160
	PS	SI-ATRP		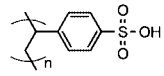	Sulfonation: chlorosulfonic acid	Proton conducting membrane	727
	PAHMA	SI-RAFT	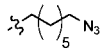	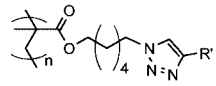	R'-C≡CH, CuBr/PMDETA	Nanoparticle surface modification	626
	PCMS	SI-RAFT	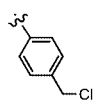	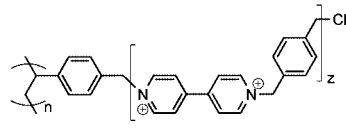	Reaction with an equimolar mixture of 1,4-di-(chloromethyl)benzene and 4,4'-bipyridine	Redox responsive surface	118
	PSLS	SI-ATRP		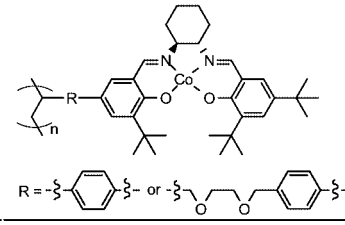	Metalation: refluxing a solution of anhydrous Co^{II} acetate in methanol, 40 h.	Catalyst for hydrolytic kinetic resolution of racemic epoxides	627

Table 21. Overview of Postmodification Reactions That Have Been Used To (Selectively) Modify the Chain End of Polymer Brushes Prepared via SI-CRP

	Polymer brush substrate	SI-CRP technique	Modified polymer brush	Reaction conditions	Application	Ref
Chain end and side chain modification	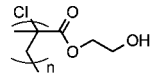 (PHEMA)	SI-ATRP	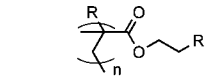	1. Chlorination ($SOCl_2$) 2. Collagen immobilization R = collagen	Cell immobilization	358
	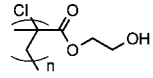 (PHEMA)	SI-ATRP	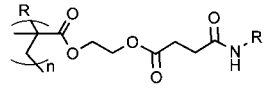	1. Succinic anhydride, DMAP/TEA 2. Collagen or gentamicin, NHS/EDC R = collagen, gentamicin	Antibacterial and osteoblast cell adhesion surfaces	387
	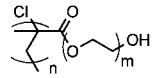 (PPEGMA)	SI-ATRP	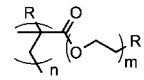	1. Chlorination ($SOCl_2$) 2. Heparin/formamide R = heparin	Antifouling and antithrombogenic surfaces	352
	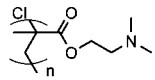 (PDMAEMA)	SI-ATRP	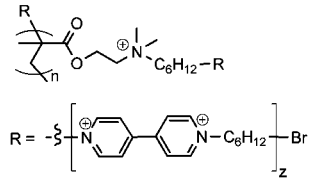	Reaction with a stoichiometric mixture of 4,4'-bipyridine and 1,6-dibromohexane	Antibacterial surfaces	349
Selective chain end modification	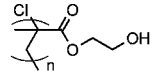 (PHEMA)	SI-ATRP	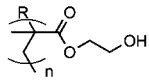	Reaction of active chloride end group with collagen. R = collagen	Cell adhesion	358,387
	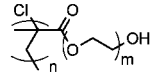 (PPEGMA)	SI-ATRP	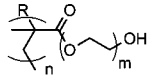	Heparin/formamide R = heparin	antithrombogenic surfaces	352
	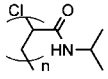 (PNIPAM)	SI-ATRP	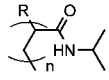	Coupling of chloride end group with heparin. R = heparin	biomedical applications: heparin delivery (anti-thrombotic)	375
	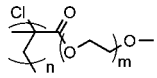 (PPEGMEMA)	SI-ATRP	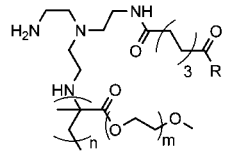	1. Tris-(2-aminoethyl)-amine 2. Disuccinimidyl octanedioate/DMAP 3. Protein immobilization. R = horseradish peroxidase or chicken immunoglobulin	Protein immobilization	628
	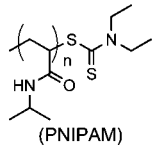 (PNIPAM)	SI-PIMP	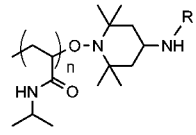	1. Exchange reaction of diethyldithiocarbamyl end group with stable 4-amino-TEMPO radicals 2. Coupling of fluorescamine R = fluorescamine	-	212
	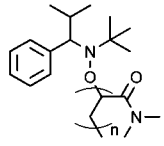 (PDMAM)	SI-NMP	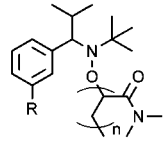	Nitroxide radical exchange during polymerization. R = biotin or pyrene functionalized substituent.	Protein immobilization (biotin-streptavidin)	630
	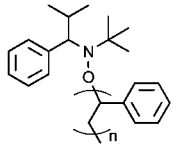 (PS)	SI-NMP	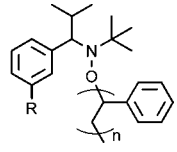	Nitroxide radical exchange during polymerization. R = pyrene functionalized substituent.	Protein immobilization (biotin-streptavidin)	630
	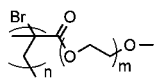 (PPEGMEMA)	SI-ATRP	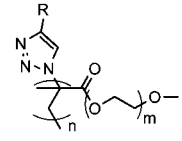	1. NaN_3 2. Acetylenyl group-containing compound, CuBr/PMDETA R= butyl, hydroxybutyl, propanoic acid, benzoate group, biotin-containing compound	Functionalization of nonbiofouling surfaces	629

3. Characterization

The characterization of polymer brushes can be a challenging task, since many of the analytical tools in polymer science are solution-based techniques. Table 22 provides an overview of the different techniques that have been used to characterize polymer brushes. For a broad variety of polymer brush properties, Table 22 lists the analytical methods that are available to study that particular property. Instead of

discussing the technical details of all the analytical techniques, this section will highlight how some of the most prominent properties of a polymer brush can be studied with the analytical tools that are currently available.

A wide range of techniques can be used to probe the chemical composition and structure of a polymer brush. IR spectroscopy is a useful tool to qualitatively provide evidence for the presence of certain functional groups. For the characterization of very thin films, the sensitivity can be improved by using special techniques such as grazing-angle reflection−absorption infrared spectroscopy.[310] XPS can provide quantitative information about the chemical composition of a polymer brush and can also give insight into the chemical structure of the analyzed material. Depending on the sample that is investigated, the penetration depth of the X-ray beam varies from 2 to 10 nm. One of the attractive features of XPS is that it also allows depth profiling[631] and mapping analysis.[555,594] Time-of-flight secondary ion mass spectroscopy (TOF-SIMS) has also been used by different groups.[632] This method gives information on the chemical surface composition and also allows depth profiling analysis[213] and surface mapping.[385] Auger electron spectroscopy (AES) can also be used to determine chemical composition, but in contrast to XPS, this technique requires conducting samples.[633] Near-edge X-ray absorption fine structure (NEXAFS) analysis provides information on the bond-type and molecular orientation of the chemical groups populating the top 3 nm of a polymer brush-covered substrate.[162]

Ellipsometry is a convenient and accurate tool to determine the thickness of an initiator monolayer or a polymer brush. Alternatively, AFM can also be used, but this requires the use of patterned brushes or mechanically removing (scratching) part of the polymer brush coating prior to the analysis. It has been observed, however, that, under high load conditions, the AFM tip can compress the brush, leading to an underestimation of the film thickness.[30,204,553,558] Other techniques that have been used to determine brush thickness include X-ray reflectivity (XRR)[634,635] and, for brushes grafted on particles, transmission electron microscopy (TEM),[636] dynamic light scattering (DLS),[109,533,637] and thermogravimetric analysis (TGA).[109,384]

In principle, information about the molecular weight and molecular weight distribution of the surface-attached polymer chains can be obtained by GPC analysis after cleavage of the brush from the substrate.[3,56] In practice, however, this requires high surface area substrates (e.g., silica particles) that can provide sufficient material for GPC analysis as well as special linkers that facilitate brush cleavage. The use of strong acids such as hydrochloric acid[638] or hydrofluoric acid[376] to cleave the brush bears the possible risk of undesired side-reactions. An alternative approach that is frequently used to assess the molecular weight of surface-grafted polymers is based on the addition of a sacrificial initiator to the polymerization reaction. Marutani et al. found that the molecular weight of the polymer generated in solution from the sacrificial initiator was in good agreement with that of the polymer chains that were cleaved from the particle surface.[376] However, in spite of these encouraging results, the validity of comparing the results of a solution/bulk polymerization with that of a surface-initiated polymerization remains a matter of debate. As reported by Bruening, Baker, and co-workers, surface-initiated polymerizations are inherently heterogeneous processes and the diffusion of monomer, catalyst, or ligands to the surface may be a limiting factor. Therefore, the rate-limiting steps and kinetics for surface-initiated polymerizations may be different compared to those for homogeneous solution/bulk processes.[74] Moreover, the substrate geometry was shown to drastically affect the molecular weight and polydispersity of surface-tethered chains. Gorman, Petrie, and Genzer studied the effect of confinement on polymer growth and compared the molecular weight and polydispersity of PMMA prepared in solution with those obtained from polymerization from flat and concave substrates. These authors concluded that introducing confinement induces a dramatic decrease of the molecular weight of the surface-attached polymer chains.[346] In addition to GPC, AFM can also be used to obtain information about the molecular weight and molecular weight distribution of polymer brushes. By analyzing the extension profiles of poly(*N*,*N*-dimethylacrylamide) and poly(*N*-isopropyl acrylamide) brushes grown via SI-ATRP, Goodman et al. obtained contour length distributions from which molecular weights were calculated that corresponded well with results obtained by GPC.[312,639]

The number-average molecular weight of the surface-grafted polymer chains can be used to calculate the grafting density (σ) of the brush. From the dry thickness of the polymer brush (h), the density of the polymer (ρ) and the number-average molecular weight of the grafted polymer chains (M_n), σ can be calculated according to $\sigma = (h\rho N_a)/M_n$.[640,641] For polymer brushes grafted from particles, the dry brush thickness that is needed to calculate the grafting density cannot be obtained from ellipsometry. In this case, however, grafting density can be determined from the weight loss observed upon thermogravimetric analysis in combination with the number-average molecular weight of the grafted polymer chains and the specific surface area of the particle substrate.[183] It is of interest to compare the grafting density of a polymer brush with the surface concentration of initiator/iniferter groups, since it can provide information about the efficiency of the initiation step of the SI-CRP process. The surface concentration of polymerization initiators/iniferters can be determined using XPS,[111,294] in particular when the polymerization active group contains a halogen atom, as is the case for ATRP initiators.[359,634] Other techniques that have been used to determine initiator surface concentrations include TGA[384] and elemental analysis.[302,642] The initiation efficiency of surface-attached initiators has been reported to vary from 5 to 30%, depending on the shape of the substrate, the type of surface-tethered initiator, and the polymerization conditions.[166,295,303,416,643]

The topography and surface structure of polymer brushes has been investigated by AFM,[555] optical microscopy,[644] scanning electron microscopy (SEM),[230] fluorescence microscopy,[582] XPS "mapping",[555,594] and X-ray reflectivity.[634,635]

The mechanical and viscoelastic properties of a polymer brush not only depend on the chemical composition of the brush but also on the conformation of the surface-tethered polymer chains and changes therein (swelling, collapse). QCM (quartz crystal microbalance) and QCM-D (quartz crystal microbalance with dissipation monitoring) are useful tools to *in situ* monitor such conformational changes.[613,645,646] Ellipsometry has also been used to study conformational changes in polymer brushes.[566,647] Scanning probe microscopy is attractive, since the behavior of surface-attached polymer chains can be studied as a function of temperature,[227] in liquid media,[423,558,586,648,649] or in a controlled vapor

Table 22. Overview of Analytical Techniques That Are Available for the Characterization of Polymer Brushes

	Methods													
Property	SPM[b]	Optical and electron microscopy	Electrochemistry	Ellipsometry	Infrared spectroscopy	Contact angle measurement	SPR[c]	TOF-SIMS[d]	QCM(-D)[e]	XPS[f]	XRR[g]	TGA[h]	NR[i]	GPC[j]	NEXAFS[k]
Chemical composition and structure					×	×		213, 632		×					162
Thickness	204, 553	636		×							634, 635	109, 384	×		
Molecular weight and molecular weight distribution	312, 639													3, 56	
Brush density[a]	×			×								183		×	
Topography and surface structure	×	230, 644				×		385		555, 594	634, 635				
Stiffness	×								×						
Conformation and swelling	423, 586		649, 662	566, 647	×	×	423, 604		613, 646				×		276
Polymerization kinetics	×			×					208, 658						
Electronic and electrochemical properties			345, 598												

[a] To determine the density of a polymer brush, a combination of different methods has to be used. [b] SPM: scanning probe microscopy. [c] SPR: surface plasmon resonance. [d] TOF-SIMS: time-of-flight secondary ion mass spectroscopy. [e] QCM(-D): quartz crystal microbalance (with dissipation monitoring). [f] XPS: X-ray photoelectron spectroscopy. [g] XRR: X-ray reflectivity. [h] TGA: thermogravimetric analysis. [i] NR: neutron reflectivity. [j] GPC: gel permeation chromatography. [k] NEXAFS: near edge X-ray absorption fine structure analysis.

atmosphere.[562] Not only scanning probe microscopy has been used to visualize conformational changes. By covering the back-side of a cantilever with a polymer brush, changes in the cantilever deflection can also be used as a read-out to monitor conformational transitions.[650–652] Yim et al. and Zhang et al. used neutron reflectivity experiments to probe temperature-dependent conformational changes in PNIPAM brushes that were prepared using SI-ATRP.[653,654] Several other techniques have been used to probe the swelling and collapse of polymer brushes. Wu et al., for example, used NEXAFS analysis to study the spatial concentration of surface-tethered PAA chains at different ionic strengths.[276] Aoki et al. used fluorescence depolarization experiments to study nanosecond dynamics of PMMA brushes in both poor and good solvents.[655] In another study on solvent responsive polymer brushes, microfocus grazing incidence small-angle X-ray scattering (μ-GISAXS) measurements were performed to elucidate the behavior of PMMA brush-backcoated micromechanical cantilevers.[656] Surface plasmon resonance (SPR)[604] and SPR-related methods[423] can also be used to probe conformational changes of polymer brushes. Li et al. showed that collapse/swelling of P4VP brushes grafted from gold nanoparticles resulted in a shift of the SPR peak.[423] ^{1}H NMR spectroscopy cannot be used to study brushes grown from planar substrates but is a useful technique to characterize brushes grafted from nanoobjects, such as nanotubes or nanoparticles, that can be dispersed in solvent.[241,447,657]

The kinetics of SI-CRP are typically monitored by preparing a series of brushes with different polymerization times and subsequently measuring the brush thickness with AFM or ellipsometry. In addition to these *ex situ* methods, SI-CRP can also be monitored *in situ* using QCM.[81,101,208,296,658–660]

Electrochemical methods, including electrochemical impedance spectroscopy (EIS),[661,662] chronoamperometry,[663] and cyclic voltammetry (CV)[345,664] have been used to probe electronic properties such as the resistance, the capacitance, the charge, as well as the redox properties of polymer brushes. It was demonstrated that those methods can be used to monitor the swelling/collapse of polymer brushes upon ion exchange[649,662] or ionic strength variations.[663] Furthermore, based on electrochemical impedance spectroscopy measurements, Jennings and co-workers developed an equivalent electronic circuit model for polymer brush coated substrates.[597,598]

4. Properties and Applications of Polymer Brushes

4.1. Responsive Surfaces

Depending on the architecture and chemical composition of the surface-attached polymer chains, the conformation and structure of a polymer brush can be manipulated using a variety of external stimuli. These responsive properties potentially provide the basis for the development of "smart" surfaces. In the following sections, the influence of solvent, temperature, pH, and ions on the conformation, structure, and properties of polymer brushes prepared via SI-CRP will be discussed.

4.1.1. Solvent Responsive Polymer Brushes

The conformation of polymer brushes is highly dependent on the solvent. In the presence of a good solvent, the polymer chains will try to maximize the polymer/solvent contacts and

swell, while in a poor solvent the brush will collapse in order to reduce polymer/solvent interactions. This section will successively discuss the influence of solvent on the structure and properties of homopolymer, diblock copolymer, and triblock copolymer brushes, as well as binary polymer brushes.

Chen et al. used AFM and ellipsometry to study the behavior of PMMA brushes in water and THF, which are poor and, respectively, good solvents for this polymer.[583] Upon immersion in water, a decrease in layer thickness and a reduction of surface roughness was observed, indicating the collapse of the brush. Other studies looked at the behavior of PMMA brushes using a micromechanical cantilever, which was coated on one side with a PMMA brush. Upon changing the solvent from isopropanol (a poor solvent) to ethyl acetate (a good solvent), a deflection of the cantilever was observed.[656,665,666] When going back to isopropanol, the deflection reached its initial value. The swelling or the collapse of the polymer chains induces a mechanical stress and results in the bending of the cantilever. When the brush was exposed to an isopropanol/ethyl acetate mixture that contains a small amount of ethyl acetate, the brush showed an intermediate behavior that was related to the fact that solvent only absorbed in the top layer.[665] This special regime was found to be very quickly and fully reversible, because the trapped solvent molecules can easily leave the polymer chains. Similar swelling behavior was observed when a PMMA brush was alternatively exposed to nitrogen and saturated toluene vapor.[666] Aoki et al. used fluorescence depolarization to study the dynamic swelling properties of PMMA brushes in benzene (a good solvent) and acetonitrile (a bad solvent).[655] It was observed that the thickness of the polymer layer was around two times lower in acetonitrile than in benzene. Furthermore, the motion of the polymer chains was faster in the good solvent. The authors also studied the influence of brush density on the swelling properties. For low density polymer brushes, in which the polymer chains could easily change their conformation, a fast response to solvent-exchange was observed. On the other hand, in the case of high density brushes, the layer was found to be almost nonresponsive to solvent-exchange. Aoki et al. proposed that, due to their high density, the polymer chains interact strongly with each other and adopt a stretched conformation, even in a poor solvent. An example of an application of solvent responsive homopolymer brushes was reported by Li et al., who demonstrated that carbon nanotubes coated with poly(butyl acrylate) or poly(acrylic acid) brushes can be used as gas sensors.[463] The electrical resistance of the polymer brush-coated carbon nanotubes increased upon exposure to organic vapor. The polymer brush-coated carbon nanotubes showed a good sensitivity to organic vapors such as acetone, chloroform, methanol, or toluene with a fast and reproducible response. The chemoselectivities and maximum response values of the polymer brush-modified nanotubes toward organic vapors were found to correlate with the solubility of the pure polymers in the respective solvents.

The response of a diblock copolymer brush to changes in solvent quality is more complex than that of a simple homopolymer brush. This is schematically illustrated in Figure 9. In the presence of solvent B, which is a good solvent for both blocks, the system will be fully extended. In contact with solvent A, which is a good solvent for the blue part of the brush but a poor solvent for the red one, the blue block will swell while the red block will collapse and eventually (depending on the nature of the blue segment) penetrate the other block in order to minimize as much as possible its contact with the solvent. Depending on the interaction parameter between the two blocks, this can lead to the formation of nanosized surface patterns.

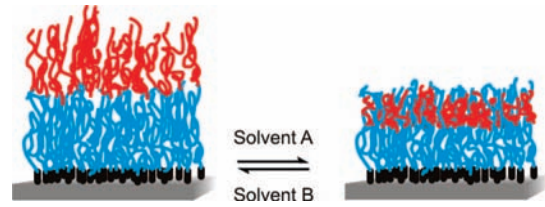

Figure 9. Structural changes in a diblock copolymer brush upon variations in solvent quality; solvent B is a good solvent for both blocks, while solvent A is a good solvent for the blue block but a nonsolvent for the red block.

Granville et al. studied the behavior of different semifluorinated diblock copolymer brushes (PS-*b*-PPFS, PS-*b*-PHDFDA, PS-*b*-PPFEA, PS-*b*-PPFPA, PMA-*b*-PPFS, PMA-*b*-PDHFDA, PMA-*b*-PPFEA, and PMA-*b*-PPFPA).[667] Rowe et al. performed similar studies on PS-*b*-PAA, PS-*b*-PNIPAM, and PMA-*b*-PDMAEA diblock copolymer brushes.[668] In these studies, the brushes were first exposed to a good solvent for both blocks. After that, the brushes were exposed to a poor solvent for the outer block and a good solvent for the inner block. The contact angle of the brush after this second step was close to the value expected for the inner block, indicating a swelling of the inner block and a strong collapse of the outer one (reversible rearrangement). These observations were confirmed by XPS measurements, which revealed a change in the surface atomic composition upon the solvent treatment. Similar behavior was observed by Yu et al. for PS-*b*-(PMMA-*co*-PCDMA) diblock copolymer brushes.[635]

Xu et al. investigated the wetting properties of three groups of PBMA-*b*-PDMAEMA brushes composed of a uniform PBMA inner block and a molecular weight gradient PDMAEMA outer block.[287] The block copolymer brushes were treated with hexane and water and characterized by water contact angle measurements, which revealed three different response regimes. When the PDMAEMA block was short, the PBMA segment dominated the surface after hexane treatment. In the partial response regime, the PDMAEMA and PBMA blocks coexisted at the air interface. Further increase in the PDMAEMA block length was found to suppress the rearrangement of the PBMA blocks after hexane treatment.

Gao et al. studied the solvent-induced formation of nanoscale patterns on PPEGMA-*b*-PMMA diblock copolymer brushes.[669] These brushes were produced by SI-ATRP from a silicon wafer and consisted of an inner PPEGMA block with a thickness of 23.4 nm and an outer PMMA block with thicknesses ranging from 1.6 to 31.0 nm. The formation of nanoscale patterns in these brushes was studied by means of AFM, ellipsometry, and water contact angle measurements. Depending on the PMMA block length, different phase segregation regimes were observed. In the case of PMMA layer thicknesses < 4 nm, spherical PMMA domains were observed. The size of these spherical features increased with increasing PMMA block length until they started to come into contact and merge into "wormlike" structures at PMMA layer thicknesses of 10.5 nm. Further increase in the PMMA layer thickness resulted in the formation of striped patterns. The formation of these phase-separated

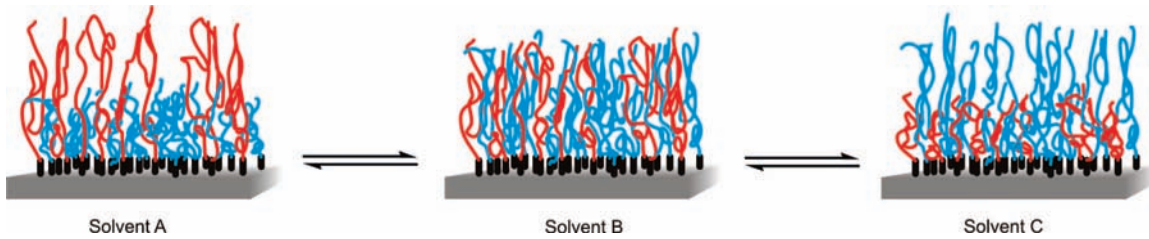

Figure 10. Solvent responsiveness of a binary mixed homopolymer brush: solvent B is a nonselective solvent, whereas solvents A and C are selective for the red and blue segments, respectively.

structures was attributed to the fact that the PMMA chains tried to minimize the contact with the solvent but could not go inside the PPEGMA layer due to the relatively long ethylene glycol side chains in this block.[670] Similar observations were reported by Santer et al., who used the topographical switching properties of PMMA-*b*-PGMA brushes to drive the motion of silica nanoparticles deposited onto the brush.[671,672] Using AFM and contact angle measurements, Xu et al. studied PMMA/PHEMA gradient copolymer brushes.[271] They observed that, upon treatment with CH_2Cl_2 (a selective solvent for PMMA), the MMA-rich segments of the polymer chains swelled and migrated to the surface in order to maximize the contact between the solvent and the MMA-rich segments while at the same time the HEMA-rich segments collapsed and penetrated inside the polymer brush to reduce their interaction with the solvent. These solvent-induced rearrangements resulted in changes in surface roughness.

In addition to diblock copolymer brushes, several groups have also studied the solvent response of triblock copolymer brushes. Boyes et al. examined the swelling behavior of PS-*b*-PMMA-*b*-PS and PMMA-*b*-PS-*b*-PMMA triblock copolymer brushes.[216] These brushes were exposed to a solvent that was a good solvent for the middle block but a nonsolvent for the tethered and outer blocks. For both systems, reversible and reproducible changes in the contact angle were observed, which indicated a conformational rearrangement and migration of the nonsoluble blocks inside the brush and the soluble block to the surface. XPS measurements revealed changes in the surface atomic concentration, and AFM showed an increase in roughness upon the solvent treatment, indicating the formation of micellar structures due to the migration of the outer blocks inside the layer. Similar observations were made by Huang et al., who investigated PMMA-*b*-PDMAEMA-*b*-PMMA and PMA-*b*-PMMA-*b*-PHEMA triblock copolymer brushes.[218]

The solvent responsiveness of mixed homopolymer brushes is different from that of block copolymer brushes. Exposure to a specific solvent triggers a selective swelling of one of the components of the brush and at the same time a collapse of the other polymer chains, leading to a phase separation and the formation of nanoscale surface patterns (Figure 10).

Zhao et al. studied mixed PMMA/PS brushes, which were grown from a flat silicon wafer using a difunctional "Y-shaped" initiator (section 2.2.3).[238] A series of mixed brushes with a constant PMMA molecular weight of 17 500 g/mol and PS molecular weights ranging from 4 300 to 26 100 g/mol were investigated. Water contact angle measurements on films exposed to chloroform (a nonselective solvent) indicated a gradual transition from 74°, the value expected for pure PMMA, to 91°, the value for pure PS, with increasing PS molecular weight. Exposure to cyclohexane, which is a selective solvent for PS, did not lead to any changes in surface topography but did induce a reorganization that drives the PMMA chains to the interior of the brush to avoid unfavorable PMMA/cyclohexane contacts. Exposure of mixed brushes with PS segments slightly shorter or similar in length to the PMMA segments to acetic acid (a PMMA selective solvent), in contrast, resulted in the formation of micellar nanodomains with PMMA chains shielding a PS core. Zhao and co-workers also used their "Y-shaped" initiator to grow binary mixed PAA/PS brushes from silica nanoparticles.[241] Tyndall scattering and ^{1}H NMR spectroscopy experiments demonstrated that the brush-coated particles could be dispersed both in chloroform, a PS selective solvent, as well as in methanol, a PAA selective solvent, which reflects the ability of the surface-tethered polymer chains to undergo structural changes in response to changes in solvent quality. Santer et al. have extensively studied solvent-induced topographical changes in PS/PMMA binary brushes.[672,673] These authors found that these mixed brushes can form microdomains upon exposure to solvents that are selective to the PS (toluene) or PMMA (acetone) segments. Upon monitoring the resulting surface topographical changes with AFM over several switching cycles, it was observed that several microdomains recover their initial state after multiple acetone/toluene exposures. This memory effect has been proposed as a possible mechanism to direct movement of objects on these "smart" surfaces.

4.1.2. Thermoresponsive Polymer Brushes

Thermoresponsive polymer brushes prepared by SI-CRP have been explored for a wide variety of applications including chromatography,[302,642,674–676] controlled cell adhesion,[206,250,520] modulating membrane transport,[677] as well as catalysis.[531] Most of the thermoresponsive brushes that have been reported show lower critical solution temperature (LCST) behavior. At temperatures below the LCST, these brushes are hydrophilic, while raising the temperature above the LCST leads to a collapse of the brushes when they are exposed to water and results in a hydrophobic surface. Table 23 provides an overview of different thermoresponsive polymer brushes that have been prepared using SI-CRP and also lists their transition temperatures as well as the nature of the transition. This section will highlight the thermoresponsive properties of various surface-attached polymer brushes and successively discusses homopolymer, random copolymer, and block copolymer brushes.

PNIPAM is one of the most studied thermoresponsive polymers, and surface-tethered PNIPAM brushes have attracted much attention in the past two decades.[678] Whereas in solution PNIPAM shows a sharp LCST at 32 °C,[679] the LCST transitions observed for PNIPAM brushes are broader, start at lower temperature, and occur over a wider temperature range (from ~29 to ~40 °C).[136,418,657,680] Analogous to the free polymer in solution, the phase transition temperature of PNIPAM brushes also depends on the salt concentration.[645]

Table 23. Overview of Thermoresponsive Polymer Brushes Prepared by SI-CRP

Polymer brush	Transition temperature	Transition	Method[a]	Ref
PNIPAM	~29−40 °C	LCST	WCA[i] QELS[g] WCA[i] SPR[h]	136, 418, 657, 680
$PPEGMEMA_2$	~21−25 °C	LCST	DLS[e] ^{1}H NMR	687
$PPEGMEMA_2$	32.3 °C	LCST	WCA[i]	689
$PPEGMEMA_3$	~42−52 °C	LCST	DLS[e] ^{1}H NMR	687
$PPEGMEMA_3$	~40−50 °C	LCST	DLS[e]	531
PSBMA	~40−50 °C	UCST	WCA[i]	633
PNIPAM-*co*-PAA (3 mol % AA)[b]	~21 °C (pH 2) ~24 °C (pH 4) ~32 °C (pH 7) ~36 °C (pH 9) ~45 °C (pH 11)	LCST	WCA[i]	690
$PPEGMEMA_2$-*co*-$PPEGMEMA_{8.5}$ (5 mol % $PEGMEMA_{8.5}$)[b]	~36 °C	LCST	WCA[i]	689
$PPEGMEMA_2$-*co*-$PPEGMEMA_{8.5}$ (10 mol % $PEGMEMA_{8.5}$)[b]	~40 °C			
PNIPAM-*co*-PDMAEMA (17 mol % DMAEMA)[c]	~40.7 °C	LCST	UV/vis	642
PNIPAM-*co*-PDMAEMA (20 mol % DMAEMA)[c]	~56.1 °C			
PNIPAM-*co*-PDMAEMA (37 mol % DMAEMA)[c]	~64.6 °C			
PNIPAM-*co*-PMBAM (0.74 mol % MBAM)[b]	31.26 °C	LCST	DSC AFM[d]	227
PNIPAM-*co*-PMBAM (0.5 mol % MBAM)[b]	~32 °C	LCST	SPR[h]	424
PNIPAM-*co*-PMBAM (1 mol % MBAM)[b]	~34 °C			
PNIPAM-*co*-PMBAM (2 mol % MBAM)[b]	~36 °C			
PDMAM-*b*-PNIPAM (61.3 mol % PDMAM)[c]	~25−32 °C	LCST	PCS[f]	538
PSEMA-*b*-PNIPAM	no LCST observed	LCST	AFM[d]	328
PNIPAM-*b*-PPEGMEMA	~33 °C (PNIPAM segment) ~55 °C (PPEGMEMA segment)	LCST	DSC, DLS,[e] SPR[h]	422

[a] Techniques used to determine the transition temperature. [b] Molar percentage of the monomer in the polymerization mixture (i.e., feed composition). [c] Molar percentage in the copolymer determined via ^{1}H NMR. [d] AFM: atomic force microscopy. [e] DLS: dynamic light scattering. [f] PCS: photon correlation spectroscopy. [g] QELS: quasi-elastic light scattering. [h] SPR: surface plasmon resonance. [i] WCA: water contact angle.

However, in contrast to the linear decrease of the phase transition temperature with increasing salt concentration observed for the free polymer, surface-attached PNIPAM brushes display a nonlinear behavior. Whereas changes in salt concentration markedly affect the LCST behavior of PNIPAM brushes, Rahane et al. found that varying pH between 3 and 8 has almost negligible impact on the swelling properties.[681] This difference between the solution properties of PNIPAM and the properties of thin, surface-attached PNIPAM brushes has been attributed to the high chain density in the latter case. The LCST transition of a PNIPAM brush is accompanied by an increase in the water contact angle of ~10−30°[418,682] as well as a decrease of the polymer brush thickness[418,647,657,683] and stiffness.[212] Yim et al. used neutron reflectivity to investigate the collapse of PNIPAM brushes upon temperature increase. They observed that the brush contraction was not monotonic and that, upon heating or cooling, phase separation occurred in the temperature range of ~30−33 °C.[653,684] ^{1}H NMR analysis (in D_2O) of PNIPAM brush-coated gold nanorods[657] and carbon nanotubes[447] revealed that, upon temperature increase, the intensity of the proton signals of the PNIPAM units became weaker and could hardly be detected for temperatures > 40 °C, which was attributed to the transition of the polymer brush from a hydrophilic to a hydrophobic state upon passing the LCST.

Several parameters have been found to influence the LCST behavior of PNIPAM brushes such as the brush thickness and grafting density. Yim et al. used neutron reflectivity to study the influence of the polymer molecular weight and brush density on the temperature-induced conformational changes of PNIPAM brushes.[685,686] For PNIPAM brushes with a high grafting density (0.0031 chains/Å^2), samples composed of lower molecular weight polymer chains were found to experience larger conformational changes upon varying the temperature across the LCST as compared to higher molecular weight PNIPAM brushes.[685] The authors, however, also noticed that low molecular weight brushes present a more complex behavior and exhibit phase separation.[684] Temperature-dependent neutron reflectivity experiments on low density (0.00063 chains/Å^2) PNIPAM brushes with different molecular weights revealed opposite behavior;[686] whereas the high molecular weight (152 000 g/mol) brush displayed conformational changes, the neutron reflectivity data did not reveal any conformational changes for the low molecular weight (33 000 g/mol) brush. Conformational changes were most prominent for brushes with intermediate grafting densities and high molecular weights. Plunkett et al. studied the PNIPAM chain collapse as a function of brush molecular weight and grafting density using water contact angle and surface force measurements, among others.[297] Surface force measurements showed that the chain collapse above the LCST decreased with decreasing grafting density and molecular weight. Above the LCST, the advancing water contact angle increases sharply on high molecular weight and dense PNIPAM brushes, whereas these changes are less pronounced on low molecular weight brushes at lower densities. Similar observations have been reported by Idota et al.[674] The wettability of PNIPAM brushes further depends on the roughness of the substrate from which they are grafted.[680] For PNIPAM brushes grown from flat surfaces, Sun et al. determined water contact angles of 63.5° and 93.2° at 25 °C and, respectively, 40 °C. When these brushes were grown from structured surfaces patterned with microgrooves of 6 μm in width and 5 μm in depth, the water contact angles changed to 0° (25 °C) and, respectively, 149.3° (40 °C) and the brushes could be reversibly switched from a superhydrophilic to a superhydrophobic state.

The presence of cross-linking can also influence the LCST of PNIPAM brushes. Li et al. studied the behavior of a random copolymer brush made of *N*-isopropylacrylamide (NIPAM) and *N*,*N*′-methylenebisacrylamide (MBAM) with various amounts of MBAM.[424] The influence of the amount of cross-linker on the LCST of the PNIPAM-*co*-PMBAM brushes was studied. It was found that 0.5 mol % (molar ratio in polymerization mixture) of MBAM did not affect the LCST value of the polymer brush, whereas the LCST increased to 34 and 36 °C when the amount of MBAM was increased to 1 or 2 mol %, respectively.

In addition to NIPAM, another monomer that has been widely used to prepare thermosensitive polymer brushes is poly(poly(ethylene glycol) methyl ether methacrylate) (PPEGMEMA). Li et al. studied the thermosensitivity of poly(di(ethylene glycol) methyl ether methacrylate) (PPEGMEMA$_2$) and poly(tri(ethylene glycol) methyl ether methacrylate) (PPEGMEMA$_3$) brush-coated silica particles and compared the phase transitions of the polymer brushes with those of the corresponding free polymers in water.[687] For both polymer brushes, as for PNIPAM brushes, no sharp transitions were observed compared to the case of the free polymer in solution. The transition began at lower temperature compared to the case of the free polymer and occurred over a broader temperature range (from ∼21 to ∼25 °C for PPEGMEMA$_2$ brushes and from ∼42 to ∼52 °C for PPEGMEMA$_3$ brushes). These differences were attributed to the close packing of the chains in the brush compared to the case of the free chains in solution. In a subsequent publication, the same authors reported the preparation of Pd-loaded poly(acrylic acid) nanoparticles modified with a thermosensitive PPEGMEMA$_3$ brush, which were explored as recyclable catalysts for biphasic hydrogenation reactions.[531] Jonas et al. studied the effect of the nanoconfinement on the thermal behavior of PPEGMEMA$_2$ brushes.[575] They noticed that, compared to a nonstructured polymer brush, patterned brushes showed an increased temperature-induced vertical swelling. The authors attributed this phenomenon to the different packing of the chains, since in the patterned brushes the chains are initially less stretched than in an "infinite", i.e. nonstructured, brush and thus the chains are able to swell more.

Homopolymer brushes displaying upper critical solution temperature (UCST) behavior have been reported by Azzaroni et al.[633] These authors grafted poly(sulfobetaine methacrylate) (PSBMA) brushes via SI-ATRP from gold surfaces and followed the changes in the water contact angle with temperature. Due to the UCST behavior, PSBMA brushes are hydrophobic at room temperature (water contact angle ∼79°) and more hydrophilic at high temperature (water contact angle ∼58°). As for the LCST transition, the authors observed that the UCST of PSBMA brushes is different from the free PSBMA in solution (i.e., 33 °C)[688] and occurs over a wider temperature range (from 40 to 50 °C).

Surface-initiated random copolymerization is an attractive strategy to tune the thermosensitive properties of polymer brushes. Jonas et al. demonstrated that thermosensitive polymer brushes with LCSTs between 32 and 40 °C can be prepared by surface-initiated atom transfer radical copolymerization of di(ethylene glycol) methyl ether methacrylate and poly(ethylene glycol) methacrylate.[689] The LCST values of the copolymer brushes were found to depend linearly on the comonomer composition. When the second monomer that is used for the preparation of the copolymer brushes is sensitive to another stimulus than temperature, then dual responsive surfaces can be produced. This was shown by Xia et al., who grafted PNIPAM-based brushes containing 3 mol % acrylic acid from silicon substrates.[690] The copolymerization of acrylic acid introduced a pH-sensitive component, and the authors demonstrated that the LCST of the brushes varied from 21 to 45 °C depending on the pH.

In addition to homopolymer and random copolymer brushes, also thermosensitive block copolymer brushes have been prepared and investigated. Brooks and co-workers used SI-ATRP to prepare PDMAM-*b*-PNIPAM-modified PS latex particles.[538] Evaluation of the hydrodynamic thickness of the brush layer as a function of temperature revealed a gradual decrease in layer thickness over a broad temperature range (20−38 °C), in contrast to the sharp LCST that is observed for PNIPAM in solution. Li et al. have prepared double thermosensitive block copolymer brushes by consecutive SI-ATRP of NIPAM and PEGMEMA from initiator-modified gold nanoparticles. Temperature-dependent dynamic light scattering experiments revealed two thermal transitions, corresponding to the LCSTs of the different blocks.[422] Other double responsive diblock copolymer brushes that have been prepared are composed of a pH-sensitive block and a thermosensitive block. Wang et al. used AFM to study the thermoresponsiveness of symmetric poly(2-succinyloxyethyl methacrylate)-*b*-poly(*N*-isopropylacrylamide) brushes.[328] Whereas at pH 9 an increase in temperature from 25 to 50 °C resulted in a decrease in film thickness, the brush seemed to be temperature-insensitive at pH 4. This loss of thermal responsiveness was attributed to hydrogen bonding between the constituent blocks. Dual (pH/temperature) responsive block copolymer brushes were also studied by Rahane et al.[681] In contrast to the example by Wang et al., the PMAA-*b*-PNIPAM brushes prepared by these authors showed temperature-dependent swelling properties between pH 3 and 8. Rahane et al. noted that although hydrogen bonding interactions influence the pH-dependent actuation, it did not influence the LCST of the PNIPAM blocks, even if the transition was broad. LeMieux et al. prepared diblock copolymer brushes via successive photoiniferter-mediated polymerization of NIPAM and glycidyl methacrylate (GMA) followed by grafting of carboxylic acid-terminated poly(*n*-butyl acrylate).[631] Nanomechanical analysis of the film indicated that the elastic response can be tuned by external temperature.

4.1.3. pH- and Ion-Sensitive Polymer Brushes

Polyelectrolyte brushes are composed of polymer chains that contain charged repeating units. Depending on the nature of the charged groups, polyelectrolyte brushes are classified as strong or weak polyelectrolyte brushes.[691] In strong polyelectrolyte brushes, the number and position of charges along the chain is fixed. In this case, variation of pH or ionic strength will not influence the number of charges. In weak polyelectrolyte brushes, in contrast, the charge density is not fixed but strongly depends on pH and ionic strength. The response of polyelectrolyte brushes to changes in pH and ionic strength has been the subject of intense research efforts. The following two sections successively discuss the effects of changes in pH and ionic strength on the structure and properties of polyelectrolyte brushes prepared via SI-CRP.

4.1.3.1. pH-Sensitive Polymer Brushes. A large number of reports have been published that describe the pH-sensitivity of polyelectrolyte brushes prepared via SI-CRP.

This section will start with a basic discussion of the pH-induced conformational changes of two prototypical polyelectrolyte brushes: namely PAA as an example of a polyacid brush and PDMAEMA as an example of a polybase brush. After that, several other characteristics of homopolyelectrolyte brushes will be highlighted. Finally, the pH-sensitivity and properties of random and block copolymer brushes will be discussed.

In the case of PAA, the addition of base deprotonates the pendant acidic groups along the polymer brush backbone, introducing charges within the layer. As a consequence, the polymer brush will swell due to Coulombic repulsions between the charged polymer chains. Brittain and co-workers observed a linear increase in PAA brush thickness from ~16 to ~26 nm upon increasing the pH from 2 to 8.[615] Further increasing the pH to ~10 was found to result in a small decrease in brush thickness. Two possible mechanisms were proposed to explain the observed decrease in brush thickness with increasing pH at pH > 8. A first possible explanation could be cleavage of the ester group of the surface-immobilized initiator. Second, the addition of additional ions (through the continued addition of base) to a fully deprotonated brush can lead to screening of the charges along the polymer backbone, which could also explain the observed decrease in brush thickness. Wu et al. have studied the effect of grafting density on the pH-induced conformational changes of PAA brushes.[276] In the osmotic brush regime, the degree of swelling of the PAA brushes was found to depend on brush density at pH 4 and 5.8, but was independent of grafting density at pH 10. These results indicate that, at pH 4 and 5.8, the PAA brush behaves as a weak polyelectrolyte, whereas at pH 10 its behavior resembles that of a strong polyelectrolyte.

The pH-response of polybase brushes such as PDMAEMA is opposite to that of polyacid brushes; their wet thickness decreases with increasing pH due to deprotonation of the charged side groups. The pH-induced conformational changes of PDMAEMA brushes have been studied using various techniques. Sanjuan et al., for example, used neutron reflectivity measurements to compare the swelling behavior of PDMAEMA at pH 2, 7, and 10.[692] The results indicated that the brushes adopted a less extended conformation as the pH of the solution became more basic. Neutron reflectivity has also been used by other groups to probe the pH-responsiveness of PDMAEMA brushes.[648,693] The study by Geoghegan et al. revealed that the brushes swell by a factor of 2 at low pH, with the onset of swelling being dependent on grafting density.[693] More densely grafted brushes were found to swell at a lower pH, reflecting a shift in pK_a as the grafting density changes. Furthermore, for swollen brushes, the composition-depth profile obtained from the reflectivity experiments pointed torward a region depleted in polymer between the substrate and the extended part of the brush. The pH-induced conformational changes of PDMAEMA brushes grafted from particles can be conveniently monitored with dynamic light scattering.[109,533] For PDMAEMA brushes grafted from polystyrene latex particles, Zhang et al. observed changes in particle size diameter of more than a factor of 2 by changing the pH from 3 to 10.[533] The pH-induced conformational changes of polyelectrolyte homopolymer brushes have been used for various applications. Several groups, for example, have described quartz crystal microbalance (QCM)-based pH-sensors, which were produced by modifying the resonator with a PAA brush coating.[613,694] Furthermore, the pH-induced swelling/collapse of polyelectrolyte brushes can be used to control the flocculation behavior of the corresponding polymer brush-coated particles. This has been reported for particles coated with PDMAEMA,[109] PSS(Na),[109] PVB(Na),[109] and P4VP brushes,[423,637] among others. The pH-induced conformational changes of polyelectrolyte brushes have also been used to actuate AFM cantilevers.[651] This was demonstrated by Huck and co-workers, who modified AFM cantilevers with a poly(2-methacryloyloxyethyl phosphate) (PMEP) brush coating. At pH < 2, the polymer brush is water insoluble and collapses, while at very high pH values the surface-tethered polymer chains experience strong repulsive interactions. Both conditions lead to compressive stresses and a deflection of the cantilever. The protonation/deprotonation of the surface-tethered polyelectrolyte chains can also influence the wettability of the polymer brushes. Zhou and Huck, for example, found that PMEP brushes exhibited a three stage switching of wettability.[562] After exposure to pH < 1 solutions, the brushes were relatively hydrophobic (advancing contact angle > 65°). After immersion into a pH 4 solution, the brushes became more hydrophilic (contact angle ~ 49°). Treatment with basic aqueous solution (pH > 13) yielded almost completely wetting surfaces. Similar observations were also reported by Zhang et al., who demonstrated that the pH-sensitivity of PDMAEMA brushes can be used to change the wettability of rough silicon surfaces from almost completely wetting at pH < 3 to very hydrophobic (water contact angle > 115°) at pH > 5.[695]

Surface-initiated copolymerization of oppositely charged monomers results in so-called polyampholyte brushes. Zauscher and co-workers modified microcantilevers with PNIPAM-*co*-PNVI brushes and demonstrated that the cantilever deflected linearly with a sensitivity of ~121 nm/pH over the range from pH 4 to 6.[650] Sanjuan and Tran used neutron reflectivity to study the pH-response of PMAA-*co*-PDMAEMA copolymer brushes.[641] At low and high pH, these brushes acted as neutral polyelectrolyte brushes. For low net charge, however, i.e. at the isoelectric point, the polyampholyte effect results in a collapsed brush.

Ayres et al. studied the pH-responsiveness of poly(acrylic acid)-*b*-poly(vinylpyridine) block copolymer brushes.[106] Evaluation of the film thickness of brushes composed of blocks of similar lengths as a function of pH indicated that these films are swollen at extreme pH values but collapsed at intermediate pHs due to the polyampholyte effect. In asymmetric block copolymer brushes with a relatively long poly(vinylpyridine) segment, this behavior was also observed, though less pronounced. Quaternization of the vinylpyridine units significantly changed the pH-sensitivity and resulted in a system that showed a continuous decrease in film thickness with increasing pH.

4.1.3.2. Ion-Sensitive Polymer Brushes. In addition to pH, polyelectrolyte brushes are also sensitive to variation in ionic strength. Genzer, Szleifer, and co-workers carried out theoretical and experimental studies to investigate the behavior of surface-attached polyelectrolytes.[276,696] Theoretical considerations predicted a different behavior for strong and weak polyelectrolyte brushes. For strong polyelectrolytes, the electrostatic interactions are largely screened at high salt concentrations, and the brush behaves as a neutral, i.e. collapsed, brush. Decreasing the salt concentration generates an unbalance between the ion concentration inside and outside the brush and results in electrostatic interactions that lead to swelling of the brush. This regime is referred to as

the salted brush regime. Upon further decreasing the salt concentration, the brush enters the osmotic brush regime, where co-ions are expelled from the brush and the layer thickness reaches a limiting value. For weak polyelectrolyte brushes, the scenario is different. In the neutral and salted brush regimes, the salt concentrations inside and outside the brush are approximately equal and the internal degree of dissociation is the same as in bulk solution. In the osmotic brush regime, however, a significant electric potential difference is developed between the brush and the bulk solution, and in addition, the salt concentration inside the brush is considerably higher. These unfavorable electrostatic conditions result in a discharge of the electrolyte groups and a collapse of the layer thickness. Experimental investigations of the wet thickness of PAA brushes at different pH values and a range of salt concentrations were in good agreement with the predicted behavior of weak polyelectrolyte brushes. In the salted brush regime, Szleifer, Genzer, and co-workers found that above the mushroom-to-brush transition, which was observed at a brush density (σ) of 0.08 chains/nm^2, the wet PAA layer thickness (H) increased with increasing brush density.[276] The increase in wet PAA thickness followed a scaling law $H \sim \sigma^n$ with $n \approx 0.29-0.31$, which was in good agreement with the theoretically predicted $^1/_3$. The behavior of the PAA brushes in the osmotic brush regime was more complex. In contrast to theory, which predicted a decrease in wet thickness with increasing grafting density and an increase in wet thickness with increasing ionic strength, the experimental results revealed an increase in brush swelling with increasing brush density. Furthermore, the increase in wet layer thickness at high brush densities was found to increase with increasing ionic strength. Ayres et al. reported the effects of mono- and divalent salts on the behavior of PMAA brushes.[608,615] Upon decreasing the salt concentration, it was found that the threshold concentration that marks the onset of brush expansion was higher for the monovalent salt. Huck and co-workers have extensively studied the influence of the counterion on the structure and properties of PMETAC brushes.[649,652,663] In contrast to many other studies that use highly hydrated and mobile counterions, these authors investigated scarcely hydrated anions, which can undergo ion-pairing interactions with the quaternary ammonium groups in the brush.[558,646,697] The characteristics of the brush (e.g., wettability) were found to be very sensitive to the nature of the counterion. Upon exchanging the original chloride counterion with a variety of other counterions, it was found that the wettability of the counterion-modified brushes increased from $ClO_4^- > SCN^- > I^- > Br^- > Cl^- > PO_4^{3-}$, which correlates with the Hofmeister classification of the hydrophobicity of these anions.[698]

4.2. Nonbiofouling Surfaces

Materials with nonbiofouling surface properties, i.e. materials that resist the nonspecific adsorption of proteins, cells, or other biological species, are important for a wide variety of applications in fields ranging from medical implants to contact lenses, drug delivery, biosensors, as well as marine applications such as the coating of ship hulls. Polymer brushes are very attractive candidates for the development of ultrathin nonbiofouling coatings. In particular, the use of SI-CRP techniques allows access to polymer brushes with well-defined thickness, composition, and architecture. Hydrophilic polymer brushes can form highly hydrated ultrathin coatings that provide an effective enthalpic and entropic barrier to nonspecific protein adsorption.[699,700] If a protein adsorbs on a hydrophilic polymer brush, water molecules associated with the polymer chains will be released into the bulk, and the chains will be compressed. The increase in enthalpy due to chain dehydration and the decrease in entropy due to chain compression (even though the latter term may be small) are both unfavorable and provide the thermodynamic basis for the nonbiofouling properties of the coating.[700] Theoretical considerations predicted an enhanced resistance to nonspecific protein adsorption and cell adhesion with increasing grafting density and chain length.[699] As a consequence, polymer brushes prepared via SI-CRP were expected to possess better nonbiofouling properties than oligo(ethylene glycol) self-assembled monolayers (SAMs). Results from several reports indeed support this hypothesis.[162,701,702] During cell adhesion studies with osteoblast-like cells, Raynor et al., however, observed that the difference in nonbiofouling behavior of polymer (PPEGMA) brushes and oligo(ethylene glycol) SAMs only became apparent for incubation times > 7 days.[389] The nonbiofouling polymer brushes that have been prepared via SI-CRP so far can be subdivided into two groups. The first group is obtained by SI-CRP of neutral monomers. An overview of these nonbiofouling polymer brushes is given in Table 24. The second class of nonbiofouling polymer brushes is obtained by SI-CRP of zwitterionic monomers. Examples of this second class of brushes and their properties are summarized in Table 25.

4.2.1. Neutral Nonbiofouling Polymer Brushes

The majority of the neutral, nonbiofouling polymer brushes has been prepared from 2-hydroxyethyl methacrylate (HEMA) and poly(ethylene glycol) methacrylate (PEGMA). These monomers are attractive, since SI-CRP results in ultrathin polymer coatings that have similarities to poly(ethylene glycol) (PEG), which is a well-known biocompatible polymer with nonbiofouling properties.[703,704] In addition, the presence of the hydroxyl group in the side chain of these monomers provides opportunities for postmodification (section 2.5.1). The oligo(ethylene glycol) side chains, however, may be susceptible to oxidation and interchain transesterification reactions, which may lead to cross-linking of the brushes. *In vivo* the hydroxyl end-groups at the side chains of these brushes may be oxidized by alcohol dehydrogenase into aldehyde groups, which may react with proteins.[705,706] This problem may be prevented by using the corresponding methoxy end-functionalized monomer, poly(poly(ethylene glycol) methyl ether methacrylate) (PPEGMEMA). In addition to HEMA and PEG(ME)MA, NIPAM is another monomer that has been widely used to prepare nonbiofouling polymer brushes.[234,565,707,708] The attractive feature of PNIPAM is that it possesses a lower critical solution temperature (LCST), which allows switching the surface properties from a hydrophilic, protein and cell resistant state, to a hydrophobic state that readily adsorbs proteins and cells.

Brush thickness and grafting density are important parameters that determine the nonbiofouling properties. A number of reports have investigated the effect of brush density. PPEGMEMA brushes with a thickness of 4 nm grown from a gold substrate modified with a 0.2/0.8 mixture of ATRP initiator-functionalized and polymerization inactive thiols were found to effectively prevent nonspecific adsorption of fibronectin.[294] In another report, 40-nm-thick PPEGMA brushes prepared from glass slides modified with a 0.6/

Table 24. Overview of Neutral Nonbiofouling Polymer Brushes Prepared via SI-CRP[a]

Polymer brush	Substrate	Thickness (nm)	Cell/protein	Exposure time	Detection method	Comments	Ref
PPEGMEMA	Au	5−20	Fibronectin, 1 mg/mL FBS[b]	20 min	SPR	Amount of adsorbed proteins at or below the detection limit of the instrument (1 ng/cm^2).	292
PPEGMEMA	Au	1−60	Fibronectin, 0.5 mg/mL	10 min	SPR	Protein resistance increases with increasing grafting density and thickness. Protein adsorption below the SPR detection limit (270 Fn molecules/cm^2).	294
PPEGMA	Glass	20−100	Fibrinogen, 1 μM	24 h	Fluorescence	Threshold for protein adsorption at initiator/dummy feed ratio 0.2/0.8, more efficient at feed ratio >0.6/0.4. Protein resistance decreases with the incubation time.	254
PPEGMA	Au	1−20	GRGDS peptide MC3T3 fibroblast cells	60 s 8 h	SPR	Effect of grafting density: crossover grafting density to repress adsorption related to peptide radius and the adsorption potential on the bare surface. No adsorption in the brush regime.	298
PPEGMA PHEMA	Si	100−120	Cy5 AGT-ACP[d]	2 h	Fluorescence	$PPEGMA_6$ exhibits slightly better resistance than $PPEGMA_{10}$. PHEMA had lower protein resistance than $PPEGMA_6$ and $PPEGMA_{10}$.	602
PPEGMA	Si	5−15	MC3T3-E1 Osteoblast like cells	56 d	SPR	PEG SAMs show comparable resistance in short terms, but after 7 days only brushes maintain the ability to prevent cell adsorption.	389
PPEGMEMA	Si	1.4−100	Fibronectin, 1 mg/mL BSA,[c] 1 mg/mL Lysozyme, 1 mg/mL FBS,[b] 1 mg/mL	1 h	Ellipsometry	Increase in thickness above 1.4 nm lead to drastic decrease in protein adsorption.	567
PPEGMA	Fe_3O_4 particles				Microscopy	Coated magnetic nanoparticles provide prolonged circulation time. Not uptaken by microphages.	377
PPEGMA	PDMS		Fibrinogen, 1 μM	30 min	Fluorescence	12-fold improvement in resisting adsorption of fibrinogen-Alexa Fluor 647 conjugate compared to bare poly(dimethylsiloxane).	517
PSPEG	Si	5−15	IgG,[e] 10 μg/mL Fibronectin, 20 μg/mL Collagen, 20 μg/mL BSA,[c] 20 μg/mL Mast cells	90 min 3 h	Fluorescence	Better protein and cell resistance than SAMs.	162
PPEGMEMA	Ti Stainless steel	30	3T3 Swiss albino fibroblast	4 h	Fluorescence	Cell adhesion reduced to 1 cell/mm^2.	385
PPEGMEA	PHEMA-*co*-PMMA hydrogel		Green fluorescent protein, 0.15 mg/mL β-lactamase, 0.3 mg/mL Lens epithelial cells	3 d 150 min 5 d	Fluorescence UV/vis spetroscopy	The polymer brush reduced nonspecific protein adsorption and cell adhesion to the hydrogel substrate.	483
PPEGMEMA	Si Au	3	Fibrinogen, 1 mg/mL BSA,[c] 1 mg/mL Streptavidin, 1 mg/mL	30 min	Ellipsometry	Polymer brushes thicker than 3 nm adsorbed less than 0.3 ng/cm^2 (within experimental error).	307
PPEGMEMA	Ti	100	3T3 Swiss albino fibroblast	80 d	Fluorescence	Longer side chains provide better cell antifouling properties (visible after 5 weeks).	393
PHEMA	Si	1−10	Fibronectin, 25 μg/mL NIH3T3 fibroblasts	5 h	Fluorescence Ellipsometry	Increasing the grafting density decreased the protein and cell adsorption due to the lower fibronectin preadsorption.	278
PNIPAM	Au	40	BSA[c]	1 h	Fluorescence	Nonbiofouling behavior below the lower critical solution temperature and fouling above.	565
PAM	PDMS		Lysozyme, 100 nM	10 min	Fluorescence	20-fold improvement in resisting adsorption of lysozyme compared to bare poly(dimethylsiloxane).	501

[a] In addition to the brush composition and thickness and the substrate from which the brush was grown, the table also shows for each entry which proteins/cells were used to evaluate the nonbiofouling properties, as well as the exposure time and the detection method that were employed. [b] FBS: fetal bovine serum. [c] BSA: bovine serum albumin. [d] Cy5 AGT-ACP: carboxymethylindocyanine-O^6-alkylguanine-DNA-alkyltransferase acyl carrier protein. [e] IgG: immunoglobulin G.

Table 25. Overview of Zwitterionic Nonbiofouling Polymer Brushes Prepared via SI-CRP[a]

Polymer brush	Substrate	Thickness (nm)	Cell/protein	Exposure time	Detection method	Comments	Ref
PMPC	Si	1−7	Platelet-poor plasma	3 h	UV/vis spetroscopy (QuantiPro BCA assay)	Polymer brushes synthesized in nanopores. Protein resistance independent of thickness in the 1−7 nm range	815
PMPC	Si	2−20	Fibrinogen Lysozyme	2 h	Radiolabeling	98% reduction of protein adsorption compared to silicon. Increase in resistance with thickness. Adsorbed lysozyme, fibrinogen molar ratio reflected the one in the solution	709
PMPC	Si	2−25	Fibrinogen, 0.05 mg/mL or 1 mg/mL	2 h	Radiolabeling	Resistance increases with increasing grafting density and thickness	301
PMPC	Si	0.5−25	Fibrinogen Lysozyme	2 h	Radiolabeling	Similar performance of PMPC and PPEGMA	711
PSBMA	Au	5 − 12	Fibrinogen, 1 mg/mL	20 min	SPR	Protein adsorption under the detection limit of SPR (0.3 ng/cm^2)	825
PSBMA	Si	7	Fibrinogen, 1 mg/mL γ-globulin, 1 mg/mL HSA[b], 1 mg/mL Platelet poor plasma Platelets (10^5 cells/mL)	20 min	SPR SEM	Fibrinogen < 2 ng/cm^2 Plasma proteins < 1.76 nm/cm^2 Better performance than PEG SAMs Independent of ionic strength and temperature (22−37 °C) Fouling at pH = 3 due to the protein denaturation	701
PMPDSAH	Au	20	Fibrinogen, 1 mg/mL Lysozyme, 1 mg/mL BSA,[c] 1 mg/mL RNase A,[d] 1 mg/mL	4 min	SPR	Amount of adsorbed proteins was below the detection limit of the instrument (1 ng/cm^2)	845
PSBMA PPEGMEMA PCBMA	Au	15−25	Fibrinogen, 1 mg/mL Human serum Human plasma	10 min	SPR	Comparison of SAMs, PPEGMEMA, PSMBA, and PCBMA. PCBMA showed the best performance	702
PSBMA PPEGMEMA PCBMA	Au	15−25	Fibrinogen, 1 mg/mL Blood plasma Platelets (10^7 cell/mL)	1 h	SPR	Comparison with SAMs: similar resistance with respect to fibrinogen and platelets, but better resistance to blood plasma	898
PSBMA PCBMA	Glass	10−15	Fibrinogen, 1 mg/mL Bovine aortic endothelial cells	90 min 24 h	ELISA[f]	∼95% reduction in protein adsorption compared to glass No cells found onto PSBMA and PCBMA	817
PCMA	Au	5−15	Fibrinogen, 1 mg/mL Lysozyme, 1 mg/mL hCG,[e] 1 mg/mL Bovine aortic endothelial cells	20 min	SPR	Fibrinogen and lysozyme < 0.3 ng/cm^2 for PCMA modified with anti-hCG[e]	612
hPCBAM[g]	Au	5−20	Fibrinogen, 1 mg/mL	15 min	SPR	Polymers with short (−CH_2− and −$(CH_2)_3$−) spacers < 0.3 ng/cm^2. Polymers with −$(CH_2)_5$− spacer absorbed 1.5 ng/cm^2 of fibrinogen	616
PMETAC-*co*-PSPMA(K)	Au	15−40	Fibrinogen, 1 mg/mL BSA,[c] 1 mg/mL Lysozyme, 1 mg/mL	10 min	SPR	Copolymer brush The best nonbiofouling surface was found for the statistical copolymer brushes formed from a 1:1 monomer ratio	712

[a] In addition to the brush composition and thickness and the substrate from which the brush was grown, the table also shows for each entry which proteins/cells were used to evaluate the nonbiofouling properties, as well as the exposure time and the detection method that were employed. [b] HSA: human serum albumin. [c] BSA: bovine serum albumin. [d] RNase A: ribonuclease A. [e] hCG: human chorionic gonadotropin. [f] ELISA: enzyme-linked immunosorbent assay. [g] hPCBAM: hydrolyzed poly(carboxybetaine derivatized acrylamide).

0.4 mixture of ATRP active and ATRP inactive trimethoxysilanes were found to suppress nonspecific adsorption of fibrinogen.[254] To prevent nonspecific adsorption of smaller molecules such as the GRGDS peptide, PPEGMA brushes with a thickness of 10 nm generated from a substrate modified with a mixture of thiols containing 70 mol % of the ATRP active component were necessary.[298] PPEGMA brushes grafted from a silicon substrate exclusively modified with an ATRP initiator-functionalized trichlorosilane and a thickness of 1.4 nm already significantly reduced nonspecific protein adsorption.[567] At brush thicknesses of 9.5 nm or larger, the amount of adsorbed proteins on these brushes was below the detection limit.

Although the long-term stability of nonbiofouling polymer brushes is very important for many biomedical applications, this topic has received only relatively limited attention. Messersmith and co-workers carried out an 80 day study in which fibroblasts were seeded twice a week onto Ti surfaces coated with PPEGMEMA brushes with three different PEG side chain lengths.[393] During the first three weeks, all brushes effectively prevented cell attachment. After that, however, the effect of the ethylene glycol side chain length became apparent. $PPEGMEMA_4$ brushes were essentially nonbiofouling for 28 days and cell attachment to the $PPEGMEMA_9$ and $PPEGMEMA_{23}$ brushes only became significant after 35 days. Ultimately, all three types of brushes were covered with a confluent cell monolayer, which was reached after 7, 10, and 11 weeks for the $PPEGMEMA_4$, $PPEGMEMA_9$, and $PPEGMEMA_{23}$ brushes, respectively. The authors hypothesized that the loss of nonbiofouling properties could be due to degradation of the ethylene glycol side chains, cleavage of the Ti−catechol bond that anchors the polymer brush to

the substrate, or hydrolysis of the ester group, which links the PEG side chain to the poly(methacrylate) backbone.[393] In another study that addressed long-term stability and nonbiofouling properties, it was found that PPEGMA brushes grafted from silicon oxide can detach upon exposure to cell culture medium.[254] As no detachment was observed in pure water, it was hypothesized that complexation of salts from the buffer solution by the PEG side chains of the brush creates an osmotic stress, which adds to the entropically unfavorable stretched chain conformation and facilitates cleavage of the siloxane bond that connects the polymer brush to the substrate. This cleavage process may be further facilitated by the relatively ill-defined nature of the trialkoxysilane-based initiator layer that was used in this study. Brushes with lower grafting densities were stable under cell culture conditions for more than 7 days, while high density ones were stable only for one day.

4.2.2. Zwitterionic Nonbiofouling Polymer Brushes

In addition to the neutral polymer brushes discussed in the previous section, a second major class of nonbiofouling polymer brushes are those that can be obtained by SI-CRP of zwitterionic monomers (Table 25). Similar to their neutral counterparts, zwitterionic polymer brushes also form highly hydrated ultrathin polymer coatings that present both enthalpic and entropic barriers to nonspecific adsorption of proteins and cells.

Several authors have extensively studied the nonbiofouling properties of poly(2-(methacryloyloxy)ethyl phosphorylcholine) (PMPC) brushes prepared by SI-ATRP.[301,612,709] The nonbiofouling properties of these brushes were evaluated using binary (fibrinogen/lysozyme) protein mixtures rather than single proteins. These experiments revealed that the adsorbed lysozyme/fibrinogen ratio reflected the solution molar ratio.[709] This suggests that PMPC brushes are equally efficient in preventing the adsorption of small (lysozyme) and large (fibrinogen) proteins. Further, it was pointed out that the adsorption does not occur by penetration through the graft layer to the silicon interface (i.e., primary adsorption),[710] since in that case it would be expected that the larger protein was more effectively resisted than the smaller one, but rather by the secondary adsorption at the outer surface of the graft layer. An increase in thickness and grafting density leads to improved protein resistance, as was the case for PPEGMEMA.[301,711] This is closely related to the observed increase in hydrophilicity by water contact angle measurements of the PMPC layer when those two parameters increase.[301] In another study, Brash and co-workers compared the nonbiofouling properties of PPEGMEMA and PMPC brushes.[711] Using radiolabeled fibrinogen, it was found that protein adsorption on PMPC and PPEGMEMA brushes for a given chain length and density was essentially the same. As a result of these experiments, the authors suggested that the principal factor determining nonbiofouling behavior is the "water barrier layer" resulting from the hydrophilic character of the brushes, which in turn depends on monomer density in the surface-grafted polymer layer. Polymer brushes obtained by SI-CRP of sulfobetaine methacrylate (SBMA) have also been widely used as nonbiofouling coatings. PSBMA brushes have been demonstrated to withstand nonspecific adsorption of fibrinogen even under high ionic strength conditions at 37 °C and pH values ranging from 5 to 11.[701] At pH values below 5, some fibrinogen adsorption occurred even though the PSBMA brushes display a very hydrophilic surface at that pH. The increased nonspecific protein adsorption at these low pH values was attributed to protein denaturation.[701] Bernard et al. demonstrated that polymer brushes with nonbiofouling properties similar to PSBMA could be obtained by surface-initiated atom transfer radical copolymerization of (2-(methacryloyloxy)ethyl) trimethylammonium chloride and 3-sulfopropyl methacrylate potassium salt.[712] In another study, Ladd et al. compared the nonbiofouling properties of PSBMA and poly(carboxybetaine methacrylate) (PCBMA) brushes with those of PPEGMEMA brushes, oligo(ethylene glycol) SAMs, as well as mixed SAMs of 1-mercapto-11-*N*,*N*,*N*-trimethylammonium chloride (TMA) and 1-mercapto-11-undecylsulfonic acid, or TMA and 1-mercapto-11-undecylcarboxylic acid.[702] Exposure of these different coatings to human serum and human plasma revealed that the polymer brushes were superior in preventing nonspecific protein adsorption. Among the three polymer brushes, the PCBMA coating proved to be the most efficient in preventing nonspecific protein adsorption. The difference in nonbiofouling properties of the PCBMA and PSBMA brushes has been attributed to the different number of methylene units that separate the positive and negative charge in those monomers. In the SBMA monomer, the cationic and anionic components are separated by three methylene units. In the CBMA monomer, the spacer is one methylene group shorter. The closer proximity of the two ionic groups in the CBMA monomer increases the interactions between the hydration shells around the two ionic groups and creates a more spatially uniform and stronger hydratation layer.

4.3. Cell Adhesive Surfaces

The surface of artificial biomaterials plays a key role in guiding and directing cellular behavior and function and, as a consequence, is of critical importance for regenerative medicine and tissue engineering.[713,714] Polymer brushes are attractive tools to control and direct cell adhesion on artificial materials surfaces. Table 26 gives an overview of different polymer brush-based coatings obtained via SI-CRP which have been used for this purpose. The polymer brushes listed in Table 26 are classified into three categories: the first group consists of nonbiofouling polymer brushes which are functionalized with an extracellular matrix (ECM) protein or a cell adhesion peptide derived thereof; the second group includes various nonbiofouling polymer brushes that have been used to pattern cell adhesive substrates and geometrically control cell adhesion; the third category consists of polymer brushes that possess a lower critical solution temperature (LCST) and that can be thermally triggered to change from a hydrophobic cell adhesive to a hydrophilic nonbiofouling state. Each of these classes will be discussed in more detail below.

4.3.1. Peptide/Protein-Functionalized Polymer Brushes

Cell adhesion to synthetic materials can be guided by specific cell surface receptor interactions by modifying the substrate surface with a nonbiofouling polymer brush that is functionalized with short peptide sequences derived from extracellular matrix (ECM) proteins. Most commonly, these cell adhesion peptides are based on the RGD (arginine-glycine-aspartic acid) sequence, which is derived from the cell attachment domain of fibronectin and specifically binds to integrin receptors that are present on the cell surface.[715] Tugulu et al. studied the adhesion and proliferation of human

Table 26. Overview of Polymer Brush Coatings Obtained via SI-CRP That Have Been Used To Control and Direct Cell Adhesion

	Polymer brush	Thickness [nm]	Peptide/Protein [density]	Type of cells	Comments	Ref
Peptide/Protein-functionalized polymer brushes	PPEGMA PHEMA	20	GGGRGDS [0.5-12 pmol/cm^2]	Human umbilical vein endothelial cells	Different focal adhesions on PPEGMA and PHEMA. An increase in the ligand density leads to an increase in the number of adhered cells. > 5 pm/cm^2 confluent cell layer. The adhesion is sufficiently strong to allow cell adhesion upon exposure to a fluid shear stress.	600
	PPEGMA	5–15	GFOGER [27.8 pmol/cm^2]	MC3T3-E1 osteoblast like cells	GFOGER derived from I collagen. Adhered cells exhibited well spread morphology and an increase in cell numbers with culture time.	389
	PPEGMA	13.5	$FNIII_{7-10}$ [~ 1 pmol/cm^2] GRGDSPC [~ 6 pmol/cm^2]	Rat bone marrow stromal cells	$FNIII_{7-10}$ targets $\alpha_5\beta_1$, GRGDSPC targets $\alpha_v\beta_3$ integrins *In vivo*: $FNIII_{7-10}$ ligand provides better cell adhesion, osteoblastic differentiation and osseointegration compared to GRGDSPC.	601
	PPEGMA	1–20	RGD	MC3T3 fibroblasts	Cell adhesion mediated by non-specifically adsorbed RGD peptide. Increase in the brush thickness reduced the GRGDS peptide adhesion and consequently cell adhesion.	298
	PMAA	5–100	GRGDS [0-20 nmol/cm^2]	3T3 fibroblasts	RGD functionalized thickness gradient PMAA brushes: cell adhesive and noncytotoxic. Cell density increases with increasing ligand density.	281
	PMAA	5–100	RGD	Human osteoblastic bone cells (MG63)	Influence of RGD position within the brush was studied. Little influence on viability, remarkable influence on cell morphology. Surface coupled RGD: focal points marked at the surface. Buried RGD: focal points concentrated towards nucleus.	213
	PHEMA	3–14	Fibronectin	MC3T3-E1 osteoblasts	PHEMA gradient: Non-specific fibronectin adsorption at low PHEMA densities facilitated cell adhesion.	291
	PHEMA	1–8	Fibronectin	NIH3T3 fibroblasts	PHEMA gradient: Non-specific fibronectin adsorption at low PHEMA densities facilitated cell adhesion.	276
	PHEMA	20–40	Collagen	3T3 fibroblasts	The higher the content of immobilized collagen, the higher the density of viable cells to the surface.	358
	PHEMA	-	Collagen	3T3 fibroblasts 3T3 osteoblasts	Collagen promotes cell adhesion and proliferation. Adhesion under centrifugal forces showed that osteoblasts adhere much stronger onto collagen modified Ti surfaces than onto unmodified titanium.	387
Patterned polymer brushes	PPEGMA	20	poly(L-lysine)	Chinese hamster ovary cells	Micropatterns of PPEGMA polymer brushes and poly(L-lysine). Cell adhesion directed onto poly(L-lysine) areas.	604
	PPEGMEMA	14	Fibronectin	NIH3T3 fibroblasts	Cell adhesion on a patterned substrate covered with fibronectin regions separated by nonbiofouling brush areas.	292
	PPEGMEMA	30	-	3T3 Swiss albino fibroblasts	Micropatterns of PPEGMEMA that direct the cell adhesion onto bare titanium surface.	385
	PSPEG	5–15	DNP[a]-BSA[c]	anti-DNP[a] IgE[b] sensitized Chinese hamster ovary and RBL mast cells	PSPEG patterns onto silicon substrate. DNP[a]-BSA[c] was used to facilitate cell attachment of RBL mast cells.	162
	PMPC	1–15	-	L929 mouse fibroblasts	UV patterned PMPC polymer bushes on silicon substrates. Increased brush thickness improves geometrical control over cell adhesion.	577
Thermoresponsive polymer brushes	PNIPAM	2–65	-	Bovine carotid artery endothelial cells	Cell adhesion decreases above the LCST (~32 °C) with increasing brush thickness.	520
	PNIPAM	100–250	-	NIH3T3 fibroblasts	Little cell attachment at 37 °C; increased cell adhesion at 40 °C.	708
	PNIPAM *-co-* PPEGMA PNIPAM *-b-* PPEGMA	3–31	-	3T3 fibroblasts	Enhancing the hydration of PNIPAM by copolymerization with PEGMA leads to faster cell detachment, but also to lower cell adhesion and proliferation; Block copolymer had very similar behavior as PNIPAM in terms of cell attachment/detachment.	234
	PGMA *-cb-* PNIPAM	32–45	-	3T3 fibroblasts	Enhancing the hydration of PNIPAM polymerized from the terminus and side chains of modified PGMA: hydroxyl groups, from opened epoxy rings, provide hydrophilic environment for accelerated cell detachment.	250
	PNIPAM	-	Collagen	Smooth muscle cells	Cells on thicker and collagen coated PNIPAM adhered better; Changes in the cell morphology upon detachment.	103
	$PPEGMEMA_9$ *-co-* $PPEGMEMA_2$	-	-	L929 mouse fibroblasts	Thermoresponsive polymer for controlled cell attachment/detachment; Alternative to PNIPAM.	103

[a] DNP: dinitrophenyl. [b] IgE: immunoglobulin E. [c] BSA: bovine serum albumin.

umbilical vein endothelial cells (HUVECs) on RGD-functionalized PHEMA and PPEGMA brushes.[600] Immunofluorescence staining of the focal adhesions revealed differences between the adhesion of HUVECs on PHEMA brushes versus the adhesion of HUVECs on PPEGMA brushes. While for PHEMA brushes relatively large and mature focal adhesions were observed, which were located mainly at the cell periphery, a relatively large number of small focal adhesions together with fibrilar adhesions were found in the case of the PPEGMA brushes. These differences were attributed to differences in water swellability between the different brushes and to the different ethylene glycol spacer lengths that connect the RGD ligand to the polymer brush backbone. It was proposed that the PPEGMA brushes represent a softer support with a more flexible peptide ligand leading to a reduced ligand−integrin affinity. Navarro et al. prepared RGD-functionalized PMAA brushes and investigated the effect of the RGD attachment site along the polymer brush on the adhesion of MG63 osteoblasts.[213] Whether the ligand was at the top of polymer brush or buried about 15 nm below the surface had very little influence on cell density and viability. However, the morphology of cells was affected. Cells spread well with marked focal adhesion points at the periphery of the cytoplasm on samples with

RGD motifs coupled on the surface, whereas in the case of the samples where RGD was buried, cells were found to adopt a rounded morphology and focal adhesions concentrated toward the internal part of the cell. Petrie et al. have demonstrated that the modification of clinical-grade titanium implants with a nonbiofouling polymer brush coating that presents appropriate biochemical cues can facilitate tissue healing and specifically osseointegration. PPEGMA brushes that presented the $\alpha_5\beta_1$-intergrin specific fibronectin fragment $FNIII_{7-10}$ enhanced osteoblast differentiation and improved functional implant osseointegration compared to RGD-functionalized and unmodified Ti-substrates.[601]

In addition to covalently immobilizing ECM (derived) peptides/proteins, cell adhesive substrates can also be obtained by (nonspecific) physisorption of such peptides/proteins on nonbiofouling polymer brushes. Since highly dense nonbiofouling brushes can be very efficient in preventing nonspecific adsorption of peptides and proteins, control of brush density is very important to allow integrin-mediated cell-adhesion following this approach. A number of reports, however, has successfully demonstrated that this is a feasible strategy to prepare cell adhesive PHEMA- and PPEGMA-based surface coatings. Washburn and co-workers, as well as the laboratory of Genzer, have studied cell adhesion on gradient PHEMA brushes that were precoated with fibronectin.[278,291] While the high density PHEMA brushes were effective in preventing fibronectin adsorption and, consequently, cell adhesion, Washburn and co-workers demonstrated that fibronectin was adsorbed on the lower density brushes, allowing adhesion and spreading of fibroblasts. Using X-ray reflectivity experiments, the authors demonstrated that the high density, nonadhesive brushes were in the brush regime, while the less dense PHEMA brushes that enabled fibronectin deposition and cell attachment had a mushroom structure. Similar results were reported by Husson and co-workers, who investigated the effect of brush density and thickness on the adhesion of mouse MC3T3 fibroblasts and GRGDS precoated PPEGMA brushes.[298] In an attempt to distinguish between the effect of polymer molecular weight and chain density (which both influence the conformation of the surface-tethered polymer chains), Bhat et al. studied fibronectin adsorption and cell attachment on orthogonal molecular weight/density gradient PHEMA brushes.[291] From these experiments, it was concluded that neither molecular weight nor density, but rather PHEMA surface coverage, was the decisive factor in determining protein adsorption and cell attachment.

4.3.2. Patterned Polymer Brushes

Instead of using polymer brushes as a platform to present ECM derived peptide ligands, surface-initiated polymerization can also be used to create nonbiofouling patterns on cell adhesive substrates and geometrically direct and/or confine cell adhesion. Chilkoti and co-workers, for example, used microcontact printing techniques to modify gold substrates with circular and striped PPEGMEMA micropatterns.[292] Incubation of these patterned substrates with fibronectin leads to the selective adsorption of the protein in those areas that are not covered by the PPEGMEMA brush and subsequently allows spatial control of cell adhesion. Lee et al. used microcontact printing to pattern *N*,*N*′-disuccinimidyl carbonate-activated PPEGMA brushes with poly(L-lysine).[604] After passivation of any remaining *N*-hydroxysuccinimide carbonate ester groups with 2-(2-aminoethoxy)ethanol, deposition of Chinese hamster ovary cells resulted in selective attachment on the poly(L-lysine)-covered areas of the brush. Ober and co-workers have studied the localization of antidinitrophenyl-immunoglobulin E sensitized RBL mast cells on patterned oligo(ethylene glycol)-modified polystyrene brushes with different feature sizes.[162] Cell adhesion to these substrates was mediated by dinitrophenyl-bovine serum albumin (DNP-BSA), which was preadsorbed on areas not covered by the nonbiofouling polymer brush. Linear patterns with feature sizes of 50 and 90 μm and a spacing of 50 μm showed a high degree of spatial control over cell adhesion. On patterns with a line width of 10 μm and a spacing of 30 μm, however, some regions showed cells located on the PEG surface between the DNP-BSA lines. This was attributed either to imperfections in the patterning process or to bridging of cells across the DNP-BSA lines. Iwata et al. studied the influence of brush thickness on the adhesion of fibroblasts to patterned PMPC brush surfaces.[577] A minimum brush thickness of 5 nm was needed to confine cell adhesion to the regions defined by the polymer brush pattern.

4.3.3. Thermoresponsive Polymer Brushes

Polymers that show LCST behavior, i.e. polymers that can be thermally switched from a hydrated, extended state into a dehydrated collapsed state, offer the possibility to generate surface coatings that can be thermally triggered from a nonbiofouling to a cell adhesive state. Such switchable surface coatings are of interest, as they provide a noninvasive means to produce cell sheets that can be used in regenerative medicine. The most widely used polymer for this purpose is PNIPAM, which has a solution LCST of 32 °C. Okano and co-workers have intensively explored the use of thermoresponsive surfaces for cell sheet engineering and have used SI-ATRP to grow PNIPAM brushes from polystyrene culture dishes.[520] The authors found that, above the LCST, cell adhesion decreased with increasing brush thickness, which was attributed to a high degree of hydration of the thicker brushes. PNIPAM brushes with thicknesses between 2 and 65 nm released most of the adhered cells within 120 min after reducing the temperature from 37 to 20 °C. The cell adhesion and detachment properties of PNIPAM-based polymer brushes can be tuned by engineering the architecture and composition of the brushes. Xu et al., for example, demonstrated that cell detachment can be accelerated by surface-initiated copolymerization of NIPAM with a very small amount of PEGMA (0.5−1.0 mol %).[234] However, the enhanced cell detachment below the LCST was compromised by reduced cell adhesion and growth at 37 °C, especially for copolymer brushes that were prepared with 1 mol % PEGMA. Cell detachment can also be facilitated via engineering of the brush architecture. Xu et al. have compared cell detachment on PGMA-*b*-PNIPAM brushes with that of comb-type PNIPAM brushes that were produced by postmodification of the epoxide side chains of a PGMA brush, followed by SI-ATRP of NIPAM.[250] Whereas 40 min was required for complete cell detachment for the PGMA-*b*-PNIPAM surface, this process required 25 min for the comb-type analogue. The enhanced cell detachment from the comb-type brushes was attributed to the presence of hydroxyl groups, which are formed during postmodification of the PGMA with an ATRP initiator and which generate a local hydrophilic environment. Random copolymers of di(ethylene glycol) methyl ether methacrylate and poly(ethylene glycol)

methyl ether methacrylate prepared via controlled radical polymerization are an interesting alternative to PNIPAM. By varying the $PEGMEMA_9$ content from 5 to 8 and 10 mol %, the cloud point of these copolymers can be tuned from 32 to 39 °C.[103] Wischerhoff et al. used SI-ATRP to prepare ($PPEGMEMA_9$-*co*-$PPEGMEMA_2$) brushes that allowed spreading and adhesion of fibroblasts at 37 °C but that were cell-repellent and induced cell detachment at 25 °C.

4.4. Protein Binding and Immobilization

Polymer brushes are very attractive platforms to bind or immobilize proteins, which makes them of interest, for instance, as the active layer in protein microarrays or as tools for protein purification. There are several characteristics that set polymer brushes apart from, for example, self-assembled monolayers and which makes them very attractive for these applications. First of all, polymer brushes can be prepared with excellent nonbiofouling properties (see section 4.2). A nonbiofouling background is important for microarray applications, to avoid nonspecific protein adsorption, which could lead to an enhanced background noise, as well as to prevent denaturation of surface-immobilized proteins. Furthermore, polymer brushes can be considered as three-dimensional films with a significant internal volume. As a consequence, polymer brushes can present a very high surface concentration of functional groups that can be used to bind or immobilize proteins. Table 27 presents an overview of the different strategies that have been used so far to bind or immobilize proteins onto polymer brushes prepared via SI-CRP. The approaches listed in Table 27 are subdivided into two categories: (i) noncovalent protein binding and (ii) covalent protein immobilization. In the remainder of this section, each of these binding/immobilization strategies will be discussed in more detail. In particular, examples will be highlighted that demonstrate the use of (protein modified)-polymer brushes for microarray applications or in protein purification.

4.4.1. Noncovalent Protein Binding

A variety of strategies has been used to noncovalently bind proteins to polymer brushes. Proteins can be bound to polymer brushes either via nonspecific noncovalent interactions, such as hydrophobic or electrostatic interactions, or via directed noncovalent interactions, such as metal-coordination or receptor−ligand interactions. In contrast to nonspecific interactions, directed noncovalent interactions allow control over the orientation of the immobilized proteins, which may be advantageous for microarray applications, for example. Below, the different noncovalent strategies that have been used to bind proteins to polymer brushes prepared via SI-CRP will be discussed in more detail.

Polymers such as PNIPAM that show LCST behavior offer interesting opportunities to reversibly bind proteins via nonspecific hydrophobic interactions. Protein binding takes place above the LCST of the polymer, when the polymer brush is in the hydrophobic, collapsed state. The adsorbed proteins are released once the brush is in the hydrated state, i.e. below the LCST. Alexander and co-workers have studied the adsorption of fluorescent labeled (FITC) BSA to micropatterned PNIPAM brushes.[565] Confocal microscopy experiments revealed that rinsing protein-loaded substrates below the LCST indeed resulted in release of protein from the PNIPAM-covered areas. When protein binding and release was studied over a larger number of thermal cycles, however, a more complex protein adsorption pattern was observed, suggesting that longer term adsorption is not only determined by the LCST behavior of the brush but also by other factors such as protein−polymer hydrogen bonding interactions, steric exclusion, surface disorder, and denaturation.

Polyelectrolyte brushes can bind proteins via electrostatic interactions. Protein binding by polyelectrolyte brushes via electrostatic interactions is influenced by two factors: (i) the pH, which determines the overall net charge of molecules, and (ii) the ionic strength, which affects the interactions among charged species. Kusumo et al. exploited electrostatic interactions to absorb a net negatively charged protein (BSA, pI $\sim$ 4.7) onto positively charged PDMAEMA brushes (pK_a = 7.5) at pH 5.8 and low ionic strength (1 mM NaCl).[299] The extent of uptake was independent of grafting density and scaled linearly with the surface mass concentration of the polymer, as measured by surface plasmon resonance (SPR). It was found that BSA binds at the constant ratio of 120 DMAEMA monomer units per protein molecule. When a protein with the same net charge as the brush (lysozyme, pI = 11) was taken, charge repulsions did not allow any absorption to take place. The large BSA uptake was, therefore, explained by electrostatically driven penetration through the oppositely charged polymer brush layer. Desorption of BSA from the brush could be accomplished by lowering the pH to 4 and/or increasing the salt concentration from 1 mM to 1 M. Similar findings were reported by Baker, Bruening, and co-workers, who studied protein adsorption on negatively charged PAA brushes.[610] Whereas no detectable adsorption of BSA could be observed, the PAA brushes were found to bind as much as 16.2 $\mu g/cm^2$ lysozyme. Due to their high binding capacity and charge selectivity, polyelectrolyte brushes are very attractive for protein separation and purification. Husson and co-workers prepared high capacity membrane absorbers by growing a PAA brush from the surfaces of regenerated cellulose membranes.[469] Depending on the polymerization time, PAA-modified membranes with maximum lysozyme binding capacities of 98 mg/mL (static) or 71 mg/mL (dynamic) could be prepared. Polymerization times longer than 1 h resulted in some pore blocking and a decrease in protein capacity. In comparison with commercial membranes, the polymer brush-functionalized membranes exhibited a 2−3 times higher lysozyme binding capacity. In another study, porous silica inorganic membranes were coated with PGMA brushes and subsequently modified with diethylamine to obtain a polymer brush coating that allowed immobilization of BSA.[622]

Metal-ion affinity interactions, in particular using nitrilotriacetate (NTA)−metal ion complexes, have been extensively used to prepare protein binding polymer brushes. The attractiveness of the use of NTA−metal ion complexes lies in the fact that the selectivity of the binding process can be tuned by varying the metal ion. Moreover, due to the strong coordination of, for example, histidine residues to the metal complex, the presence of water is not problematic. Finally, using appropriate competitive ligands, such as for example EDTA, bound proteins can be released and the polymer brush regenerated by loading with the appropriate metal ion.

Protein binding to NTA-Cu^{II} complexes involves coordination of histidine residues to the metal ion. Bruening, Baker, and co-workers reported binding of 5.8 $\mu g/cm^2$ BSA, 7.7 $\mu g/cm^2$ myoglobin, and 9.6 $\mu g/cm^2$ anti-IgG with 55-nm-thick NTA-Cu^{II}-functionalized PAA brushes.[610] As there is

Table 27. Overview of Different Noncovalent and Covalent Strategies That Have Been Used To Bind or Immobilize Proteins on Polymer Brushes Prepared via SI-CRP

	Immobilization strategy	Polymer brush	Protein(s)	Comment	Ref
Non-covalent protein binding	Hydrophobic interactions	PNIPAM	BSA[a]	Temperature-controlled protein attachment/detachment. Protein adsorbed only at the surface of the polymer brush.	565
	Electrostatic interactions	PDMAEMA	BSA[a]	Adsorption possible only at low ionic strength. pH dependent, charge selective	299
	Electrostatic interactions	PAA	Lysozyme	Charge selective: ~ 80 monolayer of lysozyme into 55-nm-thick brush.	469,610
	Electrostatic interactions	PMES	Lysozyme	Similar immobilization of proteins as on PAA.	113
	NTA-Ni^{II}	PHEMA	His-tag proteins	Selective binding of oligohistidine-tagged proteins. Protein purification.	367
	NTA-Cu^{II}	PAA PHEMA PMES	BSA[a] Myoglobin Anti-IgG[b] RNase A[c]	Site specific binding to histidine residues.	113,366,610,611
	NTA-Fe^{III}	PHEMA	Phosphoangiotensin (pA) H_5 peptide β-casein Ovalbumin digests	Selective binding of phosphopeptides.	605,606
	Biotin-streptavidin	PPEGMA	Streptavidin	Rhodamine conjugated streptavidin binding. Improved binding capacity and signal/noise ratio compared to corresponding SAMs. Saturation thickness of 20 nm beyond which no more streptavidin could enter the biotinylated polymer brush.	604
	Biotin-streptavidin	PAA	Streptavidin Fluoresceinated biotin	Protein patterned surfaces.	582
Covalent protein immobilization	NHS[d]	PAA	BSA[a] Biotinylated BSA[a] RNase A[c] Avidin	Competitive NHS[d] ester hydrolysis.	582,610,611
	NHS[d]	PCBMA	Anti-human chorionic gonadotropin (anti-hCG)	Selective binding of human chorionic gonadotropin (hCG) while maintaining a high resistance to non-specific protein adsorption.	612
	NHS[d]	crosslinked PPEGMA	Anti-mouse IgG[b]	*In situ* polymerization of acrylated antibodies with PEGMA.	718
	CDI[e]	PPEGMA *-co-* PPEGMEMA	IgG[b]	Surface concentration of IgG[b] could be varied by changing the relative amounts of PEGMA and PEGMEMA.	552
	Epoxide	PGMA	Glucose oxidase	Amount of immobilized protein increases with increasing brush thickness. Immobilized enzyme has superior stability compared to the corresponding free enzyme.	355
	Epoxide	PGMA-*co*-PDHPMA	BSA[a] Penicillin G acylase	Copolymerization with 2,3-dihydroxypropyl methacrylate to produce water-dispersible magnetic microspheres.	619,719
	Pyridyl disulfide	PMPC-*b*-PGMA PMPC-*co*-PGMA	Antibody Fab' fragments	Site specific, oriented immobilization of Fab' antibody fragments.	620,621
	O^6-benzylguanine	PPEGMA	AGT fusion proteins	Site specific, oriented immobilization	602,720

[a] BSA: bovine serum albumin. [b] IgG: immunoglobulin G. [c] RNase A: ribonuclease A. [d] NHS: *N*-hydroxysuccinimide. [e] CDI: 1,1′-carbonyldiimidazole.

no apparent correlation between binding capacity and protein size, it was proposed that protein binding is mainly governed by the number of histidine residues in the protein and their accessibility. Similar binding capacities were reported for NTA-Cu^{II}-functionalized PMES brushes.[113] The BSA binding capacity increased nonlinearly with increasing PMES brush thickness and reached a plateau value of 7.2 $\mu g/cm^2$ for a brush thickness of 85 nm. The high binding capacities and the increase in binding capacity with brush thickness suggest that binding occurs both at the brush surface and inside the brushes. Bruening, Baker, and co-workers evaluated the activity of NTA-Cu^{II} immobilized proteins by measuring the binding of antirabbit IgG to PAA-bound protein A.[610] The authors found that about 27 times less anti-IgG was found than would be expected for a 1:1 protein/anti-IgG complex and attributed this difference to the limited free space in the polymer brush after immobilization of protein A. Cullen et al. studied the activity of ribonuclease A (RNase A) bound to a PAA brush via NTA−Cu^{II} affinity interactions.[611] The RNase activity was found to increase with

increasing surface density, but it started to level off at a surface concentration of 3.5 μg/cm^2. The authors postulated that, at higher surface densities, steric crowding prevented the RNA substrate from accessing the active site.

The coordination of histidine to NTA−Ni^{II} is relatively weak compared to the NTA−Cu^{II} histidine binding. NTA−Ni^{II} complexes, however, very efficiently bind oligohistidine sequences, which makes the NTA−Ni^{II} motif very attractive for protein purification. Following this strategy, oligohistidine-tagged ubiquitin was separated from a phosphate buffer solution that also contained BSA and myoglobin and was isolated in >99% purity using porous alumina membranes, which were modified with a PHEMA-NTA-Ni^{II} brush coating.[367] Along the same lines, coating matrix-assisted laser desorption/ionization sample plates with a PHEMA brush derivatized with NTA−Fe^{III} complexes allowed selective, efficient phosphopeptide enrichment prior to mass spectrometric analysis.[605,606]

The binding of biotin to (strept)avidin provides another noncovalent strategy to immobilize proteins to polymer brushes prepared via SI-CRP. Dong et al. demonstrated that biotinylated BSA that was covalently attached to a PAA brush could be used to noncovalently immobilize streptavidin.[582] Using SPR experiments, Lee et al. compared the binding of streptavidin to biotinylated PPEGMA brushes with that on biotin-functionalized SAMs.[604] The biotinylated PPEGMA brushes showed a ~2.5-fold higher binding capacity and a signal-to-noise ratio that was 10 times better than that of the biotin-modified SAM. Signal-to-noise ratios were determined by comparing the quantity of bound streptavidin with the amount of a model protein (fibrinogen, lysozyme) that was adsorbed on the same surface. Thickness-dependent measurements revealed that both the streptavidin binding capacity and the streptavidin/fibrinogen signal-to-noise ratio reached a plateau value at a brush thickness of 20 nm.

4.4.2. Covalent Protein Immobilization

Table 27 lists a number of strategies that have been used to covalently bind proteins to polymer brushes grown via SI-CRP. In contrast to the noncovalent approaches that were discussed above, the different covalent immobilization protocols result in a robust link between the polymer brush and the protein, which also withstands intensive washing, for example. As a consequence, covalent protein immobilization is very attractive to fabricate protein microchips.

Active ester chemistry represents a very convenient way to immobilize proteins on carboxylic acid brushes such as PAA. PAA brushes are usually activated with *N*-hydroxysuccinimide (NHS) using a carbodiimide reagent to mediate the reaction.[582,610,611] NHS-activated PAA brushes have been successfully used to covalently immobilize a variety of proteins. A drawback of the use of NHS to activate carboxylic acid-containing polymer brushes is the susceptibility of the corresponding active esters toward hydrolysis. Upon exposure to an aqueous solution containing the protein of interest, NHS ester hydrolysis competes with covalent protein immobilization, which limits the maximum amount of protein that can be bound. Furthermore, the postmodification of polymeric NHS esters with primary amines has been found to be accompanied by the formation of ring-opened and glutarimide-bound conjugates.[716] Whereas the former reaction results in conjugation via a hydrolytically unstable linkage, the latter side reaction limits the maximum degree of postmodification. These side reactions, however, can be reduced to a minimum by properly adjusting the reaction conditions.[717] Cullen et al. compared the relative activity of RNase A bound to a PAA brush via NTA-Cu^{II} affinity interations with that of RNase A covalently bound to a PAA brush using NHS/EDC chemistry.[611] The covalently bound enzyme was found to show a higher relative activity. Furthermore, temperature-dependent activity experiments revealed that the covalently immobilized enzyme behaved similar to native RNase A, whereas the NTA-Cu^{II} bound enzyme showed no temperature dependence. The latter observation was attributed to conformational changes in the active site of the protein. Zhang et al. used NHS active ester chemistry to immobilize antihuman chorionic gonadotropin (anti-hCG) onto poly(carboxybetaine methacrylate) (PCB-MA) brushes.[612] Using SPR measurements, the authors could demonstrate that the antibody-modified polymer brush was able to specifically bind hCG while resisting the nonspecific adsorption of other proteins. A slightly different approach, which also involved the use of NHS activation chemistry, to prepare covalent protein-functionalized brushes was reported by Sebra et al. In this case, an acrylated antibody was prepared using NHS chemistry. The acrylated antibody was subsequently incorporated in a poly(poly(ethylene glycol) acrylate) brush via surface-initiated, iniferter-mediated copolymerization with poly(ethylene glycol) acrylate.[718]

Covalent coupling of proteins to hydroxyl-functional polymer brushes such as PPEGMA can be achieved using activating agents such as 1,1′-carbonyldiimidazole (CDI) to generate carbamate groups that can react with amine groups of proteins. This strategy was successfully used by Xu et al. to prepare patterned biofunctional surfaces consisting of IgG-functionalized PPEGMA-*co*-PPEGMEMA domains and a nonbiofouling PPEGMEMA background.[552] The authors demonstrated that the surface concentration of immobilized IgG could be varied by adjusting the relative amounts of PEGMA and PEGMEMA in the protein-presenting domains.

Epoxide groups can react irreversibly with various nucleophiles, which makes them attractive candidates for the covalent immobilization of proteins. Xu et al. have explored the reactivity of epoxide groups to immobilize the enzyme glucose oxidase (GOD) on PGMA brushes prepared via SI-ATRP.[355] Upon increasing the brush thickness from ~5 to ~55 nm, an increase in both the total amount of immobilized GOD as well as the total immobilized GOD activity was observed. With increasing brush thickness, however, the relative activity, i.e. the activity of the immobilized enzyme compared to that of an equivalent amount of the free enzyme, was found to continuously decrease, which was attributed to changes in protein tertiary structure and/or diffusion limitation of the substrate. Interestingly, the storage stability of the covalently immobilized GOD was superior to that of the free enzyme, which was ascribed to stabilization of the active conformation by multipoint bond formation between the enzyme and the polymer brush. A drawback of PGMA is that it is not water-soluble and as a consequence cannot be used to coat microspheres that need to be dispersed in aqueous media for the separation, purification, or detection of biological analytes. This problem can be overcome by copolymerization of GMA with an appropriate hydrophilic comonomer. Huang et al., for example, have demonstrated that surface-initiated copolymerization of mixtures of glycidyl methacrylate and 2,3-dihydroxypropyl methacrylate can be used to prepare water-dispersible magnetic microspheres.[619,719]

These microspheres were subsequently used to immobilize BSA and penicillin G acylase. In line with the observations by Xu et al.,[355] these authors also found that the stability of the immobilized penicillin G acylase toward changes in temperature and pH was superior compared to that of the corresponding free enzyme.[619]

The active ester, 1,1′-carbonyldiimidazole, and epoxide chemistries that have been discussed so far to immobilize proteins on polymer brushes are very attractive, as they create multiple, robust covalent linkages between the protein of interest and the polymer brush substrate. These approaches, however, also have some limitations which are primarily related to the nonchemoselective nature of the immobilization reaction and the lack of control over the orientation of the immobilized protein. The reactive groups that have been discussed so far can undergo reaction with a variety of nucleophilic groups in proteins such as amino and hydroxyl groups. Due to the high natural abundance of amino acids containing such nucleophilic groups in their side chains, this can result in multipoint attachment and makes it difficult to control the orientation of the immobilized protein. Furthermore, since the abundant amino and hydroxyl side chain functional amino acids do not only prevail in the protein of interest but are also present in many other proteins, selective immobilization of the protein of interest out of a complex mixture, e.g. a cell lysate, containing many other proteins, is not possible with the chemistries discussed so far. A few studies have been published, in which it was attempted to address these problems and to improve the chemoselectivity of the immobilization reaction and the orientation of the protein. One strategy is based on the use of less abundant side chain functional amino acids for the immobilization reaction. Cysteine is a very attractive amino acid in this respect, as it has a much lower natural abundance compared to, for example, lysine and serine and its side chain thiol group can undergo a variety of interesting coupling reactions. When proteins are used that contain a single reactive cysteine moiety, this method allows the oriented immobilization of the protein of interest. This strategy was explored by Iwasaki and co-workers, who successfully immobilized antibody fragments via a thiol−disulfide interchange reaction between the cysteine thiol group of the protein and a pyridyl disulfide-functionalized PMPC brush.[620,621] Another concept that has been successfully used to covalently immobilize proteins on polymer brushes prepared via SI-CRP involves the use of fusion constructs of the protein of interest and an enzyme. In this way, incubation of a polymer brush that is modified with the enzyme's substrate allows covalent immobilization of the fusion protein in a highly chemoselective fashion. The feasibility of this concept has been demonstrated using fusion constructs of various proteins with an engineered mutant of the DNA repair protein O^6-alkylguanine-DNA-alkyltransferase (AGT). The engineered AGT mutant can react in a highly chemoselective fashion with O^6-benzylguanine derivatives, resulting in transfer of the benzyl group of the substrate to one of the cysteine residues of AGT. By postmodification of PHEMA and PPEGMA brushes with O^6-benzylguanine moieties, Tugulu et al. successfully used this strategy to covalently immobilize AGT fusion proteins.[602] In various proof-of-concept experiments, it was demonstrated that the immobilized proteins do not lose their activity throughout the immobilization process. Most importantly, due to the extraordinary chemoselectivity of the immobilization reaction, this strategy does not require the use of purified proteins, but the immobilization reaction can be carried out using cell lysates.[720]

4.5. Chromatography Supports

SI-CRP techniques have been widely used to modify the properties of chromatography stationary phases. Table 28 gives an overview of different chromatography supports, which have been modified using SI-CRP.

Porous silica particles have been modified with hydrophobic polymer brushes to facilitate the chromatographic separation of polycyclic aromatic hydrocarbons (PAHs).[721–723] Mallik et al. prepared poly(octadecyl acrylate)-modified silica beads via SI-ATRP. The chromatographic behavior of these particles was investigated by retention studies of PAHs and compared with that of identical polymer-modified beads, which were produced via the grafting onto approach.[721] For silica beads that were modified using SI-ATRP, longer retention times and greater selectivity toward PAHs were observed. In addition to silica particles, also polymer-based stationary phases have been modified using SI-CRP techniques.[504,724] Unsal et al., for example, have modified polymer microparticles with poly(potassium 3-sulfopropyl methacrylate) (PSPMA(K)) brushes and subsequently used the modified particles as an ion-exchange stationary phase to allow protein separation.[504] Coad et al. have grafted poly(*N*,*N*-dimethylacrylamide) (PDMAM) brushes onto porous polymer microparticles, which were used as the stationary phase for protein separation by entropic interaction chromatography.[724] In addition to silica- and polymer-based particles, also a variety of other chromatographic supports has been modified using SI-CRP techniques. Lee and co-workers used SI-ATRP to modify the surface of polymer-based capillary electrophoresis microchips with a PPEGMEMA brush coating.[497,725] The polymer brush coating was found to reduce electroosmotic flow and nonspecific protein adsorption on the chip surface. One of the first reports to describe the modification of capillary chromatography supports using SI-CRP was published by Wirth and co-workers in 1998.[232] One of the motivations of these authors to use SI-ATRP was that this technique allows a surface-confined polymerization and avoids clogging of pores due to free polymer formed during polymerization. In this study, the performance of capillaries coated with linear and cross-linked poly(acrylamide) brushes with regard to the electrophoresis separation of strongly basic proteins was investigated. It was found that cross-linked polymer brush coatings resulted in a higher reproducibility with respect to migration time compared to the linear coatings. Idota et al. derivatized fused silica capillaries with a thermoresponsive PNIPAM brush and demonstrated that these surface-modified capillaries can be used to thermally regulate aqueous capillary chromatography.[674] Miller et al. grafted PHEMA brushes from the inside of silica capillaries and subsequently postmodified the polymer brush coating with ethylenediamine and octanoyl chloride.[726] These modified capillaries showed an improved performance as stationary phases for open-tubular electrochromatography of phenols and anilines compared to the bare capillaries.

4.6. Membrane Applications

In addition to the derivatization of stationary phases for chromatography applications, SI-CRP has also been used to prepare or tailor the properties of membranes. An overview of different porous inorganic and polymer-based support

Table 28. Overview of Chromatography Supports Modified with Polymer Brushes Produced via SI-CRP

Substrate	Polymer brush	SI-CRP technique	Application and remarks	Ref
Porous silica particles *(diameter, 5 μm; pore size, 12 nm)*	PODA	SI-ATRP	Stationary phase in HPLC	721, 722
Porous silica particles *(diameter, 5 μm; pore size, 12 nm)*	PODVBPheA	SI-ATRP	Packing materials for HPLC	723
Porous silica particles *(diameter, 5 and 10 μm; pore size, 20 nm)*	PSBMA, PS, PMA, PBMA, PGMA	SI-ATRP	Functionalization of stationary phases for HPLC	339
Silica monoliths *(pore size, 50 and 80 nm)*	PHEMA	SI-ATRP	Stationary phase in HPLC	766
Toyopearl AF-amino 650M *(amino functionalized porous polymer beads; diameter, 65 μm; pore size, 100 nm)*	PDMAM	SI-ATRP	Stationary phase in entropic interaction chromatography	724
PDHPMA-*co*-PEDMA[a] porous particles *(diameter, ∼6 μm; pore size, ∼40 nm)*	PSPMA(K)	SI-ATRP	Preparation of a polymer-based ion-exchange support for HPLC	504
PGMA-*co*-PMMA-based microchips *(channel dimensions: w, 49−115 μm; h, 33 μm)*	PEGMEMA	SI-ATRP	Capillary electrophoresis	725
PMMA-based microchip *(channel dimensions: w, 49−115 μm; h, 33 μm)*	PEGMEMA	SI-ATRP	Capillary electrophoresis	497
Fused silica capillary (*inner diameter, 50 μm*)	PNIPAM	SI-ATRP	Thermally regulated capillary chromatography	674
Fused silica capillary (*inner diameter, 75 μm*)	PAM	SI-ATRP	Capillary electrophoresis; protein separation	232
Fused silica capillary (*inner diameter, 100 μm*)	Ethylenediamine and octanoyl chloride postmodified PHEMA	SI-ATRP	Stationary phases for open-tubular capillary electrochromatography	726

[a] PDHPMA-*co*-PEDMA: poly(dihydroxypropyl methacrylate)-*co*-poly(ethylene glycol dimethacrylate).

Table 29. Overview of Porous Membranes That Have Been Modified Using SI-CRP

Substrate	Polymer brush	SI-CRP technique	Application and remarks	Ref
Anodic alumina oxide membrane *(pore size, 20 nm)*	PEGDMA, PHEMA	SI-ATRP	Composite membrane gas separation	255
Anodic alumina oxide membrane *(pore size, 20 nm)*	Postmodified PHEMA	SI-ATRP	Pervaporation membranes	365
Anodic alumina oxide membrane *(pore size, 100 nm)*	P4VP-*co*-PEGDMA	SI-ATRP	Template synthesis of molecularly imprinted polymer nanotube membranes	364
Regenerated cellulose membrane	PEGDMA-*co*-PMAA	SI-PIMP	Molecularly imprinted polymer membranes	228
Regenerated cellulose membranes *(MWCO: 100, 300, and 1000 kDa)*	PPEGMA	SI-ATRP	Control of membrane pore size, water flux, and molecular weight cutoff	470
Au-coated polycarbonate track-etched membrane *(pore size, 80−200 nm)*	PNIPAM	SI-ATRP	Thermal or flow properties	677
Chloromethylated poly(phthalazione ether sulfone ketone) membrane (*microporous membrane*)	PPEGMEMA	SI-ATRP	Membrane with controlled solute rejection and antifouling properties	542
PVDF-*g*-PVBC	PS, PS-*b*-P*t*BA (postderivatized)	SI-ATRP	Proton conducting membranes	727
PVDF microfiltration membranes	PMMA, PPEGMEMA	SI-RATRP	Membrane with antifouling properties under continuous-flow conditions	550

membranes that have been modified with polymer brushes grown using SI-CRP techniques is given in Table 29.

Balachandra et al. used SI-ATRP to modify the surface of porous alumina membranes with a ∼50−100-nm-thick cross-linked PPEGDMA or linear PHEMA brush.[255] Gas permeation studies indicated that the PPEGDMA-based membranes have CO_2/CH_4 selectivities of ∼15−20 and O_2/N_2 selectivities of ∼2. The PHEMA-modified membranes,

in contrast, only showed very little selectivity. The performance of the PHEMA-based membranes could be significantly improved and reached CO_2/CH_4 selectivities of ~6−8 after postmodification of the hydroxyl side-chain functional groups with pentadecafluorooctanoyl chloride. Along these lines, the same laboratory also grafted PHEMA brushes from alumina membranes and subsequently postmodified the polymer brush coating with octanoyl chloride, palmitoyl chloride, and pentadecafluorooctanoyl chloride.[365] These postmodified polymer brush-coated alumina supports were studied as pervaporation membranes for the separation of volatile organic compounds (VOCs) from water. Wang et al. used the interior pore surface of alumina membranes to template the formation of molecularly imprinted polymer nanotube membranes.[364] The imprinted polymer nanotubes adsorbed significantly larger amounts of steroids with an approximately 2-fold higher preference for β-estradiol over estrone and cholesterol compared to a nonimprinted reference sample. Molecularly imprinted polymer brush membranes were also prepared by Hattori et al., who have used SI-PIMP to graft theophylline imprinted brushes onto regenerated cellulose membranes.[228] Singh et al. used SI-ATRP to modify regenerated cellulose ultrafiltration membranes having molecular weight cut-offs of 100, 300, and 1000 kDa with a PPEGMA brush coating.[470] The authors demonstrated that the water flux across these modified membranes decreased with increasing polymerization time (i.e., brush thickness) and also found that the polymer brush surface modification resulted in reduced molecular weight cut-offs. Lokuge et al. grafted thermosensitive PNIPAM brushes on the exterior surface of gold-coated polycarbonate track-etched membranes.[677] The LCST behavior of the PNIPAM coating was successfully used to control the flow properties across the membrane. Chloromethylated poly(phthalazinone ether sulfone ketone) membranes have been modified with a thin PPEGMEMA coating, which was produced using SI-ATRP.[542] The hydrophilic polymer brush coating resulted in a decrease in pore size, increased solute rejection, and an improved fouling resistance. Proton conducting membranes have been prepared by sulfonation of polystyrene brushes, which were grown from poly(vinylidene fluoride)-*g*-poly(vinylbenzyl chloride) supports.[727] Chen et al. used surface-initiated reverse ATRP to modify PVDF microfiltration membranes with PMMA and PPEGMEMA brush coatings.[550] The PPEGMEMA-modified membranes were less susceptible to protein fouling compared to the PMMA-modified supports.

4.7. Antibacterial Coatings

Prevention and treatment of bacterial infections are important goals in modern healthcare. As a consequence, there is also a great interest in strategies to modify material surfaces with coatings that prevent biofilm formation. SI-CRP is an attractive tool to produce well-defined antibacterial coatings. Table 30 gives an overview of polymer brushes, which have been prepared to produce antibacterial surfaces. The antibacterial brushes that have been described in the literature can be subdivided into three categories. The first group are biocidal polymer brushes which kill bacteria. The second class of antibacterial polymer brushes are nonbiofouling brushes. The antibacterial properties of these coatings are due to the fact that they prevent bacterial adhesion. The third class of antibacterial polymer brushes combines biocidal and nonbiofouling properties. Examples of each of these classes of polymer brushes will be discussed in the remainder of this section.

Russell and co-workers have used SI-ATRP to graft PDMAEMA brushes on various substrates, including filter paper, glass slides, and silicon wafers.[728,729] Quaternization of these brushes with ethyl bromide resulted in quartenary ammonium-modified surfaces with substantial biocidal activity. To elucidate the influence of polymer brush chain length and grafting density on the bacterial killing properties, a combinatorial screening was developed. Surface charge density was identified as an important parameter that determines biocidal activity, and the most effective brush coatings had charge densities greater than $1-5 \times 10^{15}$ accessible quaternary ammonium groups per square centimeter.[729] Ramstedt et al. developed an alternative approach for the development of polymer brush-based coatings with biocidal properties.[730] In this case, PSPMA(K) brushes prepared via SI-ATRP were used as reservoirs that could be loaded with silver ions. The brushes showed slow leaching of silver ions but were able to maintain silver at the surface during leaching. These silver-loaded polymer brush coatings were found to effectively inhibit the growth of both Gram positive and Gram negative bacteria.

In addition to presenting biocidal functional groups or releasing biocidal agents, a second approach to prevent biofilm formation is to take advantage of the nonbiofouling properties of certain polymer brushes. Cheng et al. compared bacterial adhesion and biofilm formation on zwitterionic poly(sulfobetaine methacrylate) (PSBMA) and PPEGMEMA brush-coated substrates with that on bare glass slides and SAMs of methyl-terminated, mixed sulfate/trimethylammonium-functionalized, and oligo(ethylene glycol)-containing alkanethiols.[731] Bacterial adhesion on the polymer brush-based coatings was significantly reduced compared to the bare glass reference and the SAM-modified slides during both short-term (3 h) as well as long-term (24 h) binding studies. After 3 h of exposure, adhesion of *S. epidermidis* and *P. aeruginosa* on the polymer brush-coated substrates was reduced by 92% and, respectively, 96% compared to the bare glass control. Van der Mei and co-workers reported similar results using poly(acrylamide) (PAM) brushes.[732,733] These authors investigated the deposition, adhesion, and detachment of two bacterial strains (*S. aureus* and *S. salivarius*) and one yeast strain (*C. albicans*) and found that microbial adhesion on the polymer brush-coated substrates was reduced by 70−92% compared to unmodified silicon surfaces. Examples of other polymer brushes, which have been reported to prevent bacterial adhesion, are PMAA,[614] PAM,[732,733] and poly(2-(*tert*-butylamino)ethyl methacrylate) brushes.[233]

In addition to the examples mentioned above, also several polymer brush-based antibacterial coatings have been reported, which combine both biocidal and nonbiofouling features. Zhang et al., for example, prepared antibacterial coatings that consisted of a PHEMA brush, which was functionalized with the antibiotics gentamicin or penicillin.[387] A polymer brush coating incorporating both biocidal quaternary ammonium groups as well as nonbiofouling properties was obtained by Yao et al. by block copolymerization and subsequent quaternization of PPEGMA and PDMAEMA from polypropylene substrates.[495]

4.8. Low Friction Surfaces

SI-CRP techniques are also attractive tools to produce low friction surfaces. Sakata et al. used SI-ATRP to produce

Table 30. Overview of Antibacterial Polymer Brushes Prepared via SI-CRP

Substrate	Polymer brush	SI-CRP technique	Postmodification reaction	Brush thickness	Biocidal functionality	Bacterial strain tested	Ref
Glass slide or Whatman filter paper	PDMAEMA	SI-ATRP	Quaternization with bromoethane ($R = C_2H_5$)		Quaternary ammonium	*Escherichia coli*, *Bacillus subtilis*	728
Stainless steel	PS-*co*-PDMAEMA PBA-*co*-PDMAEMA	SI-NMP	Quaternization with bromooctane, bromododecane, benzylbromide ($R = C_8H_{17}$, $C_{12}H_{25}$, C_7H_7)	>10 nm	Quaternary ammonium	*E. coli*, *S. aureus*	191
PVBC-*co*-PEGDMA[a] microsphere	PDMAEMA	SI-ATRP	Quaternization with bromohexane, bromododecane ($R = C_6H_{13}$, $C_{12}H_{25}$)	~8 nm	Quaternary ammonium	*Escherichia coli*, *Staphylococcus aureus*	529
PVDF-*g*-PBIEA[b] copolymer microporous membrane	PDMAEMA P*t*BAEMA P*t*BAEMA-*co*-PS	SI-ATRP	Quaternization with bromohexane ($R = C_6H_{13}$)		Quaternary ammonium	*Escherichia coli*	749
Stainless steel	P*t*BAEMA-*co*-PPEGMEMA P*t*BAEMA-*co*-PAA	SI-ATRP				*Staphylococcus aureus*	233
Silicon (Si(100) wafer)	PDMAEMA	SI-ATRP	(1) quaternization with bromohexane ($R = C_6H_{13}$) (2) incorporation of viologen moieties via reaction with a stochiometric mixture of 1,6-dibromohexane and 4,4′-bipyridine	(1) 16, 28 nm (2) 18, 31 nm	Quaternary ammonium	*Pseudomona* sp.	349
Silicon wafer	PAM	SI-ATRP		20 ± 2 nm		*Staphylococcus aureus*, *Streptococcus salivarius*, *Candida albicans (yeast)*	732
Polypropylene	PDMAEMA	SI-ATRP	Quaternization with bromoethane ($R = C_2H_5$)		Quaternary ammonium	*Escherichia coli*	518
Glass slide, silicon wafer	PDMAEMA	SI-ATRP	Quaternization with bromoethane ($R = C_2H_5$)	5−123 nm	Quaternary ammonium	*E. coli*	729
Gold	PSBMA PPEGMEMA	SI-ATRP				*Staphylococcus epidermidis*, *Pseudomonas aeruginosa*	731
Gold, silicon wafer	PSPMA(K)	SI-ATRP	Loading of the polymer brush with $AgNO_3$	3−300 nm	Silver leaching	*Pseudomonas aeruginosa*, *Staphylococcus aureus*	730
Titanium oxide	PHEMA PDMAEMA	SI-ATRP	(1) succinic anhydride/DMAP, NHS/EDC, gentamicin coupling (2) (3-aminopropyl)trimethoxysilane, penicillin coupling (3) quaternization with bromohexane	PHEMA: 124 nm, PDMAEMA: 18 nm	(1) gentamicin, (2) penicillin (3) quaternary ammonium	*Staphylococcus aureus*	387
Silicon rubber	PAM	SI-ATRP		20 nm in DMF 8 nm in H_2O		*Staphylococcus aureus*, *Streptococcus salivarius*, *Candida albicans (yeast)*	733
Microporous polypropylene hollow fiber (PPHF)	(PPEGMA-*b*-PDMAEMA)	SI-ATRP	Quaternization with bromododecane ($R = C_{12}H_{25}$)		Quaternary ammonium	*Escherichia coli*, *Staphylococcus aureus*	495
Titanium oxide	PMAA	SI-ATRP	NHS/EDC activation, silk sericin coupling	>7.5 nm		*Staphylococcus aureus*, *Staphylococcus epidermidis*	614
Cellulose filter paper	PDMAEMA	SI-RAFT	Quaternization with bromooctane, bromododecane, bromohexadecane ($R = C_8H_{17}$, $C_{12}H_{25}$, $C_{16}H_{33}$)		Quaternary ammonium	*Escherichia coli*	480

[a] PVBC-*co*-PEGDMA: poly(4-vinylbenzyl chloride)-*co*-poly(ethylene glycol dimethacrylate). [b] PVDF-*g*-PBIEA: poly(vinylidene fluoride)-*g*-poly(2-(2-bromoisobutyryloxy)ethyl acrylate).

PMMA brushes with thicknesses ranging from 5 to 30 nm and densities of up to 0.56 chains/nm^2.[734] The tribological properties of these PMMA brushes were compared with that of spin coated PMMA films of similar thickness. The friction coefficient of dry PMMA brushes was found to be independent of brush thickness and sliding velocity, whereas the friction coefficient of the spin coated film increased with increasing film thickness. This difference was attributed to the highly stretched nature of the surface-tethered polymer chains. Experiments with solvent-exposed samples revealed that in the presence of good solvents (acetone, toluene), PMMA brushes can act as a lubricating layer that reduces the interactions

between the probe and the sample substrate. The same group has also prepared hydrophilic brush coatings composed of poly(2,3-dihydroxypropyl methacrylate)[625] and poly(2-(methacryloyloxy)ethyl phosphorylcholine) (PMPC)[735] via SI-ATRP. Friction experiments between PMPC brush-modified glass probes and PMPC-grafted substrates revealed very low friction coefficients, which were attributed to osmotic repulsions between the high-density grafted polymer chains. Such water-lubricating ultrathin coatings are of interest for various medical applications, e.g. in artificial hip joints.

5. Conclusions and Outlook

Thin polymer coatings have long been used to modify the surface properties of a wide range of materials. The advent of various controlled/"living" radical polymerization techniques over the past 10−15 years, however, has made it possible to produce such polymer coatings with an unprecedented level of control over composition, structure, and properties. The examples discussed in section 4 of this article give just a flavor of the possibilities that are currently offered by surface-initiated controlled polymerization techniques to produce functional surfaces. The variety of polymerization techniques, postmodification strategies, and patterning methods that were discussed earlier in this article together with the ongoing advances in each of these areas indicates that there is still plenty of room for future developments. Possible areas of application that have only received limited attention include catalysis and sensing. Due to the fact that polymer brushes produced via SI-CRP are not simple 2D films but thin 3D layers with internal chemical and physical properties that can be controlled via synthesis, these seem to be interesting application areas. Another attractive feature of SI-CRP that has not been taken much advantage of is the possibility to modify the interior surface of complex 3D support structures. This would be of interest and relevant to applications in microfluidics and tissue engineering, among others. These are just a few of the many possibilities for further developments, and we hope that this article will inspire further activities in this exciting field.

6. Acknowledgments

The work on polymer brushes in the authors' laboratory is supported by the VolkswagenStiftung, the GEBERT RÜF STIFTUNG, CTI/KTI, the Competence Centre for Materials Science and Technology (CCMX), Sensile Medical AG, and the European Community.

7. References

(1) Milner, S. T. *Science* **1991**, *251*, 905.
(2) Halperin, A.; Tirrell, M.; Lodge, T. P. *Adv. Polym. Sci.* **1992**, *100*, 31.
(3) Zhao, B.; Brittain, W. J. *Prog. Polym. Sci.* **2000**, *25*, 677.
(4) Brittain, W. J.; Minko, S. *J. Polym. Sci., Part A: Polym. Chem.* **2007**, *45*, 3505.
(5) Tsukruk, V. V. *Prog. Polym. Sci.* **1997**, *22*, 247.
(6) Brandani, P.; Stroeve, P. *Macromolecules* **2004**, *37*, 6640.
(7) Kenausis, G. L.; Vörös, J.; Elbert, D. L.; Huang, N. P.; Hofer, R.; Ruiz-Taylor, L.; Textor, M.; Hubbell, J. A.; Spencer, N. D. *J. Phys. Chem. B* **2000**, *104*, 3298.
(8) Huang, N.-P.; Michel, R.; Voros, J.; Textor, M.; Hofer, R.; Rossi, A.; Elbert, D. L.; Hubbell, J. A.; Spencer, N. D. *Langmuir* **2001**, *17*, 489.
(9) Elbert, D. L.; Hubbell, J. A. *Chem. Biol.* **1998**, *5*, 177.
(10) Lee, S.; Vörös, J. *Langmuir* **2005**, *21*, 11957.
(11) Brandani, P.; Stroeve, P. *Macromolecules* **2003**, *36*, 9492.
(12) Brandani, P.; Stroeve, P. *Macromolecules* **2003**, *36*, 9502.
(13) Papra, A.; Gadegaard, N.; Larsen, N. B. *Langmuir* **2001**, *17*, 1457.
(14) Tran, Y.; Auroy, P. *J. Am. Chem. Soc.* **2001**, *123*, 3644.
(15) Sofia, S. J.; Premnath, V.; Merrill, E. W. *Macromolecules* **1998**, *31*, 5059.
(16) Luzinov, I.; Julthongpiput, D.; Malz, H.; Pionteck, J.; Tsukruk, V. V. *Macromolecules* **2000**, *33*, 1043.
(17) Minko, S.; Patil, S.; Datsyuk, V.; Simon, F.; Eichhorn, K.-J.; Motornov, M.; Usov, D.; Tokarev, I.; Stamm, M. *Langmuir* **2002**, *18*, 289.
(18) Zhu, B.; Eurell, T.; Gunawan, R.; Leckband, D. *J. Biomed. Mater. Res.* **2001**, *56*, 406.
(19) Ostuni, E.; Yan, L.; Whitesides, G. M. *Colloids Surf., B* **1999**, *15*, 3.
(20) Roberts, C.; Chen, C. S.; Mrksich, M.; Martichonok, V.; Ingber, D. E.; Whitesides, G. M. *J. Am. Chem. Soc.* **1998**, *120*, 6548.
(21) Balazs, A. C.; Singh, C.; Zhulina, E.; Chern, S.-S.; Lyatskaya, Y.; Pickett, G. *Prog. Surf. Sci.* **1997**, *55*, 181.
(22) Rühe, J.; Knoll, W. *J. Macromol. Sci., Polym. Rev.* **2002**, *C42*, 91.
(23) Advincula, R. C. *J. Dispersion Sci. Technol.* **2003**, *24*, 343.
(24) Jennings, G. K.; Brantley, E. L. *Adv. Mater.* **2004**, *16*, 1983.
(25) Radhakrishnan, B.; Ranjan, R.; Brittain, W. J. *Soft Matter* **2006**, *2*, 386.
(26) Matyjaszewski, K. *Prog. Polym. Sci.* **2005**, *30*, 858.
(27) Braunecker, W. A.; Matyjaszewski, K. *Prog. Polym. Sci.* **2007**, *32*, 93.
(28) Edmondson, S.; Osborne, V. L.; Huck, W. T. S. *Chem. Soc. Rev.* **2004**, *33*, 14.
(29) Tsujii, Y.; Ohno, K.; Yamamoto, S.; Goto, A.; Fukuda, T. *Adv. Polym. Sci.* **2006**, *197*, 1.
(30) Pyun, J.; Kowalewski, T.; Matyjaszewski, K. *Macromol. Rapid Commun.* **2003**, *24*, 1043.
(31) Pyun, J.; Matyjaszewski, K. *Chem. Mater.* **2001**, *13*, 3436.
(32) Jordan, R.; Ulman, A.; Kang, J. F.; Rafailovich, M. H.; Sokolov, J. *J. Am. Chem. Soc.* **1999**, *121*, 1016.
(33) Advincula, R.; Zhou, Q. G.; Park, M.; Wang, S. G.; Mays, J.; Sakellariou, G.; Pispas, S.; Hadjichristidis, N. *Langmuir* **2002**, *18*, 8672.
(34) Advincula, R. *Adv. Polym. Sci.* **2006**, *197*, 107.
(35) Jordan, R.; Ulman, A. *J. Am. Chem. Soc.* **1998**, *120*, 243.
(36) Zhao, B.; Brittain, W. J. *J. Am. Chem. Soc.* **1999**, *121*, 3557.
(37) Zhao, B.; Brittain, W. J. *Macromolecules* **2000**, *33*, 342.
(38) Jaworek, T.; Neher, D.; Wegner, G.; Wieringa, R. H.; Schouten, A. J. *Science* **1998**, *279*, 57.
(39) Husemann, M.; Mecerreyes, D.; Hawker, C. J.; Hedrick, J. L.; Shah, R.; Abbott, N. L. *Angew. Chem., Int. Ed.* **1999**, *38*, 647.
(40) Kratzmüller, T.; Appelhans, D.; Braun, H. G. *Adv. Mater.* **1999**, *11*, 555.
(41) Choi, I. S.; Langer, R. *Macromolecules* **2001**, *34*, 5361.
(42) Wieringa, R. H.; Siesling, E. A.; Geurts, P. F. M.; Werkman, P. J.; Vorenkamp, E. J.; Erb, V.; Stamm, M.; Schouten, A. J. *Langmuir* **2001**, *17*, 6477.
(43) Wang, Y. L.; Chang, Y.-C. *Langmuir* **2002**, *18*, 9859.
(44) Menzel, H.; Witte, P. In *Polymer Brushes*; Advincula, R. C., Brittain, W. J., Caster, K. C., Rühe, J., Eds.; Wiley-VCH Verlag GmbH & Co. KGaA: Weinheim, 2004.
(45) Yoon, K. R.; Lee, Y.-W.; Lee, J. K.; Choi, I. S. *Macromol. Rapid Commun.* **2004**, *25*, 1510.
(46) Zeng, H. L.; Gao, C.; Yan, D. Y. *Adv. Funct. Mater.* **2006**, *16*, 812.
(47) Weck, M.; Jackiw, J. J.; Rossi, R. R.; Weiss, P. S.; Grubbs, R. H. *J. Am. Chem. Soc.* **1999**, *121*, 4088.
(48) Kim, N. Y.; Jeon, N. L.; Choi, I. S.; Takami, S.; Harada, Y.; Finnie, K. R.; Girolami, G. S.; Nuzzo, R. G.; Whitesides, G. M.; Laibinis, P. E. *Macromolecules* **2000**, *33*, 2793.
(49) Juang, A.; Scherman, O. A.; Grubbs, R. H.; Lewis, N. S. *Langmuir* **2001**, *17*, 1321.
(50) Harada, Y.; Girolami, G. S.; Nuzzo, R. G. *Langmuir* **2003**, *19*, 5104.
(51) Kong, B.; Lee, J. K.; Choi, I. S. *Langmuir* **2007**, *23*, 6761.
(52) Suzuki, M.; Kishida, A.; Iwata, H.; Ikada, Y. *Macromolecules* **1986**, *19*, 1804.
(53) Tsubokawa, N.; Kogure, A.; Maruyama, K.; Sone, Y.; Shimomura, M. *Polym. J.* **1990**, *22*, 827.
(54) Ito, Y.; Inaba, M.; Chung, D.-J.; Imanishi, Y. *Macromolecules* **1992**, *25*, 7313.
(55) Ito, Y.; Nishi, S.; Park, Y. S.; Imanishi, Y. *Macromolecules* **1997**, *30*, 5856.
(56) Prucker, O.; Rühe, J. *Macromolecules* **1998**, *31*, 592.
(57) Prucker, O.; Rühe, J. *Macromolecules* **1998**, *31*, 602.
(58) Prucker, O.; Rühe, J. *Langmuir* **1998**, *14*, 6893.
(59) Prucker, O.; Schimmel, M.; Tovar, G.; Knoll, W.; Rühe, J. *Adv. Mater.* **1998**, *10*, 1073.
(60) Biesalski, M.; Rühe, J. *Macromolecules* **1999**, *32*, 2309.
(61) Peng, B.; Johannsmann, D.; Rühe, J. *Macromolecules* **1999**, *32*, 6759.
(62) Huang, W. X.; Skanth, G.; Baker, G. L.; Bruening, M. L. *Langmuir* **2001**, *17*, 1731.

(63) Schmelmer, U.; Jordan, R.; Geyer, W.; Eck, W.; Gölzhäuser, A.; Grunze, M.; Ulman, A. *Angew. Chem., Int. Ed.* **2003**, *42*, 559.
(64) Hu, S.; Wang, Y.; McGinty, K.; Brittain, W. J. *Eur. Polym. J.* **2006**, *42*, 2053.
(65) Wang, J.-S.; Matyjaszewski, K. *J. Am. Chem. Soc.* **1995**, *117*, 5614.
(66) Kato, M.; Kamigaito, M.; Sawamoto, M.; Higashimura, T. *Macromolecules* **1995**, *28*, 1721.
(67) Percec, V.; Barboiu, B. *Macromolecules* **1995**, *28*, 7970.
(68) Patten, T. E.; Matyjaszewski, K. *Adv. Mater.* **1998**, *10*, 901.
(69) Patten, T. E.; Matyjaszewski, K. *Acc. Chem. Res.* **1999**, *32*, 895.
(70) Matyjaszewski, K.; Xia, J. H. *Chem. Rev.* **2001**, *101*, 2921.
(71) Kamigaito, M.; Ando, T.; Sawamoto, M. *Chem. Rev.* **2001**, *101*, 3689.
(72) Tsarevsky, N. V.; Matyjaszewski, K. *Chem. Rev.* **2007**, *107*, 2270.
(73) Matyjaszewski, K.; Göbelt, B.; Paik, H.-J.; Horwitz, C. P. *Macromolecules* **2001**, *34*, 430.
(74) Kim, J. B.; Huang, W. X.; Miller, M. D.; Baker, G. L.; Bruening, M. L. *J. Polym. Sci., Part A: Polym. Chem.* **2003**, *41*, 386.
(75) Nanda, A. K.; Matyjaszewski, K. *Macromolecules* **2003**, *36*, 599.
(76) Nanda, A. K.; Matyjaszewski, K. *Macromolecules* **2003**, *36*, 1487.
(77) Tang, W.; Nanda, A. K.; Matyjaszewski, K. *Macromol. Chem. Phys.* **2005**, *206*, 1171.
(78) Matyjaszewski, K.; Nanda, A. K.; Tang, W. *Macromolecules* **2005**, *38*, 2015.
(79) Tang, W.; Tsarevsky, N. V.; Matyjaszewski, K. *J. Am. Chem. Soc.* **2006**, *128*, 1598.
(80) Tang, W.; Matyjaszewski, K. *Macromolecules* **2006**, *39*, 4953.
(81) Cheng, N.; Azzaroni, O.; Moya, S.; Huck, W. T. S. *Macromol. Rapid Commun.* **2006**, *27*, 1632.
(82) Huang, X. Y.; Wirth, M. *J. Anal. Chem.* **1997**, *69*, 4577.
(83) Ejaz, M.; Yamamoto, S.; Ohno, K.; Tsujii, Y.; Fukuda, T. *Macromolecules* **1998**, *31*, 5934.
(84) Matyjaszewski, K.; Miller, P. J.; Shukla, N.; Immaraporn, B.; Gelman, A.; Luokala, B. B.; Siclovan, T. M.; Kickelbick, G.; Vallant, T.; Hoffmann, H.; Pakula, T. *Macromolecules* **1999**, *32*, 8716.
(85) Wang, X.-S.; Lascelles, S. F.; Jackson, R. A.; Armes, S. P. *Chem. Commun.* **1999**, 1817.
(86) Wang, X.-S.; Armes, S. P. *Macromolecules* **2000**, *33*, 6640.
(87) Jones, D. M.; Huck, W. T. S. *Adv. Mater.* **2001**, *13*, 1256.
(88) Huang, W. X.; Kim, J. B.; Bruening, M. L.; Baker, G. L. *Macromolecules* **2002**, *35*, 1175.
(89) Matyjaszewski, K.; Shipp, D. A.; Wang, J.-L.; Grimaud, T.; Patten, T. E. *Macromolecules* **1998**, *31*, 6836.
(90) Sedjo, R. A.; Mirous, B. K.; Brittain, W. J. *Macromolecules* **2000**, *33*, 1492.
(91) Wang, Y.-P.; Pei, X.-W.; He, X.-Y.; Lei, Z.-Q. *Eur. Polym. J.* **2005**, *41*, 737.
(92) Wang, Y.-P.; Pei, X.-W.; Yuan, K. *Mater. Lett.* **2005**, *59*, 520.
(93) Jakubowski, W.; Matyjaszewski, K. *Macromolecules* **2005**, *38*, 4139.
(94) Min, K.; Gao, H. F.; Matyjaszewski, K. *J. Am. Chem. Soc.* **2005**, *127*, 3825.
(95) Jakubowski, W.; Matyjaszewski, K. *Angew. Chem., Int. Ed.* **2006**, *45*, 4482.
(96) Jakubowski, W.; Min, K.; Matyjaszewski, K. *Macromolecules* **2006**, *39*, 39.
(97) Matyjaszewski, K.; Jakubowski, W.; Min, K.; Tang, W.; Huang, J. Y.; Braunecker, W. A.; Tsarevsky, N. V. *Proc. Natl. Acad. Sci. U. S. A.* **2006**, *103*, 15309.
(98) Zhao, H. Y.; Kang, X. L.; Liu, L. *Macromolecules* **2005**, *38*, 10619.
(99) Bombalski, L.; Min, K.; Dong, H. C.; Tang, C. B.; Matyjaszewski, K. *Macromolecules* **2007**, *40*, 7429.
(100) Esteves, A. C. C.; Bombalski, L.; Trindade, T.; Matyjaszewski, K.; Barros-Timmons, A. *Small* **2007**, *3*, 1230.
(101) He, J.; Wu, Y. Z.; Wu, J.; Mao, X.; Fu, L.; Qian, T. C.; Fang, J.; Xiong, C. Y.; Xie, J. L.; Ma, H. W. *Macromolecules* **2007**, *40*, 3090.
(102) Matyjaszewski, K.; Dong, H. C.; Jakubowski, W.; Pietrasik, J.; Kusumo, A. *Langmuir* **2007**, *23*, 4528.
(103) Wischerhoff, E.; Uhlig, K.; Lankenau, A.; Börner, H. G.; Laschewsky, A.; Duschl, C.; Lutz, J.-F. *Angew. Chem., Int. Ed.* **2008**, *47*, 5666.
(104) Okelo, G. O.; He, L. *Biosens. Bioelectron.* **2007**, *23*, 588.
(105) Bao, Z.; Bruening, M. L.; Baker, G. L. *J. Am. Chem. Soc.* **2006**, *128*, 9056.
(106) Ayres, N.; Cyrus, C. D.; Brittain, W. J. *Langmuir* **2007**, *23*, 3744.
(107) Ashford, E. J.; Naldi, V.; O'Dell, R.; Billingham, N. C.; Armes, S. P. *Chem. Commun.* **1999**, 1285.
(108) Wang, X.-S.; Jackson, R. A.; Armes, S. P. *Macromolecules* **2000**, *33*, 255.
(109) Chen, X. Y.; Randall, D. P.; Perruchot, C.; Watts, J. F.; Patten, T. E.; von Werne, T.; Armes, S. P. *J. Colloid Interface Sci.* **2003**, *257*, 56.
(110) Osborne, V. L.; Jones, D. M.; Huck, W. T. S. *Chem. Commun.* **2002**, 1838.
(111) Tugulu, S.; Barbey, R.; Harms, M.; Fricke, M.; Volkmer, D.; Rossi, A.; Klok, H.-A. *Macromolecules* **2007**, *40*, 168.
(112) Sankhe, A. Y.; Husson, S. M.; Kilbey, S. M. *J. Polym. Sci., Part A: Polym. Chem.* **2007**, *45*, 566.
(113) Jain, P.; Dai, J. H.; Baker, G. L.; Bruening, M. L. *Macromolecules* **2008**, *41*, 8413.
(114) Moad, G.; Rizzardo, E.; Thang, S. H. *Aust. J. Chem.* **2005**, *58*, 379.
(115) Perrier, S.; Takolpuckdee, P. *J. Polym. Sci., Part A: Polym. Chem.* **2005**, *43*, 5347.
(116) Chiefari, J.; Chong, Y. K.; Ercole, F.; Krstina, J.; Jeffery, J.; Le, T. P. T.; Mayadunne, R. T. A.; Meijs, G. F.; Moad, C. L.; Moad, G.; Rizzardo, E.; Thang, S. H. *Macromolecules* **1998**, *31*, 5559.
(117) Baum, M.; Brittain, W. J. *Macromolecules* **2002**, *35*, 610.
(118) Yu, W. H.; Kang, E. T.; Neoh, K. G. *Ind. Eng. Chem. Res.* **2004**, *43*, 5194.
(119) Zhai, G. Q.; Yu, W. H.; Kang, E. T.; Neoh, K. G.; Huang, C. C.; Liaw, D. J. *Ind. Eng. Chem. Res.* **2004**, *43*, 1673.
(120) Chen, Y. W.; Sun, W.; Deng, Q. L.; Chen, L. *J. Polym. Sci., Part A: Polym. Chem.* **2006**, *44*, 3071.
(121) Yoshikawa, C.; Goto, A.; Tsujii, Y.; Fukuda, T.; Yamamoto, K.; Kishida, A. *Macromolecules* **2005**, *38*, 4604.
(122) Rowe-Konopacki, M. D.; Boyes, S. G. *Macromolecules* **2007**, *40*, 879.
(123) Yuan, K.; Li, Z.-F.; Lu, L.-L.; Shi, X.-N. *Mater. Lett.* **2007**, *61*, 2033.
(124) Li, D. L.; Luo, Y. W.; Li, B.-G.; Zhu, S. P. *J. Polym. Sci., Part A: Polym. Chem.* **2008**, *46*, 970.
(125) Li, L.; Kang, E.; Neoh, K. *Appl. Surf. Sci.* **2008**, *254*, 2600.
(126) Tsujii, Y.; Ejaz, M.; Sato, K.; Goto, A.; Fukuda, T. *Macromolecules* **2001**, *34*, 8872.
(127) Li, C. Z.; Benicewicz, B. C. *Macromolecules* **2005**, *38*, 5929.
(128) Li, C.; Han, J.; Ryu, C. Y.; Benicewicz, B. C. *Macromolecules* **2006**, *39*, 3175.
(129) Hong, C.-Y.; Li, X.; Pan, C.-Y. *Eur. Polym. J.* **2007**, *43*, 4114.
(130) Liu, C.-H.; Pan, C.-Y. *Polymer* **2007**, *48*, 3679.
(131) Lu, C.-H.; Zhou, W.-H.; Han, B.; Yang, H.-H.; Chen, X.; Wang, X.-R. *Anal. Chem.* **2007**, *79*, 5457.
(132) Ranjan, R.; Brittain, W. J. *Macromol. Rapid Commun.* **2007**, *28*, 2084.
(133) Hojjati, B.; Sui, R. H.; Charpentier, P. A. *Polymer* **2007**, *48*, 5850.
(134) Skaff, H.; Emrick, T. *Angew. Chem., Int. Ed.* **2004**, *43*, 5383.
(135) Perrier, S.; Takolpuckdee, P.; Westwood, J.; Lewis, D. M. *Macromolecules* **2004**, *37*, 2709.
(136) Raula, J.; Shan, J.; Nuopponen, M.; Niskanen, A.; Jiang, H.; Kauppinen, E. I.; Tenhu, H. *Langmuir* **2003**, *19*, 3499.
(137) Roy, D.; Guthrie, J. T.; Perrier, S. *Macromolecules* **2005**, *38*, 10363.
(138) Hong, C.-Y.; You, Y.-Z.; Pan, C.-Y. *Chem. Mater.* **2005**, *17*, 2247.
(139) Xu, G. Y.; Wu, W.-T.; Wang, Y. S.; Pang, W. M.; Zhu, Q. R.; Wang, P. H.; You, Y. Z. *Polymer* **2006**, *47*, 5909.
(140) Pei, X. W.; Hao, J. C.; Liu, W. M. *J. Phys. Chem. C* **2007**, *111*, 2947.
(141) Xu, G. Y.; Wu, W.-T.; Wang, Y. S.; Pang, W. M.; Zhu, Q. R.; Wang, P. H. *Nanotechnology* **2007**, *18*, 145606.
(142) Hong, C.-Y.; You, Y.-Z.; Pan, C.-Y. *J. Polym. Sci., Part A: Polym. Chem.* **2006**, *44*, 2419.
(143) Peng, Q.; Lai, D. M. Y.; Kang, E. T.; Neoh, K. G. *Macromolecules* **2006**, *39*, 5577.
(144) Zhao, Y. L.; Perrier, S. *Macromolecules* **2006**, *39*, 8603.
(145) Wang, G.-J.; Huang, S.-Z.; Wang, Y.; Liu, L.; Qiu, J.; Li, Y. *Polymer* **2007**, *48*, 728.
(146) Zhao, Y.; Perrier, S. *Macromolecules* **2007**, *40*, 9116.
(147) Stenzel, M. H.; Zhang, L.; Huck, W. T. S. *Macromol. Rapid Commun.* **2006**, *27*, 1121.
(148) Takolpuckdee, P.; Mars, C. A.; Perrier, S. *Org. Lett.* **2005**, *7*, 3449.
(149) Perrier, S.; Takolpuckdee, P.; Mars, C. A. *Macromolecules* **2005**, *38*, 6770.
(150) Rizzardo, E.; Serelis, A. K.; Solomon, D. H. *Aust. J. Chem.* **1982**, *35*, 2013.
(151) Hawker, C. J.; Barclay, G. G.; Orellana, A.; Dao, J.; Devonport, W. *Macromolecules* **1996**, *29*, 5245.
(152) Hawker, C. J. *Acc. Chem. Res.* **1997**, *30*, 373.
(153) Hawker, C. J.; Bosman, A. W.; Harth, E. *Chem. Rev.* **2001**, *101*, 3661.
(154) Studer, A.; Schulte, T. *Chem. Rec.* **2005**, *5*, 27.
(155) Ghannam, L.; Parvole, J.; Laruelle, G.; Francois, J.; Billon, L. *Polym. Int.* **2006**, *55*, 1199.
(156) Husseman, M.; Malmström, E. E.; McNamara, M.; Mate, M.; Mecerreyes, D.; Benoit, D. G.; Hedrick, J. L.; Mansky, P.; Huang, E.; Russell, T. P.; Hawker, C. J. *Macromolecules* **1999**, *32*, 1424.
(157) Fischer, H. *Chem. Rev.* **2001**, *101*, 3581.
(158) Devaux, C.; Chapel, J. P.; Beyou, E.; Chaumont, P. *Eur. Phys. J. E* **2002**, *7*, 345.
(159) Devaux, C.; Chapel, J.-P. *Eur. Phys. J. E* **2003**, *10*, 77.
(160) Mulfort, K. L.; Ryu, J.; Zhou, Q. Y. *Polymer* **2003**, *44*, 3185.
(161) Andruzzi, L.; Hexemer, A.; Li, X.; Ober, C. K.; Kramer, E. J.; Galli, G.; Chiellini, E.; Fischer, D. A. *Langmuir* **2004**, *20*, 10498.

(162) Andruzzi, L.; Senaratne, W.; Hexemer, A.; Sheets, E. D.; Ilic, B.; Kramer, E. J.; Baird, B.; Ober, C. K. *Langmuir* **2005**, *21*, 2495.
(163) Brinks, M. K.; Hirtz, M.; Chi, L. F.; Fuchs, H.; Studer, A. *Angew. Chem., Int. Ed.* **2007**, *46*, 5231.
(164) Matsuno, R.; Yamamoto, K.; Otsuka, H.; Takahara, A. *Chem. Mater.* **2003**, *15*, 3.
(165) Matsuno, R.; Yamamoto, K.; Otsuka, H.; Takahara, A. *Macromolecules* **2004**, *37*, 2203.
(166) Kobayashi, M.; Matsuno, R.; Otsuka, H.; Takahara, A. *Sci. Technol. Adv. Mater.* **2006**, *7*, 617.
(167) Matsuno, R.; Otsuka, H.; Takahara, A. *Soft Matter* **2006**, *2*, 415.
(168) Voccia, S.; Jérôme, C.; Detrembleur, C.; Leclère, P.; Gouttebaron, R.; Hecq, M.; Gilbert, B.; Lazzaroni, R.; Jérôme, R. *Chem. Mater.* **2003**, *15*, 923.
(169) Bian, K. J.; Cunningham, M. F. *J. Polym. Sci., Part A: Polym. Chem.* **2005**, *43*, 2145.
(170) Zhao, X.; Lin, W.; Song, N. H.; Chen, X. F.; Fan, X. H.; Zhou, Q. F. *J. Mater. Chem.* **2006**, *16*, 4619.
(171) Zhao, X.-D.; Fan, X.-H.; Chen, X.-F.; Chai, C.-P.; Zhou, Q.-F. *J. Polym. Sci., Part A: Polym. Chem.* **2006**, *44*, 4656.
(172) Listigovers, N. A.; Georges, M. K.; Odell, P. G.; Keoshkerian, B. *Macromolecules* **1996**, *29*, 8992.
(173) Goto, A.; Kwak, Y.; Yoshikawa, C.; Tsujii, Y.; Sugiura, Y.; Fukuda, T. *Macromolecules* **2002**, *35*, 3520.
(174) Benoit, D.; Grimaldi, S.; Finet, J. P.; Tordo, P.; Fontanille, M.; Gnanou, Y. *Polym. Prepr. (Am. Chem. Soc., Div. Polym. Chem.)* **1997**, *38*, 729.
(175) Benoit, D.; Chaplinski, V.; Braslau, R.; Hawker, C. J. *J. Am. Chem. Soc.* **1999**, *121*, 3904.
(176) Benoit, D.; Grimaldi, S.; Robin, S.; Finet, J.-P.; Tordo, P.; Gnanou, Y. *J. Am. Chem. Soc.* **2000**, *122*, 5929.
(177) Bartholome, C.; Beyou, E.; Bourgeat-Lami, E.; Chaumont, P.; Zydowicz, N. *Macromolecules* **2003**, *36*, 7946.
(178) Parvole, J.; Montfort, J.-P.; Reiter, G.; Borisov, O.; Billon, L. *Polymer* **2006**, *47*, 972.
(179) Parvole, J.; Montfort, J.-P.; Billon, L. *Macromol. Chem. Phys.* **2004**, *205*, 1369.
(180) Parvole, J.; Billon, L.; Montfort, J. P. *Polym. Int.* **2002**, *51*, 1111.
(181) Laruelle, G.; Parvole, J.; Francois, J.; Billon, L. *Polymer* **2004**, *45*, 5013.
(182) Bartholome, C.; Beyou, E.; Bourgeat-Lami, E.; Cassagnau, P.; Chaumont, P.; David, L.; Zydowicz, N. *Polymer* **2005**, *46*, 9965.
(183) Bartholome, C.; Beyou, E.; Bourgeat-Lami, E.; Chaumont, P.; Lefebvre, F.; Zydowicz, N. *Macromolecules* **2005**, *38*, 1099.
(184) Bartholome, C.; Beyou, E.; Bourgeat-Lami, E.; Chaumont, P.; Zydowicz, N. *Polymer* **2005**, *46*, 8502.
(185) Bian, K. J.; Cunningham, M. F. *Polymer* **2006**, *47*, 5744.
(186) Konn, C.; Morel, F.; Beyou, E.; Chaumont, P.; Bourgeat-Lami, E. *Macromolecules* **2007**, *40*, 7464.
(187) Inoubli, R.; Dagréou, S.; Khoukh, A.; Roby, F.; Peyrelasse, J.; Billon, L. *Polymer* **2005**, *46*, 2486.
(188) Parvole, J.; Laruelle, G.; Khoukh, A.; Billon, L. *Macromol. Chem. Phys.* **2005**, *206*, 372.
(189) Inoubli, R.; Dagréou, S.; Delville, M. H.; Lapp, A.; Peyrelasse, J.; Billon, L. *Soft Matter* **2007**, *3*, 1014.
(190) Husemann, M.; Morrison, M.; Benoit, D.; Frommer, K. J.; Mate, C. M.; Hinsberg, W. D.; Hedrick, J. L.; Hawker, C. J. *J. Am. Chem. Soc.* **2000**, *122*, 1844.
(191) Ignatova, M.; Voccia, S.; Gilbert, B.; Markova, N.; Mercuri, P. S.; Galleni, M.; Sciannamea, V.; Lenoir, S.; Cossement, D.; Gouttebaron, R.; Jérôme, R.; Jérôme, C. *Langmuir* **2004**, *20*, 10718.
(192) von Werne, T. A.; Germack, D. S.; Hagberg, E. C.; Sheares, V. V.; Hawker, C. J.; Carter, K. R. *J. Am. Chem. Soc.* **2003**, *125*, 3831.
(193) Beinhoff, M.; Frommer, J.; Carter, K. R. *Chem. Mater.* **2006**, *18*, 3425.
(194) Blomberg, S.; Ostberg, S.; Harth, E.; Bosman, A. W.; Van Horn, B.; Hawker, C. J. *J. Polym. Sci., Part A: Polym. Chem.* **2002**, *40*, 1309.
(195) Becker, M. L.; Liu, J. Q.; Wooley, K. L. *Chem. Commun.* **2003**, 180.
(196) Otsu, T.; Yoshida, M. *Makromol. Chem. Rapid Commun.* **1982**, *3*, 127.
(197) Otsu, T.; Yoshida, M.; Tazaki, T. *Makromol. Chem. Rapid Commun.* **1982**, *3*, 133.
(198) Otsu, T. *J. Polym. Sci., Part A: Polym. Chem.* **2000**, *38*, 2121.
(199) Higashi, J.; Nakayama, Y.; Marchant, R. E.; Matsuda, T. *Langmuir* **1999**, *15*, 2080.
(200) Nakayama, Y.; Matsuda, T. *Macromolecules* **1996**, *29*, 8622.
(201) Otsu, T.; Ogawa, T.; Yamamoto, T. *Macromolecules* **1986**, *19*, 2087.
(202) Lee, H. J.; Nakayama, Y.; Matsuda, T. *Macromolecules* **1999**, *32*, 6989.
(203) Kidoaki, S.; Nakayama, Y.; Matsuda, T. *Langmuir* **2001**, *17*, 1080.
(204) Kidoaki, S.; Ohya, S.; Nakayama, Y.; Matsuda, T. *Langmuir* **2001**, *17*, 2402.
(205) Matsuda, T.; Kaneko, M.; Ge, S. R. *Biomaterials* **2003**, *24*, 4507.
(206) Matsuda, T.; Ohya, S. *Langmuir* **2005**, *21*, 9660.
(207) de Boer, B.; Simon, H. K.; Werts, M. P. L.; van der Vegte, E. W.; Hadziioannou, G. *Macromolecules* **2000**, *33*, 349.
(208) Nakayama, Y.; Matsuda, T. *Macromolecules* **1999**, *32*, 5405.
(209) Rahane, S. B.; Kilbey, S. M., II; Metters, A. T. *Macromolecules* **2005**, *38*, 8202.
(210) Luo, N.; Hutchison, J. B.; Anseth, K. S.; Bowman, C. N. *Macromolecules* **2002**, *35*, 2487.
(211) Rahane, S. B.; Metters, A. T.; Kilbey, S. M., II. *Macromolecules* **2006**, *39*, 8987.
(212) Benetti, E. M.; Zapotoczny, S.; Vancso, G. J. *Adv. Mater.* **2007**, *19*, 268.
(213) Navarro, M.; Benetti, E. M.; Zapotoczny, S.; Planell, J. A.; Vancso, G. J. *Langmuir* **2008**, *24*, 10996.
(214) Benetti, E. M.; Reimhult, E.; de Bruin, J.; Zapotoczny, S.; Textor, M.; Vancso, G. J. *Macromolecules* **2009**, *42*, 1640.
(215) Nakayama, Y.; Matsuda, T. *Langmuir* **1999**, *15*, 5560.
(216) Boyes, S. G.; Brittain, W. J.; Weng, X.; Cheng, S. Z. D. *Macromolecules* **2002**, *35*, 4960.
(217) Kim, J. B.; Huang, W. X.; Bruening, M. L.; Baker, G. L. *Macromolecules* **2002**, *35*, 5410.
(218) Huang, W. X.; Kim, J.-B.; Baker, G. L.; Bruening, M. L. *Nanotechnology* **2003**, *14*, 1075.
(219) Tomlinson, M. R.; Efimenko, K.; Genzer, J. *Macromolecules* **2006**, *39*, 9049.
(220) Mori, H.; Seng, D. C.; Zhang, M. F.; Müller, A. H. E. *Langmuir* **2002**, *18*, 3682.
(221) Mori, H.; Böker, A.; Krausch, G.; Müller, A. H. E. *Macromolecules* **2001**, *34*, 6871.
(222) Nakayama, Y.; Sudo, M.; Uchida, K.; Matsuda, T. *Langmuir* **2002**, *18*, 2601.
(223) Mu, B.; Zhao, M. F.; Liu, P. *J. Nanopart. Res.* **2008**, *10*, 831.
(224) Kim, D. J.; Kang, S. M.; Kong, B.; Kim, W.-J.; Paik, H.-J.; Choi, H.; Choi, I. S. *Macromol. Chem. Phys.* **2005**, *206*, 1941.
(225) Edmondson, S.; Huck, W. T. S. *J. Mater. Chem.* **2004**, *14*, 730.
(226) Mandal, T. K.; Fleming, M. S.; Walt, D. R. *Chem. Mater.* **2000**, *12*, 3481.
(227) Cui, Y.; Tao, C.; Zheng, S. P.; He, Q.; Ai, S. F.; Li, J. B. *Macromol. Rapid Commun.* **2005**, *26*, 1552.
(228) Hattori, K.; Hiwatari, M.; Iiyama, C.; Yoshimi, Y.; Kohori, F.; Sakai, K.; Piletsky, S. A. *J. Membr. Sci.* **2004**, *233*, 169.
(229) Rückert, B.; Hall, A. J.; Sellergren, B. *J. Mater. Chem.* **2002**, *12*, 2275.
(230) Ward, J. H.; Bashir, R.; Peppas, N. A. *J. Biomed. Mater. Res.* **2001**, *56*, 351.
(231) Pinto, J. C.; Whiting, G. L.; Khodabakhsh, S.; Torre, L.; Rodríguez, A. B.; Dalgliesh, R. M.; Higgins, A. M.; Andreasen, J. W.; Nielsen, M. M.; Geoghegan, M.; Huck, W. T. S.; Sirringhaus, H. *Adv. Funct. Mater.* **2008**, *18*, 36.
(232) Huang, X. Y.; Doneski, L. J.; Wirth, M. *J. Anal. Chem.* **1998**, *70*, 4023.
(233) Ignatova, M.; Voccia, S.; Gilbert, B.; Markova, N.; Cossement, D.; Gouttebaron, R.; Jérôme, R.; Jérôme, C. *Langmuir* **2006**, *22*, 255.
(234) Xu, F. J.; Zhong, S. P.; Yung, L. Y. L.; Kang, E. T.; Neoh, K. G. *Biomacromolecules* **2004**, *5*, 2392.
(235) Zhao, B. *Polymer* **2003**, *44*, 4079.
(236) Zhao, B. *Langmuir* **2004**, *20*, 11748.
(237) Zhao, B.; He, T. *Macromolecules* **2003**, *36*, 8599.
(238) Zhao, B.; Haasch, R. T.; MacLaren, S. *J. Am. Chem. Soc.* **2004**, *126*, 6124.
(239) Santer, S.; Kopyshev, A.; Donges, J.; Rühe, J.; Jiang, X. G.; Zhao, B.; Müller, M. *Langmuir* **2007**, *23*, 279.
(240) Zhao, B.; Haasch, R. T.; MacLaren, S. *Polymer* **2004**, *45*, 7979.
(241) Li, D. J.; Sheng, X.; Zhao, B. *J. Am. Chem. Soc.* **2005**, *127*, 6248.
(242) Zhao, B.; Zhu, L. *J. Am. Chem. Soc.* **2006**, *128*, 4574.
(243) Wang, X. J.; Bohn, P. W. *Adv. Mater.* **2007**, *19*, 515.
(244) Fréchet, J. M. J.; Henmi, M.; Gitsov, I.; Aoshima, S.; Leduc, M. R.; Grubbs, R. B. *Science* **1995**, *269*, 1080.
(245) Mori, H.; Müller, A. H. E. *Top. Curr. Chem.* **2003**, *228*, 1.
(246) Gao, C.; Muthukrishnan, S.; Li, W. W.; Yuan, J. Y.; Xu, Y. Y.; Müller, A. H. E. *Macromolecules* **2007**, *40*, 1803.
(247) Liu, P.; Wang, T. M. *Polym. Eng. Sci.* **2007**, *47*, 1296.
(248) Xu, F. J.; Yuan, Z. L.; Kang, E. T.; Neoh, K. G. *Langmuir* **2004**, *20*, 8200.
(249) Mu, B.; Wang, T. M.; Liu, P. *Ind. Eng. Chem. Res.* **2007**, *46*, 3069.
(250) Xu, F. J.; Zhong, S. P.; Yung, L. Y. L.; Tong, Y. W.; Kang, E.-T.; Neoh, K. G. *Biomaterials* **2006**, *27*, 1236.
(251) Zhai, G. Q.; Cao, Y.; Gao, J. *J. Appl. Polym. Sci.* **2006**, *102*, 2590.
(252) Yu, W. H.; Kang, E. T.; Neoh, K. G. *Langmuir* **2005**, *21*, 450.

(253) Huang, W. X.; Baker, G. L.; Bruening, M. L. *Angew. Chem., Int. Ed.* **2001**, *40*, 1510.
(254) Tugulu, S.; Klok, H.-A. *Biomacromolecules* **2008**, *9*, 906.
(255) Balachandra, A. M.; Baker, G. L.; Bruening, M. L. *J. Membr. Sci.* **2003**, *227*, 1.
(256) Luo, N.; Metters, A. T.; Hutchison, J. B.; Bowman, C. N.; Anseth, K. S. *Macromolecules* **2003**, *36*, 6739.
(257) Yu, W. H.; Kang, E. T.; Neoh, K. G. *Langmuir* **2004**, *20*, 8294.
(258) Comrie, J. E.; Huck, W. T. S. *Langmuir* **2007**, *23*, 1569.
(259) Edmondson, S.; Huck, W. T. S. *Adv. Mater.* **2004**, *16*, 1327.
(260) Edmondson, S.; Frieda, K.; Comrie, J. E.; Onck, P. R.; Huck, W. T. S. *Adv. Mater.* **2006**, *18*, 724.
(261) Loveless, D. M.; Abu-Lail, N. I.; Kaholek, M.; Zauscher, S.; Craig, S. L. *Angew. Chem., Int. Ed.* **2006**, *45*, 7812.
(262) Fu, G. D.; Shang, Z. H.; Hong, L.; Kang, E. T.; Neoh, K. G. *Macromolecules* **2005**, *38*, 7867.
(263) Fu, G.-D.; Shang, Z. H.; Hong, L.; Kang, E.-T.; Neoh, K.-G. *Adv. Mater.* **2005**, *17*, 2622.
(264) Morinaga, T.; Ohkura, M.; Ohno, K.; Tsujii, Y.; Fukuda, T. *Macromolecules* **2007**, *40*, 1159.
(265) Bhat, R. R.; Genzer, J.; Chaney, B. N.; Sugg, H. W.; Liebmann-Vinson, A. *Nanotechnology* **2003**, *14*, 1145.
(266) Bhat, R. R.; Tomlinson, M. R.; Wu, T.; Genzer, J. *Adv. Polym. Sci.* **2006**, *198*, 51.
(267) Wu, T.; Tomlinson, M.; Efimenko, K.; Genzer, J. *J. Mater. Sci.* **2003**, *38*, 4471.
(268) Genzer, J. *J. Adhes.* **2005**, *81*, 417.
(269) Luzinov, I.; Minko, S.; Tsukruk, V. V. *Soft Matter* **2008**, *4*, 714.
(270) Genzer, J.; Bhat, R. R. *Langmuir* **2008**, *24*, 2294.
(271) Xu, C.; Wu, T.; Mei, Y.; Drain, C. M.; Batteas, J. D.; Beers, K. L. *Langmuir* **2005**, *21*, 11136.
(272) Xu, C.; Barnes, S. E.; Wu, T.; Fischer, D. A.; DeLongchamp, D. M.; Batteas, J. D.; Beers, K. L. *Adv. Mater.* **2006**, *18*, 1427.
(273) Chaudhury, M. K.; Whitesides, G. M. *Science* **1992**, *256*, 1539.
(274) Wu, T.; Efimenko, K.; Vlček, P.; Šubr, V.; Genzer, J. *Macromolecules* **2003**, *36*, 2448.
(275) Wu, T.; Efimenko, K.; Genzer, J. *J. Am. Chem. Soc.* **2002**, *124*, 9394.
(276) Wu, T.; Gong, P.; Szleifer, I.; Vlček, P.; Šubr, V.; Genzer, J. *Macromolecules* **2007**, *40*, 8756.
(277) Liu, Y.; Klep, V.; Zdyrko, B.; Luzinov, I. *Langmuir* **2005**, *21*, 11806.
(278) Mei, Y.; Wu, T.; Xu, C.; Langenbach, K. J.; Elliott, J. T.; Vogt, B. D.; Beers, K. L.; Amis, E. J.; Washburn, N. R. *Langmuir* **2005**, *21*, 12309.
(279) Wang, X. J.; Tu, H. L.; Braun, P. V.; Bohn, P. W. *Langmuir* **2006**, *22*, 817.
(280) Harris, B. P.; Metters, A. T. *Macromolecules* **2006**, *39*, 2764.
(281) Harris, B. P.; Kutty, J. K.; Fritz, E. W.; Webb, C. K.; Burg, K. J. L.; Metters, A. T. *Langmuir* **2006**, *22*, 4467.
(282) Tomlinson, M. R.; Genzer, J. *Macromolecules* **2003**, *36*, 3449.
(283) Bhat, R. R.; Genzer, J. *Surf. Sci.* **2005**, *596*, 187.
(284) Tomlinson, M. R.; Genzer, J. *Chem. Commun.* **2003**, 1350.
(285) Xu, C.; Wu, T.; Drain, C. M.; Batteas, J. D.; Beers, K. L. *Macromolecules* **2005**, *38*, 6.
(286) Xu, C.; Wu, T.; Batteas, J. D.; Drain, C. M.; Beers, K. L.; Fasolka, M. J. *Appl. Surf. Sci.* **2006**, *252*, 2529.
(287) Xu, C.; Wu, T.; Drain, C. M.; Batteas, J. D.; Fasolka, M. J.; Beers, K. L. *Macromolecules* **2006**, *39*, 3359.
(288) Bhat, R. R.; Tomlinson, M. R.; Genzer, J. *J. Polym. Sci., Part B: Polym. Phys.* **2005**, *43*, 3384.
(289) Tomlinson, M. R.; Genzer, J. *Langmuir* **2005**, *21*, 11552.
(290) Bhat, R. R.; Genzer, J. *Appl. Surf. Sci.* **2006**, *252*, 2549.
(291) Bhat, R. R.; Chaney, B. N.; Rowley, J.; Liebmann-Vinson, A.; Genzer, J. *Adv. Mater.* **2005**, *17*, 2802.
(292) Ma, H.; Hyun, J.; Stiller, P.; Chilkoti, A. *Adv. Mater.* **2004**, *16*, 338.
(293) Nath, N.; Hyun, J.; Ma, H.; Chilkoti, A. *Surf. Sci.* **2004**, *570*, 98.
(294) Ma, H.; Wells, M.; Beebe, T. P., Jr.; Chilkoti, A. *Adv. Funct. Mater.* **2006**, *16*, 640.
(295) Jones, D. M.; Brown, A. A.; Huck, W. T. S. *Langmuir* **2002**, *18*, 1265.
(296) Moya, S. E.; Brown, A. A.; Azzaroni, O.; Huck, W. T. S. *Macromol. Rapid Commun.* **2005**, *26*, 1117.
(297) Plunkett, K. N.; Zhu, X.; Moore, J. S.; Leckband, D. E. *Langmuir* **2006**, *22*, 4259.
(298) Singh, N.; Cui, X. F.; Boland, T.; Husson, S. M. *Biomaterials* **2007**, *28*, 763.
(299) Kusumo, A.; Bombalski, L.; Lin, Q.; Matyjaszewski, K.; Schneider, J. W.; Tilton, R. D. *Langmuir* **2007**, *23*, 4448.
(300) von Natzmer, P.; Bontempo, D.; Tirelli, N. *Chem. Commun.* **2003**, 1600.
(301) Feng, W.; Brash, J. L.; Zhu, S. P. *Biomaterials* **2006**, *27*, 847.
(302) Nagase, K.; Kobayashi, J.; Kikuchi, A. I.; Akiyama, Y.; Kanazawa, H.; Okano, T. *Langmuir* **2008**, *24*, 511.
(303) Bao, Z. Y.; Bruening, M. L.; Baker, G. L. *Macromolecules* **2006**, *39*, 5251.
(304) Ulman, A. *Chem. Rev.* **1996**, *96*, 1533.
(305) Bain, C. D.; Whitesides, G. M. *J. Am. Chem. Soc.* **1988**, *110*, 6560.
(306) Bain, C. D.; Evall, J.; Whitesides, G. M. *J. Am. Chem. Soc.* **1989**, *111*, 7155.
(307) Brown, A. A.; Khan, N. S.; Steinbock, L.; Huck, W. T. S. *Eur. Polym. J.* **2005**, *41*, 1757.
(308) Tsukagoshi, T.; Kondo, Y.; Yoshino, N. *Colloids Surf., B* **2007**, *54*, 94.
(309) Tsukagoshi, T.; Kondo, Y.; Yoshino, N. *Colloids Surf., B* **2007**, *54*, 101.
(310) Yamamoto, S.; Ejaz, M.; Tsujii, Y.; Fukuda, T. *Macromolecules* **2000**, *33*, 5608.
(311) Kizhakkedathu, J. N.; Brooks, D. E. *Macromolecules* **2003**, *36*, 591.
(312) Goodman, D.; Kizhakkedathu, J. N.; Brooks, D. E. *Langmuir* **2004**, *20*, 6238.
(313) Wu, T.; Efimenko, K.; Genzer, J. *Macromolecules* **2001**, *34*, 684.
(314) Sagiv, J. *J. Am. Chem. Soc.* **1980**, *102*, 92.
(315) Onclin, S.; Ravoo, B. J.; Reinhoudt, D. N. *Angew. Chem., Int. Ed.* **2005**, *44*, 6282.
(316) Schwartz, D. K. *Annu. Rev. Phys. Chem.* **2001**, *52*, 107.
(317) Zhao, X. L.; Kopelman, R. *J. Phys. Chem.* **1996**, *100*, 11014.
(318) Carraro, C.; Yauw, O. W.; Sung, M. M.; Maboudian, R. *J. Phys. Chem. B* **1998**, *102*, 4441.
(319) Flinn, D. H.; Guzonas, D. A.; Yoon, R. H. *Colloids Surf., A* **1994**, *87*, 163.
(320) Mcgovern, M. E.; Kallury, K. M. R.; Thompson, M. *Langmuir* **1994**, *10*, 3607.
(321) Legrange, J. D.; Markham, J. L.; Kurkjian, C. R. *Langmuir* **1993**, *9*, 1749.
(322) Bierbaum, K.; Grunze, M.; Baski, A. A.; Chi, L. F.; Schrepp, W.; Fuchs, H. *Langmuir* **1995**, *11*, 2143.
(323) Fairbank, R. W. P.; Wirth, M. J. *J. Chromatogr., A* **1999**, *830*, 285.
(324) Vallant, T.; Kattner, J.; Brunner, H.; Mayer, U.; Hoffmann, H. *Langmuir* **1999**, *15*, 5339.
(325) Fadeev, A. Y.; McCarthy, T. J. *Langmuir* **2000**, *16*, 7268.
(326) Maeng, I. S.; Park, J. W. *Langmuir* **2003**, *19*, 4519.
(327) Maeng, I. S.; Park, J. W. *Langmuir* **2003**, *19*, 9973.
(328) Wang, X.; Xiao, X.; Wang, X. H.; Zhou, J. J.; Li, L.; Xu, J. *Macromol. Rapid Commun.* **2007**, *28*, 828.
(329) Wang, Y.; Brittain, W. J. *Macromol. Rapid Commun.* **2007**, *28*, 811.
(330) Raghuraman, G. K.; Dhamodharan, R.; Prucker, O.; Rühe, J. *Macromolecules* **2008**, *41*, 873.
(331) Wang, Y.; Hu, S. W.; Brittain, W. J. *Macromolecules* **2006**, *39*, 5675.
(332) Shimada, T.; Aoki, K.; Shinoda, Y.; Nakamura, T.; Tokunaga, N.; Inagaki, S.; Hayashi, T. *J. Am. Chem. Soc.* **2003**, *125*, 4688.
(333) Lim, J. E.; Shim, C. B.; Kim, J. M.; Lee, B. Y.; Yie, J. E. *Angew. Chem., Int. Ed.* **2004**, *43*, 3839.
(334) Roveda, C.; Church, T. L.; Alper, H.; Scott, S. L. *Chem. Mater.* **2000**, *12*, 857.
(335) Wasserman, S. R.; Tao, Y. T.; Whitesides, G. M. *Langmuir* **1989**, *5*, 1074.
(336) Sheiko, S. S.; Sun, F. C.; Randall, A.; Shirvanyants, D.; Rubinstein, M.; Lee, H.; Matyjaszewski, K. *Nature* **2006**, *440*, 191.
(337) Deng, Y.; Zhu, X. Y. *J. Am. Chem. Soc.* **2007**, *129*, 7557.
(338) Xu, F. J.; Cai, Q. J.; Kang, E. T.; Neoh, K. G. *Macromolecules* **2005**, *38*, 1051.
(339) Hemström, P.; Szumski, M.; Irgum, K. *Anal. Chem.* **2006**, *78*, 7098.
(340) Wang, L.-P.; Wang, Y.-P.; Yuan, K.; Lei, Z.-Q. *Polym. Adv. Technol.* **2008**, *19*, 285.
(341) Kasseh, A.; Ait-Kadi, A.; Riedl, B.; Pierson, J. F. *Polymer* **2003**, *44*, 1367.
(342) Chen, X. Y.; Armes, S. P.; Greaves, S. J.; Watts, J. F. *Langmuir* **2004**, *20*, 587.
(343) Edmondson, S.; Vo, C.-D.; Armes, S. P.; Unali, G.-F. *Macromolecules* **2007**, *40*, 5271.
(344) Edmondson, S.; Vo, C. D.; Armes, S. P.; Unali, G. F.; Weir, M. P. *Langmuir* **2008**, *24*, 7208.
(345) Fulghum, T. M.; Estillore, N. C.; Vo, C.-D.; Armes, S. P.; Advincula, R. C. *Macromolecules* **2008**, *41*, 429.
(346) Gorman, C. B.; Petrie, R. J.; Genzer, J. *Macromolecules* **2008**, *41*, 4856.
(347) Kruk, M.; Dufour, B.; Celer, E. B.; Kowalewski, T.; Jaroniec, M.; Matyjaszewski, K. *Macromolecules* **2008**, *41*, 8584.
(348) Buriak, J. M. *Chem. Rev.* **2002**, *102*, 1271.
(349) Xu, F. J.; Yuan, S. J.; Pehkonen, S. O.; Kang, E. T.; Neoh, K. G. *NanoBiotechnology* **2006**, *2*, 123.
(350) Xu, F. J.; Wuang, S. C.; Zong, B. Y.; Kang, E. T.; Neoh, K. G. *J. Nanosci. Nanotechnol.* **2006**, *6*, 1458.
(351) Xu, F. J.; Kang, E. T.; Neoh, K. G. *Macromolecules* **2005**, *38*, 1573.
(352) Xu, F. J.; Li, Y. L.; Kang, E. T.; Neoh, K. G. *Biomacromolecules* **2005**, *6*, 1759.

(353) Xu, F. J.; Kang, E. T.; Neoh, K. G. *J. Mater. Chem.* **2006**, *16*, 2948.
(354) Xu, F. J.; Song, Y.; Cheng, Z. P.; Zhu, X. L.; Zhu, C. X.; Kang, E. T.; Neoh, K. G. *Macromolecules* **2005**, *38*, 6254.
(355) Xu, F. J.; Cai, Q. J.; Li, Y. L.; Kang, E. T.; Neoh, K. G. *Biomacromolecules* **2005**, *6*, 1012.
(356) Peng, Q.; Xie, M.-G.; Neoh, K.-G.; Kang, E.-T. *Chem. Lett.* **2005**, *34*, 1628.
(357) Peng, J. W.; Huang, W.; Kang, E. T.; Neoh, K. G. *Surf. Rev. Lett.* **2006**, *13*, 251.
(358) Xu, F. J.; Zhong, S. P.; Yung, L. Y. L.; Tong, Y. W.; Kang, E. T.; Neoh, K. G. *Tissue Eng.* **2005**, *11*, 1736.
(359) Xu, D.; Yu, W. H.; Kang, E. T.; Neoh, K. G. *J. Colloid Interface Sci.* **2004**, *279*, 78.
(360) Yu, W. H.; Kang, E. T.; Neoh, K. G.; Zhu, S. P. *J. Phys. Chem. B* **2003**, *107*, 10198.
(361) Xu, F. J.; Cai, Q. J.; Kang, E. T.; Neoh, K. G. *Langmuir* **2005**, *21*, 3221.
(362) Belyavskii, S. G.; Mingalev, P. G.; Lisichkin, G. V. *Colloid J.* **2004**, *66*, 128.
(363) Cui, Y.; Tao, C.; Tian, Y.; He, Q.; Li, J. *Langmuir* **2006**, *22*, 8205.
(364) Wang, H.-J.; Zhou, W.-H.; Yin, X.-F.; Zhuang, Z.-X.; Yang, H.-H.; Wang, X.-R. *J. Am. Chem. Soc.* **2006**, *128*, 15954.
(365) Sun, L.; Baker, G. L.; Bruening, M. L. *Macromolecules* **2005**, *38*, 2307.
(366) Sun, L.; Dai, J.; Baker, G. L.; Bruening, M. L. *Chem. Mater.* **2006**, *18*, 4033.
(367) Jain, P.; Sun, L.; Dai, J. H.; Baker, G. L.; Bruening, M. L. *Biomacromolecules* **2007**, *8*, 3102.
(368) Fu, Q.; Rama Rao, G. V.; Basame, S. B.; Keller, D. J.; Artyushkova, K.; Fulghum, J. E.; López, G. P. *J. Am. Chem. Soc.* **2004**, *126*, 8904.
(369) Zhou, Y.; Wang, S. X.; Ding, B. J.; Yang, Z. M. *Chem. Eng. J.* **2008**, *138*, 578.
(370) Sun, Y. B.; Ding, X. B.; Zheng, Z. H.; Cheng, X.; Hu, X. H.; Peng, Y. X. *Eur. Polym. J.* **2007**, *43*, 762.
(371) Hu, B.; Fuchs, A.; Gordaninejad, F.; Evrensel, C. *Int. J. Mod. Phys. B* **2007**, *21*, 4819.
(372) García, I.; Zafeiropoulos, N. E.; Janke, A.; Tercjak, A.; Eceiza, A.; Stamm, M.; Mondragon, I. *J. Polym. Sci., Part A: Polym. Chem.* **2007**, *45*, 925.
(373) García, I.; Tercjak, A.; Zafeiropoulos, N. E.; Stamm, M.; Mondragon, I. *J. Polym. Sci., Part A: Polym. Chem.* **2007**, *45*, 4744.
(374) García, I.; Tercjak, A.; Zafeiropoulos, N. E.; Stamm, M.; Mondragon, I. *Macromol. Rapid Commun.* **2007**, *28*, 2361.
(375) Wuang, S. C.; Neoh, K. G.; Kang, E.-T.; Pack, D. W.; Leckband, D. E. *Adv. Funct. Mater.* **2006**, *16*, 1723.
(376) Marutani, E.; Yamamoto, S.; Ninjbadgar, T.; Tsujii, Y.; Fukuda, T.; Takano, M. *Polymer* **2004**, *45*, 2231.
(377) Hu, F. X.; Neoh, K. G.; Cen, L.; Kang, E.-T. *Biomacromolecules* **2006**, *7*, 809.
(378) Lattuada, M.; Hatton, T. A. *Langmuir* **2007**, *23*, 2158.
(379) An, L. J.; Li, Z. Q.; Wang, Z.; Zhang, J. H.; Yang, B. *Chem. Lett.* **2005**, *34*, 652.
(380) Vestal, C. R.; Zhang, Z. J. *J. Am. Chem. Soc.* **2002**, *124*, 14312.
(381) Parvin, S.; Sato, E.; Matsui, J.; Miyashita, T. *Polym. J.* **2006**, *38*, 1283.
(382) Parvin, S.; Matsui, J.; Sato, E.; Miyashita, T. *J. Colloid Interface Sci.* **2007**, *313*, 128.
(383) Maliakal, A.; Katz, H.; Cotts, P. M.; Subramoney, S.; Mirau, P. *J. Am. Chem. Soc.* **2005**, *127*, 14655.
(384) Babu, K.; Dhamodharan, R. *Nanoscale Res. Lett.* **2008**, *3*, 109.
(385) Fan, X. W.; Lin, L. J.; Dalsin, J. L.; Messersmith, P. B. *J. Am. Chem. Soc.* **2005**, *127*, 15843.
(386) Raghuraman, G. K.; Rühe, J.; Dhamodharan, R. *J. Nanopart. Res.* **2008**, *10*, 415.
(387) Zhang, F.; Shi, Z. L.; Chua, P. H.; Kang, E. T.; Neoh, K. G. *Ind. Eng. Chem. Res.* **2007**, *46*, 9077.
(388) Zhang, F.; Xu, F. J.; Kang, E. T.; Neoh, K. G. *Ind. Eng. Chem. Res.* **2006**, *45*, 3067.
(389) Raynor, J. E.; Petrie, T. A.; García, A. J.; Collard, D. M. *Adv. Mater.* **2007**, *19*, 1724.
(390) Marcinko, S.; Fadeev, A. Y. *Langmuir* **2004**, *20*, 2270.
(391) Fan, X. W.; Lin, L. J.; Messersmith, P. B. *Compos. Sci. Technol.* **2006**, *66*, 1198.
(392) Hamming, L. M.; Fan, X. W.; Messersmith, P. B.; Brinson, L. C. *Compos. Sci. Technol.* **2008**, *68*, 2042.
(393) Fan, X.; Lin, L.; Messersmith, P. B. *Biomacromolecules* **2006**, *7*, 2443.
(394) Liu, P.; Wang, T. M. *Curr. Appl. Phys.* **2008**, *8*, 66.
(395) Ok, J.; Matyjaszewski, K. *J. Inorg. Organomet. Polym. Mater.* **2006**, *16*, 129.
(396) Chang, M.-J.; Tsai, J.-Y.; Chang, C.-W.; Chang, H.-M.; Jiang, G. J. *J. Appl. Polym. Sci.* **2007**, *103*, 3680.
(397) Chen, R. X.; Zhu, S. P.; Maclaughlin, S. *Langmuir* **2008**, *24*, 6889.
(398) Liu, P.; Wang, T. M. *Ind. Eng. Chem. Res.* **2007**, *46*, 97.
(399) Liu, P.; Wang, T. M.; Su, Z. X. *J. Nanosci. Nanotechnol.* **2006**, *6*, 1684.
(400) Liu, P.; Guo, J. S. *Colloids Surf., A* **2006**, *282*, 498.
(401) Wang, L.-P.; Wang, Y.-P.; Pei, X.-W.; Peng, B. *React. Funct. Polym.* **2008**, *68*, 649.
(402) Li, C.-P.; Huang, C.-M.; Hsieh, M.-T.; Wei, K.-H. *J. Polym. Sci., Part A: Polym. Chem.* **2005**, *43*, 534.
(403) Lego, B.; Skene, W. G.; Giasson, S. *Langmuir* **2008**, *24*, 379.
(404) Wang, L.-P.; Wang, Y.-P.; Wang, R.-M.; Zhang, S.-C. *React. Funct. Polym.* **2008**, *68*, 643.
(405) Datta, H.; Bhowmick, A. K.; Singha, N. K. *J. Polym. Sci., Part A: Polym. Chem.* **2008**, *46*, 5014.
(406) Burkett, S. L.; Ko, N.; Stern, N. D.; Caissie, J. A.; Sengupta, D. *Chem. Mater.* **2006**, *18*, 5137.
(407) Di, J. B.; Sogah, D. Y. *Macromolecules* **2006**, *39*, 1020.
(408) Mittal, V. *J. Colloid Interface Sci.* **2007**, *314*, 141.
(409) Weimer, M. W.; Chen, H.; Giannelis, E. P.; Sogah, D. Y. *J. Am. Chem. Soc.* **1999**, *121*, 1615.
(410) Zhao, H. Y.; Farrell, B. P.; Shipp, D. A. *Polymer* **2004**, *45*, 4473.
(411) Zhao, H. Y.; Argoti, S. D.; Farrell, B. P.; Shipp, D. A. *J. Polym. Sci., Part A: Polym. Chem.* **2004**, *42*, 916.
(412) Böttcher, H.; Hallensleben, M. L.; Nuss, S.; Wurm, H.; Bauer, J.; Behrens, P. *J. Mater. Chem.* **2002**, *12*, 1351.
(413) Salem, N.; Shipp, D. A. *Polymer* **2005**, *46*, 8573.
(414) Saunders, J. M.; Saunders, B. R. *J. Macromol. Sci., Part B: Phys.* **2007**, *46*, 547.
(415) Leach, E. S. H.; Hopkinson, A.; Franklin, K.; van Duijneveldt, J. S. *Langmuir* **2005**, *21*, 3821.
(416) Shah, R. R.; Merreceyes, D.; Husemann, M.; Rees, I.; Abbott, N. L.; Hawker, C. J.; Hedrick, J. L. *Macromolecules* **2000**, *33*, 597.
(417) Kim, J.-B.; Bruening, M. L.; Baker, G. L. *J. Am. Chem. Soc.* **2000**, *122*, 7616.
(418) He, Q.; Küller, A.; Grunze, M.; Li, J. B. *Langmuir* **2007**, *23*, 3981.
(419) Lou, X. H.; Lewis, M. S.; Gorman, C. B.; He, L. *Anal. Chem.* **2005**, *77*, 4698.
(420) Nuss, S.; Böttcher, H.; Wurm, H.; Hallensleben, M. L. *Angew. Chem., Int. Ed.* **2001**, *40*, 4016.
(421) Kang, S. M.; Lee, K.-B.; Kim, D. J.; Choi, I. S. *Nanotechnology* **2006**, *17*, 4719.
(422) Li, D. X.; Cui, Y.; Wang, K. W.; He, Q.; Yan, X. H.; Li, J. B. *Adv. Funct. Mater.* **2007**, *17*, 3134.
(423) Li, D. X.; He, Q.; Cui, Y.; Li, J. B. *Chem. Mater.* **2007**, *19*, 412.
(424) Li, D. X.; He, Q.; Cui, Y.; Wang, K. W.; Zhang, X. M.; Li, J. B. *Chem.—Eur. J.* **2007**, *13*, 2224.
(425) Duan, H. W.; Wang, D. A.; Kurth, D. G.; Möhwald, H. *Angew. Chem., Int. Ed.* **2004**, *43*, 5639.
(426) Duan, H. W.; Kuang, M.; Wang, D. Y.; Kurth, D. G.; Möhwald, H. *Angew. Chem., Int. Ed.* **2005**, *44*, 1717.
(427) Duan, H. W.; Kuang, M.; Zhang, G.; Wang, D. Y.; Kurth, D. G.; Möhwald, H. *Langmuir* **2005**, *21*, 11495.
(428) Mandal, T. K.; Fleming, M. S.; Walt, D. R. *Nano Lett.* **2002**, *2*, 3.
(429) Ohno, K.; Koh, K.; Tsujii, Y.; Fukuda, T. *Macromolecules* **2002**, *35*, 8989.
(430) Ohno, K.; Koh, K.; Tsujii, Y.; Fukuda, T. *Angew. Chem., Int. Ed.* **2003**, *42*, 2751.
(431) Roth, P. J.; Theato, P. *Chem. Mater.* **2008**, *20*, 1614.
(432) Sill, K.; Emrick, T. *Chem. Mater.* **2004**, *16*, 1240.
(433) Claes, M.; Voccia, S.; Detrembleur, C.; Jérôme, C.; Gilbert, B.; Leclère, P.; Geskin, V. M.; Gouttebaron, R.; Hecq, M.; Lazzaroni, R.; Jérôme, R. *Macromolecules* **2003**, *36*, 5926.
(434) Matrab, T.; Save, M.; Charleux, B.; Pinson, J.; Cabet-Deliry, E.; Adenier, A.; Chehimi, M. M.; Delamar, M. *Surf. Sci.* **2007**, *601*, 2357.
(435) Nguyen, M. N.; Matrab, T.; Badre, C.; Turmine, M.; Chehimi, M. M. *Surf. Interface Anal.* **2008**, *40*, 412.
(436) Matrab, T.; Chehimi, M. M.; Perruchot, C.; Adenier, A.; Guillez, A.; Save, M.; Charleux, B.; Cabet-Deliry, E.; Pinson, J. *Langmuir* **2005**, *21*, 4686.
(437) Cai, Q. J.; Fu, G. D.; Zhu, F. R.; Kang, E.-T.; Neoh, K.-G. *Angew. Chem., Int. Ed.* **2005**, *44*, 1104.
(438) Choi, K.; Buriak, J. M. *Langmuir* **2000**, *16*, 7737.
(439) Xu, F. J.; Cai, Q. J.; Kang, E. T.; Neoh, K. G.; Zhu, C. X. *Organometallics* **2005**, *24*, 1768.
(440) Kong, H.; Gao, C.; Yan, D. Y. *J. Am. Chem. Soc.* **2004**, *126*, 412.
(441) Chang, J. H.; Lee, Y. W.; Kim, B. G.; Kim, H.-K.; Choi, I. S.; Paik, H.-J. *Compos. Interfaces* **2007**, *14*, 493.
(442) Qin, S. H.; Qin, D. Q.; Ford, W. T.; Resasco, D. E.; Herrera, J. E. *J. Am. Chem. Soc.* **2004**, *126*, 170.
(443) Shanmugharaj, A. M.; Bae, J. H.; Nayak, R. R.; Ryu, S. H. *J. Polym. Sci., Part A: Polym. Chem.* **2007**, *45*, 460.
(444) Baskaran, D.; Mays, J. W.; Bratcher, M. S. *Angew. Chem., Int. Ed.* **2004**, *43*, 2138.

(445) Narain, R.; Housni, A.; Lane, L. *J. Polym. Sci., Part A: Polym. Chem.* **2006**, *44*, 6558.
(446) Kong, H.; Gao, C.; Yan, D. Y. *Macromolecules* **2004**, *37*, 4022.
(447) Kong, H.; Li, W. W.; Gao, C.; Yan, D. Y.; Jin, Y. Z.; Walton, D. R. M.; Kroto, H. W. *Macromolecules* **2004**, *37*, 6683.
(448) Gao, C.; Vo, C. D.; Jin, Y. Z.; Li, W. W.; Armes, S. P. *Macromolecules* **2005**, *38*, 8634.
(449) Kong, H.; Luo, P.; Gao, C.; Yan, D. *Polymer* **2005**, *46*, 2472.
(450) Hong, C.-Y.; You, Y.-Z.; Pan, C.-Y. *Polymer* **2006**, *47*, 4300.
(451) Matrab, T.; Chancolon, J.; L'hermite, M. M.; Rouzaud, J.-N.; Deniau, G.; Boudou, J.-P.; Chehimi, M. M.; Delamar, M. *Colloids Surf., A* **2006**, *287*, 217.
(452) Wu, W.; Tsarevsky, N. V.; Hudson, J. L.; Tour, J. M.; Matyjaszewski, K.; Kowalewski, T. *Small* **2007**, *3*, 1803.
(453) Yao, Z.; Braidy, N.; Botton, G. A.; Adronov, A. *J. Am. Chem. Soc.* **2003**, *125*, 16015.
(454) Chochos, C. L.; Stefopoulos, A. A.; Campidelli, S.; Prato, M.; Gregoriou, V. G.; Kallitsis, J. K. *Macromolecules* **2008**, *41*, 1825.
(455) Liu, Y.-L.; Chen, W.-H. *Macromolecules* **2007**, *40*, 8881.
(456) Dehonor, M.; Masenelli-Varlot, K.; González-Montiel, A.; Gauthier, C.; Cavaillé, J.-Y.; Terrones, M. *J. Nanosci. Nanotechnol.* **2007**, *7*, 3450.
(457) Dehonor, M.; Masenelli-Varlot, K.; González-Montiel, A.; Gauthier, C.; Cavaillé, J. Y.; Terrones, H.; Terrones, M. *Chem. Commun.* **2005**, 5349.
(458) Yang, Q.; Wang, L.; Xiang, W.-D.; Zhou, J.-F.; Tan, Q.-H. *J. Polym. Sci., Part A: Polym. Chem.* **2007**, *45*, 3451.
(459) Cheng, J. G.; Wang, L.; Huo, J.; Yu, H. J.; Yang, Q.; Deng, L. B. *J. Polym. Sci., Part B: Polym. Phys.* **2008**, *46*, 1529.
(460) Yang, X.-H.; Yang, Q.; Yang, H.; Wang, L.; Chen, Y.-Q. *Chin. J. Anal. Chem.* **2007**, *35*, 1751.
(461) Li, L.; Davidson, J. L.; Lukehart, C. M. *Carbon* **2006**, *44*, 2308.
(462) Li, L.; Lukehart, C. M. *Chem. Mater.* **2006**, *18*, 94.
(463) Li, L.; Li, J.; Lukehart, C. M. *Sens. Actuators, B* **2008**, *130*, 783.
(464) Liu, P.; Su, Z. X. *Polym. Int.* **2005**, *54*, 1508.
(465) Jin, Y. Z.; Gao, C.; Kroto, H. W.; Maekawa, T. *Macromol. Rapid Commun.* **2005**, *26*, 1133.
(466) Matrab, T.; Chehimi, M. M.; Boudou, J. P.; Benedic, F.; Wang, J.; Naguib, N. N.; Carlisle, J. A. *Diamond Relat. Mater.* **2006**, *15*, 639.
(467) Matrab, T.; Chehimi, M. M.; Pinson, J.; Slomkowsi, S.; Basinska, T. *Surf. Interface Anal.* **2006**, *38*, 565.
(468) Carlmark, A.; Malmström, E. *J. Am. Chem. Soc.* **2002**, *124*, 900.
(469) Singh, N.; Wang, J.; Ulbricht, M.; Wickramasinghe, S. R.; Husson, S. M. *J. Membr. Sci.* **2008**, *309*, 64.
(470) Singh, N.; Chen, Z.; Tomer, N.; Wickramasinghe, S. R.; Soice, N.; Husson, S. M. *J. Membr. Sci.* **2008**, *311*, 225.
(471) Lindqvist, J.; Malmström, E. *J. Appl. Polym. Sci.* **2006**, *100*, 4155.
(472) Carlmark, A.; Malmström, E. E. *Biomacromolecules* **2003**, *4*, 1740.
(473) Westlund, R.; Carlmark, A.; Hult, A.; Malmström, E.; Saez, I. M. *Soft Matter* **2007**, *3*, 866.
(474) Nyström, D.; Lindqvist, J.; Östmark, E.; Hult, A.; Malmström, E. *Chem. Commun.* **2006**, 3594.
(475) Lindqvist, J.; Nyström, D.; Östmark, E.; Antoni, P.; Carlmark, A.; Johansson, M.; Hult, A.; Malmström, E. *Biomacromolecules* **2008**, *9*, 2139.
(476) Castelvetro, V.; Geppi, M.; Giaiacopi, S.; Mollica, G. *Biomacromolecules* **2007**, *8*, 498.
(477) Kim, D. J.; Heo, J.-Y.; Kim, K. S.; Choi, I. S. *Macromol. Rapid Commun.* **2003**, *24*, 517.
(478) Li, N.; Bai, R. B.; Liu, C. K. *Langmuir* **2005**, *21*, 11780.
(479) Liu, P.; Su, Z. X. *Mater. Lett.* **2006**, *60*, 1137.
(480) Roy, D.; Knapp, J. S.; Guthrie, J. T.; Perrier, S. *Biomacromolecules* **2008**, *9*, 91.
(481) Roy, D.; Guthrie, J. T.; Perrier, S. *Soft Matter* **2008**, *4*, 145.
(482) Zheng, G. D.; Stöver, H. D. H. *Macromolecules* **2003**, *36*, 1808.
(483) Bozukova, D.; Pagnoulle, C.; De Pauw-Gillet, M.-C.; Ruth, N.; Jérôme, R.; Jérôme, C. *Langmuir* **2008**, *24*, 6649.
(484) Liu, Z.-T.; Sun, C.; Liu, Z.-W.; Lu, J. *J. Appl. Polym. Sci.* **2008**, *109*, 2888.
(485) Liu, P.; Su, Z. X. *Carbohydr. Polym.* **2005**, *62*, 159.
(486) Bontempo, D.; Tirelli, N.; Masci, G.; Crescenzi, V.; Hubbell, J. A. *Macromol. Rapid Commun.* **2002**, *23*, 418.
(487) Angot, S.; Ayres, N.; Bon, S. A. F.; Haddleton, D. M. *Macromolecules* **2001**, *34*, 768.
(488) Alem, H.; Duwez, A.-S.; Lussis, P.; Lipnik, P.; Jonas, A. M.; Demoustier-Champagne, S. *J. Membr. Sci.* **2008**, *308*, 75.
(489) Liu, P.; Su, Z. X. *Polym. Bull.* **2005**, *55*, 411.
(490) Kawaguchi, H.; Isono, Y.; Tsuji, S. *Macromol. Symp.* **2002**, *179*, 75.
(491) Liu, P.; Zhang, L. X. *J. Macromol. Sci., Part A: Pure Appl. Chem.* **2008**, *45*, 17.
(492) Luo, N.; Husson, S. M.; Hirt, D. E.; Schwark, D. W. *J. Appl. Polym. Sci.* **2004**, *92*, 1589.
(493) Della Martina, A.; Garamszegi, L.; Hilborn, J. G. *React. Funct. Polym.* **2003**, *57*, 49.
(494) Chen, Y.; Liu, D.; Deng, Q.; He, X.; Wang, X. *J. Polym. Sci., Part A: Polym. Chem.* **2006**, *44*, 3434.
(495) Yao, F.; Fu, G.-D.; Zhao, J. P.; Kang, E.-T.; Neoh, K. G. *J. Membr. Sci.* **2008**, *319*, 149.
(496) Liu, Y.-L.; Luo, M.-T.; Lai, J.-Y. *Macromol. Rapid Commun.* **2007**, *28*, 329.
(497) Liu, J.; Pan, T.; Woolley, A. T.; Lee, M. L. *Anal. Chem.* **2004**, *76*, 6948.
(498) Coiai, S.; Passaglia, E.; Ciardelli, F. *Macromol. Chem. Phys.* **2006**, *207*, 2289.
(499) Farhan, T.; Huck, W. T. S. *Eur. Polym. J.* **2004**, *40*, 1599.
(500) Xiao, D. Q.; Van Le, T.; Wirth, M. *J. Anal. Chem.* **2004**, *76*, 2055.
(501) Xiao, D. Q.; Zhang, H.; Wirth, M. *Langmuir* **2002**, *18*, 9971.
(502) Azzaroni, O.; Moya, S. E.; Brown, A. A.; Zheng, Z.; Donath, E.; Huck, W. T. S. *Adv. Funct. Mater.* **2006**, *16*, 1037.
(503) Huang, H.; Chung, J. Y.; Nolte, A. J.; Stafford, C. M. *Chem. Mater.* **2007**, *19*, 6555.
(504) Unsal, E.; Elmas, B.; Çaglayan, B.; Tuncel, M.; Patir, S.; Tuncel, A. *Anal. Chem.* **2006**, *78*, 5868.
(505) Zhang, H.; Shouro, D.; Itoh, K.; Takata, T.; Jiang, Y. *J. Appl. Polym. Sci.* **2008**, *108*, 351.
(506) Friebe, A.; Ulbricht, M. *Langmuir* **2007**, *23*, 10316.
(507) Liu, D. M.; Chen, Y. W.; Zhang, N.; He, X. H. *J. Appl. Polym. Sci.* **2006**, *101*, 3704.
(508) Xu, F. J.; Zhao, J. P.; Kang, E. T.; Neoh, K. G.; Li, J. *Langmuir* **2007**, *23*, 8585.
(509) Lee, H. J.; Matsuda, T. *J. Biomed. Mater. Res.* **1999**, *47*, 564.
(510) Senkal, B. F.; Bildik, F.; Yavuz, E.; Sarac, A. *React. Funct. Polym.* **2007**, *67*, 1471.
(511) Senkal, B. F.; Bicak, N. *Eur. Polym. J.* **2003**, *39*, 327.
(512) Sonmez, H. B.; Senkal, B. F.; Sherrington, D. C.; Bicak, N. *React. Funct. Polym.* **2003**, *55*, 1.
(513) Desai, S. M.; Solanky, S. S.; Mandale, A. B.; Rathore, K.; Singh, R. P. *Polymer* **2003**, *44*, 7645.
(514) Zheng, G. D.; Stöver, H. D. H. *Macromolecules* **2002**, *35*, 6828.
(515) Min, K.; Hu, J. H.; Wang, C. C.; Elaissari, A. *J. Polym. Sci., Part A: Polym. Chem.* **2002**, *40*, 892.
(516) Xu, F. J.; Zhao, J. P.; Kang, E. T.; Neoh, K. G. *Ind. Eng. Chem. Res.* **2007**, *46*, 4866.
(517) Tugulu, S.; Klok, H.-A. *Macromol. Symp.* **2009**, *279*, 103.
(518) Huang, J. Y.; Murata, H.; Koepsel, R. R.; Russell, A. J.; Matyjaszewski, K. *Biomacromolecules* **2007**, *8*, 1396.
(519) Yamamoto, K.; Miwa, Y.; Tanaka, H.; Sakaguchi, M.; Shimada, S. *J. Polym. Sci., Part A: Polym. Chem.* **2002**, *40*, 3350.
(520) Mizutani, A.; Kikuchi, A.; Yamato, M.; Kanazawa, H.; Okano, T. *Biomaterials* **2008**, *29*, 2073.
(521) Genua, A.; Alduncín, J. A.; Pomposo, J. A.; Grande, H.; Kehagias, N.; Reboud, V.; Sotomayor, C.; Mondragon, I.; Mecerreyes, D. *Nanotechnology* **2007**, *18*, 215301.
(522) Jain, P.; Dai, J.; Grajales, S.; Saha, S.; Baker, G. L.; Bruening, M. L. *Langmuir* **2007**, *23*, 11360.
(523) Dunér, G.; Anderson, H.; Myrskog, A.; Hedlund, M.; Aastrup, T.; Ramström, O. *Langmuir* **2008**, *24*, 7559.
(524) Sebra, R. P.; Kasko, A. M.; Anseth, K. S.; Bowman, C. N. *Sens. Actuators, B* **2006**, *119*, 127.
(525) Sebra, R. P.; Anseth, K. S.; Bowman, C. N. *J. Polym. Sci., Part A: Polym. Chem.* **2006**, *44*, 1404.
(526) Reddy, S. K.; Sebra, R. P.; Anseth, K. S.; Bowman, C. N. *J. Polym. Sci., Part A: Polym. Chem.* **2005**, *43*, 2134.
(527) Chen, Y. W.; Kang, E.-T.; Neoh, K.-G.; Greiner, A. *Adv. Funct. Mater.* **2005**, *15*, 113.
(528) Cheng, Z.; Zhang, L.; Zhu, X.; Kang, E. T.; Neoh, K. G. *J. Polym. Sci., Part A: Polym. Chem.* **2008**, *46*, 2119.
(529) Cheng, Z. P.; Zhu, X. L.; Shi, Z. L.; Neoh, K. G.; Kang, E. T. *Ind. Eng. Chem. Res.* **2005**, *44*, 7098.
(530) Barner, L.; Li, C.; Hao, X. J.; Stenzel, M. H.; Barner-Kowollik, C.; Davis, T. P. *J. Polym. Sci., Part A: Polym. Chem.* **2004**, *42*, 5067.
(531) Li, D. J.; Dunlap, J. R.; Zhao, B. *Langmuir* **2008**, *24*, 5911.
(532) Zhang, M. M.; Liu, L.; Wu, C. L.; Fu, G. Q.; Zhao, H. Y.; He, B. L. *Polymer* **2007**, *48*, 1989.
(533) Zhang, M. M.; Liu, L.; Zhao, H. Y.; Yang, Y.; Fu, G. Q.; He, B. L. *J. Colloid Interface Sci.* **2006**, *301*, 85.
(534) Mittal, V.; Matsko, N. B.; Butté, A.; Morbidelli, M. *Macromol. Mater. Eng.* **2008**, *293*, 491.
(535) Mittal, V.; Matsko, N. B.; Butté, A.; Morbidelli, M. *Polymer* **2007**, *48*, 2806.
(536) Guerrini, M. M.; Charleux, B.; Vairon, J.-P. *Macromol. Rapid Commun.* **2000**, *21*, 669.
(537) Kizhakkedathu, J. N.; Norris-Jones, R.; Brooks, D. E. *Macromolecules* **2004**, *37*, 734.

(538) Kizhakkedathu, J. N.; Kumar, K. R.; Goodman, D.; Brooks, D. E. *Polymer* **2004**, *45*, 7471.
(539) Jayachandran, K. N.; Takacs-Cox, A.; Brooks, D. E. *Macromolecules* **2002**, *35*, 4247.
(540) Goodman, D.; Kizhakkedathu, J. N.; Brooks, D. E. *Langmuir* **2004**, *20*, 2333.
(541) Kizhakkedathu, J. N.; Goodman, D.; Brooks, D. E. In *Advances in Controlled/Living Radical Polymerization*; Matyjaszewski, K., Ed.; 2003; Vol. 854.
(542) Zhu, L.-P.; Dong, H.-B.; Wei, X.-Z.; Yi, Z.; Zhu, B.-K.; Xu, Y.-Y. *J. Membr. Sci.* **2008**, *320*, 407.
(543) Cheng, Z. P.; Zhu, X. L.; Kang, E. T.; Neoh, K. G. *Macromolecules* **2006**, *39*, 1660.
(544) Meyer, U.; Svec, F.; Fréchet, J. M. J.; Hawker, C. J.; Irgum, K. *Macromolecules* **2000**, *33*, 7769.
(545) Moine, L.; Deleuze, H.; Degueil, M.; Maillard, B. *J. Polym. Sci., Part A: Polym. Chem.* **2004**, *42*, 1216.
(546) Barner, L.; Zwaneveld, N.; Perera, S.; Pham, Y.; Davis, T. P. *J. Polym. Sci., Part A: Polym. Chem.* **2002**, *40*, 4180.
(547) Barner, L.; Perera, S.; Sandanayake, S.; Davis, T. P. *J. Polym. Sci., Part A: Polym. Chem.* **2006**, *44*, 857.
(548) Barsbay, M.; Güven, G.; Stenzel, M. H.; Davis, T. P.; Barner-Kowollik, C.; Barner, L. *Macromolecules* **2007**, *40*, 7140.
(549) Kiani, K.; Hill, D. J. T.; Rasoul, F.; Whittaker, M.; Rintoul, L. *J. Polym. Sci., Part A: Polym. Chem.* **2007**, *45*, 1074.
(550) Chen, Y. W.; Deng, Q.; Mao, J. C.; Nie, H. R.; Wu, L. C.; Zhou, W. H.; Huang, B. W. *Polymer* **2007**, *48*, 7604.
(551) Yamamoto, K.; Tanaka, H.; Sakaguchi, M.; Shimada, S. *Polymer* **2003**, *44*, 7661.
(552) Xu, F. J.; Li, H. Z.; Li, J.; Eric Teo, Y. H.; Zhu, C. X.; Kang, E. T.; Neoh, K. G. *Biosens. Bioelectron.* **2008**, *24*, 773.
(553) Farhan, T.; Azzaroni, O.; Huck, W. T. S. *Soft Matter* **2005**, *1*, 66.
(554) Xia, Y. N.; Whitesides, G. M. *Langmuir* **1997**, *13*, 2059.
(555) Zhou, F.; Zheng, Z. J.; Yu, B.; Liu, W. M.; Huck, W. T. S. *J. Am. Chem. Soc.* **2006**, *128*, 16253.
(556) van Poll, M. L.; Zhou, F.; Ramstedt, M.; Hu, L.; Huck, W. T. S. *Angew. Chem., Int. Ed.* **2007**, *46*, 6634.
(557) Azzaroni, O.; Trappmann, B.; van Rijn, P.; Zhou, F.; Kong, B.; Huck, W. T. S. *Angew. Chem., Int. Ed.* **2006**, *45*, 7440.
(558) Azzaroni, O.; Moya, S.; Farhan, T.; Brown, A. A.; Huck, W. T. S. *Macromolecules* **2005**, *38*, 10192.
(559) Azzaroni, O.; Brown, A. A.; Cheng, N.; Wei, A.; Jonas, A. M.; Huck, W. T. S. *J. Mater. Chem.* **2007**, *17*, 3433.
(560) Jeon, N. L.; Choi, I. S.; Whitesides, G. M.; Kim, N. Y.; Laibinis, P. E.; Harada, Y.; Finnie, K. R.; Girolami, G. S.; Nuzzo, R. G. *Appl. Phys. Lett.* **1999**, *75*, 4201.
(561) Jones, D. M.; Smith, J. R.; Huck, W. T. S.; Alexander, C. *Adv. Mater.* **2002**, *14*, 1130.
(562) Zhou, F.; Huck, W. T. S. *Chem. Commun.* **2005**, 5999.
(563) Kim, D. J.; Lee, K.-B.; Lee, T. G.; Shon, H. K.; Kim, W.-J.; Paik, H. J.; Choi, I. S. *Small* **2005**, *1*, 992.
(564) Zhou, F.; Liu, Z. L.; Li, W. N.; Hao, J. C.; Chen, M.; Liu, W. M.; Sun, D. C. *Chem. Lett.* **2004**, *33*, 602.
(565) Alarcón, C. D. H.; Farhan, T.; Osborne, V. L.; Huck, W. T. S.; Alexander, C. *J. Mater. Chem.* **2005**, *15*, 2089.
(566) Tu, H.; Heitzman, C. E.; Braun, P. V. *Langmuir* **2004**, *20*, 8313.
(567) Ma, H.; Li, D.; Sheng, X.; Zhao, B.; Chilkoti, A. *Langmuir* **2006**, *22*, 3751.
(568) Jung, J.; Kim, K. W.; Na, K.; Kaholek, M.; Zauscher, S.; Hyun, J. *Macromol. Rapid Commun.* **2006**, *27*, 776.
(569) Dai, X.; Zhou, F.; Khan, N.; Huck, W. T. S.; Kaminski, C. F. *Langmuir* **2008**, *24*, 13182.
(570) Tsujii, Y.; Ejaz, M.; Yamamoto, S.; Fukuda, T.; Shigeto, K.; Mibu, K.; Shinjo, T. *Polymer* **2002**, *43*, 3837.
(571) He, Q.; Kueller, A.; Schilp, S.; Leisten, F.; Kolb, H.-A.; Grunze, M.; Li, J. B. *Small* **2007**, *3*, 1860.
(572) Ballav, N.; Schilp, S.; Zharnikov, M. *Angew. Chem., Int. Ed.* **2008**, *47*, 1421.
(573) Schilp, S.; Ballav, N.; Zharnikov, M. *Angew. Chem., Int. Ed.* **2008**, *47*, 6786.
(574) Ahn, S. J.; Kaholek, M.; Lee, W.-K.; LaMattina, B.; LaBean, T. H.; Zauscher, S. *Adv. Mater.* **2004**, *16*, 2141.
(575) Jonas, A. M.; Hu, Z.; Glinel, K.; Huck, W. T. S. *Nano Lett.* **2008**, *8*, 3819.
(576) Tugulu, S.; Harms, M.; Fricke, M.; Volkmer, D.; Klok, H.-A. *Angew. Chem., Int. Ed.* **2006**, *45*, 7458.
(577) Iwata, R.; Suk-In, P.; Hoven, V. P.; Takahara, A.; Akiyoshi, K.; Iwasaki, Y. *Biomacromolecules* **2004**, *5*, 2308.
(578) Kamitani, R.; Niikura, K.; Onodera, T.; Iwasaki, N.; Shimaoka, H.; Ijiro, K. *Bull. Chem. Soc. Jpn.* **2007**, *80*, 1808.
(579) Zhou, F.; Mu, Z. G.; Wang, T. M.; Liu, Z. L.; Yu, B.; Hao, J. C.; Liu, W. M. *J. Appl. Polym. Sci.* **2007**, *106*, 723.
(580) Zhou, F.; Liu, W. M.; Hao, J. C.; Xu, T.; Chen, M.; Xue, Q. J. *Adv. Funct. Mater.* **2003**, *13*, 938.
(581) Zhou, F.; Jiang, L.; Liu, W. M.; Xue, Q. J. *Macromol. Rapid Commun.* **2004**, *25*, 1979.
(582) Dong, R.; Krishnan, S.; Baird, B. A.; Lindau, M.; Ober, C. K. *Biomacromolecules* **2007**, *8*, 3082.
(583) Chen, J.-K.; Hsieh, C.-Y.; Huang, C.-F.; Li, P.-M.; Kuo, S.-W.; Chang, F.-C. *Macromolecules* **2008**, *41*, 8729.
(584) Zapotoczny, S.; Benetti, E. M.; Vancso, G. J. *J. Mater. Chem.* **2007**, *17*, 3293.
(585) Kaholek, M.; Lee, W.-K.; LaMattina, B.; Caster, K. C.; Zauscher, S. *Nano Lett.* **2004**, *4*, 373.
(586) Kaholek, M.; Lee, W.-K.; Ahn, S.-J.; Ma, H. W.; Caster, K. C.; LaMattina, B.; Zauscher, S. *Chem. Mater.* **2004**, *16*, 3688.
(587) Hou, S. F.; Li, Z. C.; Li, Q. G.; Liu, Z. F. *Appl. Surf. Sci.* **2004**, *222*, 338.
(588) Piner, R. D.; Zhu, J.; Xu, F.; Hong, S. H.; Mirkin, C. A. *Science* **1999**, *283*, 661.
(589) Tsai, Y. S.; Wang, W.-C. *J. Appl. Polym. Sci.* **2006**, *101*, 1953.
(590) Liu, Y.; Klep, V.; Luzinov, I. *J. Am. Chem. Soc.* **2006**, *128*, 8106.
(591) Ejaz, M.; Yamamoto, S.; Tsujii, Y.; Fukuda, T. *Macromolecules* **2002**, *35*, 1412.
(592) Teare, D. O. H.; Schofield, W. C. E.; Garrod, R. P.; Badyal, J. P. S. *Langmuir* **2005**, *21*, 10818.
(593) Jiang, X. W.; Chen, H.-Y.; Galvan, G.; Yoshida, M.; Lahann, J. *Adv. Funct. Mater.* **2008**, *18*, 27.
(594) Slim, C.; Tran, Y.; Chehimi, M. M.; Garraud, N.; Roger, J.-P.; Combellas, C.; Kanoufi, F. *Chem. Mater.* **2008**, *20*, 6677.
(595) Becer, C. R.; Haensch, C.; Hoeppener, S.; Schubert, U. S. *Small* **2007**, *3*, 220.
(596) Sankhe, A. Y.; Booth, B. D.; Wiker, N. J.; Kilbey, S. M., II. *Langmuir* **2005**, *21*, 5332.
(597) Bantz, M. R.; Brantley, E. L.; Weinstein, R. D.; Moriarty, J.; Jennings, G. K. *J. Phys. Chem. B* **2004**, *108*, 9787.
(598) Brantley, E. L.; Jennings, G. K. *Macromolecules* **2004**, *37*, 1476.
(599) Brantley, E. L.; Holmes, T. C.; Jennings, G. K. *Macromolecules* **2005**, *38*, 9730.
(600) Tugulu, S.; Silacci, P.; Stergiopulos, N.; Klok, H.-A. *Biomaterials* **2007**, *28*, 2536.
(601) Petrie, T. A.; Raynor, J. E.; Reyes, C. D.; Burns, K. L.; Collard, D. M.; García, A. J. *Biomaterials* **2008**, *29*, 2849.
(602) Tugulu, S.; Arnold, A.; Sielaff, I.; Johnsson, K.; Klok, H.-A. *Biomacromolecules* **2005**, *6*, 1602.
(603) Diamanti, S.; Arifuzzaman, S.; Elsen, A.; Genzer, J.; Vaia, R. A. *Polymer* **2008**, *49*, 3770.
(604) Lee, B. S.; Chi, Y. S.; Lee, K.-B.; Kim, Y.-G.; Choi, I. S. *Biomacromolecules* **2007**, *8*, 3922.
(605) Dunn, J. D.; Igrisan, E. A.; Palumbo, A. M.; Reid, G. E.; Bruening, M. L. *Anal. Chem.* **2008**, *80*, 5727.
(606) Wang, W.-H.; Bruening, M. L. *Analyst* **2009**, *134*, 512.
(607) Gauthier, M. A.; Klok, H.-A. *Chem. Commun.* **2008**, 2591.
(608) Ayres, N.; Boyes, S. G.; Brittain, W. J. *Langmuir* **2007**, *23*, 182.
(609) Sanjuan, S.; Tran, Y. *J. Polym. Sci., Part A: Polym. Chem.* **2008**, *46*, 4305.
(610) Dai, J.; Bao, Z.; Sun, L.; Hong, S. U.; Baker, G. L.; Bruening, M. L. *Langmuir* **2006**, *22*, 4274.
(611) Cullen, S. P.; Liu, X.; Mandel, I. C.; Himpsel, F. J.; Gopalan, P. *Langmuir* **2008**, *24*, 913.
(612) Zhang, Z.; Chen, S. F.; Jiang, S. Y. *Biomacromolecules* **2006**, *7*, 3311.
(613) Kurosawa, S.; Aizawa, H.; Talib, Z. A.; Atthoff, B.; Hilborn, J. *Biosens. Bioelectron.* **2004**, *20*, 1165.
(614) Zhang, F.; Zhang, Z.; Zhu, X.; Kang, E.-T.; Neoh, K.-G. *Biomaterials* **2008**, *29*, 4751.
(615) Treat, N. D.; Ayres, N.; Boyes, S. G.; Brittain, W. J. *Macromolecules* **2006**, *39*, 26.
(616) Zhang, Z.; Cheng, G.; Carr, L. R.; Vaisocherová, H.; Chen, S.; Jiang, S. *Biomaterials* **2008**, *29*, 4719.
(617) Zhang, Z.; Vaisocherová, H.; Cheng, G.; Yang, W.; Xue, H.; Jiang, S. *Biomacromolecules* **2008**, *9*, 2686.
(618) Bicak, N.; Gazi, M.; Galli, G.; Chiellini, E. *J. Polym. Sci., Part A: Polym. Chem.* **2006**, *44*, 6708.
(619) Huang, J. S.; Li, X. T.; Zheng, Y. H.; Zhang, Y.; Zhao, R. Y.; Gao, X. C.; Yan, H. S. *Macromol. Biosci.* **2008**, *8*, 508.
(620) Iwasaki, Y.; Omichi, Y.; Iwata, R. *Langmuir* **2008**, *24*, 8427.
(621) Iwata, R.; Satoh, R.; Iwasaki, Y.; Akiyoshi, K. *Colloids Surf., B* **2008**, *62*, 288.
(622) Kawakita, H.; Masunaga, H.; Nomura, K.; Uezu, K.; Akiba, I.; Tsuneda, S. *J. Porous Mater.* **2007**, *14*, 387.
(623) Zhao, J.; Shang, Z.; Gao, L. *Sens. Actuators, A* **2007**, *135*, 257.
(624) Ejaz, M.; Ohno, K.; Tsujii, Y.; Fukuda, T. *Macromolecules* **2000**, *33*, 2870.
(625) Kobayashi, M.; Takahara, A. *Chem. Lett.* **2005**, *34*, 1582.

(626) Li, Y.; Benicewicz, B. C. *Macromolecules* **2008**, *41*, 7986.
(627) Gill, C. S.; Venkatasubbaiah, K.; Phan, N. T. S.; Weck, M.; Jones, C. W. *Chem.—Eur. J.* **2008**, *14*, 7306.
(628) Yao, Y.; Ma, Y.-Z.; Qin, M.; Ma, X.-J.; Wang, C.; Feng, X.-Z. *Colloids Surf., B* **2008**, *66*, 233.
(629) Lee, B. S.; Lee, J. K.; Kim, W.-J.; Jung, Y. H.; Sim, S. J.; Lee, J.; Choi, I. S. *Biomacromolecules* **2007**, *8*, 744.
(630) Jhaveri, S. B.; Beinhoff, M.; Hawker, C. J.; Carter, K. R.; Sogah, D. Y. *ACS Nano* **2008**, *2*, 719.
(631) LeMieux, M. C.; Peleshanko, S.; Anderson, K. D.; Tsukruk, V. V. *Langmuir* **2007**, *23*, 265.
(632) Kim, Y.-P.; Lee, B. S.; Kim, E.; Choi, I. S.; Moon, D. W.; Lee, T. G.; Kim, H.-S. *Anal. Chem.* **2008**, *80*, 5094.
(633) Azzaroni, O.; Brown, A. A.; Huck, W. T. S. *Angew. Chem., Int. Ed.* **2006**, *45*, 1770.
(634) Yu, K.; Wang, H. F.; Xue, L. J.; Han, Y. C. *Langmuir* **2007**, *23*, 1443.
(635) Yu, K.; Wang, H. F.; Han, Y. C. *Langmuir* **2007**, *23*, 8957.
(636) Dey, T. *J. Nanosci. Nanotechnol.* **2006**, *6*, 2479.
(637) Li, D.; He, Q.; Yang, Y.; Möhwald, H.; Li, J. *Macromolecules* **2008**, *41*, 7254.
(638) Raghuraman, G. K.; Dhamodharan, R. *J. Nanosci. Nanotechnol.* **2006**, *6*, 2018.
(639) Goodman, D.; Kizhakkedathu, J. N.; Brooks, D. E. *Langmuir* **2004**, *20*, 3297.
(640) Biesalski, M.; Rühe, J. *Macromolecules* **2002**, *35*, 499.
(641) Sanjuan, S.; Tran, Y. *Macromolecules* **2008**, *41*, 8721.
(642) Nagase, K.; Kobayashi, J.; Kikuchi, A.; Akiyama, Y.; Kanazawa, H.; Okano, T. *Biomacromolecules* **2008**, *9*, 1340.
(643) Liu, Y.; Klep, V.; Zdyrko, B.; Luzinov, I. *Langmuir* **2004**, *20*, 6710.
(644) Azzaroni, O.; Zheng, Z. J.; Yang, Z. Q.; Huck, W. T. S. *Langmuir* **2006**, *22*, 6730.
(645) Jhon, Y. K.; Bhat, R. R.; Jeong, C.; Rojas, O. J.; Szleifer, I.; Genzer, J. *Macromol. Rapid Commun.* **2006**, *27*, 697.
(646) Moya, S. E.; Azzaroni, O.; Kelby, T.; Donath, E.; Huck, W. T. S. *J. Phys. Chem. B* **2007**, *111*, 7034.
(647) Li, J.; Chen, X. R.; Chang, Y.-C. *Langmuir* **2005**, *21*, 9562.
(648) Ryan, A. J.; Crook, C. J.; Howse, J. R.; Topham, P.; Jones, R. A. L.; Geoghegan, M.; Parnell, A. J.; Ruiz-Perez, L.; Martin, S. J.; Cadby, A.; Menelle, A.; Webster, J. R. P.; Gleeson, A. J.; Bras, W. *Faraday Discuss.* **2005**, *128*, 55.
(649) Choi, E.-Y.; Azzaroni, O.; Cheng, N.; Zhou, F.; Kelby, T.; Huck, W. T. S. *Langmuir* **2007**, *23*, 10389.
(650) Abu-Lail, N. I.; Kaholek, M.; LaMattina, B.; Clark, R. L.; Zauscher, S. *Sens. Actuators, B* **2006**, *114*, 371.
(651) Zhou, F.; Shu, W. M.; Welland, M. E.; Huck, W. T. S. *J. Am. Chem. Soc.* **2006**, *128*, 5326.
(652) Zhou, F.; Biesheuvel, P. M.; Chol, E.-Y.; Shu, W.; Poetes, R.; Steiner, U.; Huck, W. T. S. *Nano Lett.* **2008**, *8*, 725.
(653) Yim, H.; Kent, M. S.; Mendez, S.; Balamurugan, S. S.; Balamurugan, S.; Lopez, G. P.; Satija, S. *Macromolecules* **2004**, *37*, 1994.
(654) Zhang, J. M.; Nylander, T.; Campbell, R. A.; Rennie, A. R.; Zauscher, S.; Linse, P. *Soft Matter* **2008**, *4*, 500.
(655) Aoki, H.; Kitamura, M.; Ito, S. *Macromolecules* **2008**, *41*, 285.
(656) Wolkenhauer, M.; Bumbu, G. G.; Cheng, Y.; Roth, S. V.; Gutmann, J. S. *Appl. Phys. Lett.* **2006**, *89*, 054101.
(657) Wei, Q. S.; Ji, J.; Shen, J. C. *Macromol. Rapid Commun.* **2008**, *29*, 645.
(658) Fu, L.; Chen, X. N.; He, J. N.; Xiong, C. Y.; Ma, H. W. *Langmuir* **2008**, *24*, 6100.
(659) Ma, H.; Textor, M.; Clark, R. L.; Chilkoti, A. *Biointerphases* **2006**, *1*, 35.
(660) Döbbelin, M.; Arias, G.; Loinaz, I.; Llarena, I.; Mecerreyes, D.; Moya, S. *Macromol. Rapid Commun.* **2008**, *29*, 871.
(661) Zhou, F.; Hu, H. Y.; Yu, B.; Osborne, V. L.; Huck, W. T. S.; Liu, W. M. *Anal. Chem.* **2007**, *79*, 176.
(662) Yu, B.; Zhou, F.; Hu, H.; Wang, C. W.; Liu, W. M. *Electrochim. Acta* **2007**, *53*, 487.
(663) Spruijt, E.; Choi, E.-Y.; Huck, W. T. S. *Langmuir* **2008**, *24*, 11253.
(664) Sakakiyama, T.; Ohkita, H.; Ohoka, M.; Ito, S.; Tsujii, Y.; Fukuda, T. *Chem. Lett.* **2005**, *34*, 1366.
(665) Bumbu, G.-G.; Wolkenhauer, M.; Kircher, G.; Gutmann, J. S.; Berger, D. *Langmuir* **2007**, *23*, 2203.
(666) Bumbu, G.-G.; Kircher, G.; Wolkenhauer, M.; Berger, R.; Gutmann, J. S. *Macromol. Chem. Phys.* **2004**, *205*, 1713.
(667) Granville, A. M.; Boyes, S. G.; Akgun, B.; Foster, M. D.; Brittain, W. J. *Macromolecules* **2004**, *37*, 2790.
(668) Rowe, M. D.; Hammer, B. A. G.; Boyes, S. G. *Macromolecules* **2008**, *41*, 4147.
(669) Gao, X.; Feng, W.; Zhu, S. P.; Sheardown, H.; Brash, J. L. *Langmuir* **2008**, *24*, 8303.
(670) Yin, Y.; Sun, P.; Li, B.; Chen, T.; Jin, Q.; Ding, D.; Shi, A.-C. *Macromolecules* **2007**, *40*, 5161.
(671) Prokhorova, S. A.; Kopyshev, A.; Ramakrishnan, A.; Zhang, H.; Rühe, J. *Nanotechnology* **2003**, *14*, 1098.
(672) Santer, S.; Rühe, J. *Polymer* **2004**, *45*, 8279.
(673) Santer, S.; Kopyshev, A.; Donges, J.; Yang, H. K.; Rühe, J. *Adv. Mater.* **2006**, *18*, 2359.
(674) Idota, N.; Kikuchi, A.; Kobayashi, J.; Akiyama, Y.; Sakai, K.; Okano, T. *Langmuir* **2006**, *22*, 425.
(675) Seino, M.; Yokomachi, K.; Hayakawa, T.; Kikuchi, R.; Kakimoto, M.-A.; Horiuchi, S. *Polymer* **2006**, *47*, 1946.
(676) Nagase, K.; Kobayashi, J.; Kikuchi, A.; Akiyama, Y.; Kanazawa, H.; Okano, T. *Langmuir* **2007**, *23*, 9409.
(677) Lokuge, I.; Wang, X.; Bohn, P. W. *Langmuir* **2007**, *23*, 305.
(678) Schild, H. G. *Prog. Polym. Sci.* **1992**, *17*, 163.
(679) *Polymer Data Handbook*; Mark, J. E., Ed.; Oxford University Press, Inc.: 1999.
(680) Sun, T. L.; Wang, G. J.; Feng, L.; Liu, B. Q.; Ma, Y. M.; Jiang, L.; Zhu, D. B. *Angew. Chem., Int. Ed.* **2004**, *43*, 357.
(681) Rahane, S. B.; Floyd, J. A.; Metters, A. T.; Kilbey, S. M., II. *Adv. Funct. Mater.* **2008**, *18*, 1232.
(682) Balamurugan, S.; Mendez, S.; Balamurugan, S. S.; O'Brien, M. J.; López, G. P. *Langmuir* **2003**, *19*, 2545.
(683) Wu, T.; Zhang, Y. F.; Wang, X. F.; Liu, S. Y. *Chem. Mater.* **2008**, *20*, 101.
(684) Yim, H.; Kent, M. S.; Satija, S.; Mendez, S.; Balamurugan, S. S.; Balamurugan, S.; Lopez, G. P. *Phys. Rev. E: Stat., Nonlinear, Soft Matter Phys.* **2005**, *72*, 051801.
(685) Yim, H.; Kent, M. S.; Satija, S.; Mendez, S.; Balamurugan, S. S.; Balamurugan, S.; Lopez, G. P. *J. Polym. Sci., Part B: Polym. Phys.* **2004**, *42*, 3302.
(686) Yim, H.; Kent, M. S.; Mendez, S.; Lopez, G. P.; Satija, S.; Seo, Y. *Macromolecules* **2006**, *39*, 3420.
(687) Li, D. J.; Jones, G. L.; Dunlap, J. R.; Hua, F. J.; Zhao, B. *Langmuir* **2006**, *22*, 3344.
(688) Schulz, D. N.; Peiffer, D. G.; Agarwal, P. K.; Larabee, J.; Kaladas, J. J.; Soni, L.; Handwerker, B.; Garner, R. T. *Polymer* **1986**, *27*, 1734.
(689) Jonas, A. M.; Glinel, K.; Oren, R.; Nysten, B.; Huck, W. T. S. *Macromolecules* **2007**, *40*, 4403.
(690) Xia, F.; Feng, L.; Wang, S. T.; Sun, T. L.; Song, W. L.; Jiang, W. H.; Jiang, L. *Adv. Mater.* **2006**, *18*, 432.
(691) Rühe, J.; Ballauff, M.; Biesalski, M.; Dziezok, P.; Grohn, F.; Johannsmann, D.; Houbenov, N.; Hugenberg, N.; Konradi, R.; Minko, S.; Motornov, M.; Netz, R. R.; Schmidt, M.; Seidel, C.; Stamm, M.; Stephan, T.; Usov, D.; Zhang, H. N. *Adv. Polym. Sci.* **2004**, *165*, 79.
(692) Sanjuan, S.; Perrin, P.; Pantoustier, N.; Tran, Y. *Langmuir* **2007**, *23*, 5769.
(693) Geoghegan, M.; Ruiz-Pérez, L.; Dang, C. C.; Parnell, A. J.; Martin, S. J.; Howse, J. R.; Jones, R. A. L.; Golestanian, R.; Topham, P. D.; Crook, C. J.; Ryan, A. J.; Sivia, D. S.; Webster, J. R. P.; Menelle, A. *Soft Matter* **2006**, *2*, 1076.
(694) Liu, G. M.; Zhang, G. Z. *J. Phys. Chem. B* **2008**, *112*, 10137.
(695) Zhang, Q. L.; Xia, F.; Sun, T. L.; Song, W. L.; Zhao, T. Y.; Liu, M. C.; Jiang, L. *Chem. Commun.* **2008**, 1199.
(696) Gong, P.; Wu, T.; Genzer, J.; Szleifer, I. *Macromolecules* **2007**, *40*, 8765.
(697) Moya, S.; Azzaroni, O.; Farhan, T.; Osborne, V. L.; Huck, W. T. S. *Angew. Chem., Int. Ed.* **2005**, *44*, 4578.
(698) Azzaroni, O.; Brown, A. A.; Huck, W. T. S. *Adv. Mater.* **2007**, *19*, 151.
(699) Jeon, S. I.; Lee, J. H.; Andrade, J. D.; De Gennes, P. G. *J. Colloid Interface Sci.* **1991**, *142*, 149.
(700) Li, L.; Chen, S.; Zheng, J.; Ratner, B. D.; Jiang, S. *J. Phys. Chem. B* **2005**, *109*, 2934.
(701) Chang, Y.; Liao, S.-C.; Higuchi, A.; Ruaan, R.-C.; Chu, C.-W.; Chen, W.-Y. *Langmuir* **2008**, *24*, 5453.
(702) Ladd, J.; Zhang, Z.; Chen, S.; Hower, J. C.; Jiang, S. *Biomacromolecules* **2008**, *9*, 1357.
(703) Wattendorf, U.; Merkle, H. P. *J. Pharm. Sci.* **2008**, *97*, 4655.
(704) Harris, J. M. *Poly(ethylene glycol) Chemistry*; Plenum Press: New York and London, 1992.
(705) Herold, D. A.; Keil, K.; Bruns, D. E. *Biochem. Pharmacol.* **1989**, *38*, 73.
(706) Talarico, T.; Swank, A.; Privalle, C. *Biochem. Biophys. Res. Commun.* **1998**, *250*, 354.
(707) Okano, T.; Yamada, N.; Okuhara, M.; Sakai, H.; Sakurai, Y. *Biomaterials* **1995**, *16*, 297.
(708) Kim, D. J.; Kong, B.; Jung, Y. H.; Kim, K. S.; Kim, W.-J.; Lee, K.-B.; Kang, S. M.; Jeon, S.; Choi, I. S. *Bull. Korean Chem. Soc.* **2004**, *25*, 1629.
(709) Feng, W.; Zhu, S. P.; Ishihara, K.; Brash, J. L. *Langmuir* **2005**, *21*, 5980.
(710) Halperin, A.; Fragneto, G.; Schollier, A.; Sferrazza, M. *Langmuir* **2007**, *23*, 10603.

(711) Feng, W.; Zhu, S. P.; Ishihara, K.; Brash, J. L. *Biointerphases* **2006**, *1*, 50.
(712) Bernards, M. T.; Cheng, G.; Zhang, Z.; Chen, S. F.; Jiang, S. Y. *Macromolecules* **2008**, *41*, 4216.
(713) Lutolf, M. P.; Hubbell, J. A. *Nat. Biotechnol.* **2005**, *23*, 47.
(714) Stevens, M. M.; George, J. H. *Science* **2005**, *310*, 1135.
(715) Hersel, U.; Dahmen, C.; Kessler, H. *Biomaterials* **2003**, *24*, 4385.
(716) Devenish, S. R. A.; Hill, J. B.; Blunt, J. W.; Morris, J. C.; Munro, M. H. G. *Tetrahedron Lett.* **2006**, *47*, 2875.
(717) Wong, S. Y.; Putnam, D. *Bioconjugate Chem.* **2007**, *18*, 970.
(718) Sebra, R. P.; Masters, K. S.; Bowman, C. N.; Anseth, K. S. *Langmuir* **2005**, *21*, 10907.
(719) Huang, J.; Han, B.; Yue, W.; Yan, H. *J. Mater. Chem.* **2007**, *17*, 3812.
(720) Sielaff, I.; Arnold, A.; Godin, G.; Tugulu, S.; Klok, H.-A.; Johnsson, K. *ChemBioChem* **2006**, *7*, 194.
(721) Mallik, A. K.; Rahman, M. M.; Czaun, M.; Takafuji, M.; Ihara, H. *J. Chromatogr., A* **2008**, *1187*, 119.
(722) Mallik, A. K.; Rahman, M. M.; Czaun, M.; Takafuji, M.; Ihara, H. *Chem. Lett.* **2007**, *36*, 1460.
(723) Rahman, M. M.; Czaun, M.; Takafuji, M.; Ihara, H. *Chem.—Eur. J.* **2008**, *14*, 1312.
(724) Coad, B. R.; Steels, B. M.; Kizhakkedathu, J. N.; Brooks, D. E.; Haynes, C. A. *Biotechnol. Bioeng.* **2007**, *97*, 574.
(725) Sun, X. F.; Liu, J. K.; Lee, M. L. *Anal. Chem.* **2008**, *80*, 856.
(726) Miller, M. D.; Baker, G. L.; Bruening, M. L. *J. Chromatogr., A* **2004**, *1044*, 323.
(727) Holmberg, S.; Holmlund, P.; Wilén, C. E.; Kallio, T.; Sundholm, G.; Sundholm, F. *J. Polym. Sci., Part A: Polym. Chem.* **2002**, *40*, 591.
(728) Lee, S. B.; Koepsel, R. R.; Morley, S. W.; Matyjaszewski, K.; Sun, Y. J.; Russell, A. J. *Biomacromolecules* **2004**, *5*, 877.
(729) Murata, H.; Koepsel, R. R.; Matyjaszewski, K.; Russell, A. J. *Biomaterials* **2007**, *28*, 4870.
(730) Ramstedt, M.; Cheng, N.; Azzaroni, O.; Mossialos, D.; Mathieu, H. J.; Huck, W. T. S. *Langmuir* **2007**, *23*, 3314.
(731) Cheng, G.; Zhang, Z.; Chen, S. F.; Bryers, J. D.; Jiang, S. Y. *Biomaterials* **2007**, *28*, 4192.
(732) Cringus-Fundeanu, I.; Luijten, J.; van der Mei, H. C.; Busscher, H. J.; Schouten, A. J. *Langmuir* **2007**, *23*, 5120.
(733) Fundeanu, I.; van der Mei, H. C.; Schouten, A. J.; Busscher, H. J. *Colloids Surf., B* **2008**, *64*, 297.
(734) Sakata, H.; Kobayashi, M.; Otsuka, H.; Takahara, A. *Polym. J.* **2005**, *37*, 767.
(735) Kobayashi, M.; Terayama, Y.; Hosaka, N.; Kaido, M.; Suzuki, A.; Yamada, N.; Torikai, N.; Ishihara, K.; Takahara, A. *Soft Matter* **2007**, *3*, 740.
(736) Rakhmatullina, E.; Braun, T.; Kaufmann, T.; Spillmann, H.; Malinova, V.; Meier, W. *Macromol. Chem. Phys.* **2007**, *208*, 1283.
(737) El Harrak, A.; Carrot, G.; Oberdisse, J.; Jestin, J.; Boué, F. *Macromol. Symp.* **2005**, *226*, 263.
(738) Carrot, G.; El Harrak, A.; Oberdisse, J.; Jestin, J.; Boué, F. *Soft Matter* **2006**, *2*, 1043.
(739) Sha, K.; Li, D. S.; Li, Y. P.; Wang, S. W.; Wang, J. Y. *J. Mater. Sci.* **2007**, *42*, 4916.
(740) Cui, T.; Zhang, J. H.; Wang, J. Y.; Cui, F.; Chen, W.; Xu, F. B.; Wang, Z.; Zhang, K.; Yang, B. *Adv. Funct. Mater.* **2005**, *15*, 481.
(741) Topham, P. D.; Howse, J. R.; Crook, C. J.; Parnell, A. J.; Geoghegan, M.; Jones, R. A. L.; Ryan, A. J. *Polym. Int.* **2006**, *55*, 808.
(742) Vo, C.-D.; Schmid, A.; Armes, S. P.; Sakai, K.; Biggs, S. *Langmuir* **2007**, *23*, 408.
(743) Bhat, R. R.; Tomlinson, M. R.; Genzer, J. *Macromol. Rapid Commun.* **2004**, *25*, 270.
(744) Zheng, G. D.; Stöver, H. D. H. *Macromolecules* **2002**, *35*, 7612.
(745) Zhou, L.; Yuan, W.; Yuan, J.; Hong, X. *Mater. Lett.* **2008**, *62*, 1372.
(746) Gong, R.; Maclaughlin, S.; Zhu, S. P. *Appl. Surf. Sci.* **2008**, *254*, 6802.
(747) Cho, W. K.; Kang, S. M.; Kim, D. J.; Yang, S. H.; Choi, I. S. *Langmuir* **2006**, *22*, 11208.
(748) Kim, D. J.; Lee, K.-B.; Chi, Y. S.; Kim, W.-J.; Paik, H.-J.; Choi, I. S. *Langmuir* **2004**, *20*, 7904.
(749) Zhai, G. Q.; Shi, Z. L.; Kang, E. T.; Neoh, K. G. *Macromol. Biosci.* **2005**, *5*, 974.
(750) Liu, T. Q.; Jia, S. J.; Kowalewski, T.; Matyjaszewski, K.; Casado-Portilla, R.; Belmont, J. *Macromolecules* **2006**, *39*, 548.
(751) Feng, W.; Brash, J.; Zhu, S. P. *J. Polym. Sci., Part A: Polym. Chem.* **2004**, *42*, 2931.
(752) Peng, Q.; Lu, S. Q.; Chen, D. Z.; Wu, X. Q.; Fan, P. F.; Zhong, R.; Xu, Y. W. *Macromol. Biosci.* **2007**, *7*, 1149.
(753) Parnell, A. J.; Martin, S. J.; Jones, R. A. L.; Vasilev, C.; Crook, C. J.; Ryan, A. J. *Soft Matter* **2009**, *5*, 296.
(754) Parnell, A. J.; Martin, S. J.; Dang, C. C.; Geoghegan, M.; Jones, R. A. L.; Crook, C. J.; Howse, J. R.; Ryan, A. J. *Polymer* **2009**, *50*, 1005.
(755) Mulvihill, M. J.; Rupert, B. L.; He, R. R.; Hochbaum, A.; Arnold, J.; Yang, P. D. *J. Am. Chem. Soc.* **2005**, *127*, 16040.
(756) Titirici, M.-M.; Sellergren, B. *Chem. Mater.* **2006**, *18*, 1773.
(757) Raynor, J. E.; Petrie, T. A.; Fears, K. P.; Latour, R. A.; García, A. J.; Collard, D. M. *Biomacromolecules* **2009**, *10*, 748.
(758) Ramakrishnan, A.; Dhamodharan, R.; Rühe, J. *J. Polym. Sci., Part A: Polym. Chem.* **2006**, *44*, 1758.
(759) Perruchot, C.; Khan, M. A.; Kamitsi, A.; Armes, S. P.; von Werne, T.; Patten, T. E. *Langmuir* **2001**, *17*, 4479.
(760) Li, L.; Yan, G. P.; Wu, J. Y.; Yu, X. H.; Guo, Q. Z. *J. Macromol. Sci., Part A: Pure Appl. Chem.* **2008**, *45*, 828.
(761) Cummins, D.; Wyman, P.; Duxbury, C. J.; Thies, J.; Koning, C. E.; Heise, A. *Chem. Mater.* **2007**, *19*, 5285.
(762) Teare, D. O. H.; Barwick, D. C.; Schofield, W. C. E.; Garrod, R. P.; Ward, L. J.; Badyal, J. P. S. *Langmuir* **2005**, *21*, 11425.
(763) Pirri, G.; Chiari, M.; Damin, F.; Meo, A. *Anal. Chem.* **2006**, *78*, 3118.
(764) Qian, T. C.; Li, Y. F.; Wu, Y. Z.; Zheng, B.; Ma, H. W. *Macromolecules* **2008**, *41*, 6641.
(765) Zhang, K.; Li, H. T.; Zhang, H. W.; Zhao, S.; Wang, D.; Wang, J. Y. *Mater. Chem. Phys.* **2006**, *96*, 477.
(766) Yoshikawa, C.; Goto, A.; Ishizuka, N.; Nakanishi, K.; Kishida, A.; Tsujii, Y.; Fukuda, T. *Macromol. Symp.* **2007**, *248*, 189.
(767) Yoshikawa, C.; Goto, A.; Tsujii, Y.; Ishizuka, N.; Nakanishi, K.; Fukuda, T. *J. Polym. Sci., Part A: Polym. Chem.* **2007**, *45*, 4795.
(768) Lou, X. H.; He, L. *Langmuir* **2006**, *22*, 2640.
(769) Granville, A. M.; Boyes, S. G.; Akgun, B.; Foster, M. D.; Brittain, W. J. *Macromolecules* **2005**, *38*, 3263.
(770) Constable, A. N.; Brittain, W. J. *Colloids Surf., A* **2007**, *308*, 123.
(771) Lou, X. H.; Wang, C. Y.; He, L. *Biomacromolecules* **2007**, *8*, 1385.
(772) Brantley, E. L.; Holmes, T. C.; Jennings, G. K. *J. Phys. Chem. B* **2004**, *108*, 16077.
(773) Lou, X. H.; He, L. *Sens. Actuators, B* **2008**, *129*, 225.
(774) Zhang, K.; Li, H. T.; Zhao, S.; Wang, W.; Wang, S. W.; Xu, Y. X.; Yu, W. Z.; Wang, J. Y. *Polym. Bull.* **2006**, *57*, 253.
(775) Yoon, K. R.; Ramaraj, B.; Lee, S. M.; Kim, D.-P. *Surf. Interface Anal.* **2008**, *40*, 1139.
(776) Wang, J.-Y.; Chen, W.; Liu, A.-H.; Lu, G.; Zhang, G.; Zhang, J.-H.; Yang, B. *J. Am. Chem. Soc.* **2002**, *124*, 13358.
(777) Marsh, A.; Khan, A.; Garcia, M.; Haddleton, D. M. *Chem. Commun.* **2000**, 2083.
(778) Ayres, N.; Holt, D. J.; Jones, C. F.; Corum, L. E.; Grainger, D. W. *J. Polym. Sci., Part A: Polym. Chem.* **2008**, *46*, 7713.
(779) Uekusa, T.; Nagano, S.; Seki, T. *Langmuir* **2007**, *23*, 4642.
(780) Uekusa, T.; Nagano, S.; Seki, T. *Macromolecules* **2009**, *42*, 312.
(781) Tsukagoshi, T.; Kondo, Y.; Yoshino, N. *Colloids Surf., B* **2007**, *55*, 19.
(782) Duquesne, E.; Labruyère, C.; Habimana, J.; Degée, P.; Dubois, P. *J. Polym. Sci., Part A: Polym. Chem.* **2006**, *44*, 744.
(783) Ramakrishnan, A.; Dhamodharan, R.; Rühe, J. *Macromol. Rapid Commun.* **2002**, *23*, 612.
(784) Kong, X. X.; Kawai, T.; Abe, J.; Iyoda, T. *Macromolecules* **2001**, *34*, 1837.
(785) Pyun, J.; Jia, S. J.; Kowalewski, T.; Patterson, G. D.; Matyjaszewski, K. *Macromolecules* **2003**, *36*, 5094.
(786) von Werne, T.; Patten, T. E. *J. Am. Chem. Soc.* **2001**, *123*, 7497.
(787) Farmer, S. C.; Patten, T. E. *Chem. Mater.* **2001**, *13*, 3920.
(788) Ohno, K.; Morinaga, T.; Koh, K.; Tsujii, Y.; Fukuda, T. *Macromolecules* **2005**, *38*, 2137.
(789) Ohno, K.; Morinaga, T.; Takeno, S.; Tsujii, Y.; Fukuda, T. *Macromolecules* **2007**, *40*, 9143.
(790) Ohno, K.; Morinaga, T.; Takeno, S.; Tsujii, Y.; Fukuda, T. *Macromolecules* **2006**, *39*, 1245.
(791) Audouin, F.; Blas, H.; Pasetto, P.; Beaunier, P.; Boissière, C.; Sanchez, C.; Save, M.; Charleux, B. *Macromol. Rapid Commun.* **2008**, *29*, 914.
(792) Ejaz, M.; Tsujii, Y.; Fukuda, T. *Polymer* **2001**, *42*, 6811.
(793) Save, M.; Granvorka, G.; Bernard, J.; Charleux, B.; Boissière, C.; Grosso, D.; Sanchez, C. *Macromol. Rapid Commun.* **2006**, *27*, 393.
(794) Wang, T.-L.; Ou, C.-C.; Yang, C.-H. *J. Appl. Polym. Sci.* **2008**, *109*, 3421.
(795) Morinaga, T.; Ohno, K.; Tsujii, Y.; Fukuda, T. *Eur. Polym. J.* **2007**, *43*, 243.
(796) Urayama, K.; Yamamoto, S.; Tsujii, Y.; Fukuda, T.; Neher, D. *Macromolecules* **2002**, *35*, 9459.
(797) Piech, M.; Bell, N. S. *Macromolecules* **2006**, *39*, 915.
(798) Yamamoto, S.; Tsujii, Y.; Fukuda, T. *Macromolecules* **2000**, *33*, 5995.
(799) Chen, R. X.; Feng, W.; Zhu, S. P.; Botton, G.; Ong, B.; Wu, Y. L. *J. Polym. Sci., Part A: Polym. Chem.* **2006**, *44*, 1252.

(800) Zhang, H.; Lei, X. P.; Su, Z. X.; Liu, P. *J. Polym. Res.* **2007**, *14*, 253.
(801) Bell, N. S.; Piech, M. *Langmuir* **2006**, *22*, 1420.
(802) Piech, M.; George, M. C.; Bell, N. S.; Braun, P. V. *Langmuir* **2006**, *22*, 1379.
(803) Bai, J.; Qiu, K.-Y.; Wei, Y. *Polym. Int.* **2003**, *52*, 853.
(804) Rahane, S. B.; Kilbey, S. M., II; Metters, A. T. *Macromolecules* **2008**, *41*, 9612.
(805) Perruchot, C.; Khan, M. A.; Kamitsi, A.; Armes, S. P.; Watts, J. F.; von Werne, T.; Patten, T. E. *Eur. Polym. J.* **2004**, *40*, 2129.
(806) Brown, A. A.; Azzaroni, O.; Huck, W. T. S. *Langmuir* **2009**, *25*, 1744.
(807) Zhai, G. Q.; Kang, E. T.; Neoh, K. G. *Macromolecules* **2004**, *37*, 7240.
(808) Xu, F. J.; Xu, D.; Kang, E. T.; Neoh, K. G. *J. Mater. Chem.* **2004**, *14*, 2674.
(809) Feng, W.; Chen, R. X.; Brash, J. L.; Zhu, S. P. *Macromol. Rapid Commun.* **2005**, *26*, 1383.
(810) Zheng, Y.; Bruening, M. L.; Baker, G. L. *Macromolecules* **2007**, *40*, 8212.
(811) Li, D. J.; Zhao, B. *Langmuir* **2007**, *23*, 2208.
(812) He, P.; Zheng, W. M.; Tucker, E. Z.; Gorman, C. B.; He, L. *Anal. Chem.* **2008**, *80*, 3633.
(813) Chen, R. X.; Feng, W.; Zhu, S. P.; Botton, G.; Ong, B.; Wu, Y. L. *Polymer* **2006**, *47*, 1119.
(814) Fries, K.; Samanta, S.; Orski, S.; Locklin, J. *Chem. Commun.* **2008**, 6288.
(815) Hoven, V. P.; Srinanthakul, M.; Iwasaki, Y.; Iwata, R.; Kiatkamjornwong, S. *J. Colloid Interface Sci.* **2007**, *314*, 446.
(816) Pei, X. W.; Xia, Y. Q.; Liu, W. M.; Yu, B.; Hao, J. C. *J. Polym. Sci., Part A: Polym. Chem.* **2008**, *46*, 7225.
(817) Zhang, Z.; Chao, T.; Chen, S. F.; Jiang, S. Y. *Langmuir* **2006**, *22*, 10072.
(818) Yu, B.; Zhou, F.; Bo, Y.; Hou, X. M.; Liu, W. M. *Electrochem. Commun.* **2007**, *9*, 1749.
(819) Sankhe, A. Y.; Husson, S. M.; Kilbey, S. M. *Macromolecules* **2006**, *39*, 1376.
(820) Liu, Z. L.; Liu, J. X.; Hu, H. Y.; Yu, B.; Chen, M.; Zhou, F. *Phys. Chem. Chem. Phys.* **2008**, *10*, 7180.
(821) Liu, Z. L.; Hu, H. Y.; Yu, B.; Chen, M. A.; Zheng, Z. J.; Zhou, F. *Electrochem. Commun.* **2009**, *11*, 492.
(822) Kim, S.; Cheng, N.; Jeong, J.-R.; Jang, S.-G.; Yang, S.-M.; Huck, W. T. S. *Chem. Commun.* **2008**, 3666.
(823) Chen, M.; Briscoe, W. H.; Armes, S. P.; Cohen, H.; Klein, J. *ChemPhysChem* **2007**, *8*, 1303.
(824) Chen, X. Y.; Armes, S. P. *Adv. Mater.* **2003**, *15*, 1558.
(825) Zhang, Z.; Chen, S. F.; Chang, Y.; Jiang, S. Y. *J. Phys. Chem. B* **2006**, *110*, 10799.
(826) Cheng, N.; Brown, A. A.; Azzaroni, O.; Huck, W. T. S. *Macromolecules* **2008**, *41*, 6317.
(827) Zhang, Z.; Zhang, M.; Chen, S. F.; Horbett, T. A.; Ratner, B. D.; Jiang, S. Y. *Biomaterials* **2008**, *29*, 4285.
(828) Li, G. Z.; Xue, H.; Cheng, G.; Chen, S. F.; Zhang, F. B.; Jiang, S. Y. *J. Phys. Chem. B* **2008**, *112*, 15269.
(829) Choi, W. S.; Koo, H. Y.; Kim, J. Y.; Huck, W. T. S. *Adv. Mater.* **2008**, *20*, 4504.
(830) Ramstedt, M.; Ekstrand-Hammarström, B.; Shchukarev, A. V.; Bucht, A.; Österlund, L.; Welch, M.; Huck, W. T. S. *Biomaterials* **2009**, *30*, 1524.
(831) Sonnenberg, L.; Parvole, J.; Borisov, O.; Billon, L.; Gaub, H. E.; Seitz, M. *Macromolecules* **2006**, *39*, 281.
(832) Liu, T. Q.; Jia, S.; Kowalewski, T.; Matyjaszewski, K.; Casado-Portilla, R.; Belmont, J. *Langmuir* **2003**, *19*, 6342.
(833) Liu, T. Q.; Casado-Portilla, R.; Belmont, J.; Matyjaszewski, K. *J. Polym. Sci., Part A: Polym. Chem.* **2005**, *43*, 4695.
(834) Carrot, G.; Diamanti, S.; Manuszak, M.; Charleux, B.; Vairon, J.-P. *J. Polym. Sci., Part A: Polym. Chem.* **2001**, *39*, 4294.
(835) Pyun, J.; Matyjaszewski, K.; Kowalewski, T.; Savin, D.; Patterson, G.; Kickelbick, G.; Huesing, N. *J. Am. Chem. Soc.* **2001**, *123*, 9445.
(836) Yamaguchi, H.; Honda, K.; Kobayashi, M.; Morita, M.; Masunaga, H.; Sakata, O.; Sasaki, S.; Takahara, A. *Polym. J.* **2008**, *40*, 854.
(837) Hamelinck, P. J.; Huck, W. T. S. *J. Mater. Chem.* **2005**, *15*, 381.
(838) Boyes, S. G.; Akgun, B.; Brittain, W. J.; Foster, M. D. *Macromolecules* **2003**, *36*, 9539.
(839) Granville, A. M.; Brittain, W. J. *Macromol. Rapid Commun.* **2004**, *25*, 1298.
(840) Akgun, B.; Brittain, W. J.; Li, X. F.; Wang, J.; Foster, M. D. *Macromolecules* **2005**, *38*, 8614.
(841) Lei, Z. L.; Bi, S. X. *Mater. Lett.* **2007**, *61*, 3531.
(842) Retsch, M.; Walther, A.; Loos, K.; Müller, A. H. E. *Langmuir* **2008**, *24*, 9421.
(843) Snaith, H. J.; Whiting, G. L.; Sun, B. Q.; Greenham, N. C.; Huck, W. T. S.; Friend, R. H. *Nano Lett.* **2005**, *5*, 1653.
(844) Whiting, G. L.; Snaith, H. J.; Khodabakhsh, S.; Andreasen, J. W.; Breiby, D. W.; Nielsen, M. M.; Greenham, N. C.; Friend, R. H.; Huck, W. T. S. *Nano Lett.* **2006**, *6*, 573.
(845) Cho, W. K.; Kong, B. Y.; Choi, I. S. *Langmuir* **2007**, *23*, 5678.
(846) Gopireddy, D.; Husson, S. M. *Macromolecules* **2002**, *35*, 4218.
(847) Huang, X.; Wirth, M. J. *Macromolecules* **1999**, *32*, 1694.
(848) Xiao, D. Q.; Wirth, M. J. *Macromolecules* **2002**, *35*, 2919.
(849) Fu, G. D.; Lei, J. Y.; Yao, C.; Li, X. S.; Yao, F.; Nie, S. Z.; Kang, E. T.; Neoh, K. G. *Macromolecules* **2008**, *41*, 6854.
(850) Schepelina, O.; Zharov, I. *Langmuir* **2006**, *22*, 10523.
(851) Liu, P.; Guo, J. S. *J. Appl. Polym. Sci.* **2006**, *102*, 3385.
(852) Song, W. L.; Sun, T. L.; Song, Y. L.; Bai, Y. B.; Liu, F. Q.; Jiang, L. *Talanta* **2005**, *67*, 543.
(853) Zhang, K.; Ma, J.; Zhang, B.; Zhao, S.; Li, Y. P.; Xu, Y. X.; Yu, W. Z.; Wang, J. Y. *Mater. Lett.* **2007**, *61*, 949.
(854) Bi, S. X.; Wei, X. Y.; Li, N.; Lei, Z. L. *Mater. Lett.* **2008**, *62*, 2963.
(855) Fu, Q.; Rama Rao, G. V.; Ista, L. K.; Wu, Y.; Andrzejewski, B. P.; Sklar, L. A.; Ward, T. L.; López, G. P. *Adv. Mater.* **2003**, *15*, 1262.
(856) Lee, W.-K.; Patra, M.; Linse, P.; Zauscher, S. *Small* **2007**, *3*, 63.
(857) Schepelina, O.; Zharov, I. *Langmuir* **2007**, *23*, 12704.
(858) Sun, T. L.; Liu, H. A.; Song, W. L.; Wang, X.; Jiang, L.; Li, L.; Zhu, D. B. *Angew. Chem., Int. Ed.* **2004**, *43*, 4663.
(859) Chung, P.-W.; Kumar, R.; Pruski, M.; Lin, V. S.-Y. *Adv. Funct. Mater.* **2008**, *18*, 1390.
(860) Kizhakkedathu, J. N.; Janzen, J.; Le, Y.; Kainthan, R. K.; Brooks, D. E. *Langmuir* **2009**, *25*, 3794.
(861) Czaun, M.; Rahman, M. M.; Takafuji, M.; Ihara, H. *J. Polym. Sci., Part A: Polym. Chem.* **2008**, *46*, 6664.
(862) Böttcher, H.; Hallensleben, M. L.; Nuss, S.; Wurm, H. *Polym. Bull.* **2000**, *44*, 223.
(863) von Werne, T.; Patten, T. E. *J. Am. Chem. Soc.* **1999**, *121*, 7409.
(864) El Harrak, A.; Carrot, G.; Oberdisse, J.; Jestin, J.; Boué, F. *Polymer* **2005**, *46*, 1095.
(865) Savin, D. A.; Pyun, J.; Patterson, G. D.; Kowalewski, T.; Matyjaszewski, K. *J. Polym. Sci., Part B: Polym. Phys.* **2002**, *40*, 2667.
(866) El Harrak, A.; Carrot, G.; Oberdisse, J.; Eychenne-Baron, C.; Boué, F. *Macromolecules* **2004**, *37*, 6376.
(867) Jeyaprakash, J. D.; Samuel, S.; Dhamodharan, R.; Rühe, J. *Macromol. Rapid Commun.* **2002**, *23*, 277.
(868) Wang, Y.; Teng, X. W.; Wang, J.-S.; Yang, H. *Nano Lett.* **2003**, *3*, 789.
(869) Zhang, F. Z.; Lei, X. P.; Su, Z. X.; Zhang, H. *J. Polym. Res.* **2008**, *15*, 319.
(870) Jakuczek, L.; Gutmann, J. S.; Müller, B.; Rosenauer, C.; Zuchowska, D. *Polymer* **2008**, *49*, 843.
(871) Goel, V.; Chatterjee, T.; Bombalski, L.; Yurekli, K.; Matyjaszewski, K.; Krishnamoorti, R. *J. Polym. Sci., Part B: Polym. Phys.* **2006**, *44*, 2014.
(872) Lenarda, M.; Chessa, G.; Moretti, E.; Polizzi, S.; Storaro, L.; Talon, A. *J. Mater. Sci.* **2006**, *41*, 6305.
(873) Ostaci, R.-V.; Celle, C.; Seytre, G.; Beyou, E.; Chapel, J. P.; Drockenmüller, E. *J. Polym. Sci., Part A: Polym. Chem.* **2008**, *46*, 3367.
(874) Oren, R.; Liang, Z. Q.; Barnard, J. S.; Warren, S. C.; Wiesner, U.; Huck, W. T. S. *J. Am. Chem. Soc.* **2009**, *131*, 1670.
(875) Liu, P.; Su, Z. X. *J. Photochem. Photobiol., A* **2004**, *167*, 237.
(876) Fu, G. D.; Zhao, J. P.; Sun, Y. M.; Kang, E. T.; Neoh, K. G. *Macromolecules* **2007**, *40*, 2271.
(877) Lei, Z. L.; Li, Y. L.; Wei, X. Y. *J. Solid State Chem.* **2008**, *181*, 480.
(878) Tu, C.-Y.; Liu, Y.-L.; Lee, K.-R.; Lai, J.-Y. *Polymer* **2005**, *46*, 6976.
(879) Lei, Z.; Bi, S.; Hu, B.; Yang, H. *Food Chem.* **2007**, *105*, 889.
(880) He, X. Y.; Yang, W.; Pei, X. W. *Macromolecules* **2008**, *41*, 4615.
(881) Li, X.; Wei, X. L.; Husson, S. M. *Biomacromolecules* **2004**, *5*, 869.
(882) Yu, K.; Han, Y. C. *Soft Matter* **2009**, *5*, 759.
(883) Senkal, B. F.; Yavuz, E. *Polym. Adv. Technol.* **2006**, *17*, 928.
(884) Wu, Z. Q.; Chen, H.; Liu, X. L.; Zhang, Y. X.; Li, D.; Huang, H. *Langmuir* **2009**, *25*, 2900.
(885) Cullen, S. P.; Mandel, I. C.; Gopalan, P. *Langmuir* **2008**, *24*, 13701.
(886) Parvole, J.; Laruelle, G.; Guimon, C.; Francois, J.; Billon, L. *Macromol. Rapid Commun.* **2003**, *24*, 1074.
(887) Kamata, K.; Lu, Y.; Xia, Y. N. *J. Am. Chem. Soc.* **2003**, *125*, 2384.
(888) Ranjan, R.; Brittain, W. J. *Macromol. Rapid Commun.* **2008**, *29*, 1104.
(889) Liu, P.; Tian, J.; Liu, W. M.; Xue, Q. J. *Polym. Int.* **2004**, *53*, 127.
(890) Li, L.; Yan, G. P.; Cheng, Z. Y.; Wu, J. Y.; Yu, X. H.; Guo, Q. Z. *Surf. Interface Anal.* **2009**, *41*, 69.
(891) Lego, B.; François, M.; Skene, W. G.; Giasson, S. *Langmuir* **2009**, *25*, 5313.

(892) Behling, R. E.; Williams, B. A.; Staade, B. L.; Wolf, L. M.; Cochran, E. W. *Macromolecules* **2009**, *42*, 1867.
(893) Bech, L.; Elzein, T.; Meylheuc, T.; Ponche, A.; Brogly, M.; Lepoittevin, B.; Roger, P. *Eur. Polym. J.* **2009**, *45*, 246.
(894) Zou, Y. Q.; Kizhakkedathu, J. N.; Brooks, D. E. *Macromolecules* **2009**, *42*, 3258.
(895) Limé, F.; Irgum, K. *J. Polym. Sci., Part A: Polym. Chem.* **2009**, *47*, 1259.
(896) Friebe, A.; Ulbricht, M. *Macromolecules* **2009**, *42*, 1838.
(897) Li, L.; Ke, Z. J.; Yan, G. P.; Wu, J. Y. *Polym. Int.* **2008**, *57*, 1275.
(898) Zhang, Z.; Zhang, M.; Chen, S.; Horbett, T. A.; Ratner, B. D.; Jiang, S. *Biomaterials* **2008**, *29*, 4285.

CR900045A